

FOUR-DIMENSIONAL
STOCK MARKET
STRUCTURES AND CYCLES

Bradley F. Cowan

NOTICE OF TRADEMARKS

First time violations of trademark laws carry fines of up to \$250,000 and five years in jail.

"PTV" is a trademark of Bradley F. Cowan

"Price-Time Vector" is a trademark of Bradley F. Cowan

COPYRIGHT

Copyright @ 1993 by Bradley Frank Cowan

Copyright @ 1998 by Bradley Frank Cowan

All rights reserved. No part of this work covered by the copyright hereon may be reproduced or used in any form or by any means -graphic, or mechanical, including photocopying, taping, or information storage and retrieval systems - without permission of the author.

Any copy of this book issued by the author is sold subject to the condition that it **SHALL NOT BY WAY OF TRADE OR OTHERWISE, BE LENT, RE-SOLD, HIRED OUT, OR OTHERWISE CIRCULATED, WITHOUT THE AUTHOR'S PRIOR CONSENT**, in any form of binding or cover other than that in which it is published, and without a similar condition including this condition being imposed on a subsequent purchaser.

This work is dedicated to my mother, Ruby Charolotte Polhemus Miller, who never compromised the unconditional love she holds for her children. Through her love and willingness to sacrifice even the bare necessities in her life for her children, she provided the respect for life, the self-confidence, and the determination needed to produce and make available to the public this material.

TABLE OF CONTENTS

LIST OF FIGURES	iv
LIST OF TABLES	v
PREFACE	vii
ADDITIONAL SUBJECTS TO STUDY RELATED TO THIS COURSE.....	ix
INTRODUCTION	1
PART I FOUR-DIMENSIONAL PRICE-TIME STRUCTURES	5
LESSON I - PRICE-TIME RADII VECTORS (PTV).....	6
INTRODUCTION	6
DEFINITION OF THE PRICE-TIME RADIUS VECTOR (PTV).....	6
CALCULATION OF THE PTV	7
PTVs ROTATE AROUND A COMMON CENTER	9
PTV ANGLE DEFINES THE EXTENT AND DURATION OF A MOVE	11
PTV AND THE MUSICAL SCALE	12
PTVs CAN EXTEND FOR CENTURIES	13
PTVs CAN OVERLAP AND EXPERIENCE OFFSETS	15
ADVANCED TOPICS	15
CONCLUSION	16
REVIEW QUESTIONS	16
ANSWERS TO REVIEW QUESTIONS	17
LESSON II - THE ELLIPTICAL NATURE OF PRICE-TIME	22
INTRODUCTION	22
CHARACTERISTICS OF THE ELLIPSE.....	23
GRAPHICAL CONSTRUCTION OF THE ELLIPSE.....	23
EXAMPLES OF PRICE-TIME ACTION WITHIN THE ELLIPSE.....	25
ELLIPSE DEFINES ORIGIN AND TERMINUS OF PRICE-TIME CYCLES	27
MAJOR AXES OF MATED ELLIPSES FORM EQUILATERAL TRIANGLES	28
ELLIPSES ARE CONTAINED WITHIN LARGER ELLIPSES	31
LARGE SCALE ELLIPSES	31
ADVANCED TOPICS	33
CONCLUSION.....	33
REVIEW QUESTION.....	34
ANSWER TO REVIEW QUESTION	36
LESSON III - GROWTH PATTERNS	37
INTRODUCTION	37
BACKGROUND REVIEW	38
FIBONACCI	38
GOLDEN SECTION	39
DYNAMIC SYMMETRY	40
FIVE YEAR CYCLE DEFINES THE SMALLEST COMPLETED GROWTH PATTERN.....	40
ADVANCED TOPICS	46
LESSON IV - PRICE-TIME RATIOS MORE IMPORTANT THAN FIBONACCI.....	47
INTRODUCTION	47
A RATIO MUCH MORE IMPORTANT THAN FIBONACCI	47
DJIA EXAMPLES OF THE SQUARE ROOT OF TWO RATIO	51
LONG-TERM STOCK MARKET EXAMPLES OF THE SQUARE ROOT OF TWO RATIO	53
THE MOST IMPORTANT NON-INTEGRAL RATIO IN STOCK MARKET ANALYSIS	54
DJIA EXAMPLES OF THE SQUARE ROOT OF FIVE RATIO	56
LONG-TERM STOCK MARKET EXAMPLES OF SQUARE ROOT OF FIVE RATIO	57
A THIRD RATIO MORE IMPORTANT THAN FIBONNACI.....	58
DJIA EXAMPLES OF PI (3.14) RATIO	59
LONG-TERM STOCK MARKET EXAMPLE OF THE PI RATIO.....	60
A FOURTH RATIO MORE IMPORTANT THAN FIBONNACI.....	61
LONG-TERM STOCK MARKET EXAMPLES OF ROOT THREE RATIO.....	62
SUMMARY	62

LESSON V - GEOMETRIC STRUCTURES.....	64
INTRODUCTION	64
TWO-DIMENSIONAL GEOMETRY	65
DJIA EXAMPLES OF TWO-DIMENSIONAL DIVISION OF THE SQUARE.....	67
ADVANCED TOPICS IN DJIA EXAMPLES OF THE DIVISION OF THE SQUARE	70
TWO-DIMENSIONAL SQUARE STRUCTURES IN THE DJIA (1899-1932).....	70
TWO-DIMENSIONAL SQUARE STRUCTURES IN THE DJIA (1932-1987).....	73
PENTAGONAL (FIVE-FOLD) SYMMETRY OF LIVING ORGANISMS	75
DJIA EXAMPLES OF TWO-DIMENSIONAL PENTAGONAL SYMMETRY	76
SUMMARY OF TWO-DIMENSIONAL STOCK MARKET STRUCTURES.....	76
THREE-DIMENSIONAL GEOMETRY	77
TETRAHEDRON.....	78
TRIGONAL PYRAMID	79
TRIGONAL BIPYRAMID (OCTAHEDRON).....	80
DJIA EXAMPLES OF TETRAHEDRAL STRUCTURES	81
GEOMETRIC STRUCTURES CONTAINED WITHIN CUBES	82
THREE-DIMENSIONAL PERSPECTIVE OF 1966-1982 SQUARE	82
GEOMETRY OF ADJACENT CUBES.....	83
THREE-DIMENSIONAL CUBIC STRUCTURE IN THE DJIA.....	84
SUMMARY OF THREE-DIMENSIONAL STOCK MARKET STRUCTURES	87
FOUR-DIMENSIONAL CUBIC STRUCTURES IN THE DJIA.....	87
CURRENT FOUR-DIMENSIONAL CUBIC STRUCTURE OF THE DJIA.....	90
GEOMETRY OF STACKED CUBES.....	91
SIMILAR PATTERNS FORM ON CORRESPONDING FACES OF CUBES.....	92
CHAOS THEORY AND FRACTALS IN THE STOCK MARKET.....	93
SUMMARY	96
 PART II FOUR-DIMENSIONAL PRICE-TIME CYCLES	 100
INTRODUCTION TO PART II.....	101
LESSON VI - SYMPATHETIC RESONANCE AND THE LAW OF VIBRATION	102
INTRODUCTION	102
SYNCHRONY.....	103
MUSICAL SCALES	103
NODAL POINTS	105
LESSON VII - CYCLES	112
INTRODUCTION	112
BACKGROUND REVIEW	112
DJIA EXAMPLE OF APPLYING CONTEMPORARY CYCLE ANALYSIS.....	113
PROBLEMS WITH CONTEMPORARY CYCLE ANALYSIS	113
PATH OF PRICE-TIME WITHIN ELLIPSE DEFINES THE MOVING AVERAGE	115
WHY PERIODICITY OF CYCLE TOPS AND BOTTOMS VARY	116
ENERGY LEVELS OF CYCLES	119
LESSON VIII - PLANETARY CYCLES.....	122
INTRODUCTION	122
BACKGROUND REVIEW	123
SUBDIVISIONS OF THE 360° PLANETARY CYCLE	125
ANGLES BETWEEN THE PLANETS AND CORRESPONDING MUSICAL TONES.....	126
PLANETARY CYCLES AND THE FOUR-DIMENSIONAL STOCK MARKET.....	127
URANUS SIDEREAL CYCLE AND STOCK MARKET CORRELATION	128
SEVEN YEAR STOCK MARKET CYCLE	128
SATURN-URANUS SYNODIC CYCLE AND STOCK MARKET CORRELATION.....	137
HISTORICAL ANALYSIS OF SATURN-URANUS CYCLE (1896-1929).....	138
HISTORICAL ANALYSIS OF SATURN-URANUS CYCLE (1929-1937).....	140
HISTORICAL ANALYSIS OF SATURN-URANUS CYCLE (1949-1966).....	143
HISTORICAL ANALYSIS OF SATURN-URANUS CYCLE (1966-1982).....	143
HISTORICAL ANALYSIS OF SATURN-URANUS CYCLE (1981-1991).....	145
67-YEAR PERIODICITY AND SATURN-URANUS SYNODIC CYCLE.....	147
45-YEAR PERIODICITY AND SATURN-URANUS SYNODIC CYCLE.....	147
LONG-TERM HARMONICS AND STOCK MARKET TURNING POINTS.....	148
RESOLVING THE MYSTERY OF THE DISAPPEARING 52-MONTH CYCLE.....	148

SATURN SIDEREAL CYCLE AND STOCK MARKET CORRELATION	150
JUPITER-SATURN SYNODIC CYCLE AND STOCK MARKET CORRELATION.....	157
20-MONTH JUPITER-SATURN HARMONIC AND STOCK MARKET CYCLES	158
JUPITER-URANUS CYCLE AND STOCK MARKET CORRELATION	161
MARS SIDEREAL CYCLE AND STOCK MARKET CORRELATION	164
OCTAVES (1/2; 1/4; 1/8) OF MARS CYCLE AND THE STOCK MARKET.....	165
MUSICAL TWELFTH (1/3) OF MARS CYCLE AND THE STOCK MARKET.....	169
MARS TRINES IN DJIA (1/87-6/92) FORM HEBREW "STAR OF DAVID"	173
VENUS SIDEREAL CYCLE AND STOCK MARKET CORRELATION	173
12-WEEK MERCURY CYCLE AND STOCK MARKET CORRELATION	178
DETERMINING THE STRONGEST PLANETARY HARMONICS WITHIN A TIME PERIOD	179
EXAMPLE PROJECTING PRICE-TIME TURNING POINTS USING PLANETARY CYCLES	185
SUMMARY	188
LESSON IX - COMPOSITE CYCLES: PUTTING IT ALL TOGETHER	192
INTRODUCTION	192
CONTEMPORARY METHODS FOR CREATING COMPOSITE WAVES	192
USING TRIANGLE WAVES AS SIMPLE COMPONENTS	193
STOCK MARKET "BEATS"	195
COMPOSITES OF MULTIPLE CYCLES	195
CREATING THE REAL-LIFE COMPOSITE OF THE STOCK MARKET.....	198
CHANGING ORBS OF INFLUENCE.....	203
LESSON X - DIMENSIONAL ASPECTS OF TIME.....	205
INTRODUCTION	205
BACKGROUND REVIEW	205
TIME IS MOTION IN A HIGHER DIMENSION	206
FOUR-DIMENSIONAL PRICE-TIME	208
TIME CONTINUUM	209
APPENDIX A - CRASH OF 1987 ANALYSIS OF RETRACEMENT RATIO.....	210
APPENDIX B - EQUATIONS FOR DETRENDING MONTHLY STOCK MARKET DATA SINCE 1790.....	211
APPENDIX C - W.D. GANN'S ANNUAL FORECASTS	212
APPENDIX D - TWENTY YEAR PRESIDENTAL CYCLE.....	214
APPENDIX E - FORMAT OF DATA AND TABLES USED IN THIS COURSE	216
FORMAT OF STOCK MARKET DATA.....	216
FORMAT OF TABLES USED IN THIS COURSE	216
APPENDIX F - URANUS CYCLE AND THE PERIODICITY OF WAR IN THE UNITED STATES.....	218
APPENDIX G - SQUARE ROOT OF FIVE STOCK MARKET GROWTH SPIRALS	221
STOCK MARKET EXAMPLES OF THE SQUARE ROOT OF FIVE GROWTH SPIRAL.....	222

LIST OF FIGURES

1.1	Definition of the price-time radius vector (PTV)	8
1.2	Decreasing angle between PTV and time axis, showing decreasing price component and increasing time component.....	13
2.1	Characteristics of the ellipse.....	22
2.2.a	Graphical construction of the ellipse using two circles	23
2.2.b	Construction of the ellipse with pencil and string.....	24
2.3	Diagonal triangle formed within the ellipse.....	26
2.4	Equilateral triangles progressively rotated clockwise, showing.....	27
3.1	Side view of conical helix	34
3.2	Golden Spiral.....	35
3.3	Golden Section derived from diagonal of half square	36
3.4	Squares from Chart III.A (DJIA 3/08/1982 - 3/27/1986).....	38
4.1	Diagonal of the square.....	44
4.2	Two concentric circles with radii in the ratio of root two.....	45
4.3	Successive energy levels: (a) with squares and; (b) without squares	46
4.4.a	Diagonal of two squares showing square root of five ratio	51
4.4.b	Fibonacci ratio derived from two adjacent squares	51
4.5	Diameter of circle equals the side length of the enclosing square.....	54
4.6	Both perimeters of the ellipse shown in Figure 3.4 (3/09/1982 - 3/27/1986).....	55
4.7	Diagonal of a cube showing square root of three ratio.....	57
5.1	Two-dimensional geometric growth process defined by root two	61
5.2	Two-dimensional squares containing the PTVs from 1966 to 1982.....	63
5.3	Combined radii vectors EF, FG, EG from Figure 5.2	64
5.4	Two-dimensional square structures in the DJIA from 12/1899 - 7/1932 (See Chart V.B).....	66
5.5	Two-dimensional square structures in the DJIA from 7/1932 - 12/1987.....	69
5.6	Pentagonal form	70
5.7	Three-dimensional view of the PTV decomposition shown in Figure 5.3.....	73
5.8	Central angle of the tetrahedron.....	74
5.9	Composites of tetrahedral structures.....	75
5.10	Tetrahedral structures in daily DJIA (3/1991 - 10/1991)	75
5.11	Two tetrahedra from Figure 5.10 placed together with triangles ABF and EHK as the common faces	76
5.12	Cube centered tetrahedron.....	77
5.13	Cube centered tetrahedron unfolded into two dimensions	77
5.14	Geometry of two adjacent cubes with a common face.....	79
5.15	Two-dimensional representation of the squares that formed in the DJIA between 1914 and 1966.....	82
5.16	Four-dimensional cubic structure of DJIA between 1899 and 1982.....	84
5.17	Four-dimensional cubic structure of DJIA from 2/1966 to the present.....	85
5.18	Two stacked cubes in the DJIA from 1899-present showing the 1966-1982 square as the common face.....	86
5.19	Two-dimensional representation of stacked cubes	90
6.1	Musical intervals and corresponding frequency ratios.	105
6.2	Musical intervals and corresponding major planetary cycles with Saturn-Uranus cycle as fundamental tone.....	106
6.3	Musical intervals and corresponding minor planetary cycles with the Mars cycle as the fundamental tone.....	107
7.1	Difference between the PTV and the moving average.....	112
7.2	Configurations of adjacent equilateral triangles defining variance	113
7.3	Extremes reached by the rotating PTV define the circle and the square.....	115
7.4	Two energy levels of electrons orbiting a nucleus.....	116
7.5	Square defining separation between two successive PTV energy levels	117
8.1	Subdivision of the heavens into twelve 30° divisions.....	123
8.2	Quarter-cycles of Uranus showing dates of squares between 1794-2194 (See Charts VIII.A and VIII.B)	128
8.3	Mars trines synchronized with 15° axes of Jupiter-Uranus cycle in DJIA between 1/1987-6/1992.....	161
8.4	The two Mars trines in the DJIA between 1/23/1987 and 6/5/1992 that are synchronized with the Jupiter-Uranus 15° axes form the Hebrew "Star of David". (See Figure 8.4 and Charts VIII.S and VIII.T).....	163
8.5	Two possible subdivisions of the Saturn-Uranus cycle by the Jupiter-Saturn and Jupiter-Uranus cycles	171
8.6	Two possible harmonic divisions of the Jupiter-Saturn cycle: 15° and 22°30'	174
8.7	Locations of major planetary harmonics and Mars trines between January 11, 1973 and December 12, 1974.....	180
9.1	"Sum of Sin Waves": The traditional method of creating composites	183
9.2	Composite of simple triangle waves	183
9.3	Composite of 52, 20, 14, 2 month triangle waves	185
9.4	Composite of triangle waves from Figure 9.3 with linear trend added.....	186
9.5	Planetary cycles defining simple components of DJIA composite wave 8/1982 to 12/1987 (See Chart IX.A)	191
9.6.a	Composite of individual planetary cycles shown in Figure 9.5.....	192
9.6.b	Linear trend of one point per trading day (1982-1987).....	192
10.1	The three dimensions	194
10.2	Motion of a three-dimensional color wheel through a two-dimensional plane.....	195
10.3	Two-dimensional time chart of three-dimensional rotating color wheel.....	195
10.4	Three-dimensional cube rotating through the perception of a two-dimensional observer.....	196
C.1	W.D. Gann's annual stock market forecast for 1922; and stock market 10 & 20 years earlier (1902 & 1912).	204
D.1	Locations of the seven Jupiter-Saturn conjunctions between 1841 and 1961 defining the triplicity.....	206
F.1	Coincidence of Uranus Squares With American Wars	211
G.1	Square root of five growth spiral	214
G.2	Similar triangles formed by PTVs between 1914 - 1942	216

LIST OF TABLES

1.1	PTV Calculations for Chart I.A; Dow Jones Industrial Average (DJIA) 3/1991-12/1991	9
1.2	PTV Calculations for Vectors Rotating About Point "C" on Chart I.A.	11
1.3	PTV Calculations for Vectors Rotating About Point "I" on Chart I.A.....	11
1.4	PTV Calculations for Vectors on Chart I.B.	14
1.5	PTV Calculations for Vectors on Chart I.C.	14
3.1	PTV Calculations for Chart III.A Showing Completed Five Year Growth Pattern.....	37
4.1	PTV Calculations for Chart IV.A; Ratios in DJIA (2/1966 - 12/1987).....	48
4.2	PTV Calculations for Charts IV.B and IV.C (12/1914 - 2/1966).....	50
4.3	PTV Calculations for Chart IV.D; Square Root of Three Ratios in DJIA (12/1914 - 6/1949).....	58
5.1	PTV Calculations for Figure 5.4 (See Chart V.B).....	66
6.1	Frequency Ratios of Diatonic Major Scale With C As The Fundamental Tone (Key of C)	99
6.2	Heliocentric Sidereal and Synodic Periods of the Planets	100
8.1	Names of the Thirty Degree Divisions of the Heavens	122
8.2	Names of Planetary Angles And Corresponding Musical Tones	123
8.3	21-Year Stock Market Half-Cycle And Ninety Degree Motions of Uranus (Quarter-Cycle) (See Charts VIII.A and VIII.B).....	126
8.4.a	Seven Year Stock Market Cycles And Thirty Degree Heliocentric Motion of Uranus (1806-1914) (See Chart VIII.A).....	130
8.4.b	Seven Year Stock Market Cycles And Thirty Degree Heliocentric Motion of Uranus (1914-1942) (See Charts VIII.C and VIII.D).....	131
8.4.c	Seven Year Stock Market Cycles And Thirty Degree Heliocentric Motion of Uranus (1942-1988) (See Chart VIII.D).....	131
8.5.a	Saturn-Uranus Synodic Divisions of Fifteen Degrees And Corresponding Turning Points in the DJIA (1896-1929) See Chart VIII.E.....	133
8.5.b	Saturn-Uranus Synodic Movements of Thirty Degrees And Corresponding Turning Points in the DJIA (9/1929 - 8/1937) See Chart VIII.F.....	134
8.5.c	Saturn-Uranus Synodic Movements of Fifteen Degrees And Corresponding Turning Points in the DJIA; Showing The 52-Month Cycle Between 1949-1966 (See Chart VIII.G).....	136
8.5.d	Saturn-Uranus Synodic Movements of Fifteen Degrees And Corresponding Turning Points in the DJIA; Showing The 42-Month Cycle Between 1966-1982 (See Chart VIII.H).....	137
8.5.e	Saturn-Uranus Synodic Movements of Fifteen Degrees And Corresponding Turning Points in the DJIA; Between 1981-1991; Showing The 52-Month Cycle (See Chart VIII.I).....	138
8.6	Sixty-Seven Year Stock Market Patterns And 540° Saturn-Uranus Synodic Movements (See Chart V.E).....	139
8.7	Saturn-Uranus Half-Cycle of 22 Years And Corresponding Turning Points in Stock Market (1792-2019)	140
8.8.a	Five Year Stock Market Cycles And Sixty Degree Sidereal Motions of Saturn (1859-1914) (See Charts VIII.K, VIII.L).....	144
8.8.b	Five Year Stock Market Cycles And Sixty Degree Sidereal Motions of Saturn (1914-1987) (See Charts VIII.L, VIII.M, VIII.N)	145
8.9	Saturn Five Year Cycles Within Uranus Quarter-Cycles (Uranus Quarter-Cycles Are Shown in 8.3)	147
8.10.a	Jupiter-Saturn Synodic Movements of Fifteen Degrees And Corresponding Turning Points in the DJIA From 1981 to the Crash of 1987 (See Chart VIII.O).....	150
8.10.b	Jupiter-Saturn Synodic Movements of Fifteen Degrees And Corresponding Turning Points in the DJIA After the Crash of 1987 (See Chart VIII.O)	151
8.11.a	Jupiter-Uranus Synodic Movements of Fifteen Degrees And Corresponding Turning Points in the DJIA (3/1980 - 10/1987) See Chart VIII.P.....	153
8.11.b	Jupiter-Uranus Synodic Movements of Fifteen Degrees And Corresponding Turning Points in the DJIA After Crash of 1987 (See Chart VIII.P)	154
8.12.a	Mars Scorpio Cycle And Corresponding Turning Points in the DJIA (5/1969-11/1991) (See Chart VIII.Q).....	157
8.12.b	Mars Virgo Cycle And Corresponding Turning Points in the DJIA (1/1967-7/1991) (See Chart VIII.Q).....	158
8.12.c	Mars 180° Harmonics And Corresponding Turning Points in the DJIA (10/2/1987 - 6/8/1992) (See Charts VIII.R and VIII.T)	159
8.12.d	Mars 120° Harmonics And Corresponding Turning Points in the DJIA (1/23/1987 - 8/11/1989) (See Figure 8.4.a and Chart VIII.S)	162
8.12.e	Mars 120° Harmonics And Corresponding Turning Points in the DJIA (1/3/1990 - 6/5/1992) (See Figure 8.4.b and Chart VIII.T).....	162
8.13.a	Venus Ninety Degree Motions And Corresponding Eight-Week Cycle in the DJIA (8/1989 - 7/1990) (See Chart VIII.V).....	165
8.13.b	Venus Cycle And Corresponding Turning Points in the DJIA (10/1987 - 3/1991) (See Chart VIII.U).....	167
8.14	Twelve-Week Mercury Cycle And Corresponding Turning Points in the DJIA (12/1987 - 1/1991) (See Chart VIII.W).....	169
G.1	Angles of PTVs in Figure G.2 Relative to the Price and Time Axe	216

ADDITIONAL SUBJECTS TO STUDY RELATING TO THIS COURSE

W.D. Gann's "Master Course for Stocks" And "Master Course for Commodities"

These courses are actually a series of courses offered by W.D. Gann from 1935 to 1955. To the novice they appear nebulous. However, with this course many of the things about which Mr. Gann wrote will become clear.

Contemporary Methods of Cycle Analysis

Although these techniques are primitive, they provide a basic foundation upon which to build. The work by the Foundation for the Study of Cycles is a good starting point.

Radii Vectors

Review what radii vectors are and how to derive them.

Musical Scales

Study how the "Diatonic Major" scale is constructed; including the frequency relationships between successive tones in the musical scale as well as to the fundamental tone.

The same simple mathematical ratios found in sounds that are pleasing to the human ear are also present in another reflection of human activity, financial markets.

Patterns in Nature

Naturally occurring phenomena unfold in a limited number of recurring patterns. These patterns differ between living organisms and inanimate, statically symmetrical, objects.

Fibonacci Number Series

Although the terminal points of stock market growth patterns are defined by a root five geometric relationship, it is helpful to understand Fibonacci to gain a basic understanding of the internals of this growth process.

WWW.FOREX-WAREZ.COM
ANDREYBBRY@GMAIL.COM SKYPE: ANDREYBBRY

Dynamic Symmetry

Financial markets act like bodies in motion, demonstrating dynamic symmetry.

Sympathetic Resonance

Study how two systems in unison resonate when one is set into vibration. This is the physical law upon which the radio is based.

Characteristics of Revolving Bodies

Specifically, study elliptical motion. George Bayer and W.D. Gann used ellipses to define the containment perimeter of price-time action. What was never revealed by either of these analysts are the geometric structures formed by the major axes of these ellipses.

Contemplative Geometry

Sometimes called "Sacred Geometry" this applies geometry to life much the way as did the ancient Greeks.

Vibration

Everything exists in a state of vibration. In 1921, a physicist named Louis de Broglie postulated "Wave-Particle Duality", which simply states that matter and vibration are indistinguishable. An equation was developed giving a wavelength to particles. While it is not necessary to master the physics behind this postulate, it is helpful to know the importance of wave mechanics.

Crystallography

Understanding the general theory of the crystal lattice structure of matter is helpful for learning the geometry of a financial market.

Basic Astronomy

PREFACE

The 1998 edition differs from the 1993 in that references were added and a few typographical errors were corrected. The reader will notice two reference types, “Technical References” are typically those of college or graduate level science or engineering. “References” require no technical background. A reference list is provided in the back.

Previous researchers of financial markets have uncovered pieces of the puzzle behind the nature of financial market activity. However, either they did not put all these pieces together, or they chose to not present their knowledge to the public. Because these researchers made contributions which must be acknowledged,

**IT IS THE AUTHOR'S INTENTION THROUGHOUT THIS COURSE
TO GIVE CREDIT FOR ANY MATERIAL THAT HAS BEEN
PREVIOUSLY PRESENTED BY ANOTHER AUTHOR.**

Two books are provided with this course. The first book contains written text describing charts, contained in the second book. Two books allow the reader to have the charts and the descriptions in front of him at the same time without flipping forward and backward in the book looking for charts.

It is necessary for the reader to keep the chart under study in front of him. Without referencing the charts the written text will make little sense.

Even though the concepts presented in this course are not difficult, they will not be entirely understood with a single reading. It is such a new approach to market analysis that it takes a little practice to adjust thinking in such a way to fully comprehend what is presented. It is recommended the reader pass over information he initially finds confusing. When rereading the course many things will be seen that were missed the first or second time through.

INTRODUCTION

Financial markets provide a unique laboratory to study the free expression of human nature with the opportunity to see man pressed to his extreme emotions of hope, fear, and greed. These extreme emotional swings have been recorded for centuries in the form of price-time charts.

As man, in mass, is dominated by the feeling of hope, he competes with other men, bidding prices higher and higher until the dominant emotional mood swings to fear, which leads to financial market panics.

This course shows how these dominant emotional swings can be forecast well into the future and, ultimately, provides illumination into their nature and cause. These swings are present throughout all human activity, but are uniquely expressed and recorded in financial markets.

THERE ARE NO RANDOM MOTIONS IN FINANCIAL MARKETS. All ups and downs, twists and turns, booms and crashes follow clear, easy to understand, natural laws, which can be represented and modeled with applications of basic science.

Libraries around the country are filled with books on financial market analysis, which basically cover the same worn out subjects. They can all be placed into one of three categories:

- (1) Fundamental analysis
- (2) Technical analysis
- (3) Cycle analysis

And within the category of technical analysis either they use momentum indicators, relative strength indexes (RSI), pattern recognition, Elliott Waves, trend lines, stochastics, or some other subject that has been beaten to death over the years by hundreds of authors and analysts. All these techniques and many more have been thoroughly studied by the author and found to have limited value. And few provide any insight into what is truly happening in financial market activity.

The author's intention in producing this course is to provide unique material to students of mass human behavior who find the currently available material on this subject not only lacking dependability and applicability, but also without insight into its true driving forces. The goal has been to produce an original source of financial market analysis, and provide it at a price affordable to anyone genuinely interested in the motivating forces behind human behavior.

This course is the result of over ten years of full time research into financial market timing and many thousands of dollars devoted to researching the subject material presented. In addition, over a year was spent by the author compiling the data and writing

this course. The material presented here is **UNIQUE, POWERFUL, AND IS NOT AVAILABLE FROM ANY OTHER SOURCE**. Not only are many valuable timing techniques presented, but also insight into the driving forces behind financial market price-time changes. No one will be able to read this course and say, "I knew all that".

This is not a "get rich quick" scheme. Truly understanding financial markets requires study and hard work. No one becomes an expert on any subject, including financial markets, without putting in the required effort. The reader's advantage as a student of this material is that much of the work has been done for him. For every path researched that produced results, at least one hundred dead ends were explored. Remember, most things that relate to an understanding of nature are simple to understand when presented, but can be very difficult to discover. Einstein's theory of relativity, $E=MC^2$, is a simple equation, but could you have derived it?

Contrary to claims of many market analysts who charge exorbitant sums for such things as simple pattern recognition gimmicks, and claim to hold the "secret of the universe", mastering the subject of financial market analysis requires hard work. However, the analyst who spends the time to study this course will broaden his base of knowledge well beyond what he currently knows, regardless of his current level of expertise. For those who do not want to put in the work, possibly they would be better off chasing one of those "secret of the universe" gimmicks, or maybe buying lottery tickets.

The works of the great masters throughout time have been researched. While many of these analysts had great discoveries, for the most part it appears the general rule has been to keep these discoveries secret and hidden from the public.

There is no mystery to the author's techniques. They are based on simple application of science and proven natural law. The author does not dance around a subject with unclear and hidden messages. All material is supported with extensive and direct examples in financial market charts.

The reader may have noticed that the market forecasters with the most respectable records rarely come from academia. Rather, their backgrounds often hold a common thread of the arts. Musicians, especially, seem to have a predisposition for accurate market timing. The reason for this will become apparent, as the lessons of this course unfold. People with a special affinity for music are in harmony with the natural laws governing proportion and ratios, as experienced through sound. These same laws govern financial market activity as movements divide and subdivide into the same ratios present in the "Just Diatonic" musical scale. In more ways than one, these market analysts are "playing the market".

Similarly, artists are talented with a special understanding of proportion and symmetry experienced through vision. These laws manifest in financial markets as they

progress through their natural growth patterns, which demonstrate the same dynamic symmetry the artist employs when he expresses his talent.

Initially, it may not be clear how some of the material presented in this course relates to financial markets. However, be aware that the author has focused his efforts on providing only necessary material, while always keeping in mind the words of William Shakespeare, "Brevity is the soul of wit".

Those topics that may seem irrelevant are in reality intimately tied to the ultimate goal of understanding mass human behavior as reflected in financial markets. They are presented to the reader as physical proof of the omnipresence of natural law. Physical laws that govern the universe, ranging from bodies in motion to the growth of living organisms, are also present in the price-time action of financial markets. Albert Einstein said, "The only randomness is the natural law which we do not yet understand". The proof of this is to follow.

This course is presented in two parts. The first five lessons define Part One and the last five lessons compose Part Two.

Part One introduces the new concept of multi-dimensional analysis to financial markets. The tools for viewing markets in more than the traditional two dimensions of price and time are developed. After these tools are mastered, they are used to identify the true geometric structures and ratios, which lie at the heart of financial market activity. The completed geometric solid that formed between 1899 and 1982 is closely analyzed.

Part Two presents a unique method of analyzing financial market cycles. This is not the traditional cycle analysis currently practiced by many analysts. Rather, the application of a scientific phenomenon known as sympathetic resonance is used to isolate cyclical influences in financial markets, focusing on those in the Dow Jones Industrial Averages (DJIA).

The ten lessons are organized as follows:

Lesson I introduces a new way of looking at financial markets by presenting the "Price-Time Radius Vector". This vector allows the analyst to work with price and time as a single unified element. By looking at price-time as a unified element, various spatial relationships become evident.

Lesson II uses the vectors studied in Lesson I to define axes of ellipses that contain financial market action.

Lesson III takes the reader through the natural growth process of financial markets. Many analysts have studied Growth patterns in the past, but none have understood the true spatial and multi-dimensional relationships necessary to master this topic.

Lesson IV identifies ratios in price-time much more valuable as timing tools than the celebrated Fibonacci ratio (1.62). These ratios are visible when a multi-dimensional perspective is applied.

Lesson V puts together the material presented in previous lessons, and identifies the geometry of the four-dimensional structures hidden in the two-dimensional price-time charts of the stock market.

Lesson VI presents the scientific concept of sympathetic resonance and identifies several examples in nature.

Lesson VII describes what a real cycle is, how varying energy levels define the duration of these cycles, and explains the age-old problem of varying periodicity of cycle tops and bottoms.

Lesson VIII shows the correlation between motions of planets and cycles in the Dow Jones Industrial Average.

Lesson IX shows how to add together all the individual influences in the stock market to arrive at the true composite effect.

Lesson X describes how the multi-dimensional perspective of financial markets affects the time element of two-dimensional price-time charts. Traditionally, financial market analysts have incorrectly represented time as a single dimension along the horizontal axis of the price-time chart. This lesson will show what is truly happening in the dimension called time.

PART ONE

FOUR-DIMENSIONAL

PRICE-TIME STRUCTURES

LESSON I

PRICE-TIME RADII VECTORS (PTV)

*"Gott wurfelt nicht"
God does not play dice*

Albert Einstein

INTRODUCTION

A variety of techniques attempt to forecast prices in financial markets. However, relatively few deal with the most important element in financial market timing, i.e., time. Traditional cycle analysis is the most commonly used of these techniques, but even the so-called experts on this subject acknowledge the great limitations of their approach. Cycles (or more correctly, rhythms) tend to suddenly disappear, only to reappear at a later date with phase shifts from their original pattern. Contemporary cycle analysts cannot explain why cycles "disappear", why they reappear with a phase shift, and a variety of other characteristics that will be explained in this course.

DEFINITION OF THE PRICE-TIME RADIUS VECTOR (PTV)¹

To begin the analysis of the dimension of time it must be understood that financial market movements are defined within the limits of radii vectors. These vectors allow analysts to expand their thinking beyond one dimension at a time, i.e., only price levels or only time values, and to **START VIEWING PRICE-TIME AS A SINGLE UNIFIED ELEMENT**. For, as will be shown in this course, **PRICE AND TIME ARE INTIMATELY CONNECTED**.

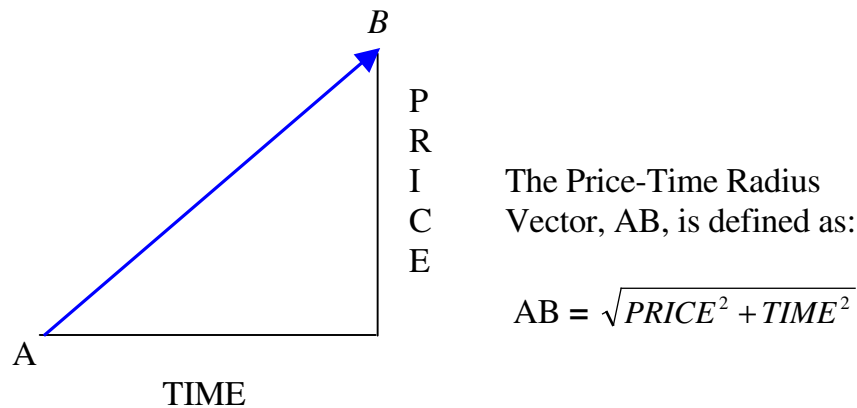
On a traditional price-time chart of any financial market, the price-time radius vector is defined as shown in Figure 1.1. For the sake of brevity, the price-time radius vector will, hereafter, be referred to as **PTV**.

This is an application of the Pythagorean theorem taught in high school geometry classes, which states that the sum of the squares of the sides of a right triangle is equal to the square of the hypotenuse. In this case, the sides of the right triangle are time and price, and the hypotenuse is the PTV.²

¹ Please note that "PTV" and "Price-Time Vector" are registered trademarks.

² The concept of applying the Pythagorean Theorem to price and time simultaneously was discovered by the author.

For those without a scientific background, a radius vector simply measures the distance and direction from one point in space to another point in space. On price-time charts of financial markets, a point in space is a specific price at a specific time. For example, if stock XYZ traded at 33 on January 14th, that would be a point in space on a price-time chart.

**Figure 1.1**

Definition of the Price-Time Radius Vector (PTV)

THE PTV HAS CONSTANT LENGTH AND DEFINES THE INTERVAL OF OPERATION WITHIN SPECIFIED MARKET CONDITIONS.

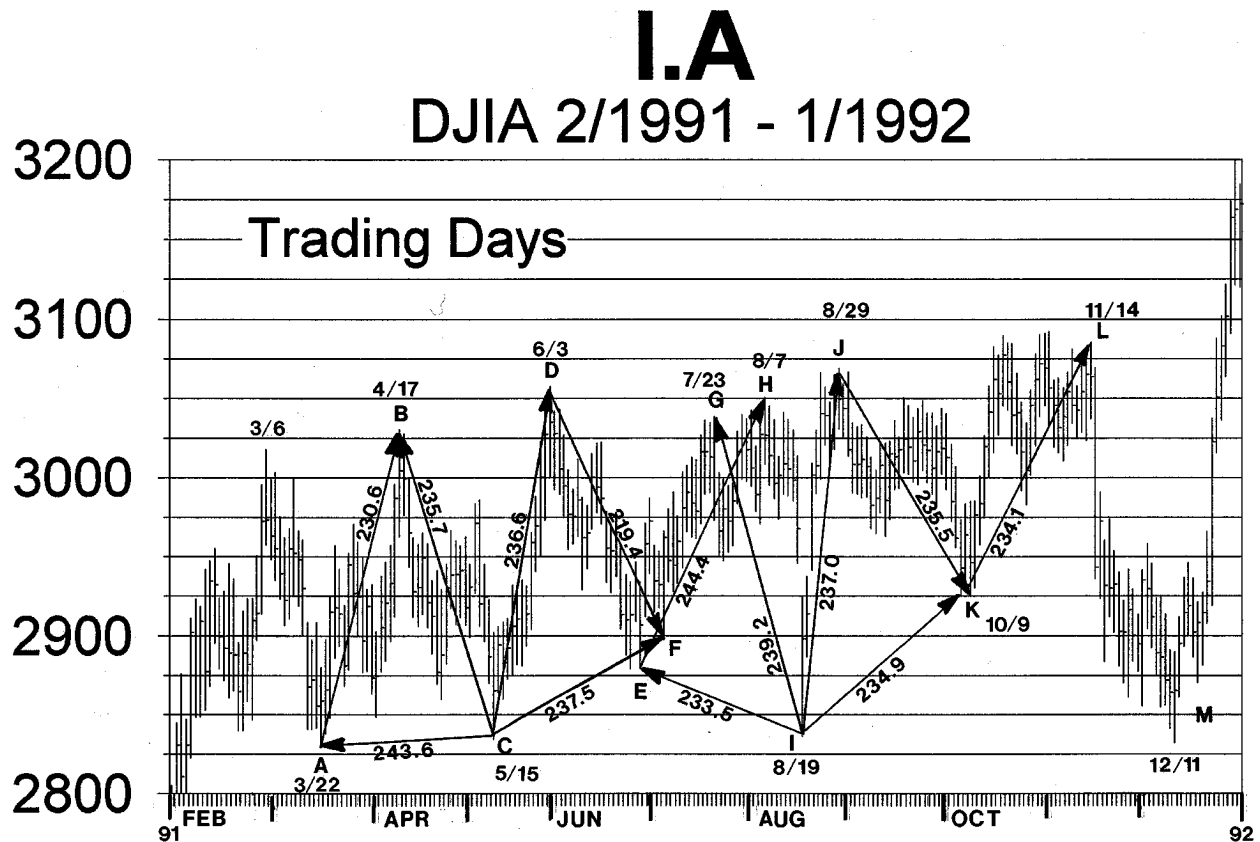
CALCULATION OF THE PTV

Chart I.A is used to demonstrate how the PTV is calculated. On this price-time chart the time distance between the two points labeled B and C was 131 trading hours.³ The price change between these same two points was 195.9 points. Therefore, using the equation from Figure 1.1, the PTV, BC, is calculated to be the square root of $(131^2 + 195.9^2)$, which equals 235.7. This technique is repeated for each of the PTVs shown on Chart I.A, and the results are contained in Table 1.1.

Tables similar to Table 1.1 will be used throughout Part I of this course. They contain the data used to calculate all PTVs. It is highly recommended the reader reference Appendix E at this point to avoid any possible confusion about how the data used in this course is collected or calculated. If the reader is not interested in verifying the data used to calculate the PTVs, then the only necessary part of these tables is the last column, which contains the final values of the PTVs. For example, in Table 1.1 the first row of data shows the PTV, AB, to equal 230.6.

When the PTV values from column eight of Table 1.1 are studied, one of the first things noticed is that they are all approximately the same length. The only deviation occurred at the bottom labeled F (radius vector DF = 219.4), which was caused by the overlapping radius vector EH. On Chart I.A note that F lies on the line connecting E and H.

³ Twenty trading days times 6.5 hours/day, plus one extra hour from 2pm to 3pm, equals 131 trading hours.



One reason why market analysts have failed to notice that all these market movements were equal in length is that the scales of the price and time axes must be just right in order for this phenomenon to be immediately visible on a price-time chart. Specifically, the price axis must reflect one unit of price for each unit of time.⁴ As the scales deviate from this one-to-one relationship the appearance of the vectors will be more and more distorted from their actual size. To make this clearer, refer again to Chart I.A. Notice that radius vector CD appears to be longer than radius vector CF. However, calculations have proven they are equal in length. The distortion is caused because Chart I.A is not "squared out". If the time scale of this chart was stretched out these vectors would appear to be closer in length. Regardless of the scales used for the two axes on a chart, by employing the technique described above the actual length of the radius vector is determined, and the graphical approach is unnecessary.

⁴ This is what W.D. Gann referred to when he spoke of "squaring your charts". This is a very important concept that allows a graphical approach to price-time geometry. The subject of squaring of charts is covered in depth in W.D. Gann's, *Master Course For Stocks*.

Table 1.1
PTV Calculations for Chart I.A
Dow Jones Industrial Average (DJIA) 3/1991-12/1991

Price-Time Radius Vector	Date & Time of High	PTV Price High	Date & Time of Low	PTV Price Low	Time Change (hours)	Price Change (points)	Vector Value (PTV)
AB	4/17 2PM	3030.5	3/22 12PM	2829.2	112.5	201.3	230.6
BC	4/17 2PM	3030.5	5/15 3PM	2834.5	131	195.9	235.7
CD	6/03 4PM	3057.5	5/15 3PM	2834.5	79.0	223.0	236.6
DF	6/03 4PM	3057.5	7/08 10AM	2897.4	150	160.1	219.4
EH	8/07 12PM	3050.5	6/28 1PM	2879.3	174.5	171.2	244.4
GI	7/23 10AM	3038.2	8/19 3PM	2836.3	128.5	201.9	239.2
IJ	8/29 10AM	3068.6	8/19 3PM	2836.3	47.0	232.3	237.0
JK	8/29 10AM	3068.6	10/9 3PM	2925.5	187	143.11	235.5
KL	11/14 11AM	3085.0	10/8 1PM	2927.8	173.5	157.2	234.1

PTVs ROTATE AROUND A COMMON CENTER

On Chart I.A the points "C" and "I" hold special significance. These two points represent the center points about which these two radii vectors rotate in a clockwise direction. The "C" radius vector starts with CA, sweeps through CB, over to CD, and finally terminates with CF. The "I" radius vector starts with IE, sweeps through IG, over to IJ, and finally terminates with IK.

An interesting concept is that these two rotating radii vectors have their beginning points defined before their center points have been reached in time. For example, at point A the radius vector swinging from A to B is already moving within the limits of the radius vector centered at point C, **EVEN THOUGH POINT C HAD YET TO OCCUR IN TIME.**

The following radii vectors are equal length:⁵

$$\begin{aligned} CA &= 243.6 \\ CB &= 235.7 \\ CD &= 236.6 \\ CF &= 237.5 \end{aligned}$$

The values used for the calculation of these radii vectors are contained within Table 1.2. Similarly, Table 1.3 shows that the radii vectors rotating around point "I" have equal lengths:

$$\begin{aligned} IE &= 233.5 \\ IG &= 239.3 \\ IJ &= 237.0 \\ IK &= 234.9 \end{aligned}$$

Table 1.2
PTV Calculations for Vectors
Rotating About Point "C" on Chart I.A.

Price-Time Radius Vector	Date & Time of High	PTV Price High	Date & Time of Low	PTV Price Low	Time Change (hours)	Price Change (points)	Vector Value (PTV)
CA	5/15 3PM	2834.5	3/22 12PM	2829.2	243.5	5.3	243.6
CB	4/17 2PM	3030.5	5/15 3PM	2834.5	131.0	195.9	235.7
CD	6/03 4PM	3057.5	5/15 3PM	2834.5	79.0	223	236.6
CF	7/08 10AM	2897.4	5/15 3PM	2834.5	229.0	62.9	237.5

The reason why radius vector DF was shorter than the other vectors is now apparent. The sequence of radii vectors rotating around point C terminated with radius vector CF. However, the radii vectors rotating around point I began with radius vector IE. This means the two cycles overlapped by the amount EF, causing the terminal point of DF to be "pulled up" by the radius vector rotating around point I.

⁵ These values are equal within the resolution of the intraday data used for their calculation. The non-homogeneous nature of the DJIA index also negatively affects these results.

Table 1.3
PTV Calculations for Vectors
Rotating About Point "I" on Chart I.A.

Price-Time Radius Vector	Date & Time of High	PTV Price High	Date & Time of Low	PTV Price Low	Time Change (hours)	Price Change (points)	Vector Value (PTV)
IE	6/28 1PM	2879.3	8/19 3PM	2836.3	229.5	43	233.5
IG	7/23 10AM	3038.2	8/19 3PM	2836.3	128.5	201.9	239.3
IJ	8/29 10AM	3068.7	8/19 3PM	2836.3	47.0	232.34	237.0
IK	10/07 11AM	2926.2	8/19 3PM	2836.3	217.0	89.9	234.9

THE PTV ANGLE DEFINES THE EXTENT AND DURATION OF A MOVE

Since the length of the PTV is constant, it follows that as the time component decreases the price component increases, and vice-versa.

By knowing the length of the radius vector the analyst is able to project the magnitude and **DURATION** of a move. If a fast advance is under way he knows it will not last very long. Similarly, a slowly advancing market will show little price gain because the length of the radius vector will be consumed by the component of time, leaving little for price.

In Figure 1.2 the PTVs OA, OB, and OC are all equal length. OA advanced very quickly to its maximum length, i.e., T_1 is a very short time interval; consequently, the price component of OA, P_1 , is very large.

As the angle between the PTV and the time axis decreases, the time component increases and the price component decreases. That is, the time component of OB, T_2 , is longer than the time component of OA, T_1 . And the price component of OB, P_2 , is less than the price component of OA, P_1 .

Similarly, as the angle becomes even flatter with the time axis, as with OC, the time component, T_3 , becomes greater than that of either OA or OB. And the price component of OC becomes less than that of either OA or OB.

A real-life example of a PTV similar to OA is shown on Chart I.A between points C and D. The time component of CD was short, only 79 hours. Hence, its price component must be long in order to maintain a constant length radius vector. In fact, the price component of CD was 223 points, which approaches the maximum amount for a PTV at this energy level.

An example of a PTV similar to OB is shown on Chart I.A, between points E and H. Between those two points the time component was 174.5 hours. Hence, the price component must be shorter than it was in CD to maintain the constant length radius vector. In fact, the price component was 171.2 points.

PTV AND THE MUSICAL SCALE

The frequency of notes on the musical scale are defined by ratios of simple integers relative to the fundamental tone (such as the octave=2:1, the fifth=3:2, the fourth=4:3, etc).⁶ Similarly, lengths of PTVs are defined by the same ratios as found on the musical scale.

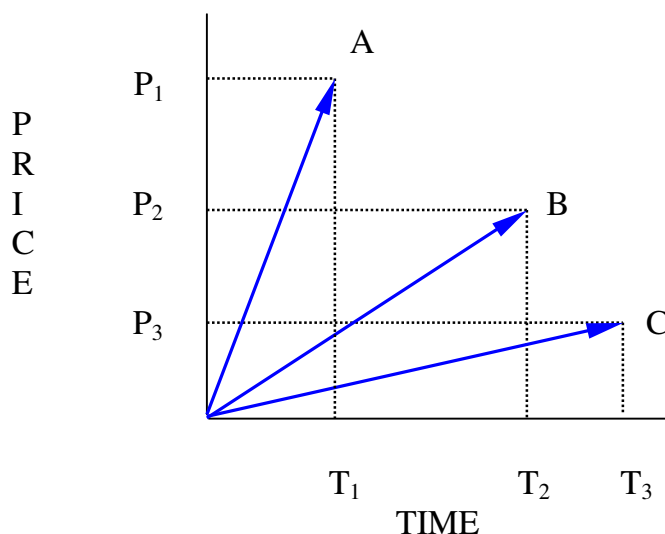


Figure 1.2

Decreasing angle between PTV and the time axis, showing decreasing price component and increasing time component

For example, Chart I.B (Table 1.4) is a continuation of Chart I.A. On Chart I.B, between points M and N, the time distance was 185 hours and the price component was 443.2 points. Using the technique described above, the PTV between points M and N (hereafter, referred to as MN) is calculated to be 480.3, which is two times (the octave) the amount calculated for the radii vectors on Chart I.A. The octave above PTV, MN, can be seen on Chart I.B, between points M and O (hereafter, referred to as MO) where the time component was 773 hours and the price component was 552.5 points. Hence, the PTV, MO, is calculated to be 950.2, which is twice (the octave) the length of MN and four times (the double octave) the radii vectors shown on Chart I.A.

⁶ More on the "Diatonic Major" musical scale is included in Lesson VI, **SYMPATHETIC RESONANCE AND THE LAW OF VIBRATION**. This was one of the items included as a subject to study relating to this course.

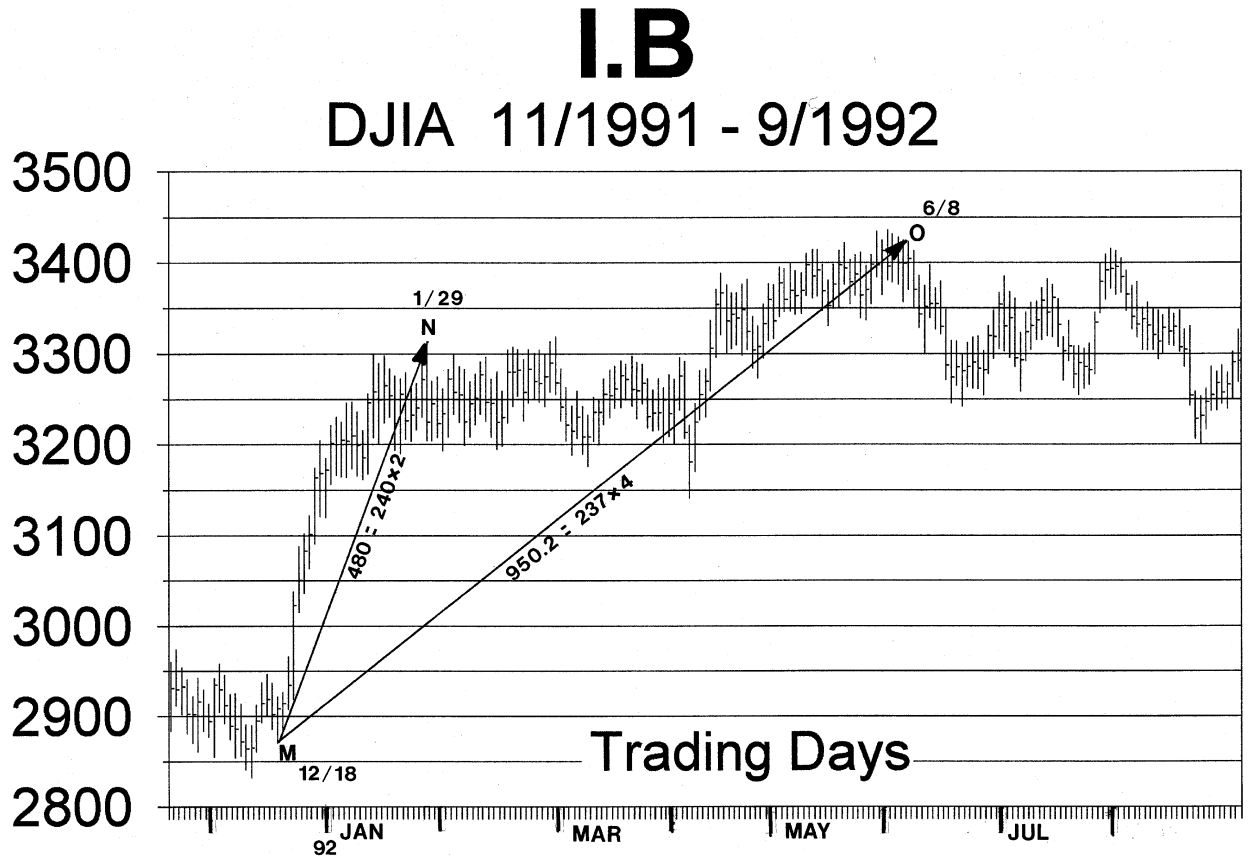


Table 1.4
PTV Calculations for
Vectors on Chart I.B.

Price-Time Radius Vector	Date & Time of High	PTV Price High	Date & Time of Low	PTV Price Low	Time Change (hours)	Price Change (points)	Vector Value (PTV)
MN	1/29 1PM	3313.5	12/18 10AM	2870.3	185	443.2	480.3
MO	6/08 4PM	3422.8	12/18 10AM	2870.3	773	552.5	950.2 = MNx2

PTVs CAN EXTEND FOR CENTURIES

Application of the PTV is not limited to daily charts. In fact, there is no limit to how large (or small) a PTV can be. For example, Chart I.C is a chart of the stock market from 1929 to 1966, where the PTV, AE, is calculated using weekly data to be 1997 price-time units in length. The values used for this calculation are shown in Table 1.5. This PTV will be used in later lessons to show the geometric structure during this time period.

I.C

PTVs ON MONTHLY SCALE

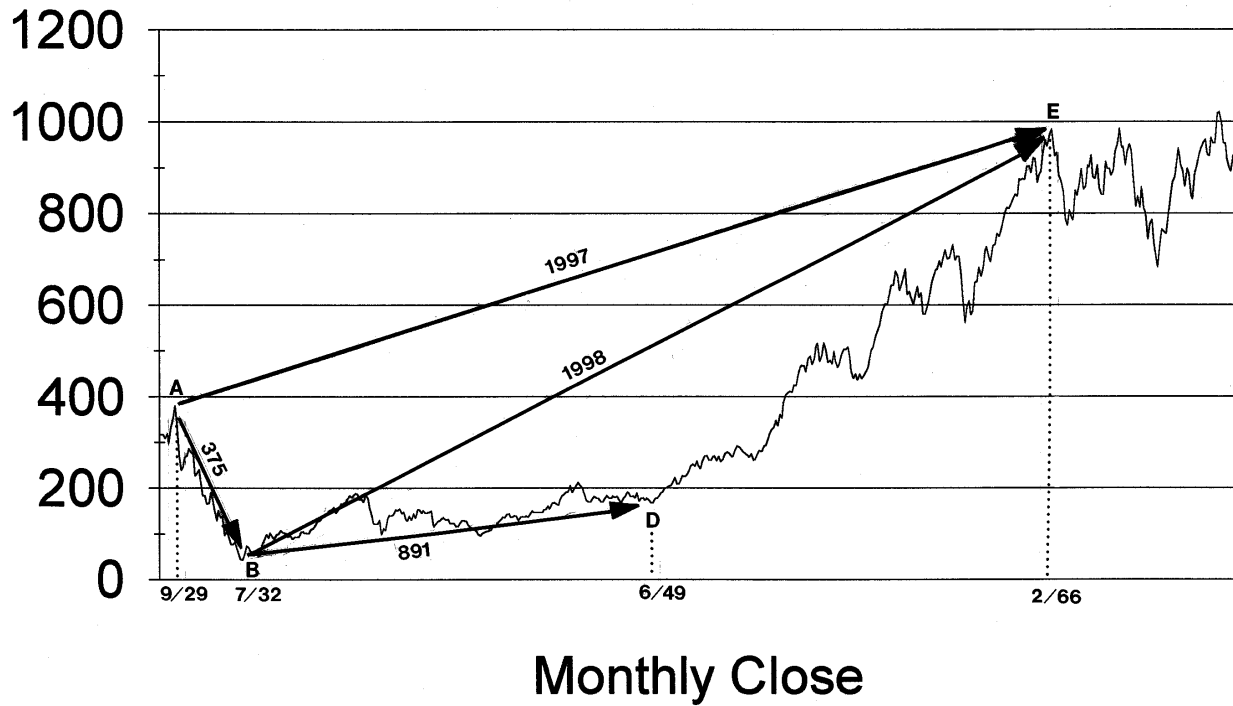


Table 1.5
PTV Calculations for
Vectors on Chart I.C.

Price-Time Radius Vector	Date & Time of High	PTV Price High	Date & Time of Low	PTV Price Low	Time Change	Price Change (points)	Vector Value (PTV)
AE	2/09 1966	1001	9/3 1929	386	1900 Weeks	615	1997
AB	9/3 1929	386.1	7/8 1932	41	148 Weeks	345	375

PTVs CAN OVERLAP AND EXPERIENCE OFFSETS

The origin or terminus of a PTV does not necessarily coincide with the origin or terminus of another PTV. In other words, PTVs can overlap and they can experience offsets.

An example of overlapping PTVs can be seen on Chart I.A where the PTV defining the top at point H originated at point E. However, the PTVs preceding EH terminated at point F. Hence, they overlapped by the amount EF. Similarly, the terminus of EH overlapped the terminus of IG.

Vertical offsets typically occur with "gaps". Chart I.D is used in the "Review Questions" section of this lesson. On this chart the origin of the PTV terminating on 3/6/1991 is shown to be the bottom on 1/23/1991, which occurred after the gap on 1/17/1991. The concept of vertical offsets is expanded in Lesson VII, **CYCLES**.

The possibility that PTVs can overlap and experience offsets complicates the analysis. However, with practice and experience the precise beginning point of a PTV can be determined, even if it lies within the field of a previous radius vector. This subject is covered in greater detail later in this course.

ADVANCED TOPICS

This section is added for those who feel comfortable with an explanation that appears to be more advanced than that encountered in the previous analysis.

On Chart I.A since the radii vectors CA, AB, and BC are all equal length, they form three legs of an equilateral triangle.⁷ In addition, the radii vectors CF, CD, and DF form three legs of another equilateral triangle. These two triangles are contained within the semi-cycle, ABDF. Similarly, the remaining semi-cycle, EHJK, contains two equilateral triangles. The significance of this will be left as an exercise for the reader. But, as a hint, try to find how many equilateral triangles fit into a circle with each leg equal to the radius of the circle. This creates a geometric figure.

Students of relativity are familiar with the concept of "curvilinear time", as popularized by Albert Einstein. Traditional charts of financial markets provide an oversimplified two-dimensional representation of what is actually a multi-dimensional phenomenon. Price-time charts simply reflect a "shadow" of this multi-dimensional action. Time is not a linear dimension and hence, cannot be accurately represented by a straight one-dimensional axis across the bottom of a chart.⁸ When price-time is forced onto a two-dimensional chart, the resultant appearance is that of price-time twisting and turning into and out of the page of observation. The PTV, as described above, allows the analyst to better represent and predict this complicated motion.

⁷ An equilateral triangle has all three legs equal and the three inner angles equal to 60° .

⁸ Technical Reference: *Modern Physics*, P. 20 – 21.

Spend a few moments thinking about the time concepts presented in this lesson. As mentioned earlier and repeated here, Chart I.A showed that the price-time action was contained within the radius vector originating at point C. When the market was at point A and moving to point B it was under the influence of a radius vector whose origin at point C had yet to occur in time.

CONCLUSION

It is important the material presented in this lesson is mastered because the following lessons rely heavily on the PTV.

At this point in the course the reader should be able to:

1. Determine the PTV between any two points on a price-time chart.
2. Project a price value from any top or bottom given the expected number of days from that top or bottom.
3. Project when a top or bottom will occur given the dominant resistance or support level.

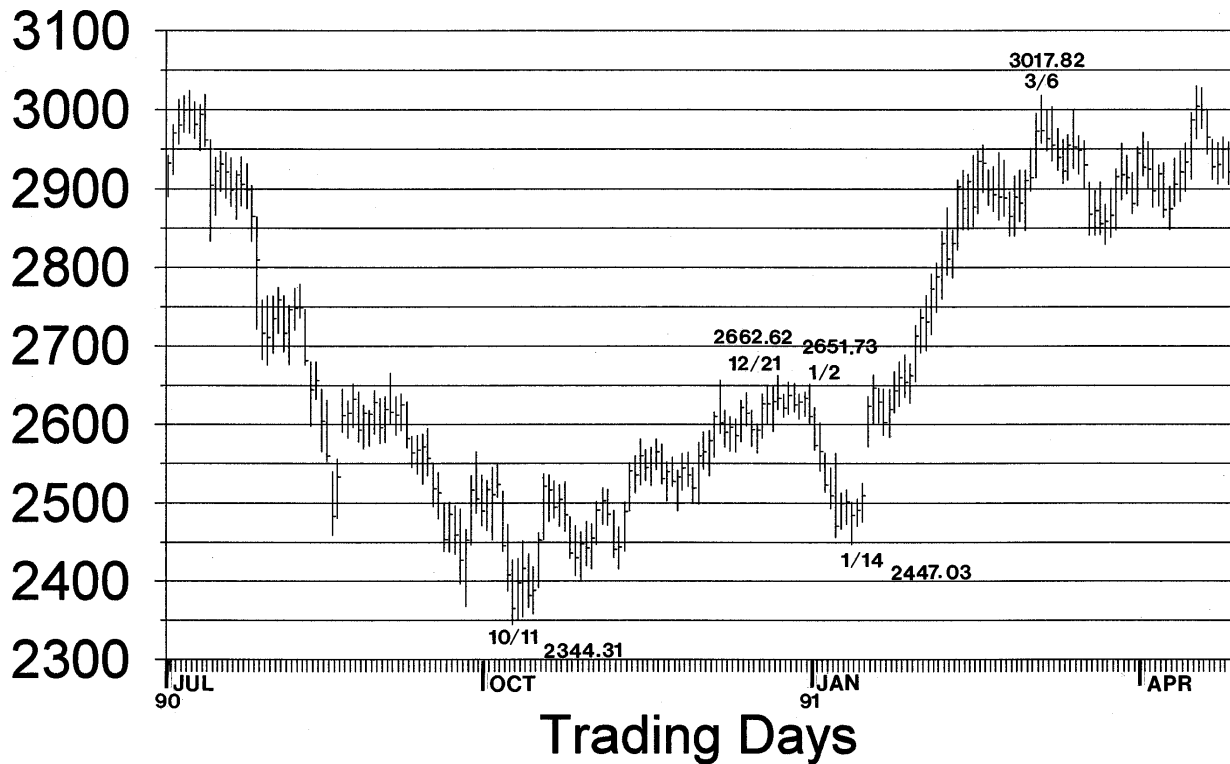
REVIEW QUESTIONS

The following questions refer to Chart I.D

1. On 10/11/1990 at 2 pm the DJIA bottomed at 2344.31, intraday. Fifty-six days later, on 1/2/91 at 10 am, the DJIA reached its top at 2651.73. What is the PTV from this low to high?
2. On 1/14/91 the DJIA bottomed at 2447.03 at 3 pm. What is the PTV from the top of 2662.62, on 12/21/90 at 3pm, to the low on 1/14/91?
3. On 1/23/91 at 11 am the DJIA bottomed at 2584.65. Your cycle analysis has advanced to the stage where you expect a significant advance that will top out 29 days later, on 3/6/91. What value will you expect for the DJIA at that time?
4. On 10/11/90 at 2 pm the DJIA bottomed at 2344.31. Your understanding of resistance levels has advanced to the stage where you can project the DJIA to advance to a value of 3020. What day will this top occur?
5. In 1908 W.D. Gann amazed reporters and traders by stating "Union Pacific will not trade at 169 before it has a good break". At the time of this statement Union Pacific was trading at 168 1/8. Union Pacific did not reach 169. Gann said his ability to make such a statement was based on the "Law of Vibration". Based on the PTV, how could such a statement be made?

I.D

DJIA 7/1990 - 4/1991



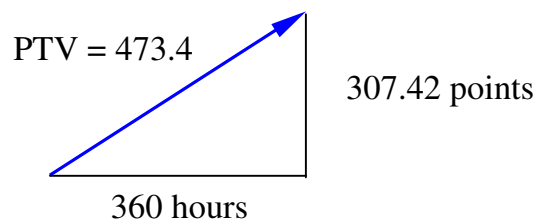
ANSWERS TO REVIEW QUESTIONS

1. Step (1) The price change is:
 $2651.73 - 2344.31 = 307.42$ points.

- Step (2) The time change is:
 $56 \text{ days} \times 6.5 \text{ hours/day} = 364 \text{ hours}$

The four hours from 10am to 2pm are subtracted from this value, to arrive at the final time difference of 360 hours.

- Step (3) These values define the PTV as below:



$$PTV = \sqrt{307.42^2 + 360^2} = 473.4$$

The value of this PTV is twice that measured earlier in this lesson. That is,

$$473.4 = 236.6 \times 2.$$

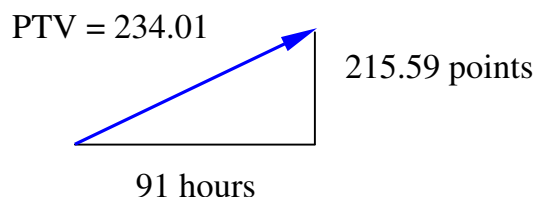
It is also equal to the value calculated in Table 1.4 for MN.

2. Step (1) The price change is:
 $2662.62 - 2447.03 = 215.59$ points.

- Step (2) The time change is $14 \text{ days} \times \frac{6.5 \text{ hours}}{\text{day}} = 91$ hours.

Since, the high and low occurred at the same time of day (3 pm), there are no additional hours to add or subtract.

- Step (3) These values define the PTV as below:



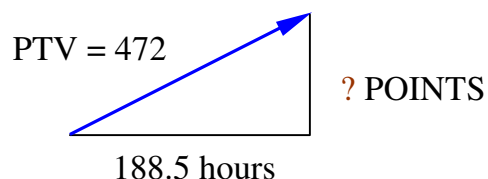
$$PTV = \sqrt{215.59^2 + 91^2} = 234.01$$

3. Step (1) The time value is $29 \text{ days} \times 6.5 \text{ hours/day} = 188.5$ hours.

- Step (2) Since a significant advance is expected, the PTV value will be the octave of the base value of 236. Or,

$$2 \times 236 = 472.$$

- Step (3) The above values for the PTV and time, define the points component, as below:



The PTV formula is applied, in reverse, to find the number of points, given the PTV value and time value. That is,

$$PTV = 472 = \sqrt{188.5^2 + POINTS^2}$$

Or, solving this equation for *POINTS*:

$$POINTS = \sqrt{472^2 - 188.5^2} = 432.73$$

Adding this to the low of 2584.65, projects the top to be:

$$2584.65 + 432.73 = 3017.38.$$

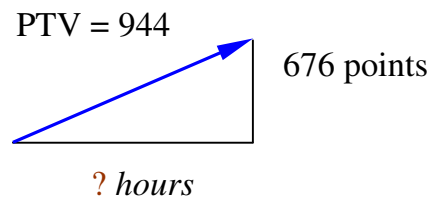
THE ACTUAL HIGH ON 3/6/91 WAS 3017.82, A DIFFERENCE OF ONLY 0.44 POINTS, OR 0.015%.

4. Step (1) The price change is:

$$3020 - 2344 = 676 \text{ points.}$$

- Step (2) Since the price value is so large, the PTV will be the double octave. Or, $4 \times 236 = 944$.

- Step (3) The above values for the PTV and price, define the time component, as below:



The PTV formula is applied, in reverse, to find the number of hours, given the PTV value and price value. That is,

$$944 = \sqrt{hours^2 + 676^2}$$

Or, solving for time,

$$\sqrt{944^2 - 676^2} = 658.9 \text{ hours} = 101 \text{ days}$$

The actual number of trading days between 10/11/90 and 3/6/91 was 100 days, a difference of one day from the projected value, or 1% error. This is well within the resolution of the available data.

5. In 1908 when Union Pacific traded at 168 1/8 it was at a point where the PTV from its previous bottom had reached its maximum length, based upon the length of PTVs immediately preceding it. This maximum length was calculated as demonstrated in this lesson. Since the PTV had reached its end, the only direction for the stock to move was down or sideways.

LESSON II

THE ELLIPTICAL NATURE OF PRICE-TIME⁹

*... there is another kind of curved space, "elliptical space", that excels in its simplicity, since all points in it are equivalent.
Albert Einstein ...The Theory of Relativity*

INTRODUCTION

Albert Einstein was known for carefully choosing his words, especially in his writings. In the above quote Einstein did not say that all points in the ellipse are **EQUAL**. He said all points in the ellipse are **EQUIVALENT**. Equivalence has special meaning in the world of science. It is recommended the reader reference one of the many sources of modern physics concerning the topic of equivalence.

Elliptical motion is consistent throughout nature. The planets move around the sun in elliptical orbits. The sun moves around the galaxy in an elliptical path. The electron moves around the nucleus of the atom in an elliptical orbit. In fact, any body set revolving about a center will assume an elliptical orbit. The circle is a special example of elliptical motion. That is, the circle is an ellipse with eccentricity of zero.¹⁰

Lesson I introduced "price-time radii vectors", showed how the length of these vectors are constant, and that their lengths are often integral multiples of smaller vectors. The vector allows the analyst to expand his perspective of financial market charts beyond the single dimensions of price or time. With the PTV, direct measurements can be made from one point of force to another within a two-dimensional plane. Lesson II will explain the nature of these vectors and show that they define the axes of ellipses. The PTV defines the two-dimensional spacing between two points of force. The ellipse defines the potential deviation from this PTV as the price-time action is contained within its perimeter.

PRICE-TIME ACTION IS CONTAINED WITHIN THE PERIMETER OF ELLIPSES, WHOSE MAJOR AND MINOR AXES ARE "PRICE-TIME RADII VECTORS".

⁹ Ellipses were used by a trader, George Bayer, in the San Francisco area shortly after the turn of the century. He wrote a small amount of material about ellipses. The relevant points of his writing are contained within this course. In addition, the concept is greatly advanced beyond anything previously written by any author.

¹⁰ For those who are mathematically inclined, the ellipse is represented by the equation, $(X^2/A^2)+(Y^2/B^2) = 1$, where A is the semi-major axis, B is the semi-minor axis, and $A^2 = B^2 + C^2$. C represents the distance from the center to a focus, and X,Y represents a point on the perimeter.

CHARACTERISTICS OF THE ELLIPSE

Figure 2.1 shows the ellipse with the relevant characteristics marked for future reference.

There are many good mathematics books that describe in detail the characteristics of the ellipse. This information will not be repeated here. However, there are certain characteristics of the ellipse that must be examined, because they are directly related to the work presented here.

The ellipse has a major and a minor axis. The major axis defines the longest distance across the ellipse, and the minor axis defines the shortest width passing through the center point.

The ellipse has two foci, F_1 and F_2 . In the case of the solar system, the sun occupies one focus and the other is vacant. The sum of the distances from these two foci to any point on the perimeter of the ellipse is a constant value. This is demonstrated in Figure 2.1, where the sum of the distances $F_1a + F_2a$ equals the sum of the distances $F_1b + F_2b$.

In addition to the properties listed above, a body moving around the foci in an elliptical orbit will achieve its greatest velocity when closest to a focus (at perihelion with the planets). The slowest velocity occurs at the greatest distance from a focus (aphelion with the planets).

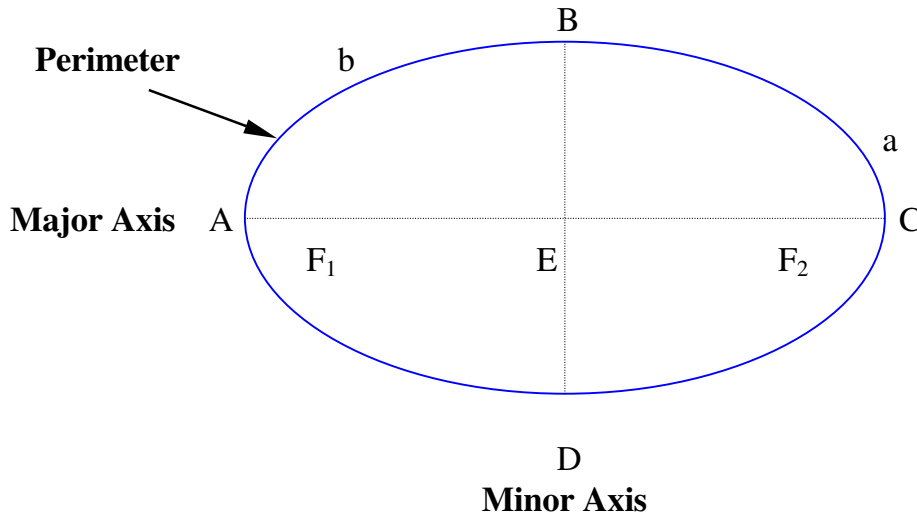


Figure 2.1
Characteristics of the ellipse

GRAPHICAL CONSTRUCTION OF THE ELLIPSE

One way to construct an ellipse is with two circles, as shown in Figure 2.2.a. The method used is described below.

1. Draw two concentric circles, the radii of which define the major and minor axes of the ellipse.

2. Draw a line through the center of the concentric circles and extend it to the perimeter of the larger circle, such as AB in Figure 2.2.a.
3. At the two points where the line drawn in step 2 crosses the perimeter of the inner circle, draw two lines parallel to the horizontal axis, such as ih and jk.
4. At the two points where the line drawn in step 2 crosses the perimeter of the outer circle, draw two lines parallel to the vertical axis, such as Bd and Ac.
5. Where the lines drawn in steps 3 and 4 intersect, such as points l and m, a point on the perimeter of the ellipse is defined.
6. Repeat steps 2-5 for several additional points on the perimeter of the ellipse.

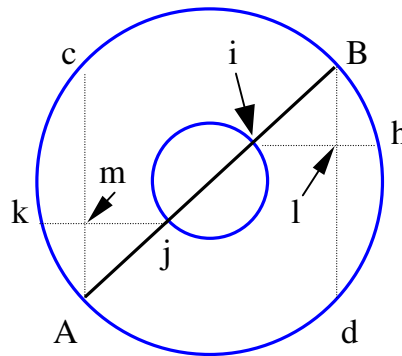


Figure 2.2.a

Graphical construction of the ellipse using two circles¹¹

In Figure 2.2.b the two foci, F_1 and F_2 , anchor a string that is used to draw around the perimeter of the ellipse. Since the length of the string is constant, the distance $F_1p + F_2p$ is constant all the way around the ellipse. This is one definition of the ellipse.

¹¹ There is special significance in using two concentric circles to construct the ellipse. As W.D. Gann stated, in his *Master Course For Stocks*, "... there is an inner circle and an inner square, as well as an outer square and an outer circle which prove the **FOURTH DIMENSION** in working out market movements." Mr. Gann never stated that these two circles define the major and minor axes of the ellipse. Remember the above statement from Mr. Gann. It will be discussed further in this section under "Advanced Topics".

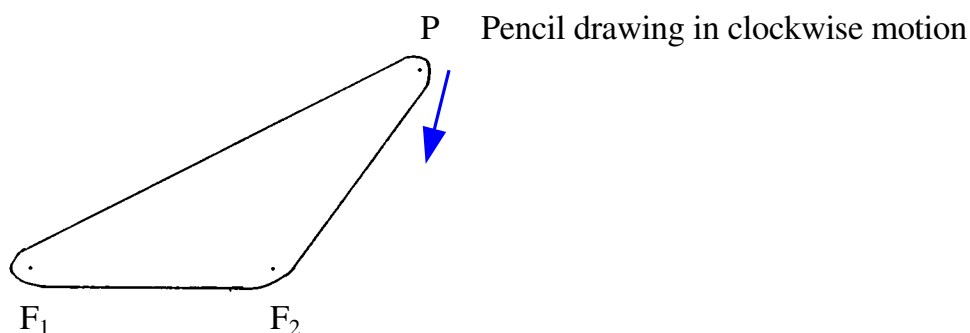


Figure 2.2.b

Construction of the ellipse with pencil and string

EXAMPLES OF PRICE-TIME ACTION WITHIN THE ELLIPSE

Four possible paths are followed by the price-time action as it moves within an ellipse. First, the action can follow the ellipse along the upper perimeter, as shown in Figure 2.1 along path ABC.

Second, the action can follow the ellipse along the lower perimeter, as shown in Figure 2.1 along path ADC.

Third, the action can follow the major axis along path AEC.

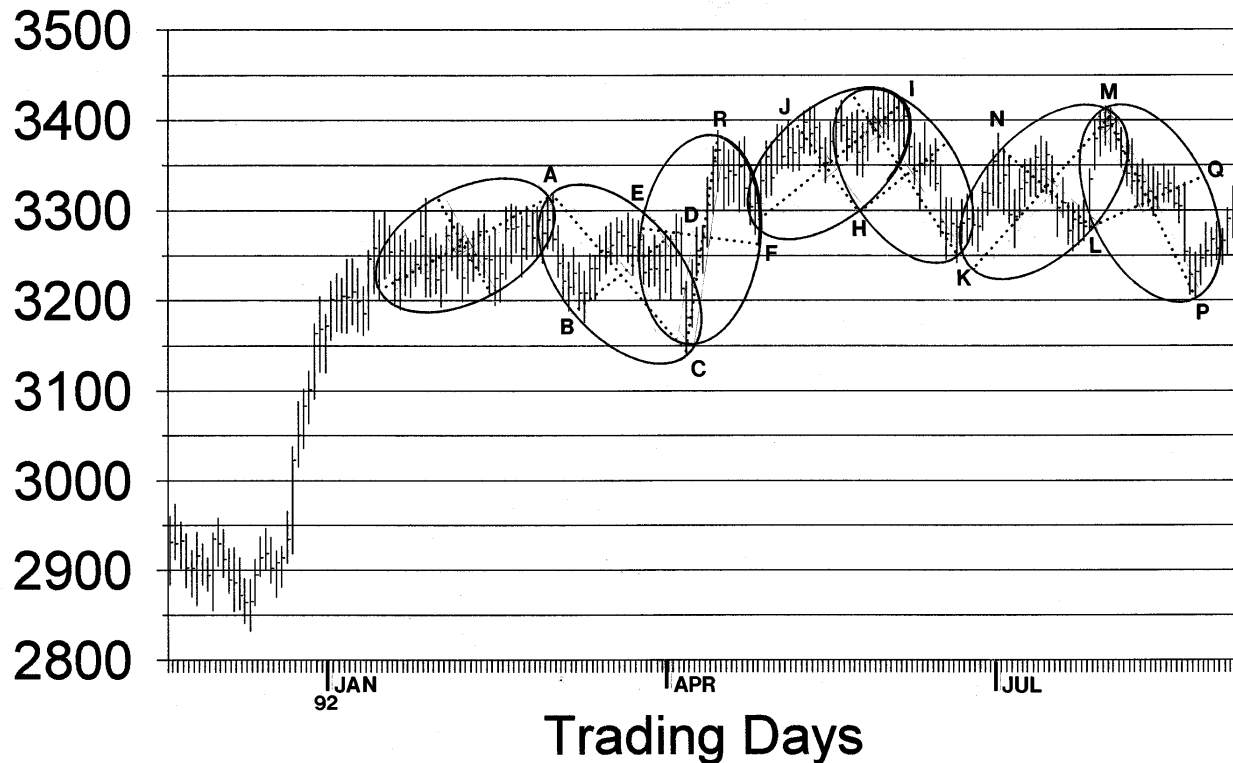
And fourth, the action can follow the minor axis along path BED. This fourth path typically occurs as a reaction to the major trend. For example, if the major trend is up, that is, the major axis of the ellipse is pointing toward increasing prices as time progresses, the price-time action may start moving along the upper perimeter of the ellipse, or it may move along the major axis, until the minor axis is reached, which is point B on the perimeter or E on the axis in Figure 2.1. Then a countertrend reaction will occur with the price-time action following the minor axis of the ellipse until the lower perimeter is reached, along arc DC in Figure 2.1.

For example, refer to Chart II.A, which has the ellipses drawn for a period of nine months. In ellipse KLMN the trend began upward at point K. That is, the major axis of ellipse KLMN is pointing toward higher prices as time progresses. When the price-time action reached the minor axis at point N it turned down and followed the minor axis, NL, until the lower perimeter of the ellipse was reached at point L. When this point was reached the price-time action swung upward until the end of the major axis was reached at point M. At this point the ellipse was complete and the price-time action moved into the new ellipse, MLPQ.

Within this new ellipse, MLPQ, the price-time action followed the major axis, MP, until the minor axis was reached, LQ. At this point a countertrend rally occurred, carrying prices upward until the price-time action was directly over the end point of the major axis at point P. When this occurred the price-time action swung down dramatically for two days to reach the end point of the major axis at point P. At this point, ellipse MLPQ was complete and the price-time action moved into the next ellipse.

II.A

ELLIPSES IN DJIA 12/1991 - 9/1992



When the price-time action follows the perimeter of the ellipse and the minor axis is encountered, the action does not necessarily swing all the way to the opposing perimeter of the ellipse. This is a function of the energy placed into the countertrend movement at that time. An example of this occurs on Chart II.A with ellipse FHIJ. Ellipse FHIJ contained the price-time action along its upper perimeter until the minor axis was reached at point J, where the action swung down to the support line along the major axis. From this point the action oscillated between the major axis and the upper perimeter until the end point of the major axis was reached at point I.

Other examples of this same type of action are shown on Chart I.A. The radii vectors EH and KL defined the major axes of two ellipses that contained the price-time action between the upper perimeter of the ellipse and the major axis. It is this type of elliptical formation that explains the pattern known as the diagonal triangle in Elliott Wave and traditional technical analysis. It also explains why this type of formation occurs in the fifth wave position in Elliott Wave analysis, as shown in Figure 2.3.

Since the ellipse is nearing completion, the distance between the major axis and the upper perimeter is narrowing as time progresses, causing the "coil" appearance of the price-time action. For the Elliott Wave analyst who is aware of the ellipse and the

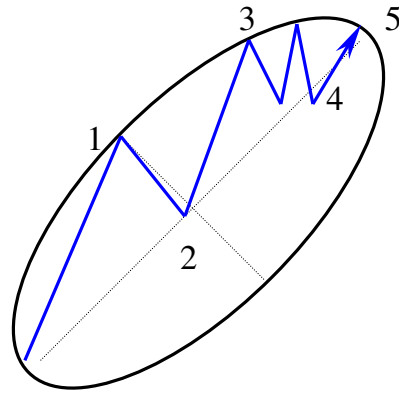


Figure 2.3
Elliott Wave diagonal triangle formed within the ellipse

beginning point of the radius vector, the end point of this fifth wave can be pinpointed, even if it involves a "fifth wave failure" as described in Elliott Wave parlance. A good example of a diagonal triangle defined within an ellipse is on Chart I.A, with KL the major axis of the ellipse.

The rapid decline that follows the diagonal triangle is also explained by this phenomenon, and will be further explained later in this lesson.

On Chart II.A the mirror image of ellipse KLMN is ellipse ABCD. Note the equal price and time components of these two ellipses. The price-time action of ABCD pointed downward, i.e., the major axis pointed toward decreasing prices as the time component progressed. The price-time action followed the lower perimeter of the ellipse until the minor axis was reached at point B. After which, a countertrend rally occurred carrying the action to the upper perimeter of the ellipse at point E. From there, the action oscillated between the major axis and the upper perimeter until the terminal point of the ellipse was reached at point C.

ELLIPSE DEFINES THE ORIGIN AND TERMINUS OF PRICE-TIME CYCLES

Chart II.A makes it apparent why the terminal point of radius vector MO on Chart I.B was chosen to be point O, rather than the actual price high, which occurred four days earlier. This was because ellipse FHIJ was not complete until point I had been reached. Similarly, on Chart I.A ellipse KL terminated at point L. However, the actual price high was reached nine days earlier. The price action moved sideways within the ellipse until it had time to complete.

As stated in Lesson I, it is necessary to know the origin of the radius vector if the terminus is to be determined in advance. For example, the origin of ellipse FHIJ was at point F, rather than point R. With the ellipses drawn as they are on Chart II.A, it is clear why point F was chosen. That is the point where the price-time action moved out of the previous ellipse CFR. Ellipse CFR was pointing in a nearly vertical direction, consequently when the price-time action reached the end of the major axis there was still

considerable space left within ellipse CFR, specifically, the distance from point R to point F. The action drifted along the outer perimeter of the ellipse until time had progressed enough for it to move out of the ellipse. This was the origin of ellipse FHIJ.

MAJOR AXES OF MATED ELLIPSES FORM EQUILATERAL TRIANGLES

A very powerful, yet simple, technique that allows the analyst to fix in advance a specific point in price-time will now be explained. This technique is another of many provided in this course that were discovered by the author and are not available from any other source. This simple technique allows not only accurate price projects to be made, but even more importantly, identifies WHEN these price levels will be reached.

The "Advanced Topics" section of Lesson I explained that price-time radii vectors formed the sides of equilateral triangles. Basic geometry identifies the inner angle of an equilateral triangle as 60 degrees. Also, Lesson I demonstrated that the length of the PTV is fixed. Therefore, given the angle and the length of the vector, the future point in price-time is fixed. For example, on Chart I.A when the location of radius vector AB had been fixed point C was fixed in price-time as well. This is because the angle from the AB axis is 60 degrees, and the length of the radius vector is constant, i.e., 236.

This is graphically demonstrated in Figure 2.4, where three different orientations of an equilateral triangle are shown. The triangles shown in these three figures are the same, but are progressively rotated in a clockwise direction.

In Figure 2.4.a the PTV, AB, that forms the first side of the equilateral triangle is nearly vertical causing its mated PTV, BC, to have very little price depreciation, since its direction is more parallel to the time axis. A slowly declining market consuming considerable time characterizes this orientation of mated ellipses. A good example in the DJIA of this type of configuration is shown on Chart II.B, where points F, G, H correspond with points A, B, C from Figure 2.4.a. Since FG was nearly vertical, its mated PTV, GH, moved sideways along the time axis resulting in very little price depreciation.

In Figure 2.4.b the first side of the equilateral triangle represented by PTV, DE, angles more toward the time axis causing its mated PTV, EF, to point down more in price than the one in Figure 2.4.a. A good example of this type of orientation is shown on Chart II.B, where the points A, B, C correspond with points D, E, F in Figure 2.4.b. Notice that the PTV, AB, was angled more toward the time axis than was FG. This means that the PTV that was the mate of AB pointed down in price more than the PTV that was the mate of FG, i.e., BC drops much more in price and consumes less time doing so than does GH.

In Figure 2.4.c, the PTV, GH, points nearly parallel to the time axis causing its mated PTV, HI, to point nearly straight down in price. This type of market is very dangerous for traders because the slow sideways movement along GH puts traders to sleep and they lose their immediate attention to what is happening in the market. However, when GH has run its course its mated PTV, HI, represents a dramatic decline in prices in a very short time span. An example of this type of market configuration is shown on Chart II.B, where DE angled more toward the time axis than did either FG or AB. Notice that along DE almost all the price appreciation occurred

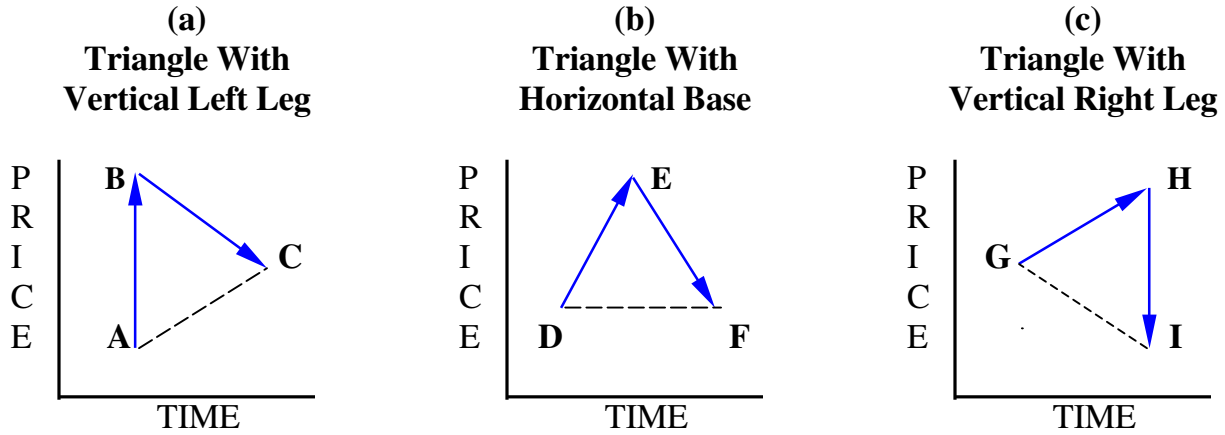
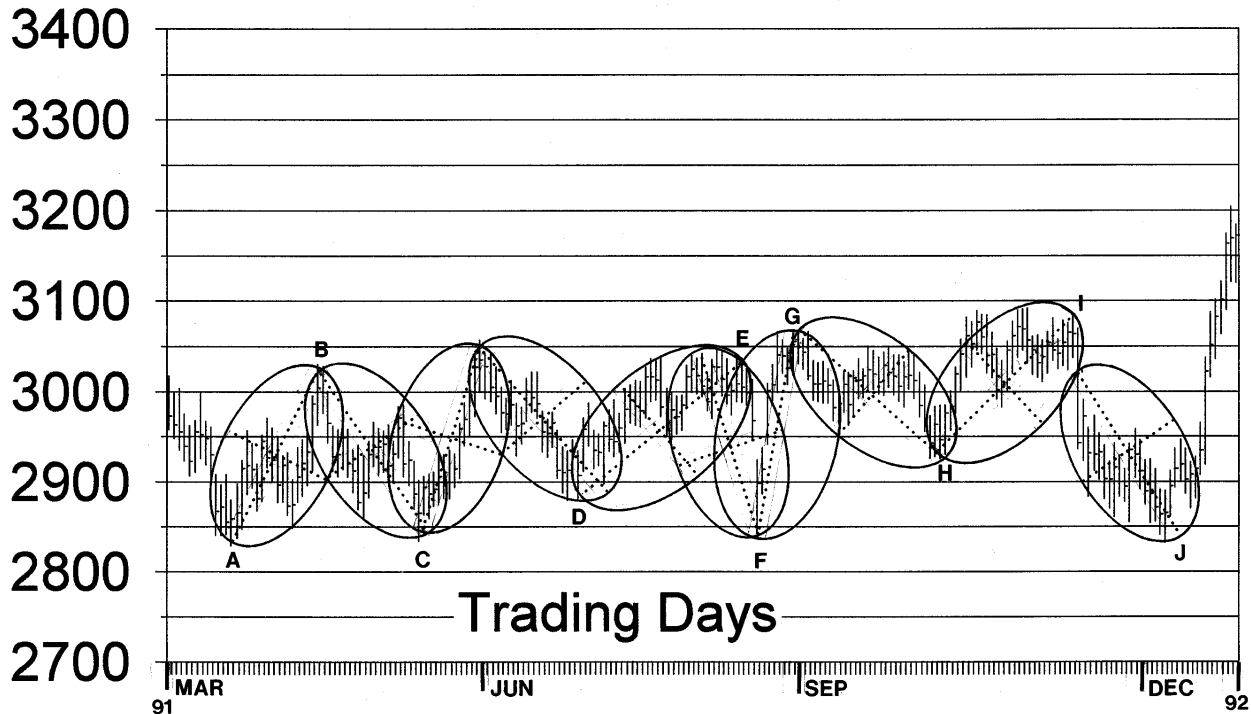


Figure 2.4
Equilateral triangles progressively rotated clockwise, showing progressively steeper movements down the price axis. (HI is steeper than EF; EF is steeper than BC)

II.B

ELLIPSES IN DJIA 2/1991 - 1/1992



during the first nine days. After which, the market moved sideways along the upper perimeter of the ellipse for nearly a month, showing no price change during this time.

While the market moved sideways many traders became "bored" with what was called a "dead market". Several analysts appeared on television talking about the "dull market". These analysts lost their attention to the clear signals the market was giving of the hazard lying directly ahead. However, when the end of DE was reached at point E, its mated PTV, EF, pointed nearly straight down in price, dropping 200 points in a very short time span. These "bored" traders were caught unprepared for such a quick decline. One thing is certain, they were no longer bored.

Another example of the market configuration shown in Figure 2.4.c is shown on Chart II.B, with the two mated ellipses, HI and IJ. Nearly identical conditions occurred within this triangle as occurred within triangle DEF. The PTVs, DE and HI, are parallel. Notice the slow sideways movement just before the dramatic decline along IJ. Traders with knowledge of the PTV would not have been caught sleeping when point I arrived because it was clearly the terminal point of the advance from point H.¹² The ellipse terminating at point J originated at the perimeter of ellipse HI rather than the terminus of its major axis. The major cycle bottom on 12/11/1991 caused this shifting.

The configuration shown in Figure 2.4.c is also present on Chart II.A, with triangle FIK.

If the scales of Chart I.A are "squared out", as previously described, this can be tried as an exercise: (1) lay sketch paper over Chart I.A, (2) draw the two lines AB and BC. (3) rotate the sketch paper so points A and B overlay points C and D on the chart, (4) notice, how the radius vector on the sketch paper, BC, points directly at the terminal point of the radius vector DF. That is, point F is located in both price and **TIME**. Repeat this exercise for vectors IJ and JK. If this technique is used on a chart with different price-time scales the triangles will have to be adjusted, accordingly.

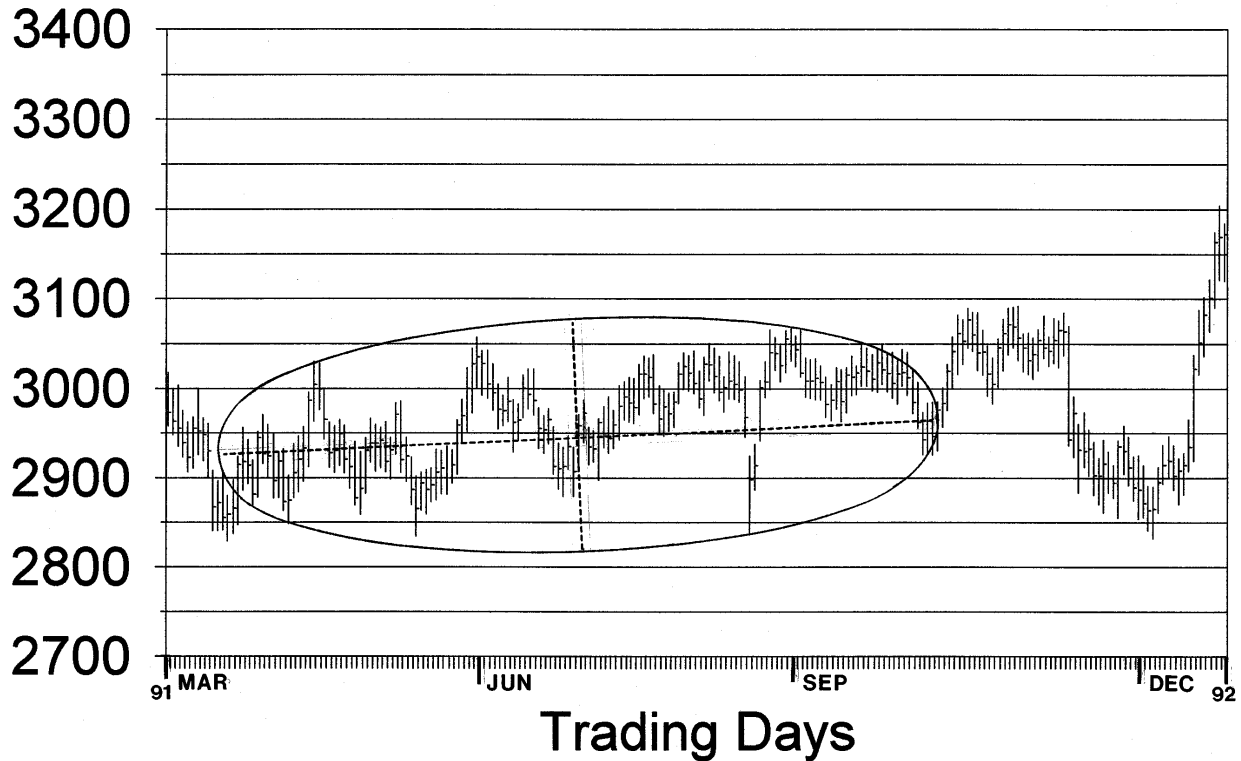
When radius vectors EH and GI are overlaid an error is seen that is not present in the other triangles. This is due to the overlapping nature of radii vectors EH and GI.

On Chart II.A the mated ellipses include KLMN and LPQM also, ABCD and CFR. Since the angle of ellipse ABCD was so flat, its mated ellipse, CFR, needed to be nearly vertical in order to maintain the constant angle between them. The reverse of this occurred with the mirror ellipse of ABCD namely, KLMN. Because the angle of KLMN

¹² This type of equilateral triangle configuration explains the phenomenon known to Elliott Wave analysts as the rapid decline after completion of the fifth wave diagonal triangle. The diagonal triangle is created as shown in Figure 2.3, i.e., due to the flat angle of the major axis of the ellipse and the narrowing distance between the major axis and the upper perimeter. The rapid decline must follow this formation because the angles between the two ellipses are constant and hence, the major axis of the second ellipse is pointing nearly straight down.

II.C

LARGER ELLIPSES CONTAIN SMALL ELLIPSES



was flat, its mated ellipse LPQM had to decline very rapidly in order to maintain the fixed angle between them.

ELLIPSES ARE CONTAINED WITHIN LARGER ELLIPSES

Table 1.4 showed that PTV lengths are often integral multiples of smaller PTVs. Since radii vectors define the major axes of ellipses, it follows that ellipses exist in sizes that are multiples of each other. For example, the ellipses on Chart II.A are all contained within a larger ellipse. This ellipse is in turn, contained within an even larger ellipse, and so on, ad infinitum. Notice how the smaller ellipses from Chart II.B fit into the larger ellipse shown on Chart II.C.

LARGE SCALE ELLIPSES

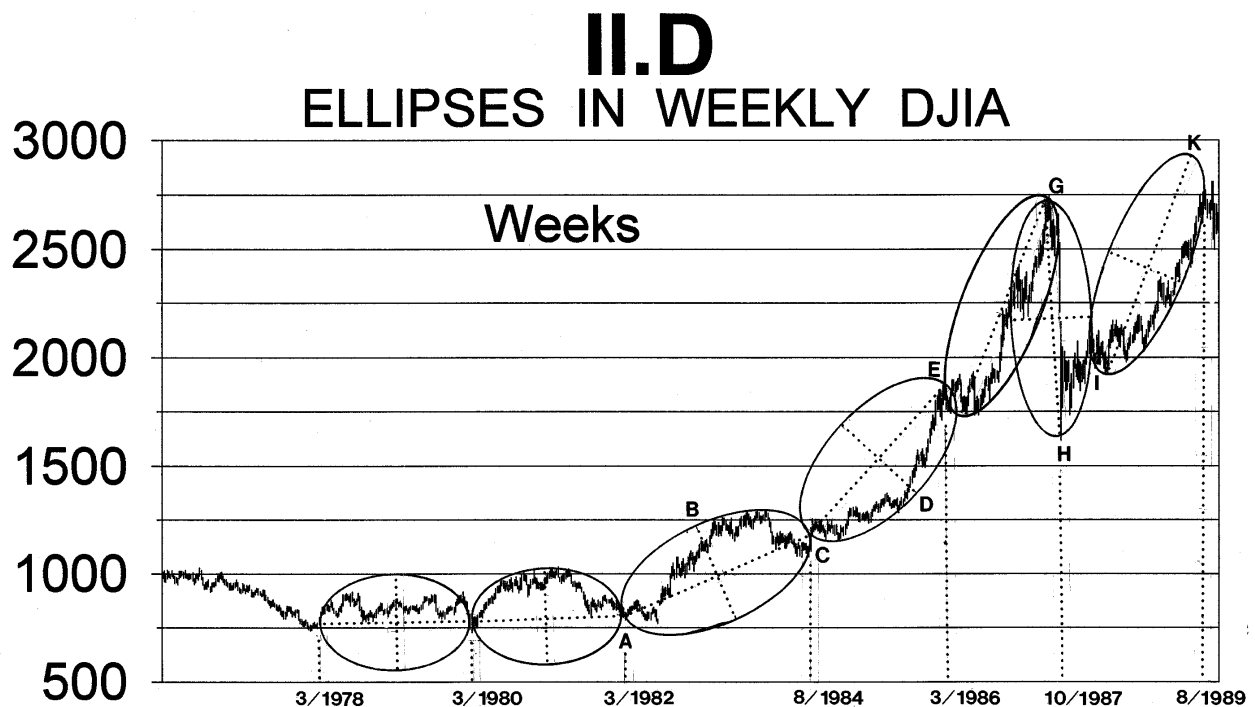
Chart II.D demonstrates the phenomenon of ellipses contained within ellipses on a much larger scale. This chart contains a wealth of information and will be referenced in later lessons. The price-time action between points A and C was contained within the indicated ellipse, with the majority of the action occurring between the upper perimeter and the major axis. The action broke away from the upper perimeter in two significant

areas. The first occurred with the drop into the June-August, 1982 low. The second occurred when several major cycles turned down in January, 1984. In the later case the energy of the down cycle was sufficient to carry the action all the way down to the lower perimeter of the ellipse. However, note that the lower perimeter contained the decline. After this decline the action quickly snapped upward, meeting the terminal point of the major axis of the ellipse in August, 1984.

The action between C and E was also contained within an ellipse the same size as ellipse ABC. The action within ellipse CDE followed the lower perimeter. When September, 1985 arrived the action was not only setting on the lower perimeter of the ellipse, but also had a great deal of price distance to cover in a short time period, in order to reach the terminal point of the major axis at point E. This explains the rapid advance between September, 1985 and March, 1986.

Chart II.E shows an enlarged view of ellipses EG and IK. The lower perimeter of EG contained the action during the beginning phase of the ellipse, i.e., between March 1986 and November, 1986. When the action reached the point in time that is directly below the center of the ellipse in January, 1987, a "quarter-cycle" had completed¹³, and a rapid advance followed carrying the action up to the major axis in March, 1987. This axis contained the action until the terminal point of the ellipse was reached in August, 1987.

Another very important aspect of ellipse EG must be studied. Although the terminal point occurred in August, 1987, the action did not break out of the ellipse until October 5, 1987, when the outer perimeter was pierced. At this point, in October, a new ellipse was formed with the major axis, GH, pointing directly downward, hence, the "crash of 1987". This phenomenon is the same previously described on daily Chart II.A, with ellipse CFR. In that case the major axis terminated at point R. However, the action was still contained within the ellipse until the perimeter was crossed at point F.



Ellipse GH is much simpler to describe. Simply stated, it pointed down! Within this ellipse the gap occurred when the action reached the center point of the ellipse along the major axis.

The same phenomenon occurred between ellipses GH and IK that occurred between ellipses EG and GH. Namely, the price action hit its low in October, 1987, when the terminal point of the major axis had been reached. However, the new ellipse, IK, did not begin until March, 1988 at point I, where the action pierced the perimeter of the previous ellipse, GH.

Ellipse IK was similar in form to ellipse CD. It followed the lower perimeter of the ellipse until the action moved directly below the center point of the ellipse. At this point in November, 1988, the "quarter-cycle" was complete and the action moved dramatically upward to reach the terminal point of the major axis at point K. The action between March, 1988 and November, 1988 defined the "base before the advance", as described above.

The ellipses contained on Charts II.D and II.E are multiples of the much smaller ellipses, shown on the daily charts II.A and II.B. Methods for determining these ratios will be presented in later lessons.

ADVANCED TOPICS

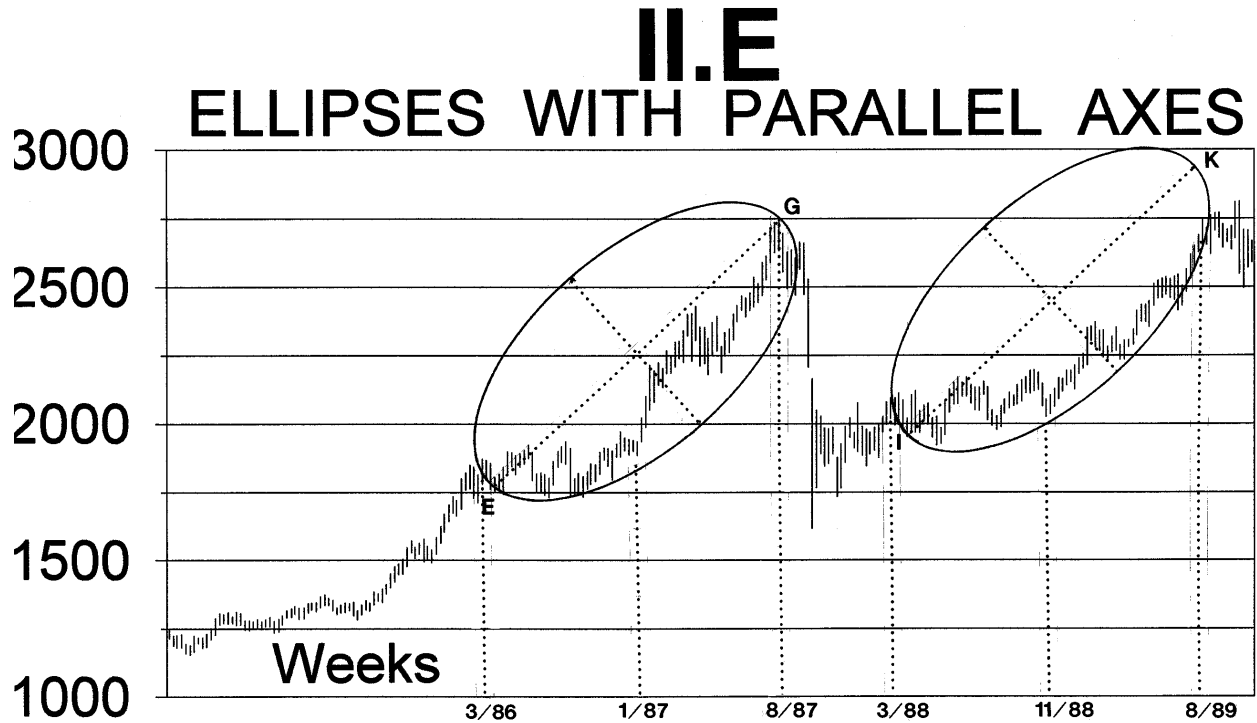
It was previously noted that there is special significance to using two circles to form the ellipse. It was also noted in Lesson I that traditional price-time charts are limited in the sense that they are two-dimensional representations of a multi-dimensional phenomenon. The inner circle of the ellipse is actually at a higher dimension than the outer circle.¹⁴ To visualize this, imagine a conic section with circles stacked on top of each other, each with a diameter smaller than the previous circle until the vortex is reached. The ellipse is formed from two such circles with the price-time action actually moving out of the limits of the two-dimensional representation of the price-time chart.

CONCLUSION

At this point in the course the reader should be able to:

- Construct an ellipse from two concentric circles.
- Identify an ellipse on a price-time chart.
- Use a PTV, as identified in Lesson I, as the major or minor axis of the ellipse and construct the ellipse.
- Recognize equilateral triangles on price-time charts and use them to project the terminal point of a PTV.
- Identify the 1/2 and 1/4 cycles of the ellipse.

¹⁴ This is what W.D. Gann meant when he stated, "... there is an inner circle and an inner square, as well as an outer square and an outer circle which prove the fourth-dimension in working out market movements."

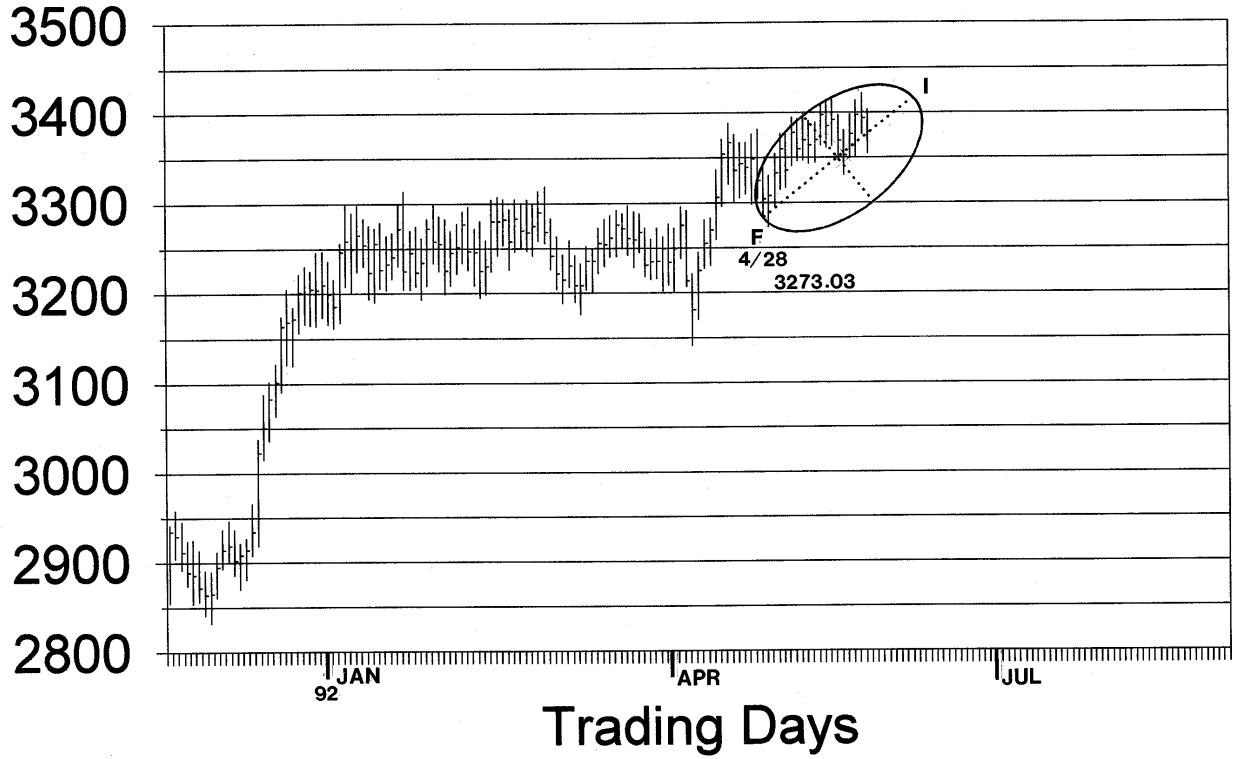


REVIEW QUESTION

Chart II.F shows the daily Dow Jones Industrial Average (Hereafter, referred to as DJIA) from the low in December, 1991 to May, 1992. Enough of ellipse FI had completed on this date to identify point F as its origin. Also, it was clear that the price-time action was following the upper perimeter of this ellipse. The ellipse is laid over the price-time action to date with the origin of the ellipse at point F and the upper perimeter containing the intraday highs. With the ellipse in place the angle of the major axis is defined. Since the length (236), angle, and origin of the major axis is known, its terminal point is also known. What is the projected date and price high for the DJIA within this ellipse?

II.F

THE ELLIPSE - REVIEW



ANSWER TO REVIEW QUESTION

Since point F had been identified as the origin of the major axis of the ellipse, it is the origin of the PTV, FI. The value of the DJIA at point F was 3273.03. Graphically measuring the time distance to the terminal point of the major axis of the ellipse, 28 trading days (182 hours)¹⁵ are expected to elapse, projecting the date of June 8, 1992.

With this date the price value is calculated as follows:¹⁶

$$236^2 = \text{price}^2 + 182^2$$

$$\text{Therefore, } \text{price}^2 = 236^2 - 182^2$$

$$\text{Or, } \text{price change} = 150.24 \text{ points}$$

Add the projected price change to the origin of the ellipse on 4/28/1992 to get the projected price top.

$$\text{Projected DJIA top} = 3273.03 + 150.24 = 3423.27$$

On 6/8/1992 the DJIA topped out at 3422.8, intraday. For an error of:

$$\frac{3423.27 - 3422.8}{3422.8} = \frac{0.47}{3422.8} = 0.014\%$$

¹⁵ Twenty-eight trading days x 6.5 hours per day = 182 hours.

¹⁶ For the mathematically inclined, the price and time components can be calculated using basic trigonometry. Since the angle and hypotenuse are known, the price is given by:

$$\text{Sin (angle)} = \frac{\text{Price}}{\text{PTV}} \quad \text{or, } \text{Price change} = \text{Sin(angle)} \times \text{PTV}$$

$$\text{Cos (angle)} = \frac{\text{Time}}{\text{PTV}} \quad \text{or, } \text{Time change} = \text{Cos(angle)} \times \text{PTV}$$

LESSON III

GROWTH PATTERNS

Here and elsewhere we shall not obtain the best insight into things until we actually see them growing from the beginning.
Aristotle (322 A.D.)

INTRODUCTION

Previous lessons taught how to determine the PTV, how to create the ellipse and apply it to financial market charts, and what angle to expect for the major axis of the ellipse.

If accurate projections of price-time are to be made, an understanding of natural growth patterns is needed. Everything in nature grows according to simple mathematical relationships and financial markets are not exempt from this law.

Financial market analysts have noticed certain recurrent ratios that exist in price-time. The most celebrated of these is the Fibonacci ratio of 1.618:1. However, even though certain ratios are known to exist, without an understanding of the natural growth process it is impossible to know when to expect these ratios to occur and when they will not. An arbitrary application of any timing technique is a sure recipe for financial disaster.

Market analysts consistently err in trying to apply growth pattern ratios to a single dimension on a price-time chart, i.e., to only price support and resistance levels, or to time cycles.

A CLEARER UNDERSTANDING OF THE UNIFIED NATURE OF PRICE-TIME IS REQUIRED IF ACCURATE PROJECTIONS ARE EXPECTED. THE PTV PROVIDES THE TOOL TO VIEW THE MULTI-DIMENSIONAL NATURE OF PRICE-TIME GROWTH PATTERNS.

This lesson will study the patterns created as financial markets proceed through their natural growth sequence. As a greater understanding of this growth process is developed the analyst will be made aware of the places in the growth process where specific ratios occur. In subsequent lessons ratios more important than the celebrated Fibonacci will be revealed.

Keep in mind throughout this lesson and the ones to follow, that the approaches used in this course are unique in the fact that a multi-dimensional approach is used. The PTV is used as a tool in a theory of unified price-time.

WWW.FOREX-WAREZ.COM
ANDREYBBRY@GMAIL.COM SKYPE: ANDREYBBRY

BACKGROUND REVIEW

In the following explanation it is assumed the reader is familiar with Fibonacci relationships, the Golden Section, Dynamic Symmetry, and basic logarithmic spirals. If not, it will be helpful to review these subjects before proceeding.

FIBONACCI

Man uses the Fibonacci number series to represent certain growth patterns in nature. For example, the distribution of seeds on the head of a sunflower follow the Fibonacci series, as do the distribution of florets in pinecones and daisies. That is not to say some divine spirit developed a number series and ordained all plants to grow according to it. The plant grows in a manner that best suits its environment, filling space in as efficient manner as possible. The Fibonacci number series is simply man's attempt to model and understand the results of this growth.

This number series progresses as follows:

1, 1, 2, 3, 5, 8, 13, 21, 34, 55, 89,

Fibonacci is a summation series, with each element the sum of the two preceding elements. Two is the sum of one plus one; eight is the sum of five plus three; and so on. This series is especially prevalent in growth patterns that follow a conical helix, shown in Figure 3.1.



Note the similarity between this figure and Figure 2.2.a, which showed a two-dimensional representation of two stacked circles used to construct the ellipse.¹⁷

Figure 3.1

Side view of conical helix¹⁸

After the Fibonacci series progresses past the first few terms, each successive element is in the ratio of 1.618:1 to the one preceding it. This ratio is the well-known "Golden Section" used by many market analysts to establish support and resistance levels.

¹⁷ The ellipse contains the price-time action, which exists in more than two dimensions. The two circles used to construct the ellipse are two successive wraps in a conical helix. As the price-time action swings through the ellipse, what is actually seen is a "slice" out of the conical helix. This can be visualized by seeing a marble rolling down a coiled spiral, and you only see the marble when it rolls past in front of you.

¹⁸ Technical Reference: *Fundamentals of Physics Extended*, P. 709-710.

As will be shown in later lessons, this ratio is not the most important ratio in financial market analysis. In fact, it is far down the list. However, due to its popular understanding and general applicability to this subject it is included here.

GOLDEN SECTION

One of the many interesting things about the Golden Section is that it does not matter what two numbers are used to start the series. If the summation process is continued enough times the ratio of successive terms will converge on the ratio, 1.618:1. For example, if we arbitrarily select two numbers, such as 520 and 12, as the first two numbers of the summation series and proceed as described above, the successive terms will converge on 1.618:1. This series will progress as follows:

520, 12, 532, 544, 1076, 1620, 2696, 4316, ...

The last two terms of this series had already approached 1.618:1. The actual ratio at this point in the progression is $4316/2696 = 1.6009:1$.

This number series is the basis for the "Golden Spiral", shown in Figure 3.2, which has each successive radius vector equal to a Fibonacci number.

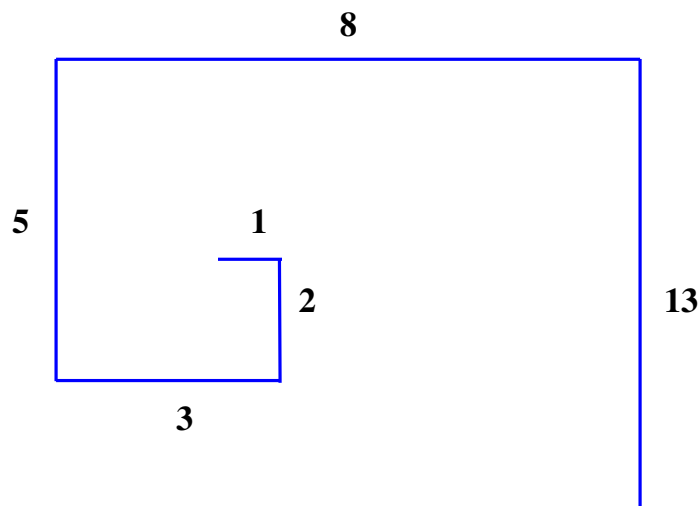


Figure 3.2
Golden Spiral

ON A TWO-DIMENSIONAL PRICE-TIME CHART THE GOLDEN SPIRAL CANNOT BE DIRECTLY SEEN BEYOND THE FIRST FEW TERMS.

As described earlier, the price-time action gives the appearance of twisting and turning into and out of the page of observation. To determine the location of the Golden Spiral, we must first look for the successive terms in the Fibonacci series, then apply the principles of Dynamic Symmetry to locate where the next turn in the spiral will lead.

DYNAMIC SYMMETRY

Dynamic symmetry is the name given to the design found in living and growing plants and animals.¹⁹ This is in contrast to static symmetry, which is present in inanimate objects. Artists use the principles of dynamic symmetry to create a more "living" appearance in their work. Not only are contemporary artists using these principles, but artists for hundreds of years have been using them. Many ancient works of art, especially Greek, show deliberate incorporation of Dynamic Symmetry. Dynamic Symmetry utilizes geometry to obtain the proportions present in living organisms. This produces a variety of geometric designs, including those with the Golden Section.

A graphical representation of how dynamic symmetry is used to derive the Golden Section from a square is shown in Figure 3.3.

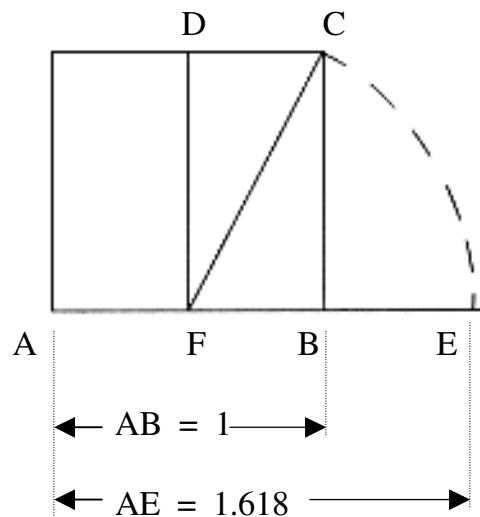


Figure 3.3

Golden Section derived from diagonal of half-square

In this example of dynamic symmetry, square AC is divided into two equal 1x2 rectangles, AD and DB. The diagonal of one of these rectangles, FC, is used as a radius vector centered at point F, and drawn down to intersect a line segment extended from the bottom of the square, AE. Hence, $FC=FE$ and the ratio between this extended line, AE, and the side of the square, AB, is 1.618:1.

FIVE-YEAR CYCLE DEFINES SMALLEST COMPLETED GROWTH PATTERN

Before the relationships described above are related to financial markets, some price-time measurements are necessary. The weekly chart will be used, extending over a period of several years, to be sure an entire growth pattern is included in the field of vision. If only a

¹⁹ Reference: *Elements of Dynamic Symmetry*.

daily chart is used the time frame would be too short for a growth pattern to complete and only a piece of the pattern would be seen.

Chart III.A shows a weekly chart referenced in Lesson II, with the price and time components of the radii vectors included. The data used for the calculation of these radii vectors are contained in Table 3.1.

Table 3.1
PTV Calculations for Chart III.A
Showing Completed Five-Year Growth Pattern

Price-Time Radius Vector	Date of Low	Closing Low	Date of High	Closing High	Time Change	Price Change (points)	Vector Value (PTV)
AC	3/08 1982	795.47	8/07 1984	1204.62	613 DAYS	409	737
CE	8/07 1984	1204.62	3/27 1986	1821.72	413 DAYS	617	742
EG	3/27 1986	1821.72	10/2 1987	2641	384 DAYS	819	904
IK	3/02 1988	2071.29	8/11 1989	2684	366 DAYS	612	713
AE	3/08 1982	795.47	3/27 1986	1821.72	1026 DAYS	1026	1451
AG	3/08 1982	795.47	10/2 1987	2641	1410 DAYS	1846	2323

Several facts must be noted about the values in Table 3.1 and the corresponding cycles shown on Chart III.A.

(1) Whether the value is time or price, they are all integral multiples of a "base" value of approximately 205. This is demonstrated in Figure 3.4, where only the integral multiples are shown. That is, 2 on Figure 3.4 represents $2 \times 205 = 410$, 3 equals $3 \times 205 = 615$, 5 equals $5 \times 205 = 1025$. The points A, C, and E are the same as shown on Chart III.A. On Chart III.A the ellipse AC has a time component of 613 days, which is three times 205, and a price component of 409, which is two times 205. Therefore, the rectangle that has 613 days as a side and 409 points as a side is a 3x2 rectangle.

(2) The two radii vectors, AC and CE, which define the major axes of the corresponding ellipses, are of equal length.

(3) Ellipse CE is the inverse of ellipse AC. That is, the time component of CE is 413 days, which equals the price component of ellipse AC. And the price component of ellipse CE is 617, which equals the time component of ellipse AC. Therefore, ellipse CE has price-time components of a 2x3 rectangle.

Ellipse AC contains the action along the upper perimeter and ellipse CE along the lower perimeter. If these two ellipses are overlaid an ellipse with both perimeters outlined is seen.

(4) The two cycles, AC and CE, are defined within a square, AE, with sides equal to 1026, which equals 205 times 5.

(5) Since Figure 3.4 is a square, it follows that its diagonal, AE, must form an angle of 45 degrees with the time axis.²⁰ This figure actually contains three squares with sides two, three, and five. These numbers are successive terms in the Fibonacci number series. Compare this figure with Figure 3.2, the "Golden Spiral".

To practice visualizing how spirals unfold in three dimensions, try to view the

III.A PRICE-TIME COMPONENTS



²⁰ This is W.D. Gann's 45-degree angle. It is the diagonal of the square. When the square has completed forming, as at point E, the 45-degree angle is reached and significant resistance is encountered.

Which angle the price-time action follows depends upon the current stage of the growth process. For example, if the price-time action is following the lower perimeter of the ellipse the 1x2 angle will dominate early in the cycle, then the 45, then the 2x1. The angle gets progressively steeper as the growth process increases at a greater rate, while being contained within the ellipse.

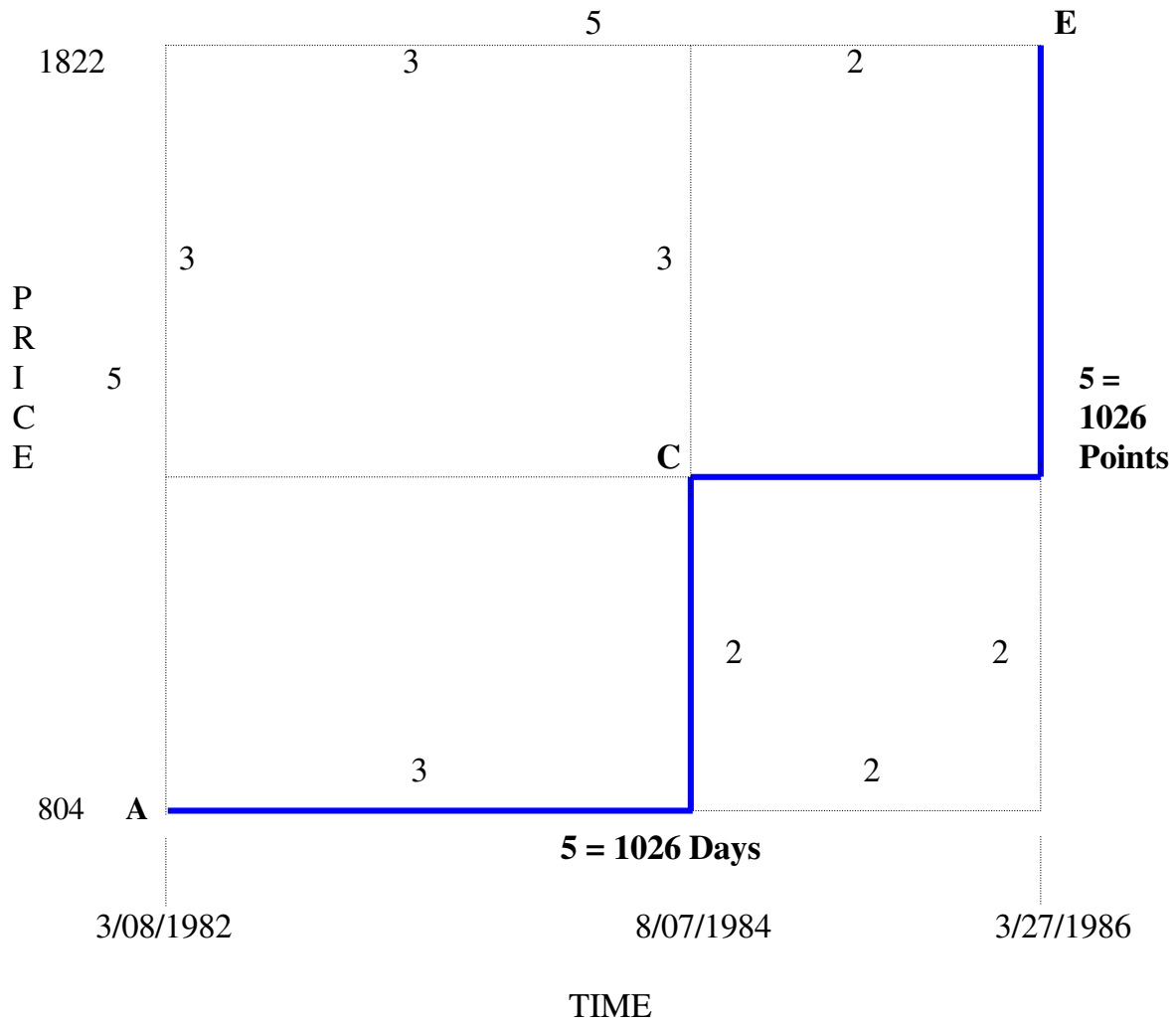


Figure 3.4
Squares from Chart III.A (DJIA 3/08/1982 - 3/27/1986)

On Chart III.A the action started at point A and moved along the upper perimeter of ellipse AC until strong cyclic effects caused it to be **PULLED DOWN**²¹ into the low of June-August, 1982. When this cycle bottomed the action moved up and oscillated between the upper perimeter of the ellipse, providing resistance, and the diagonal of the square, AE, which provided support. Several points can be seen where the action touched both these lines. In January, 1984 the support line, AE, and the resistance perimeter of the ellipse came together. At this point a rapid decline began, dropping the action to the lower perimeter of the ellipse, which provided the support until the ellipse was complete at point C.

²¹ The cycle that caused this price-time action to be pulled down into the 1982 low will be explained later in this course.

After ellipse AC completed, its inverse contained the action as it moved upward until point E was reached. Point E not only represented the point where ellipse CE was complete, but also the completion of square AE. At this point the market was up 1026 points in 1026 trading days, defining the square with sides 1026 x 1026.

Square AE has many notable characteristics:

- (1) The diagonal of the square provided a support line until it was broken in January, 1984.
- (2) Two large ellipses, AC and CE, are contained within this square.
- (3) The terminus of ellipse AC and the origin of ellipse CE occurred at point C. **THIS POINT IS NOT DIRECTLY ON THE DIAGONAL OF THE SQUARE.** Rather, the location of point C defined the Golden Spiral within the square.²²

When a living cell has reached maturity it reproduces by separating into two parts, ultimately creating two cells with twice the volume of the original cell.

In geometry, to create a square with twice the area of the original square the diagonal of the first square is used as the side of the new square.²³ The diagonal of the square shown on Chart III.B extends from point A to point E and has length of 1451, as calculated in Table 3.1. With this line used as the base, the new square, AEMN, is constructed. This square is used to locate the next point on the curve of the Golden Spiral, using the principles of Dynamic Symmetry, as shown in Figure 3.3. At point E the spiral had progressed in the Fibonacci series through the number five: 1,1,2,3,5. These numbers and their corresponding squares are shown on Chart III.B. The next number in the series is 8.

Within the new square, AENM, the diagonal of the half-square, PN, is drawn. This line, PN, has length of 1622,²⁴ which is eight times the base value of 205, and defines the length of the next PTV on the Golden Spiral. This PTV originates at point P and is graphically extended forward in time by drawing the arc, NG. Along this arc are defined

²² The Golden Section divides a square with side length equal to five into two parts with the ratio 3:2. These are two terms early in the Fibonacci number series, upon which the Golden Section is based.

²³ This is because the diagonal of a square with side length of one is $\sqrt{2}$. And the area of a square with side length equal to $\sqrt{2}$ is $\sqrt{2}$ squared, which equals 2. This will be explained further in Lesson IV.

²⁴ The diagonal of a half-square is defined as $\sqrt{5}$ times the short side of the half-square. In the example shown on Chart III.B, PE is the short side of the half-square. Therefore, the diagonal, PN, to this half-square is given by; $PN = \sqrt{5} \times PE$; or $PN = 2.236 \times 725.5 = 1622$.

the limits of the next turn on the Golden Spiral. As can be seen on Chart III.B, this arc touches the market high just before the crash on October 2, 1987.

To verify that the theoretical values calculated above match the actual market action, EG must be shown to be in the Fibonacci ratio of 1.62 to the side of the square, AE. Table 3.1 calculated the values for EG and AE to be 904 and 1451, respectively.

Therefore,

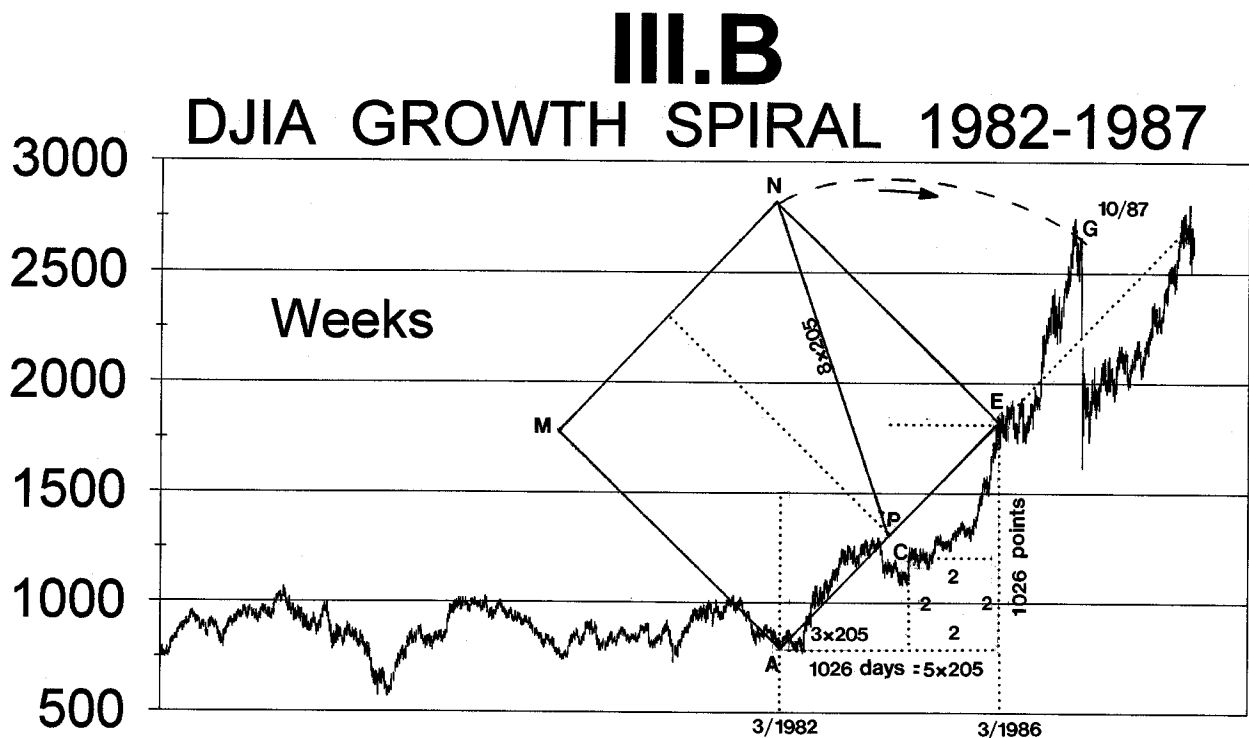
$$\frac{AE}{EG} = \frac{1451}{904} = 1.605$$

In other words, EG and AE are in the Fibonacci ratio of 1.6:1. Also, notice that the value of EG, which was determined by the root five relationship, is equal to the PTV from 1966 to 1982.

To compare how ideal theoretical values matched the actual data, the theoretical length of EG is found by dividing the side of square AE by 1.618. That is,

Since AE = 1451, the theoretical value of EG is given by;

$$\text{Theoretical value of EG} = \frac{AE}{1.618} = \frac{1451}{1.618} = 896.8$$



The actual value of EG was 904, producing an error of,

$$\frac{904-896.8}{896.8} = 0.80\% \text{ error}$$

Additional proof that the techniques of dynamic symmetry defined above identify the Golden Section within the five-year growth pattern on Chart III.B is obtained by verifying the PHI ratio between the PTVs AG and AE.

$$\frac{\underline{AG}}{\underline{AE}} = \frac{2323}{1451} = 1.6$$

ADVANCED TOPICS

The reason dynamic symmetry is an invaluable tool in determining the final turn on the spiral of the completed five-year growth cycle is that the final PTV, EG, actually turned out of the page of observation. The dimensional distortions caused by two-dimensional charts create the appearance that the action is coming toward the observer as he views the chart.

LESSON IV

PRICE-TIME RATIOS MORE IMPORTANT THAN FIBONACCI

Mathematics ... reveals the orderliness of the ratios according to which the universe is constructed and the proportion that binds things together in the cosmos.

Proclus Diadochus (485 A.D.) ...Commentary on the First Book of Euclid's Elements

INTRODUCTION

While the Fibonacci ratio (PHI=1.618) has gained recent popularity as a tool for financial market analysis, it is **NOT** the most valuable. There are several ratios that produce better results in timing financial markets if they are approached from the four-dimensional perspective. Without such a perspective the realities presented in this lesson and the lessons to follow remain unseen. The PTV provides the tool for a four-dimensional approach.

The ratios presented in this lesson are produced as markets unfold in their characteristic geometric patterns.²⁵ The only limitation in the time scale to which these ratios can be applied is the availability of reliable data. Financial markets continue to grow from their date of inception until their termination. If a financial market has been in existence for seven hundred years, (like the world-wide wheat market), PTV ratios can be calculated and applied to the geometric growth pattern for that time frame. In fact, the ratios presented in this lesson are present on price-time charts with time scales ranging from minutes to centuries.

A RATIO MUCH MORE IMPORTANT THAN FIBONACCI

The square root of two, 1.414, is **MUCH MORE IMPORTANT** in financial market analysis than Fibonacci. The square root of two relates the diagonal of a square to its side, as in Figure 4.1.

The square root of two ratio has many interesting properties, some common with Fibonacci. For example, if one is subtracted from the square root of two the result is 0.414.

$$\sqrt{2} - 1 = 0.414$$

If this value of 0.414 is divided into one, the result is one plus the square root of two.

²⁵ A more detailed explanation of financial market geometry is provided in Lesson V, **GEOMETRIC STRUCTURES**.

That is,

$$\frac{1}{0.414} = 1 + 1.414 = 2.414$$

This is similar to the Fibonacci ratio, where one subtracted from PHI equals one divided by PHI. That is,

One subtracted from PHI,

$$1.618 - 1 = 0.618$$

equals one divided by PHI,

$$\frac{1}{1.618} = 0.618$$

There are many reasons why the square root of two ratio is so prevalent in financial market price-time charts. Lesson V, **GEOMETRIC STRUCTURES**, will make these reasons clear. For now, the objective is to show that this ratio is found throughout the stock market. When the presence of this ratio is demonstrated beyond the possibility of coincidence, the next step will be to look into the resultant composite geometry. This is done in Lesson V, **GEOMETRIC STRUCTURES**.

The square root of two ratio defines the relative magnitudes of the radii of two concentric circles circumscribing and inscribing a square. If a circle is placed within a square and another circle is drawn around the square the combination will appear as in Figure 4.2.

$$AC = AB \times \sqrt{2}$$

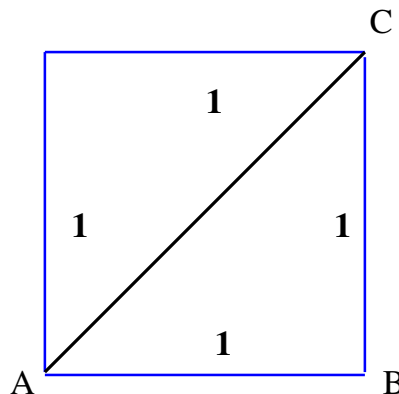


Figure 4.1
Diagonal of the square

THE SQUARE REPRESENTS THE TWO-DIMENSIONAL EXTREMES REACHED BY THE PTV IN BOTH PRICE AND TIME. IT ALSO DEFINES SUCCESSIVE GROWTH LEVELS AS ENERGY IS ADDED TO THE SYSTEM.²⁶

The radii of the two circles in Figure 4.2 are OA and OB. OA is the radius of the inner circle and OB is the radius of the outer circle. For the purpose of this analysis, radius OA is set equal to one. Triangle OBA is a right angle triangle with OA=AB=1. Lesson I showed that the distance, OB, is the hypotenuse of this right triangle, and has the value $\sqrt{2} = 1.414$. This means that the ratio of the radii of the two circles is 1.414.²⁷

The difference between the two radii in Figure 4.2 is 0.414.²⁸ This value is extremely important and will be shown in Lesson V, **GEOMETRIC STRUCTURES**, to relate the sides of the geometric structures formed in the stock market during the early part of the twentieth century to those formed more recently.

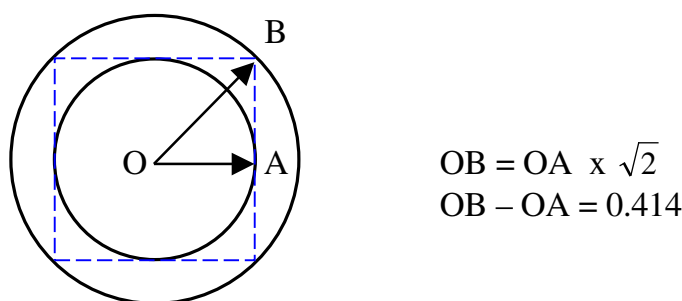


Figure 4.2

Two concentric circles with radii in the ratio of root two

²⁶ The concept of energy levels of cycles is explained in Lesson VII, **CYCLES**.

²⁷ If you own a "precision ratio divider" the ratio of the square root of two can be obtained by setting it to divide the circle into four parts. The reason why this works can be seen in Figure 4.2.

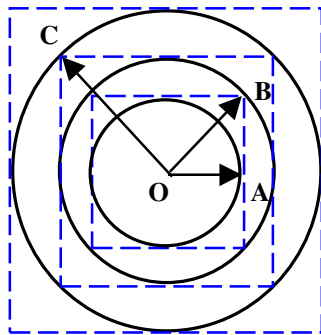
Remember, for any graphical approach to work accurately the charts must be "squared out" as described in Lesson I. This is because growth patterns do not confine themselves to a single dimension.

²⁸ Reference: *Kepler's Geometrical Cosmology*, P. 197-200.

If the growth process shown in Figure 4.2 is continued to the next energy level the pattern will look like Figure 4.3.a. And without the squares it looks like Figure 4.3.b. Compare this figure with the conical helix shown in Figure 3.1. They are the same figure. The only difference is the angle of observation. Figure 3.1 is a three-dimensional perspective of the conical helix viewed from the side. Figure 4.3.b is a two-dimensional perspective of this same helix viewed from the top looking down.²⁹

The squares in Figure 4.3 represent the successive levels of a four-sided pyramid when viewed from a three-dimensional perspective. This is the same construct found in the great pyramid at Giza, Egypt. The next lesson will show that this geometric formation defines successive energy levels of the stock market. As the conical helix unfolds, it expands.³⁰ The lengths of the sides of the squares at each energy level are defined by the extent the helix has unfolded at that particular point in time.

(a)
Three Successive Energy
Levels With Squares



$$\frac{OB}{OA} = \frac{OC}{OB} = \sqrt{2}$$

$$\frac{OC}{OA} = 2$$

(b)
Three Successive Energy
Levels Without Squares

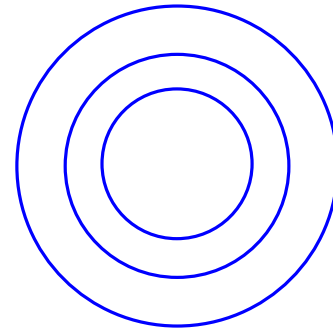


Figure 4.3

Successive root two energy levels: (a) with squares and; (b) without squares

²⁹ The figure of one circle contained within another keeps recurring in this analysis of financial markets. It was used: (1) in Lesson I to construct the ellipse; (2) in Lesson III to show the conical helix within growth patterns; (3) to demonstrate successive energy levels.

³⁰ Technical Reference: *Chemistry, Reactions, Structure and Properties*, P. 511-512

DJIA EXAMPLES OF THE SQUARE ROOT OF TWO RATIO

Chart IV.A shows the monthly DJIA from the market top in 1966 through the crash of 1987. The values for the PTVs shown on this chart are contained within Table 4.1.

Table 4.1 contains many PTVs with the 1.414 ratio.³¹ For example, the PTVs connecting the three most significant turning points within the long sideways movement in the stock market between February 9, 1966 and August 9, 1982 defined nearly perfect square root of two ratios. These three points were; the top on 2/9/1966, the bottom on 12/9/1974; and the bottom on 8/9/1982. Chart IV.A labels the three PTVs connecting these points as EF, FG, and EG, and their exact ratios are as shown below.

$$\frac{EF}{FG} = \frac{631}{447} = 1.412$$

$$\frac{EG}{EF} = \frac{891}{631} = 1.412$$

For comparison, the ideal theoretical values are:

$$(1) \quad EF = FG \times \sqrt{2} = 447 \times \sqrt{2} = 632.15$$

$$\text{Producing an error of; } \frac{632.15-631}{631} = \frac{1.15}{631} = 0.18\%$$

$$(2) \quad EG = EF \times \sqrt{2} = 631 \times \sqrt{2} = 892.37$$

$$\text{Producing an error of; } \frac{892.37-891}{891} = \frac{1.37}{891} = 0.15\%$$

And since, $\sqrt{2} \times \sqrt{2} = 2$;

$$(3) \quad FG = 447 = \frac{EG}{2} = \frac{891}{2}$$

³¹ The ratios calculated for this chart are closer to the ideal theoretical values than those calculated using older data for a variety of reasons. First, the components within the index did not change as much as in previous years. Hence, the homogeneity of the index was better maintained. Also, the techniques for recording accurate data have greatly improved.

IV.A

PTV RATIOS IN DJIA 1966-1987

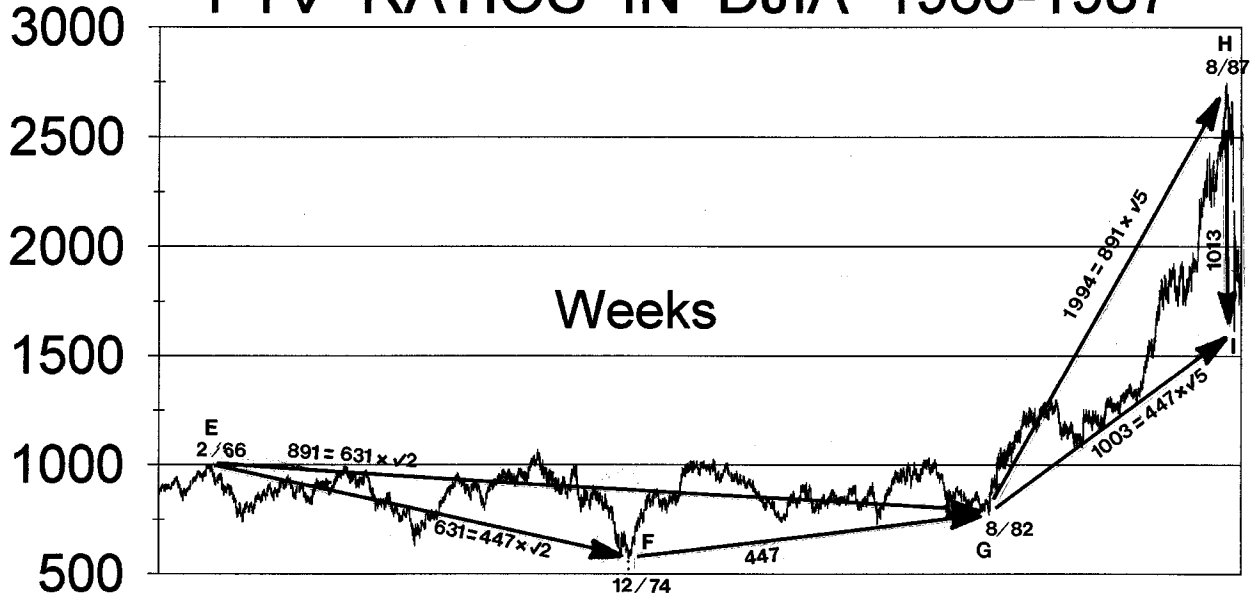


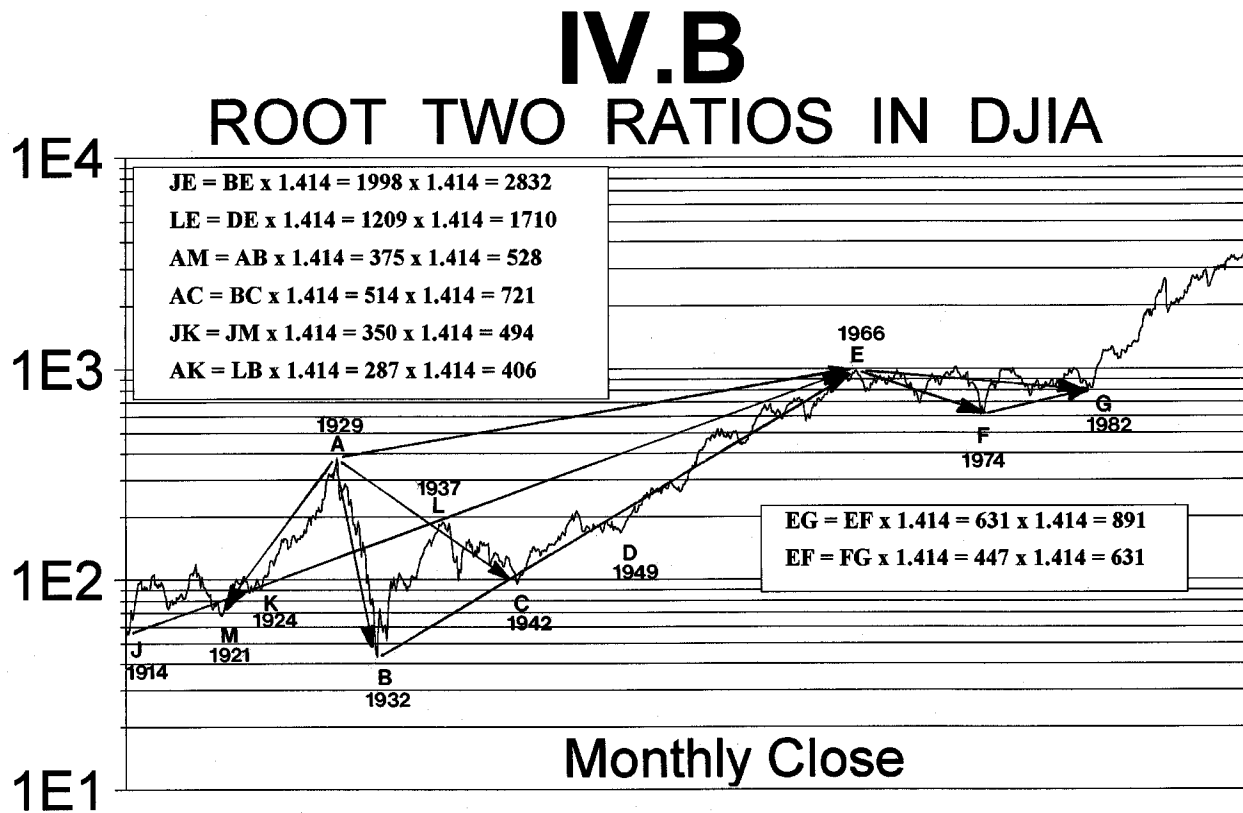
Table 4.1
PTV Calculations for Chart IV.A
Ratios in DJIA (2/1966 - 12/1987)

Price-Time Radius Vector	Date of Low	PTV Price Low	Date of High	PTV Price High	Time Change (weeks)	Price Change (points)	Vector Value (PTV)
EF	12/09 1974	570	2/09 1966	1001	461 Weeks	431 Points	631
FG	12/09 1974	570	8/09 1982	770	400 Weeks	200 Points	447
EG	8/09 1982	770	2/09 1966	1001	861 Weeks	231 Points	891
GH	8/09 1982	770	8/25 1987	2747	263 Weeks	1977 Points	1994
GI	8/09 1982	770	12/04 1987	1734	277 Weeks	964 Points	1003
EH	2/09 1966	1001	8/25 1987	2747	1124 Weeks	1746 Points	2077
HI	12/04 1987	1734	8/25 1987	2747	14 Weeks	1013 Points	1013

LONG-TERM STOCK MARKET EXAMPLES OF THE ROOT TWO RATIO

Application of the square root of two is not limited by the time scale. The division of the square to create the next level of the growth process occurs on an hourly chart, just as it does in the time frame covering the entire lifespan of the market, beginning from the date of the first official trade.

Chart IV.B shows several PTVs in the DJIA between 1914 and 1982. The data for these PTVs are included in Table 4.2.³² Described below are some of the square root of two ratios on this chart. There are many more examples of this ratio on Chart IV.B. However, only those necessary to explain the geometry of the solid they define are listed.³³ These geometric formations will be explained in the next lesson, **GEOMETRIC STRUCTURES**. Take the time to find the ratios listed below on Chart IV.B.



³² During the week of 3/6/1933 through 3/11/1933, the stock market was closed for the "Bank Holiday". One half of the next week it was also closed. Time calculations in this course using weekly data subtract the single complete week that the market was closed.

³³ Notice the smallest PTV in Table 4.2 is 287. This is W.D. Gann's second "Square of Twelve". In his *Master Course for Stocks* he provided an overlay called the "Square of Twelve", which has 0-144 on the vertical axis and 0-144 on the horizontal axis. The square of twelve is $144 = 288/2$.

Table 4.2 shows two squares of twelve defining two five-year cycles: 1932-1937 and 1937-1942. Neither of these would be visible if only the time or price axis were looked at.

The square root of two ratios within triangle EFG, between 1966 and 1982, were described in the previous section and are not repeated here.

$$JE = BE \times \sqrt{2} = 1998 \times \sqrt{2} = 2832 \quad (\text{This ratio worked out within } 0.23\% \text{ covering 52 years.})$$

$$LE = DE \times \sqrt{2} = 1209 \times \sqrt{2} = 1710$$

$$AM = AB \times \sqrt{2} = 375 \times \sqrt{2} = 528$$

$$AC = BC \times \sqrt{2} = 514 \times \sqrt{2} = 721$$

$$JK = JM \times \sqrt{2} = 350 \times \sqrt{2} = 494$$

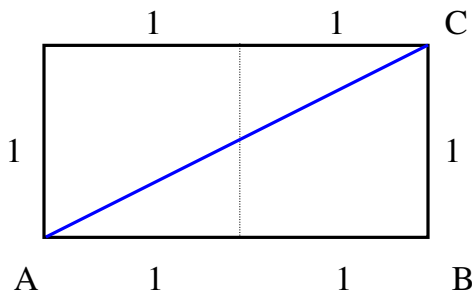
$$AK = LB \times \sqrt{2} = 287 \times \sqrt{2} = 406$$

MOST IMPORTANT NON-INTEGRAL RATIO IN STOCK MARKET ANALYSIS

The square root of five is the most important non-integral ratio in stock market analysis because it defines the growth spiral. Although a description of this spiral is included in Appendix G, it is recommended the reader study the material in the next lesson before reading that appendix.

The square root of five defines the diagonal of two adjacent squares, as shown in Figure 4.4.a, and can be considered the "grandfather" of the Fibonacci ratio, since PHI is derived from the square root of five. That is,

$$\frac{\sqrt{5}+1}{2} = 1.618 = \text{PHI}$$



$$\begin{aligned} AC &= \sqrt{AB^2 + BC^2} \\ &= \sqrt{2^2 + 1^2} \\ &= \sqrt{5} \end{aligned}$$

Figure 4.4.a

Diagonal of two squares showing square root of five ratio

Table 4.2
PTV Calculations for Charts IV.B and IV.C
12/1914 - 2/1966

Price-Time Radius Vector	Date of Low	PTV Price Low	Date of High	PTV Price High	Time Change (weeks)	Price Change (points)	Vector Value (PTV)
AB	7/8 1932	40.56	9/3 1929	386.1	148 Weeks	345	375
AC	4/28 1942	92.69	9/3 1929	386.1	659 Weeks	293	721
AE	9/3 1929	386.10	2/09 1966	1001	1900 Weeks	615	1997
AK	5/20 1924	88.33	9/3 1929	386.1	276 Weeks	298	406
AM	8/24 1921	63.9	9/3 1929	386.1	419 Weeks	322	528
BE	7/8 1932	40.56	2/09 1966	1001	1752 Weeks	960	1998
BD	7/8 1932	40.56	6/14 1949	160.62	883 Weeks	120	891
BC	7/8 1932	40.56	4/28 1942	92.69	511 Weeks	52	514
ED	6/14 1949	160.62	2/09 1966	1001	869 Weeks	840	1209
EL	3/10 1937	195.59	2/09 1966	1001	1509 Weeks	805	1710
EJ	12/24 1914	53.17	2/09 1966	1001	2669 Weeks	948	2832
JA	12/24 1914	53.17	9/3 1929	386.1	769 Weeks	333	838
JM	12/24 1914	53.17	8/24 1921	63.9	350 Weeks	10.7	350
JK	12/24 1914	53.17	5/20 1924	88.33	493 Weeks	35	494
LB	7/8 1932	40.56	3/10 1937	195.59	243 Weeks	155	288
LC	4/28 1942	92.69	3/10 1937	195.59	268 Weeks	103	287

The relationship between PHI and the square root of five is expressed geometrically in Figure 4.4.b, where PHI is derived from two adjacent squares, as was the square root of five in Figure 4.4.a. Figure 4.4.b is a double of Figure 3.3, which showed the Golden Section derived from the diagonal of the half square. Since the distances; $AE = 3.236$; and $BD = 2$; it follows,

$$\frac{AE}{BD} = \frac{3.236}{2} = 1.618$$

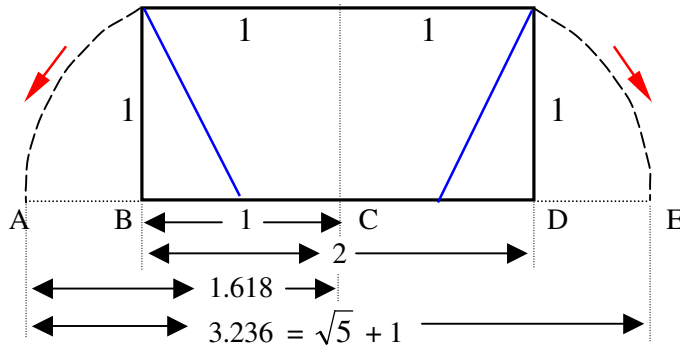


Figure 4.4.b

Fibonacci ratio derived from two adjacent squares

DJIA EXAMPLES OF THE SQUARE ROOT OF FIVE RATIO

The 2.236 ratio is obvious when the PTVs from Chart IV.A are calculated, as in Table 4.1. This table shows GH, which extended from the low on August 9, 1982 to the top on August 25, 1987, to be a nearly exact 2.236 multiple of EG, which extended from the high on February 9, 1966 to the low on August 9, 1982. That is,

$$GH = \sqrt{5} \times EG$$

Therefore, GH is the diagonal of two adjacent squares that have side length equal to EG. To check the exact ratio between these two PTVs, GH is divided by EG;

$$\frac{GH}{EG} = \frac{1994}{891} = 2.238$$

These PTVs span a time frame of over twenty-one years and still produce results with an error of less than two points. Accurately predicting a major market top that spanned a time frame of twenty-one years is quite an accomplishment.

The ideal theoretical value for GH is given by;

$$GH = EG \times \sqrt{5} = 891 \times \sqrt{5} = 1992.34$$

Producing an error of;

$$\frac{1994-1992.34}{1994} = \frac{1.66}{1994} = 0.08\%$$

Also, note that HI corrected the advance represented by GH. This value is a 50% retracement of GH.³⁴

That is,

$$\frac{HI}{GH} = \frac{1013}{1994} = 0.508 = 50.8\%.$$

This fifty percent correction gives a clue why the Fibonacci ratio, PHI = 1.62, seems to appear so often in financial market corrections.³⁵

LONG-TERM STOCK MARKET EXAMPLES OF THE ROOT FIVE RATIO

The square root of five ratio is a valuable tool for analysis as far back in time as reliable historical data is available. Chart IV.C shows the monthly stock market from 1914 to 1993. The data used to calculate the PTVs in this chart are included in Table 4.2.

The square root of five relationship between EG and GH has been previously analyzed. They are included in this chart to provide perspective on the magnitude of the time frame being studied.

The relationship between EG and GH is the same as between BD and BE. BD connects the bottom of the market in 7/1932 to the bottom in 6/1949, and has the same magnitude as EG. Also, the two PTVs, AE and BE, have the same magnitude as GH.

³⁴ Appendix B is an analysis of the retracement of 1987, known as the "crash of 1987".

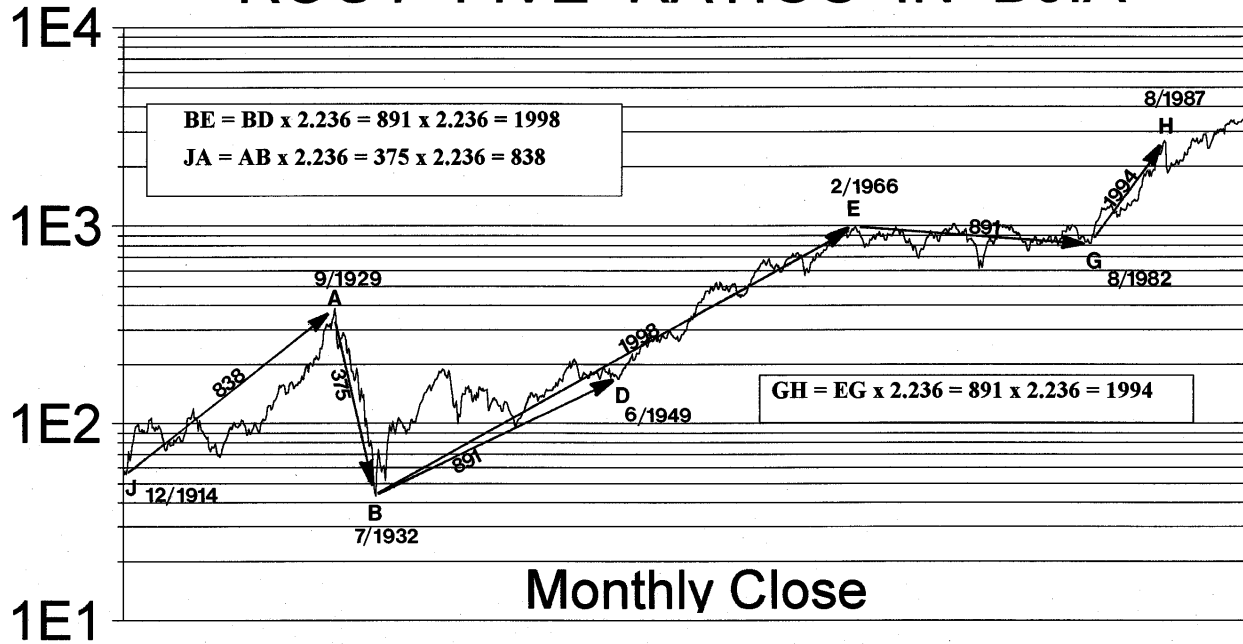
³⁵ It is worthwhile to take the time and study the following explanation, because it provides an understanding of how PHI is a product of market geometry, which will be explained in Lesson V.

- (1) From the section on the square root of two; $EG = EF \times \sqrt{2}$.
- (2) From the section on the square root of five; $GH = EG \times \sqrt{5}$.
- (3) Combining these two equations; $GH = (EF \times \sqrt{2}) \times \sqrt{5}$.
- (4) Since HI is a 50% correction; $HI = GH / 2$.
- (5) Combining the equations from (3) and (4);

$$HI = \frac{\sqrt{5} + \sqrt{2}}{2} \times EF = \frac{\sqrt{10}}{2} \times EF = 1.581 \times EF$$

(6) The end result, 1.581, is so close to 1.618, (difference of only 0.037), that many market analysts mistakenly identify a $\sqrt{10}/2$ ratio as PHI.

IV.C ROOT FIVE RATIOS IN DJIA



Therefore, the root five relationship exists between the two PTVs, AE and EG, spanning a time frame of fifty-three years from 1929 to 1982.

In summary, the three major square root of five ratios on Chart IV.C, between 1914 and 1987, are:

$$\begin{aligned}
 BE &= 1998 = BD \times \sqrt{5} = 891 \times \sqrt{5} \\
 GH &= 1994 = EG \times \sqrt{5} = 891 \times \sqrt{5} \\
 JA &= 838 = AB \times \sqrt{5} = 375 \times \sqrt{5}
 \end{aligned}$$

A THIRD RATIO MORE IMPORTANT THAN FIBONNACI

A circle is a cycle, complete when the entire circumference has been traversed. The circumference of a cycle is established when its diameter is defined. The value PI, 3.14, is the number that relates the diameter of a circle to its circumference and defines completion of the growth process.

In Figure 4.5.a the diameter, D, of the circle is AB. The circumference, C, is the distance around the circle and is defined as;

$$C = \pi \times D = 3.14 \times D$$

Another way to view Figure 4.5.a is to enclose the circle in a square, as in Figure 4.5.b. In this figure the diameter of the circle is equal to the side of the enclosing square.

That is, $D = AB$. Therefore, a circle inscribed within a square has a circumference equal to 3.14 multiplied by the length of the side of the enclosing square, $C = 3.14 \times AB$.

The previous section showed how the Fibonacci ratio, 1.62, could be derived from the square root of five. It can also be derived from PI, 3.14. That is,

$$1.62 = \frac{5}{3.14}$$

This demonstrates the intimate connection between the values of PI, PHI, and five. The **VALUE OF FIVE IS EXTREMELY IMPORTANT IN STOCK MARKET ANALYSIS** and will be covered further in Lesson V, **GEOMETRIC STRUCTURES**. Similarly, the two ratios previously described can approximate PI. That is, $\sqrt{5} \times \sqrt{2} = 3.16$. In many positions of the growth process of financial markets this value will be more applicable than the actual value of 3.14. However, for practical purposes the results obtained by using either of these values are very similar.

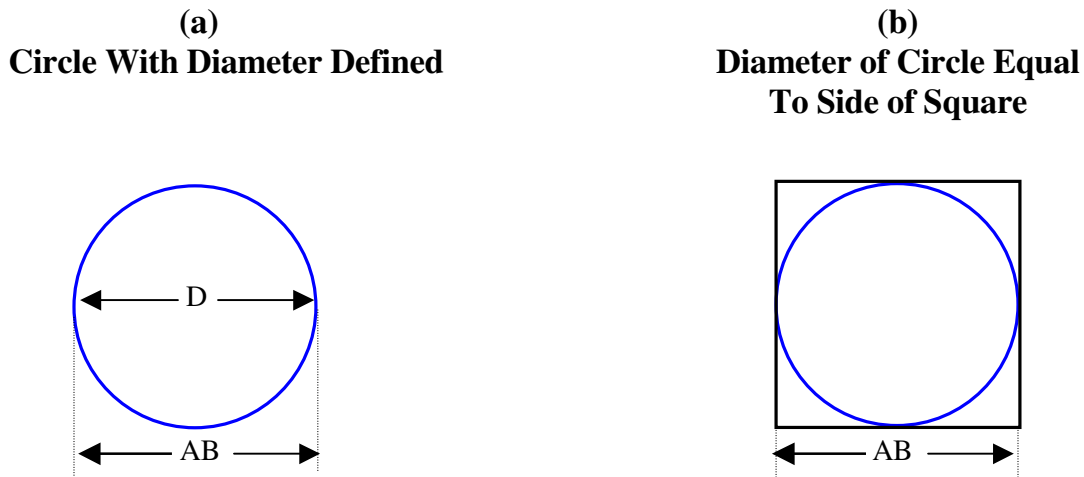


Figure 4.5
Diameter of circle equals the side length of the enclosing square.

DJIA EXAMPLES OF PI (3.14) RATIO

An application of the PI ratio is outlined below. Figure 3.4 showed that the PTV defining the major axis of the ellipse from 3/1982 to 8/1984 equaled 737. This is the same value calculated for its inverse ellipse, CE. When viewed on a two-dimensional price-time chart these two ellipses give the appearance of being contained within the limits of the larger square, AE. However, with an understanding of the three-dimensional geometry involved, these two ellipses can be seen to be different sides of the same ellipse, as shown in Figure 4.6. Only one side of an ellipse can be seen at a time on a two-dimensional price-time chart. The major axis of the ellipse in Figure 4.6 is the diameter of the larger circle from which the ellipse is derived, as was shown in Figure 2.2.a. The circumference of this circle is found by multiplying the diameter, $AC = 737$, by PI. That is,

$$\text{Circumference} = 3.14 \times 737 = 2315.$$

The result is the projected value for the completed cycle, as defined by the length of the PTV extending from the beginning of the cycle to its end. The actual length of this PTV, AG, was calculated in Table 3.1 to be 2323. This value is eight more than the theoretical value calculated above, producing an error of;

$$\frac{8}{2323} = 0.34\%$$

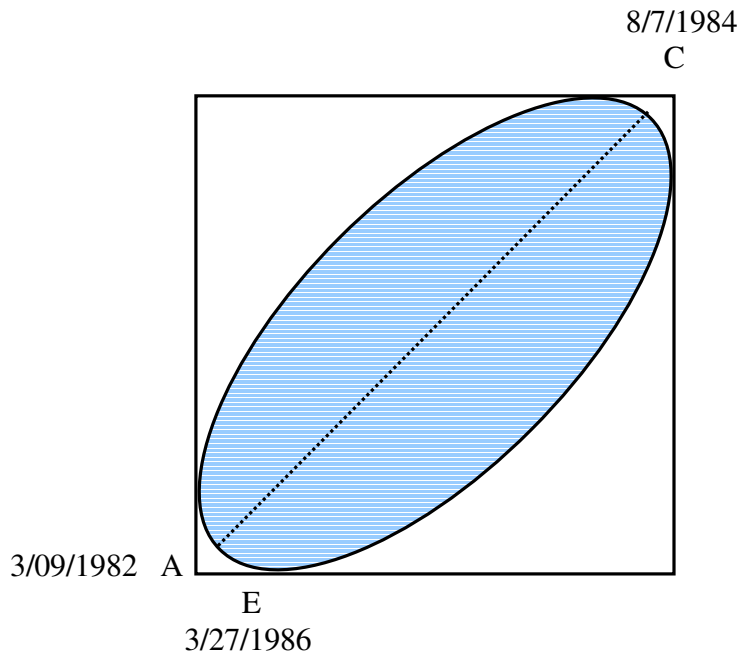


Figure 4.6

Both halves of the ellipse shown in Figure 3.4 (DJIA 3/09/1982 - 3/27/1986)

LONG-TERM STOCK MARKET EXAMPLE OF THE PI RATIO

A long-term example of the PI ratio is shown on Chart IV.A, where $EF = 631$, is multiplied by 3.14 to determine the end point of the completed growth pattern, which occurred on August 25, 1987, when GH equaled 1994. This provides a good example of the 3.16 value described earlier in this section. As previously described in the two sections on the square root of two and the square root of five, GH is defined by using the two ratios $\sqrt{2}$ and $\sqrt{5}$. That is,

$$\begin{aligned} EG &= EF \times \sqrt{2} \\ GH &= EG \times \sqrt{5} \end{aligned}$$

Combining these two results;

$$GH = (EF \times \sqrt{2}) \times \sqrt{5} = 1995.4$$

This result, 1995.4, is off from the actual value, 1994, by 1.4, for an error of;

$$\frac{1.4}{1994} = 0.07\%$$

Another application of the PI ratio using long-term historical data is shown on Chart IV.B. The PTV, JE, extends from 1914 to 1966, covering a period of fifty-two years. This PTV is the product of $\sqrt{5} \times \sqrt{2} \times EG$, where EG is the base of the square equal to 891. Previous sections in this lesson showed that;

$$\begin{aligned} AE &= EG \times \sqrt{5} = 1992 \\ JE &= AE \times \sqrt{2} \end{aligned}$$

Combining the two above equations to get the theoretical value for JE;

$$JE = (EG \times \sqrt{5}) \times \sqrt{2} = 1992 \times \sqrt{2} = 2818$$

Table 4.2 calculated the actual value for JE to be 2832, which produces an error from the theoretical value of;

$$\frac{2832-2818}{2832} = \frac{14}{2832} = 0.49\%$$

A FOURTH RATIO MORE IMPORTANT THAN FIBONNACI

To this point this lesson has focused on ratios appearing in two-dimensional growth patterns. However, as will be demonstrated in Lesson V, **GEOMETRIC STRUCTURES**, markets do not unfold within the confines of two dimensions.

If six squares are put together at right angles to each other a cube is formed, as shown in Figure 4.7. This figure also shows the diagonal of the cube, AE, crossing from one corner to the opposing corner. This diagonal has length equal to the square root of three ($\sqrt{3} = 1.73$).³⁶

Similarly, it was previously shown that the ratio between radii of two circles, one inscribed within a square and one circumscribed around a square, is the square root of two. The three-dimensional counterpart of this configuration is a sphere contained within a cube, which is itself contained within a second sphere. The ratio of the radii of two such spheres is the square root of three.

This ratio is tricky to identify on two-dimensional price-time charts because it inherently defines a three-dimensional ratio. Because this could be a source of confusion for

³⁶ Since the square has side length, EC, equal to one, the diagonal of the square, AC, is $\sqrt{2}$. With these two values the diagonal of the cube, AE, is calculated using ACE as the right triangle. That is, $AE^2 = AC^2 + CE^2 = \sqrt{2}^2 + 1^2$. Therefore, $AE = \sqrt{3} = 1.73$.

the reader, less attention will be devoted to this ratio than the three previously defined. When the reader is more comfortable with the three-dimensional geometry of financial markets, this ratio should be further studied. Until then, it is not critical to understand the square root of three ratio to practically apply the ratios previously presented.

Two examples are given of the square root of three ratio originating from the 7/1932 bottom.

$$AE = AB \times \sqrt{3}$$

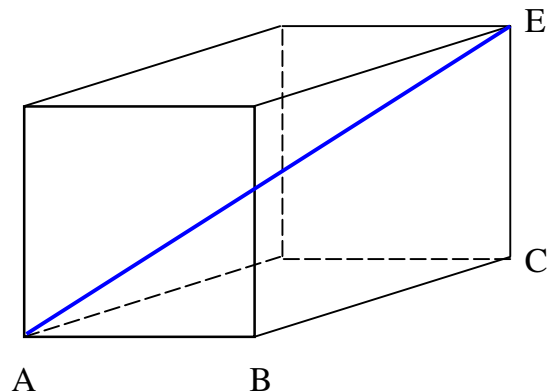


Figure 4.7

Diagonal of a cube showing square root of three ratio

LONG-TERM STOCK MARKET EXAMPLES OF THE ROOT THREE RATIO

Chart IV.D shows a sequence of PTVs with ratios equal to the square root of three. The data used to calculate these PTVs are contained in Table 4.3.

Two pairs of items in Table 4.3 are in the ratio of the square root of three.

$$BD = BC \times \sqrt{3} = 514 \times 1.73 = 891$$

$$JK = LB \times \sqrt{3} = 288 \times 1.73 = 494$$

SUMMARY

This lesson dealt with stock market ratios in two and three dimensions. Each ratio was demonstrated on its own chart to avoid cluttering. These ratios were devoted to growth patterns represented by squares and composites of squares in two and three dimensions.

In the next Lesson, these charts will be put together to see how these ratios create geometric structures in the stock market.

IV.D ROOT THREE RATIOS IN DJIA

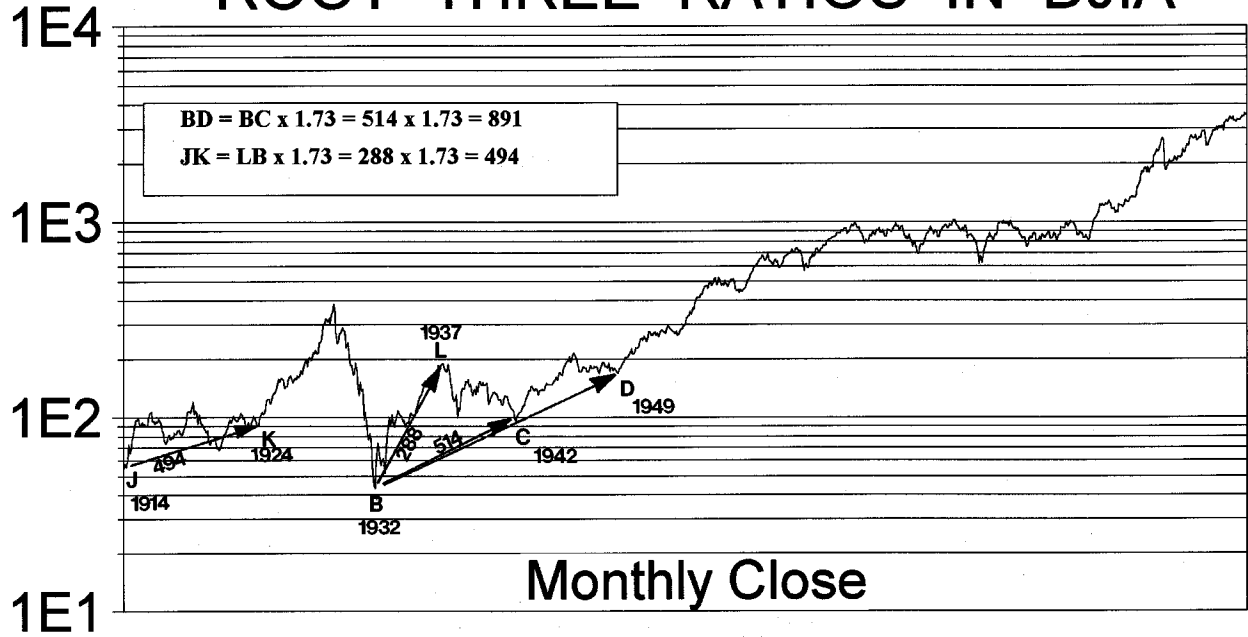


Table 4.3
PTV Calculations for Chart IV.D
Square Root of Three Ratios in DJIA
12/1914 - 6/1949

Price-Time Radius Vector	Date of Low	PTV Price Low	Date of High	PTV Price High	Time Change (weeks)	Price Change (points)	Vector Value (PTV)
BC	7/8 1932	40.56	4/28 1942	92.69	511 (Weeks)	52	514
BD	7/8 1932	40.56	6/14 1949	160.62	883 (Weeks)	120	891
JK	12/24 1914	53.17	5/20 1924	88.33	493 (Weeks)	35	494
LB	7/8 1932	40.56	3/10 1937	195.59	243 (Weeks)	155	288

LESSON V

GEOMETRIC STRUCTURES

Geometry existed before the Creation, it is co-eternal with the mind of God, is God himself.

Johannes Kepler (1630 A.D.) ...Harmonice Mundi (Harmony of the World)

INTRODUCTION

Previous lessons explained the multi-dimensional nature of price-time. This lesson will provide additional proof of this powerful concept, as price-time charts will be shown to be nothing more than a two-dimensional sequential recording of geometric solids in motion.

Financial markets unfold in price-time within the confines of predetermined points of force. The relative locations of these points in three dimensions form geometric structures. This phenomenon is not unique to financial markets. Matter creates clearly defined geometric structures when it attains a stable state. Geologists apply the "crystal lattice" structure to classify minerals by looking at the geometric arrangement of their planes of cleavage. Similarly, chemists can identify an element by looking at the geometry of its constituent atoms.³⁷ These applications are nothing more than simple three-dimensional geometry. As previously explained, financial markets are not exempt from natural law, including this one.

The reader may have had the opportunity in the past to try a puzzle where he imagined what figure is created when a piece of paper is folded along a variety of dotted lines. This type of mental exercise requires using the abstract or right hemisphere of the brain. There is very little in modern academia that encourages the development of this ability. In fact, our whole western civilization is primarily based upon usage of the logical or left hemisphere of the brain. In western society if a conclusion cannot be logically derived it is presumed fallacious.

This is not the case throughout the world. Several eastern societies demonstrate an emphasis on "intuitive wisdom", or conclusions that are not limited by the sequential derivation required of the left hemisphere of the brain. In the sixth century B.C. the Chinese philosopher, Lao Tzu, wrote the work *Tao Te Ching*, which was intentionally styled to demand an intuitive conceptualization of reality.³⁸ In fact, this philosophy held a certain contempt for logical reasoning, considering it part of an artificial world created by man.

³⁷ Technical References: *Chemistry, Reactions, Structures and Properties*, P. 500-504,
Fundamentals of Physics, P. 309, 948.

³⁸ The limited records during this time make it impossible to attribute to Lao Tzu the entire writing of *Tao Te Ching*, which literally translates as "Classic of the Way and Power". Contemporary thought is that other authors over a period of time contributed to this work.

Lao Tzu, whose name means "Old Master", originated the philosophy of Taoism.

Referring to Taoism, the philosopher, Chuang Tzu, stated in 400 B.C.;

"The most extensive knowledge does not necessarily know it; reasoning will not make men wise in it. The sages have decided against both these methods."

In this lesson the reader will use his abilities of abstraction to see the geometric patterns unfolding in the stock market. If this seems difficult at first, do not despair. This type of thinking has been practiced for centuries, and a little mental work will make this exercise much easier.

TWO-DIMENSIONAL GEOMETRY

This discussion of two-dimensional geometry is valuable as a first step to understanding true four-dimensional market geometry. As will be explained in the section on three-dimensional geometry, **ONE SIDE OF THE GEOMETRIC STRUCTURE IS VISIBLE IN OUR PERCEPTION AT A TIME.**

The limitation of a two-dimensional analysis of price-time charts is seen during the period when one side of the geometric structure completes and the entire structure appears to rotate to expose the new face. These are the periods when financial market analysts are most confused. The cycles they have been following suddenly "disappear", and a seemingly new set of cycles replaces them. These analysts find themselves waiting for cycle bottoms or tops that never arrive. To understand the transition between two-dimensional faces, three-dimensional geometry must be studied. The relationships between the sides of these three-dimensional structures are predictable if the nature of the complete geometric structure is understood. Three-dimensional geometry will be explained later in this lesson. First, a certain amount of background knowledge must be developed in the form of two-dimensional geometry.

When a living cell reproduces it internally divides in half, creating a condition where each new cell has half the area of the original cell. The cells then separate and grow to maturity with an area equal to that of the original cell. This process of fission creates two cells with a combined area twice the original cell.

Geometrically, this process of division is represented in Figure 5.1.a, where square ABC is the original area beginning the division process by dividing in half along diagonal, AC. As described in Lesson IV, **PRICE-TIME RATIOS MORE IMPORTANT THAN FIBONACCI**, this diagonal has length 1.414 times the side of the square, AB. The diagonal is the longest line that can be used within the square to divide it into two equal parts.³⁹

To create a square with twice the area of the original the diagonal, AC, of square AB is used as a side of the new square, ACDE, in Figure 5.1.b. Since the side of the new square

³⁹ References: *Connections – The Geometric Bridge Between Art and Science*, P. 451;
Sacred Geometry

is the square root of two, it follows that the area of the new square is two. The area of a square is simply the square of the side. The square root of two multiplied by itself is two.

Figure 5.1.c shows a continuation of this process to the next division of the cell. The diagonal of square, ACDE, defines the side of the next new square, ADGF. This new square has an area twice that of ACDE and four times that of the original square, ABC.

The relative relationships between these three figures are as follows:

Ratios between the lengths of the sides of the squares:

$$ABC : ACDE : ADGF = 1 : \sqrt{2} : 2$$

Ratios between the areas of the squares:

$$ABC : ACDE : ADGF = 1 : 2 : 4$$

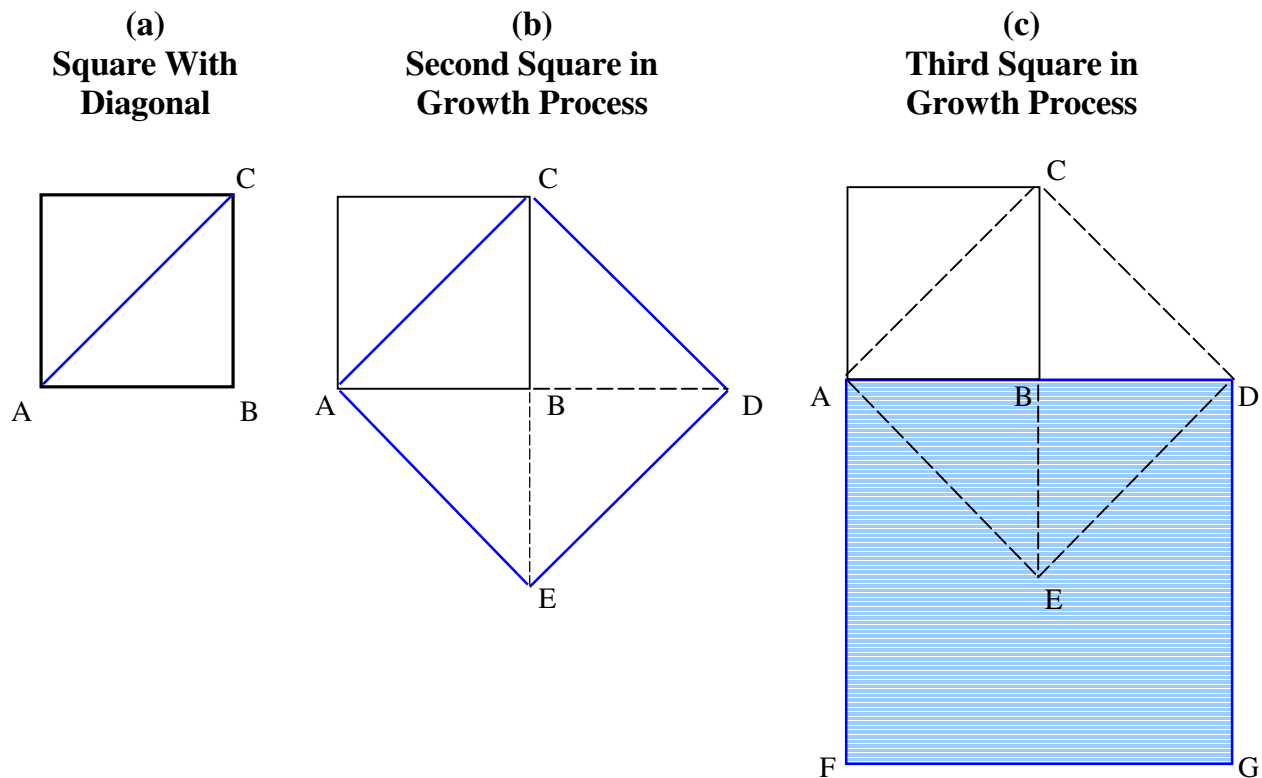


Figure 5.1

Two-dimensional geometric growth process defined by root two

DJIA EXAMPLES OF TWO-DIMENSIONAL DIVISION OF THE SQUARE

The growth process shown in Figure 5.1 was visible in the stock market during the sideways choppy market from the top in 2/9/1966 to the bottom in 8/9/1982. Because this period represented a pattern of decomposition rather than growth, successive PTV lengths **DECREASED** by the root two ratio. That is, the PTV represented by Figure 5.1.a occurred as the last vector in the sequence rather than the first.

On Chart IV.A the PTV between 12/9/1974 and 8/9/1982, FG, represents the side of the original square, as shown in Figure 5.1.a. Since FG advanced 200 points in 400 weeks, it also defined the diagonal of two smaller adjacent squares, as shown in Figure 5.2.a.⁴⁰

Table 4.1 in Lesson IV showed that the ratio between the two PTVs: FG between 12/9/1974 and 8/9/1982, and EF between 2/9/1966 and 12/9/1974 was the square root of two. Therefore, EF is the PTV representing a level of the growth process that was one higher than that represented by FG. This is graphically shown in Figures 5.1.b and 5.2.b, where EF is the diagonal of the square with side, FG.⁴¹

EG is the PTV representing the side of the square defining the complete decomposition between 1966 and 1982. This is graphically shown in Figures 5.1.c and 5.2.c. Table 4.1 in Lesson IV showed EG to have the value of the square root of two times EF or similarly, two times FG.

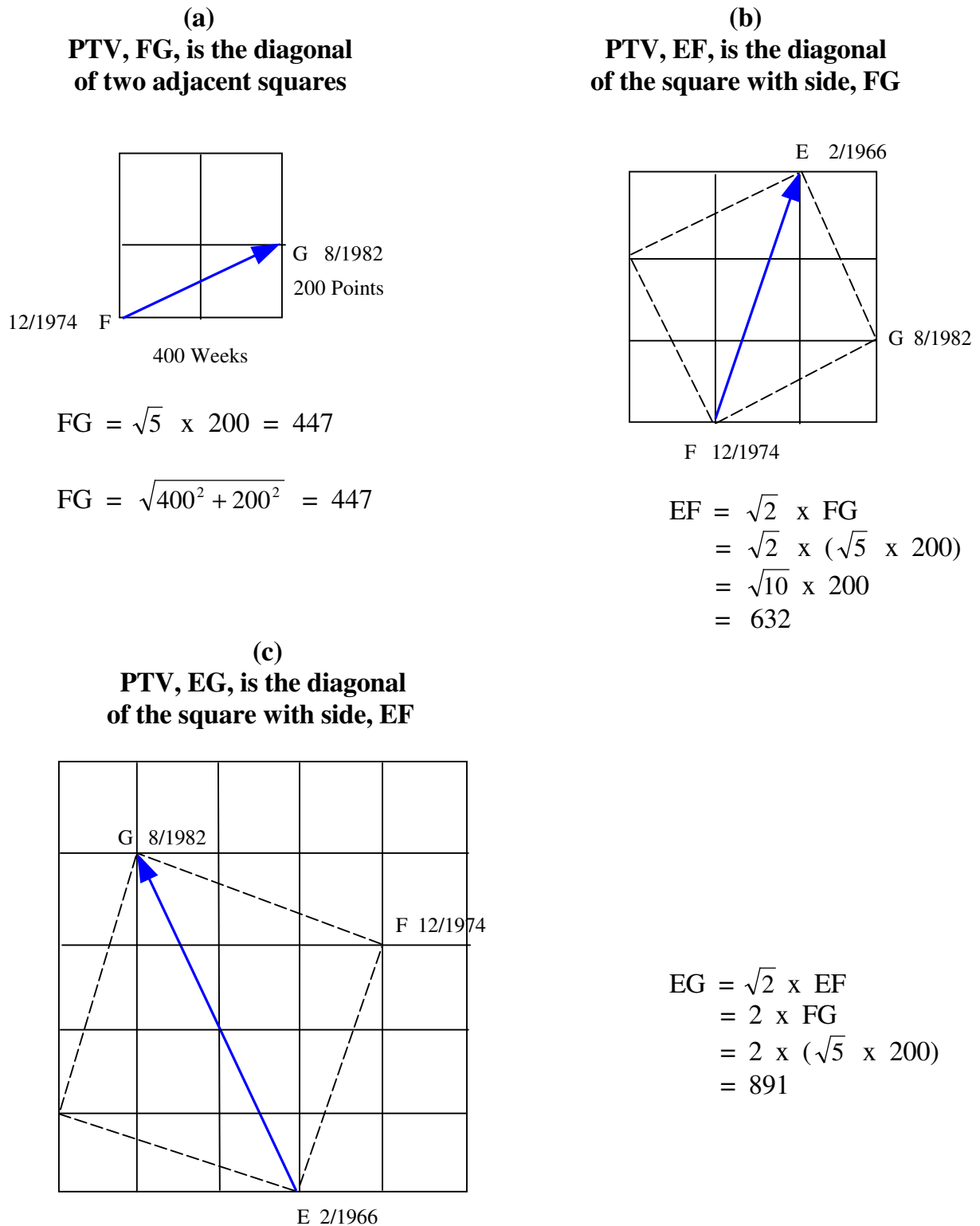
Figure 5.2 also shows why the Fibonacci growth spiral is commonly found in financial markets. When the three successive PTVs; FG, EF, and EG are placed within the squares that contain them, the side length of these squares grow in accordance with the Fibonacci sequence. Figure 5.2.a has side length of two. Figure 5.2.b has side length of three. Figure 5.2.c has side length of five. Two, three, and five are successive numbers in the Fibonacci number sequence.

At first glance it may seem that 5.2.c could be drawn with only four squares, rather than five. However, the necessity of the fifth square can be seen when the squares are placed within each other, as shown in Figure 5.3.

⁴⁰ This is the basis of W.D. Gann's 1x2 diagonal angle. It is the diagonal of two adjacent squares. As shown below Figure 5.2.a, the square root of five is the PTV that defines this geometric structure.

⁴¹ The length of EF is the square root of **TEN** times the side of one of the smaller squares. That is, $EF = \sqrt{10} \times 200 = 632$.

The square root of ten was explained in Lesson IV, **PRICE-TIME RATIOS MORE IMPORTANT THAN FIBONACCI**, as the square root of two multiplied by the square root of five. Geometrically, this is represented by a 3x1 rectangle, as shown in Figure 5.2.b.

**Figure 5.2**

Two-dimensional squares containing the PTVs from 1966 to 1982. These squares contain circles that define successive wraps on the three-dimensional conical helix.

Figure 5.3 combines the three squares from Figure 5.2 into one figure, and shows the relative growth of the magnitudes of the respective PTVs. The ratios between these PTVs display a square root of two geometric proportion. Each of these radii vectors define the interval of operation within the growth phase taking place within that square. After each growth phase completes, the next radius vector defines the next interval. If the growth process is that of decomposition, as it was during the period between 1966 and 1982, the larger radius vector, EG, decomposes by the root two proportion until decomposition is complete. The decomposition between the dates 1966 and 1982 was complete when radius vector FG completed on August 9, 1982 with a proportion to the preceding vectors, EF and EG, in the ratio of the square root of two.

The period between 1929 and 1932 also represented decomposition of the growth process taking place at that time. The length of the PTV during the decline between 1929 and 1932 was equal to the length of the PTV during the preceding advance from 1921 to 1929, divided by the square root of two. This is shown in Figure 5.4 where the two PTVs, AB and MA, are shown to be in the ratio of the square root of two.

The square shown in Figure 5.2.c extended from 1966 to 1982. This square is one face of a four-dimensional structure, which is reflected onto two dimensions in price-time charts. Only one face of this four-dimensional structure is visible at a time as it rotates into view. Price-time charts provide a convenient historic record of each of these faces as they present themselves.

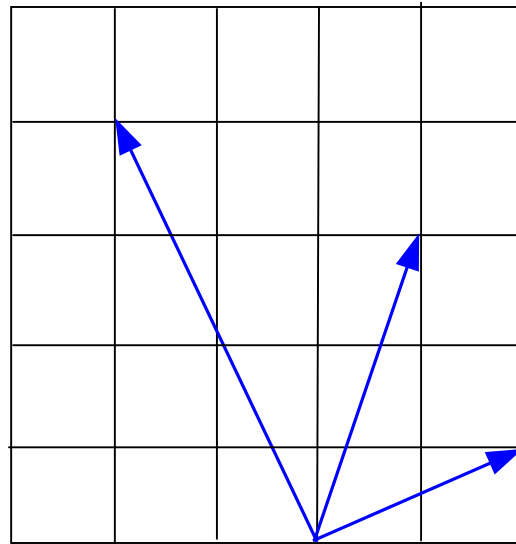


Figure 5.3

Combined radii vectors EF, FG, EG from Figure 5.2, showing root two progression in the lengths of the PTVs between 1966 and 1982

ADVANCED TOPICS IN DJIA EXAMPLES OF DIVISION OF THE SQUARE

The smaller square, defined by FG, was the next level of decomposition following the EF square. These two squares and the PTVs that defined them were intimately connected. If the orientation of one of these squares changed the other would have to adjust, accordingly.

The smaller PTV, FG, defined the diagonal of a 1x2 rectangle (200 points x 400 weeks). This PTV was the side of the square, whose diagonal, EF, was the side of the next larger square, as shown in Figure 5.2. Therefore, the length of EF is given by the diagonal of the 1x3 rectangle ($\sqrt{10}$), shown in Figure 5.2.b, **NOT THE DIAGONAL OF A 2x2 SQUARE**. That is,

$$EF = \sqrt{10} \times 200 = 632.$$

In contrast, if EF had been defined by the diagonal of the square with side 400 it would have followed the 45° angle more closely, as did the 1949-1966 square, and its length would have been;

$$EF = \sqrt{2} \times 400 = 566$$

TWO-DIMENSIONAL SQUARE STRUCTURES IN THE DJIA (1899-1949)

Figure 5.4 shows the six squares that developed in the stock market between December, 1899 and June, 1949. These six squares formed the sides of a cube that unfolded during this time. The data for Figure 5.4 are included in Tables 5.1 and 4.2.

The period between 1899 and 1914 contained two squares, which were laterally traversed, as represented by NJ. The value of NJ was 761, which was twice the value of the side of the square from 1929 to 1932, and twice the value of the square from 1942 to 1949. The stocks in the DJIA index before the close in 1914 were dramatically different than those after the reopening. This is the cause of the slight distortion between theoretical values and actual data when comparing periods before and after the close in 1914.

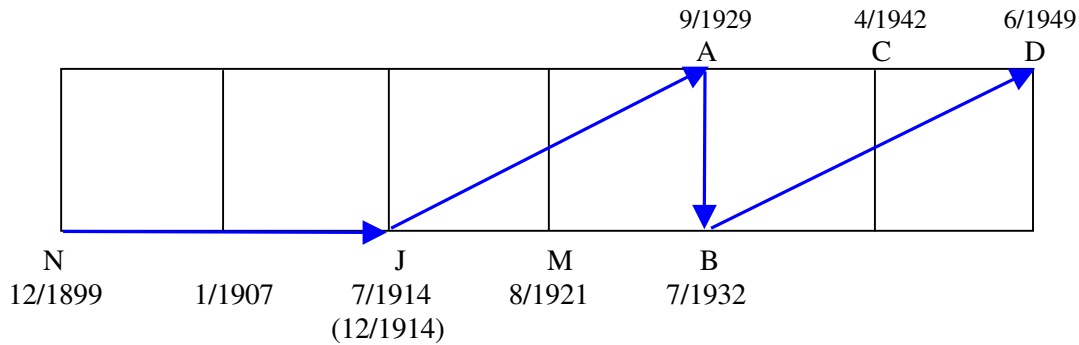
When the first square completed in 1907 the decline was dramatic enough to be called "the rich man's panic", and prices were nearly cut in half in ten months.

The two squares within NJ combined to produce the base of a larger cube, which extended from 1899 to 1982. In other words, the square that produced the base of the larger 1899-1982 structure subdivided into two parts to create squares one and two in Figure 5.4. This fact must be remembered because following sections explaining the 1899-1982 structure treat NJ as a single larger square. Similarly, the two squares from 1914 to 1929 compose a single larger square, as do the squares from 1932 to 1949. These larger squares define sides of a larger cube that contains the smaller cube shown in Figure 5.4.

Table 5.1
PTV Calculations for Figure 5.4
(See Chart V.B)

Price-Time Radius Vector	Date of Low	PTV Price Low	Date of High	PTV Price High	Time Change (weeks)	Price Change (points)	Vector Value (PTV)
AB	7/8 1932	40.56	9/3 1929	386.1	148 Weeks	345	375
CD	4/28 1942	92.69	6/14 1949	160.6	372 Weeks	67.9	378
MA	8/24 1921	63.9	9/3 1929	386.1	419 Weeks	322	528
JA	12/24 1914	53.2	9/3 1929	386.1	769 Weeks	333	838
NJ	12/2 1899	75.7	7/2 1914	80.64	761 Weeks	5	761

$$\begin{aligned}
 MA &= 528 = AB \times \sqrt{2} & BC &= 514 \cong MA \\
 JA &= 838 = AB \times \sqrt{5} & CD &= 378 = AB
 \end{aligned}$$



$$NJ = 761 = AB \times 2$$

$$AB = 375$$

Figure 5.4
 Squares forming six faces of cube in DJIA from 12/1899 to 6/1949
 (See Chart V.B)

Because the market was closed between 7/31/1914 and 12/12/1914, NJ terminated in 7/1914 and JA began in 12/1914.

Between 1914 and 1929 two squares completed. The size of these squares equaled the two squares between 1899 and 1914. The action within the 1921-1929 square differed from the three preceding it by crossing the square diagonally.

From Table 5.1 it can be seen that the length of the side of the squares during this time period was 375. That is, AB equaled 375, CD equaled 378, and twice this amount, 761, was expended in the dimension of time between 1899 and 1914.

Since it is known that the length of the side of the square during this time was 375, it follows that a diagonal of one of these squares is given by the square root of two ratio. That is,

$$\text{Diagonal of a square in Figure 5.4} = \sqrt{2} \times 375 = 530$$

This is the value of MA from the bottom on 8/24/1921 to the top on 9/3/1929.

The error between the actual value of MA and the ideal theoretical value, calculated above, is;

$$\frac{530 - 528}{530} = \frac{2}{530} = 0.38\%$$

Figure 4.4.a showed that the diagonal of two adjacent squares is $\sqrt{5}$ times the length of the side of one of the squares. Therefore, it follows that JA, which is the diagonal of the two squares from the bottom on 12/24/1914 to the top on 9/3/1929 must equal:

$$\text{Diagonal of two squares in Figure 5.4} = \sqrt{5} \times 375 = 838$$

This theoretical value matched the actual data perfectly. The diagonal of the two squares represented by JA is shown in Figure 5.4 to be 838.⁴²

Analysts applying the traditional "Gann angles" of 45^0 and $1x2$ to two-dimensional price-time charts are not aware of the geometric arrangement outlined above. This is because the diagonal of the square, MA, did not follow the 45^0 angle. Nor did the diagonal of two squares, JA, follow the $1x2$ angle. Similarly, Gann analysts drawing the $1x2$ angle from the 9/3/1929 top see the action consistently drop below that angle. Between 1929 and 1932 the market dropped 345 points in 148 weeks. In contrast, the $1x2$ angle dropped 296 points during this same time frame. The reason the action did not follow the ideal angles is:

⁴² Appendix G provides a closer look at the growth spiral that defined the squares formed between 1921 and 1932. It is recommended the reader reference that material at this time.

PRICE-TIME ACTION WITHIN A SQUARE ONLY FOLLOWS THE 1x2, 45⁰, OR 2x1 ANGLES IF THE ORIENTATION OF THE SQUARE IS ITSELF SQUARE WITH THE PRICE AND TIME AXES OF THE CHART. IF THE SQUARE CONTAINING THE ACTION IS ROTATED EITHER DIRECTION WITH RESPECT TO THE AXES OF THE CHART, THE ANGLES WITHIN THAT SQUARE ARE ALSO ROTATED, ACCORDINGLY.

The orientation of the squares containing the action between 1914 and 1932 was rotated in a clockwise direction. Appendix G showed that the relative orientation of the two PTVs, JA and AB, was fixed by the square root of five growth spiral. Consequently, the angles followed by these two PTVs were fixed relative to each other, and not the price and time axes of the chart.

This is further evidence that true geometric configurations remain unseen unless the action is viewed from a perspective not limited to a single dimension. Analysis using PTVs provides such a perspective.

TWO-DIMENSIONAL SQUARE STRUCTURES IN THE DJIA (1932-1987)

If the squares defining the market activity from the bottom in 7/1932 until after the crash of 10/1987 are placed together, the two-dimensional structure shown in Figure 5.5 is produced. The data for the PTVs in this figure are contained in Tables 4.1 and 4.2.

In this figure it is seen that BE, from 1932 to 1966, has the same length as GH, from 8/1982 to 8/1987.⁴³ Both these PTVs represent diagonals of two adjacent squares, which had side length equal to 891. Hence, their magnitude is given by the square root of five ratio. That is,

$$GH = BE = 1994 = \sqrt{5} \times 891$$

This ratio was calculated in the previous lesson, **PRICE-TIME RATIOS MORE IMPORTANT THAN FIBONACCI**. Refer to that lesson for the calculation of the small error between the actual and the ideal theoretical values.

The difference between the two squares represented by GH and BE is that one took 34 years to work out and the other took only 5 years. This is possible because the 1932 to 1966 squares are lying next to each other, and the 1982 to 1987 squares are stacked on top of each other. This can be seen in Figure 3.4, where the rectangle lying flat, AC, was formed early in the growth process when the exponential curve was relatively flat. As the curve arcs upward the squares defining the price-time action stack on top of each other, such as CE in Figure 3.4, rather than next to each other as they do early in the growth process.

⁴³ Compare Figure 5.5 with Figure 3.4, which showed two 3x2 rectangles at different points in the growth process.

Two other PTVs in Figure 5.5 have the same length. BD is the PTV from 7/1932 to 6/1949 and has the same length as EG, from 2/1966 to 8/1982. Both these PTVs equal 891 and represent the sides of completed squares.

When the squares formed during the time period between 1899 and 1949 they were at a lower energy level than those created after 1949. This is clearly seen if the entire period from 1899 to the present is graphed on the same chart. The price movements in the earlier period were only a fraction of those occurring more recently at the higher energy level. Chart I.C was intentionally graphed with a linear price scale, rather than a logarithmic scale to demonstrate the dramatic increase in price swings after 1949.

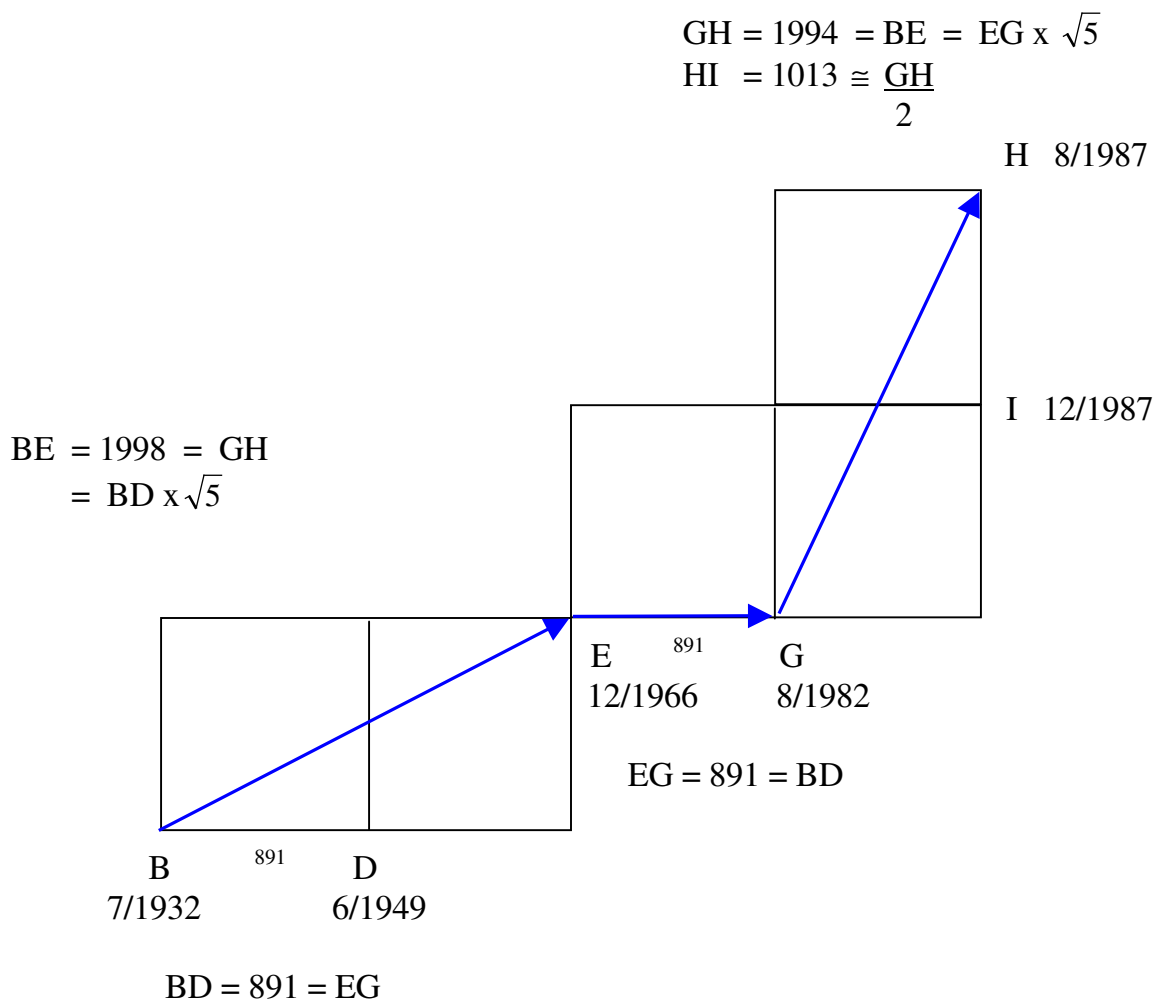


Figure 5.5

Two-dimensional square structures in the DJIA from 7/1932 - 12/1987

The magnitude of the difference between these two time periods, when measured by their PTVs, is the square root of two minus one, i.e.,

$$1.414 - 1 = 0.414.$$

To demonstrate the difference in energy levels between the smaller squares shown in Figure 5.4 and the larger squares shown in Figure 5.5, the ratios of the sides of the squares in each time period are measured and compared, i.e.,

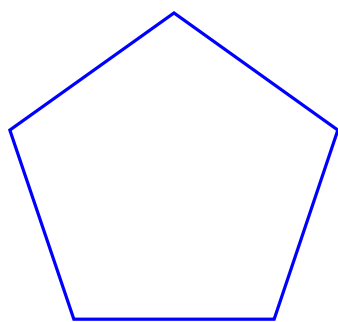
$$\frac{375}{891} = 0.42$$

For a geometric explanation of this ratio, refer to Figure 4.2 in Lesson IV, **PRICE-TIME RATIOS MORE IMPORTANT THAN FIBONACCI**.

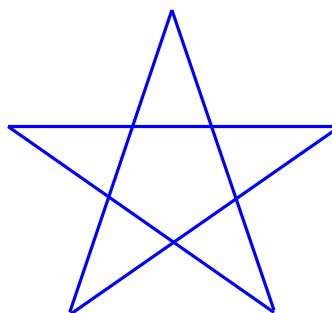
PENTAGONAL (FIVE-FOLD) SYMMETRY OF LIVING ORGANISMS

As living organisms grow they often demonstrate what is known as "five-fold symmetry". This simply means a pentagonal pattern, as shown in Figure 5.6.

The pentagon possesses many interesting characteristics including the Fibonacci ratio (PHI). Pythagoras used the pentagon to identify the select members of his very exclusive group. For centuries astrologers and mystics have used this symbol as an instrument into the world of the "supernatural".⁴⁴



PENTAGON



PENTAGRAM

Figure 5.6
Pentagonal form

⁴⁴ It is not the intention to make some mystical claim about the pentagon, rather to provide a short history of its usage. This work is only concerned with what is provable and easily demonstrated in nature and hence, financial markets.

Five-fold symmetry does not exist in inanimate objects. Only living plants and animals have five-fold symmetry. No crystal structures, whether they are snowflakes or are from the mineral world, exhibit five-fold symmetry. The most common arrangement of flower petals is five petals per stem. Horticulturists know that edible plants, or those that produce edible fruit, tend to have five leaves. In contrast, poisonous plants tend to have six or seven leaves.⁴⁵

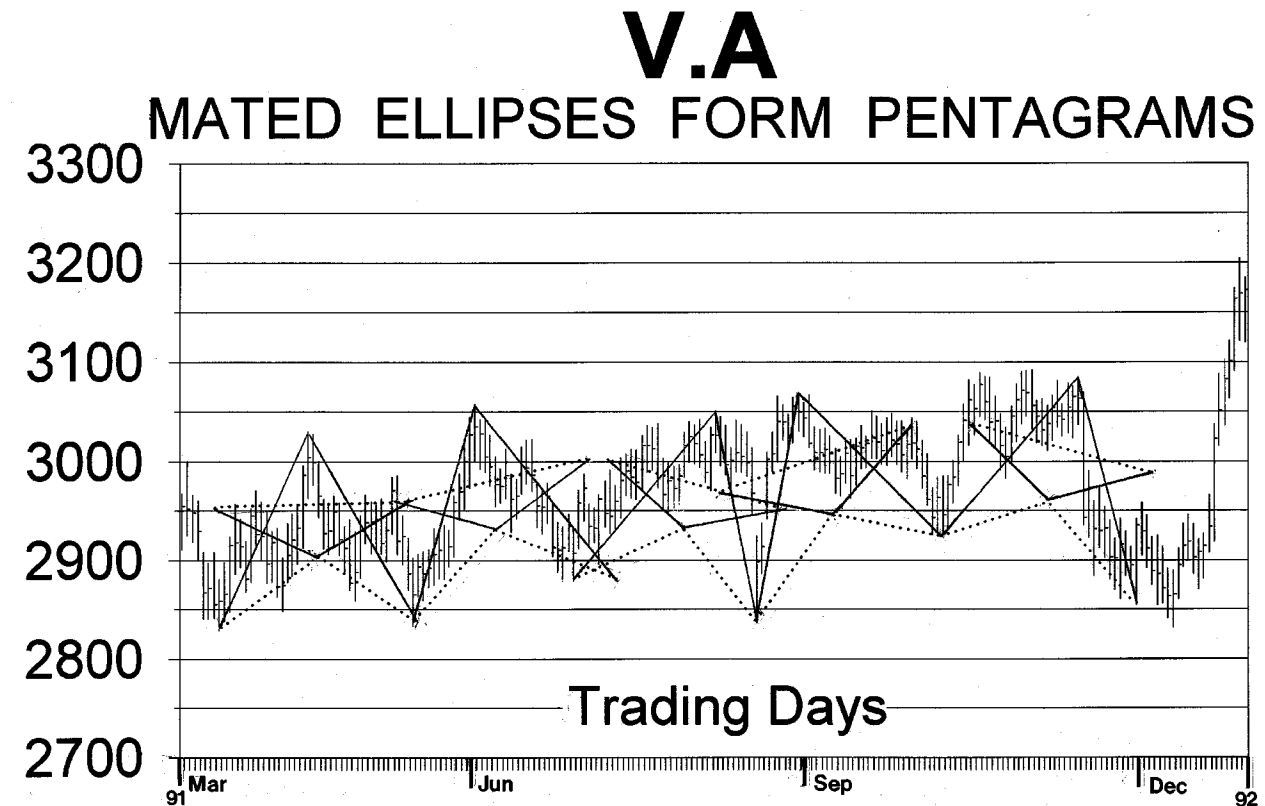
Even the human figure demonstrates five-fold symmetry with two arms, two legs, and a head, creating five appendages to the trunk. Five fingers and five toes are attached to the ends of these appendages.

DJIA EXAMPLES OF TWO-DIMENSIONAL PENTAGONAL SYMMETRY

Chart V.A shows the ellipses from Chart II.B drawn without their perimeters, i.e., only the major and minor axes of the ellipses have been drawn. This chart shows that the major and minor axes of two mated ellipses⁴⁶ interlock to form the pentagonal pattern.

SUMMARY OF TWO-DIMENSIONAL STOCK MARKET STRUCTURES

The preceding description of two-dimensional geometry showed how the diagonal of the square represents nature's division of unity into two equal parts. This ratio is seen in the



⁴⁵ Reference: *Patterns in Nature*.

Connections – The Geometric Bridge Between Art and Life, P. 405-452.

⁴⁶ Mated ellipses were described in Lesson II, **THE ELLIPTICAL NATURE OF PRICE-TIME**.

sequence of squares developing in the stock market, depending upon whether the square is crossed laterally or diagonally.

Relationships were shown identifying certain PTVs as either the side of a square, the diagonal of a square, or the diagonal of two adjacent squares. The actual values calculated from the historic data had less than one percent error when compared to the ideal theoretical values.

In the next section the arrangement of these squares will be shown to clearly form three-dimensional structures as seen on two-dimensional price-time charts.

THREE-DIMENSIONAL GEOMETRY

To this point this lesson has only addressed two-dimensional geometry. Two-dimensional analysis is useful when looking at a single face of the geometric solid at a time. However, a three-dimensional perspective is required to understand the anomalies encountered in price-time when the two-dimensional face of the structure completes its growth process and the structure rotates to expose the new face. This section provides the tools for a three-dimensional analysis of price-time geometry.

Traditional two-dimensional price-time charts of financial markets do not accurately represent the motion. This limitation of two-dimensional charts results in the appearance of price-time twisting into and turn out of the page of observation. However, as will be explained in Lesson X, **DIMENSIONAL ASPECTS OF TIME**, the price-time action is actually moving through man's three-dimensional perception, and man takes that three-dimensional perception and further reduces it to a two-dimensional price-time chart.

Further complicating the analysis, the element of time is not linear, as represented on traditional price-time charts. Albert Einstein proved this fact.

Figure 5.3 showed a two-dimensional representation of the successive decrease in PTV length, and the squares containing them, during the decomposition period from 1966 to 1982. The three-dimensional counterpart of Figure 5.3 is shown in Figure 5.7.

To help visualize the true construct present in this figure the squares are enclosed in circles, revealing a three-dimensional view of a conical helix. Compare Figure 5.7 with the conical helix shown in Figure 3.1.

With knowledge of the underlying conic helix, the three-dimensional properties of Chart IV.A can be seen. The square represented by FG is the smaller square in Figure 5.7, while the larger square in Figure 5.7 is represented by EG. The reader should review Chart IV.A, while conceptualizing the true conical structure shown in Figure 5.7.⁴⁷

⁴⁷ Technical Reference: The exponential decay of an RL circuit is mathematically similar to PTV decomposition. *Engineering Circuit Analysis*, P. 176, *Modern Control Systems*, P. 177-178. The circular fields shown in Figure 5.7 are the magnetic movement of a spinning particle, *Introduction to Physics for Scientists and Engineers*, P. 516.

Also reference, *Fundamentals of Physics – Extended*, P. 440-441;
Geometry of Art and Life, P. 124-141.

The points of force defining the price-time action moving through man's perception takes the form of a geometric solid. Each individual market has its own characteristic solid, just as each element in the mineral world has its own characteristic geometric structure.

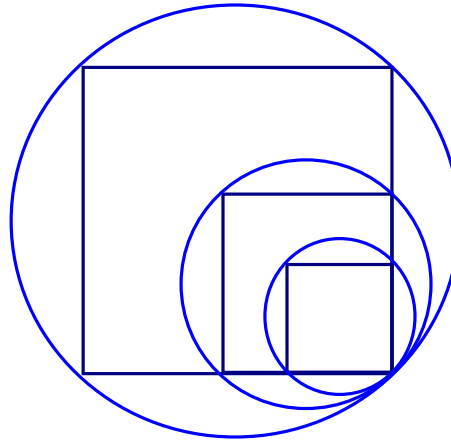


Figure 5.7

Three-dimensional view of the PTV decomposition shown in Figure 5.3

ONE SIDE OF THE STRUCTURE IS VISIBLE AT A TIME AS IT ROTATES. THE RELATIVE LOCATION WITHIN THE SIDE OF THE STRUCTURE DICTATES THE AMOUNT OF THE FACE ALREADY RECORDED ON PRICE-TIME CHARTS, AND THE AMOUNT IMMEDIATELY AVAILABLE FOR CYCLIC MODELING.

It then becomes a matter of measuring the spatial relationships between each side and putting them all together to complete the entire structure.

The cube has been presented in this course as an example of a volume. A three-dimensional volume can take many shapes other than a cube and still maintain a stable form. Which geometric shape a market takes is an individual characteristic of the specific market being studied.

TETRAHEDRON⁴⁸

Geologists recognize five volumes known as "Platonic Solids" as having special significance. These five solids are the only ones with all faces and interior angles equal to each other. They are the tetrahedron (4 faces), octahedron (8 faces), cube (6 faces), icosahedron (20 faces), and the dodecahedron (12 faces).

The tetrahedron is a shape found in many places in nature. It is the structure that provides the maximum possible separation between four bodies around a common center,

⁴⁸ Technical Reference: Study modular geometry in: *Chemical Principles*, P. 372-378

resulting in the minimum repulsion between these bodies. It is the most stable structure that can be formed from four bonds. The tetrahedron is composed of four equilateral (all sides are equal) triangles, as shown in Figure 5.9.a. In geology, the tetrahedron is a base used to classify one of only six crystal systems (tetragonal), from which a variety of minerals are composed, such as tetrahedrite, rutile, anatase, and many others.

The tetrahedral structure is a base upon which several chemical compounds are built. Some of these are listed below.

methane ⁴⁹	CH ₄	zinc	Zn	germane	GeH ₄
silane	SiH ₄	beryllium	Be		

Even the foundation of life on Earth, water (H₂O), assumes the tetrahedral form. The two hydrogen atoms form an angle of 104.6° with the central oxygen atom, as shown in Figure 5.8.b.

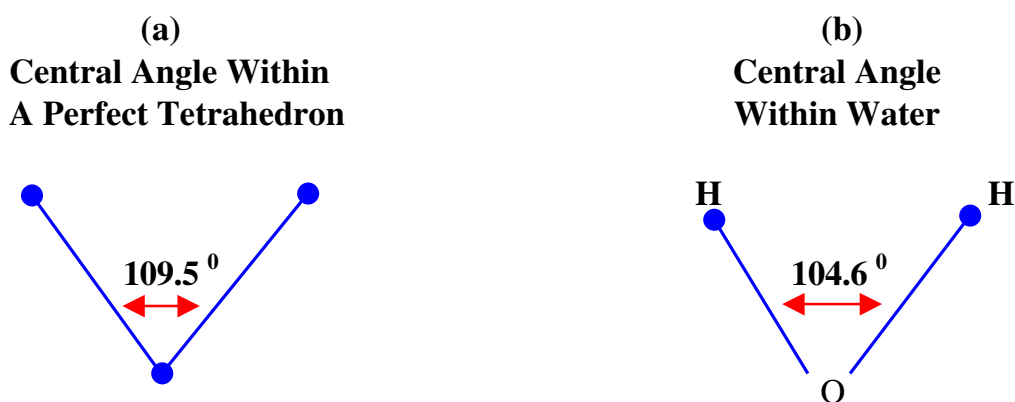


Figure 5.8
Central angle of the tetrahedron

The angle within water is slightly less than the ideal 109.5° angle found within the perfectly symmetrical tetrahedron, shown in Figure 5.8.a. The small difference is due to the two pairs of lone electrons in H₂O. Unpaired electrons require slightly more space than paired electrons. Hence, the two hydrogen atoms are pushed together five degrees from the perfect tetrahedron.

TRIGONAL PYRAMID

If two tetrahedra are placed together with one common face a trigonal pyramid is formed with a four-sided base and four faces in the form of equilateral triangles, as shown in Figure 5.9.b. An example of a chemical structure assuming the form of the trigonal pyramid

⁴⁹ Methane provides the best example of a chemical compound assuming the nearly perfect tetrahedral form.

is ammonia, NH_3 . The pyramidal shape is also found in many places in nature, as well as the man-made structure known as the "Great Pyramid" in Egypt.

TRIGONAL BIPYRAMID (OCTAHEDRON)

This process can be continued by placing two trigonal pyramids together with the square base as the common face. This structure forms another of the Platonic solids, the octahedron shown in Figure 5.9.c. An example of a mineral with octahedral symmetry is fluorite.

DJIA EXAMPLES OF TETRAHEDRAL STRUCTURES

The "Advanced Topics" section of Lesson I explained that there are four equilateral triangles shown on Chart I.A: ABC, CDF, EHI, and IJK. These four triangles fit into two groups: (1) the two triangles formed by the radius vector rotating about point C, triangles ABC and CDF; (2) the two triangles formed by the radius vector rotating about point I, triangles EHI and IJK.

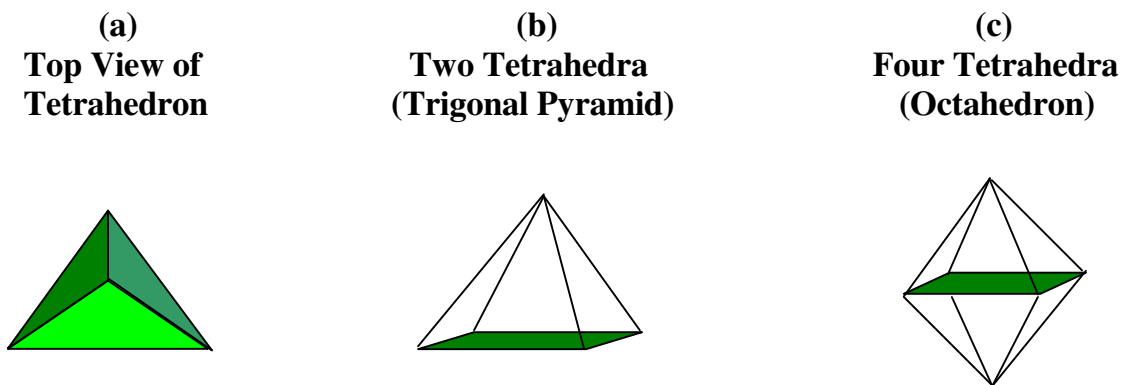


Figure 5.9
Composites of tetrahedral structures

To visualize the three-dimensional structure formed by these triangles pull them together, so the lines BC and CD come together (points B and D become the same point). Bend triangle CDF around so the distances $AF=AC=CF$. This clearly forms the tetrahedron with triangle ACF as the base. If this seems difficult, refer to Figure 5.10.a, where a top view of this tetrahedron is shown with corresponding points from Chart I.A.

Triangles ABC, CDF, ACF, and AFB(D) form the four faces of the three-dimensional tetrahedron that extends from point A to point F on the two-dimensional graph seen on Chart I.A.

The second tetrahedron on Chart I.A can be seen if HI and IJ are pulled together, (H and J become the same point), and triangle IJK is bent around so that the distances $EI=IK=EK$. This clearly forms another tetrahedron with triangle EIK as the base. This tetrahedron is shown in Figure 5.10.b.

Two tetrahedra have now been identified that formed in three dimensions between points A and K. These structures are clearly present, since the pattern of PTVs defined a series of equilateral triangles.

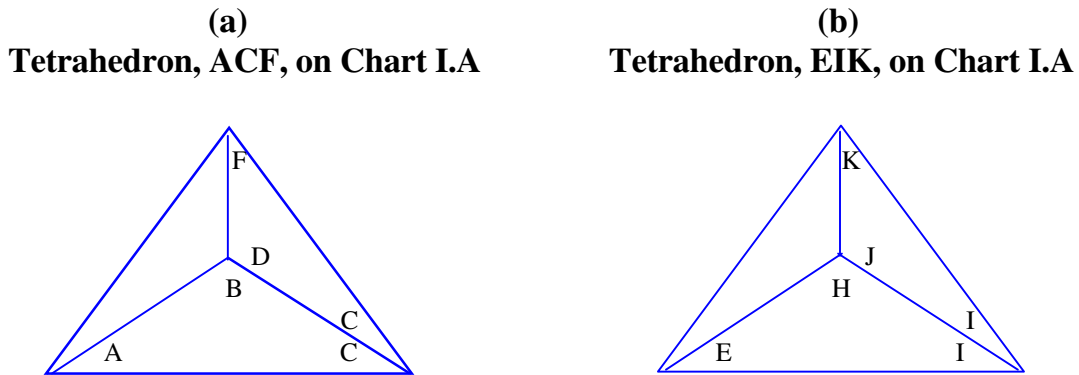


Figure 5.10
Tetrahedral structures in daily DJIA (3/1991 - 10/1991)

The next step is to see what larger structure is formed by these two tetrahedra. Wrap the two ends around and connect AB with JK. The points B, D, H, and J become the same point in this three-dimensional structure. This means that two tetrahedra have been placed together with a common face. The common faces are ABF from the first tetrahedron and EHK from the second tetrahedron. A top view of this structure is shown in Figure 5.11.

The price-time action from point A to point K completes this single geometric structure, **WHICH TAKES THE FORM OF A PYRAMID**. The base of this pyramid is a square with sides AC, CF, EI, and IK. Maybe, it is no coincidence that the great structure located in Egypt takes this form.

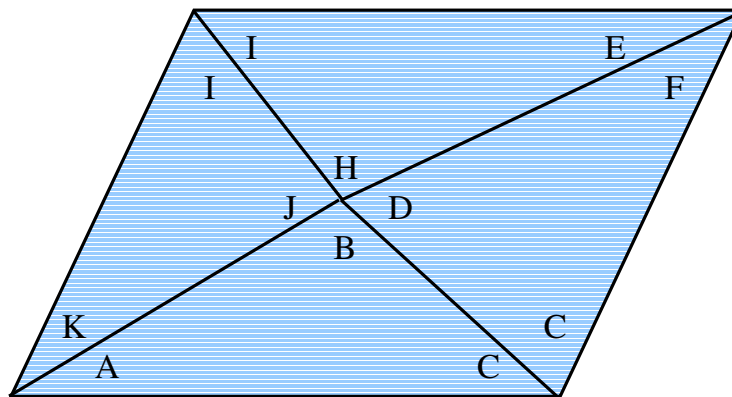


Figure 5.11
Two tetrahedra from Figure 5.10 placed together with triangles ABF and EHK as the common faces. The lettered points correspond with Chart I.A.

GEOMETRIC STRUCTURES CONTAINED WITHIN CUBES

The tetrahedron is one of two "cube-centered" structures (the other is the octahedron). That is, it can be placed symmetrically within a cube, as shown in Figure 5.12.

Each of the six squares in this figure is a face of the cube and is divided diagonally by the edges of the tetrahedron. Compare this figure with Figure 5.1.a, where the diagonal of the square was shown to be the first step in the two-dimensional growth process. Also, Lesson IV, **PRICE-TIME RATIOS MORE IMPORTANT THAN FIBONACCI**, showed that the root two ratio was found throughout the stock market.

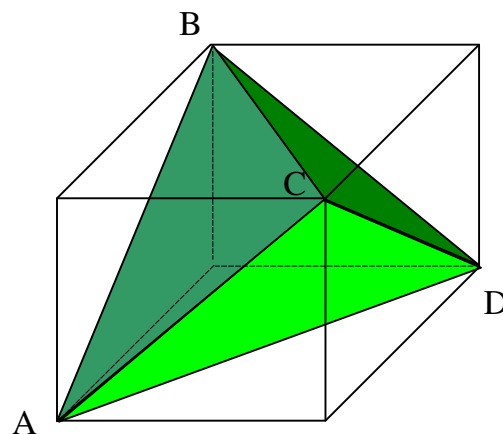


Figure 5.12

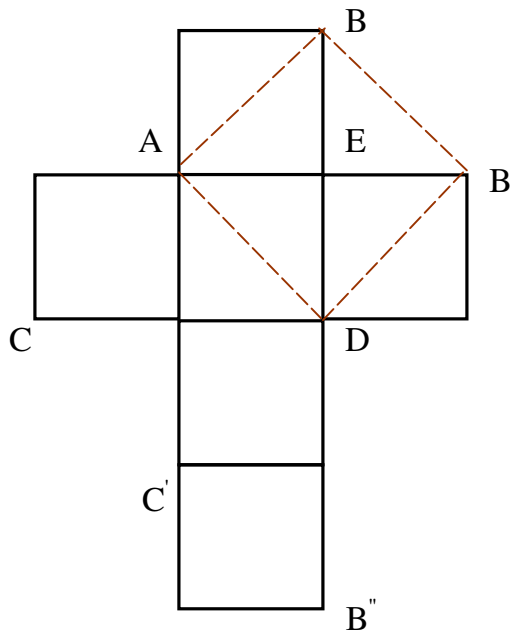
Cube centered tetrahedron

If the sides of Figure 5.12 are unfolded and laid flat onto a two-dimensional plane, as price-time charts are, the result would be Figure 5.13. The lettered points on Figure 5.13 correspond with those on the three-dimensional representation in Figure 5.12.

Figure 5.13 is a two-dimensional representation of a completed tetrahedral growth process. Compare this figure with Figure 5.1.c. At first glance their similarities might not be apparent. However, they represent the same three-dimensional cube-centered tetrahedral growth pattern reflected onto a two-dimensional plane. In Figure 5.13 the square at the top, AB, is equivalent to square ABC in Figure 5.1.c. The square formed by connecting points ABB'D in Figure 5.13, corresponds with square ACDE in Figure 5.1.c.

THREE-DIMENSIONAL PERSPECTIVE OF 1966-1982 SQUARE

On Chart IV.A EF is angled toward the observer and out of the page. At point F, FG bends at an angle away from EF and more toward the page. At point G, GH angles at a nearly right angle to EF and points into the plane of observation. Therefore, the point F on the chart is nearest the observer while point H is furthest away. The points E,F,G, and H are not only places where prices change direction, but also pivot points for the price-time action



If the six squares in this figure have side lengths equal to one, then a diagonal of one of these squares, such as DB' , is equal to the square root of two.

Similarly, a square that has DB' as its side, such as $ABB'D$, has a diagonal length, BD , of two.

Also, the two adjacent squares, DC' and $C'B''$, have a diagonal that spans both squares with a length of the square root of five.

Figure 5.13

Cube centered tetrahedron unfolded into two dimensions

in three dimensions. Look at Chart IV.A and visualize the price-time action coming toward the observer along a plane defined by EF . Similarly, view the price-time action bending at point F and turning at an angle more toward the page of observation. An easier angle to visualize is triangle GHI that clearly pivots at point G and angles into the page of observation.

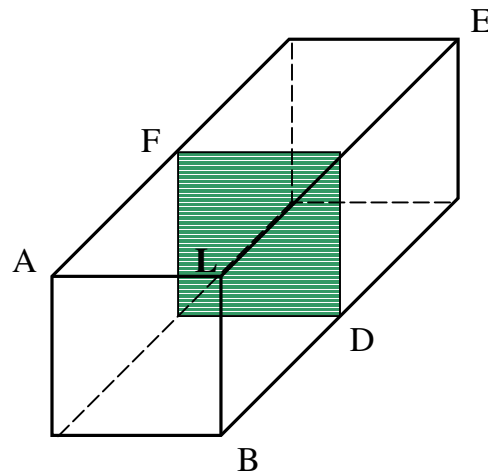
THIS EXERCISE IN VISUALIZATION IS NECESSARY BECAUSE OF THE LIMITATIONS OF TWO-DIMENSIONAL PRICE-TIME CHARTS, WHICH SEQUENTIALLY RECORD THE FOUR-DIMENSIONAL EFFECTS THAT MANIFEST IN PRICE-TIME.

GEOMETRY OF ADJACENT CUBES

If two cubes are placed next to each other with a common face, they appear as in Figure 5.14, where the following measurements can be made:

- (1) The distance, LE , is twice the length of one side of a cube.
- (2) The distance, LE , divided by the square root of two gives the diagonal, DE , of a square on the face of one of the cubes.
- (3) The side of the square, BD , multiplied by $\sqrt{5}$ gives the diagonal across two adjacent squares, represented by AE and BE .

Figure 5.14 is used as a model for two-dimensional price-time charts. Although two adjacent cubes are used in this model, in three-dimensional geometry the price-time action may be pivoting at point D, and square DE is actually the far side of the first cube represented by square DF. This would be the case if the first cube had not yet completed when point D was reached. For a cube to be complete all six sides must have unfolded.



Square, FD, is the common face between the cubes.

Figure 5.14

Geometry of two adjacent cubes with a common face

THREE-DIMENSIONAL CUBIC STRUCTURE IN THE DJIA

THE STOCK MARKET UNFOLDS WITH A CHARACTERISTIC GEOMETRIC STRUCTURE THAT IS DEFINED WITHIN THE LIMITS OF SQUARES IN TWO DIMENSIONS. SIX OF THESE SQUARES FORM THE SIDES OF A CUBE IN THREE DIMENSIONS.

Chart V.B shows the two adjacent cubes from Figure 5.14 overlaid on a chart of the DJIA from 1899 to 1993. A logarithmic price scale is used, so all the price-time action can be included on a single chart. This scale produces a distortion in the appearance of the geometric structure as prices increase up the vertical axis. However, since the proof of this analysis is provided with calculated PTVs, and not those drawn graphically, the patterns on the chart are needed for reference only.

The cubic structure on Chart V.B provides the three-dimensional perspective necessary to understand how each face of the cube develops. The lettered points on Chart V.B correspond with those in Figure 5.14.

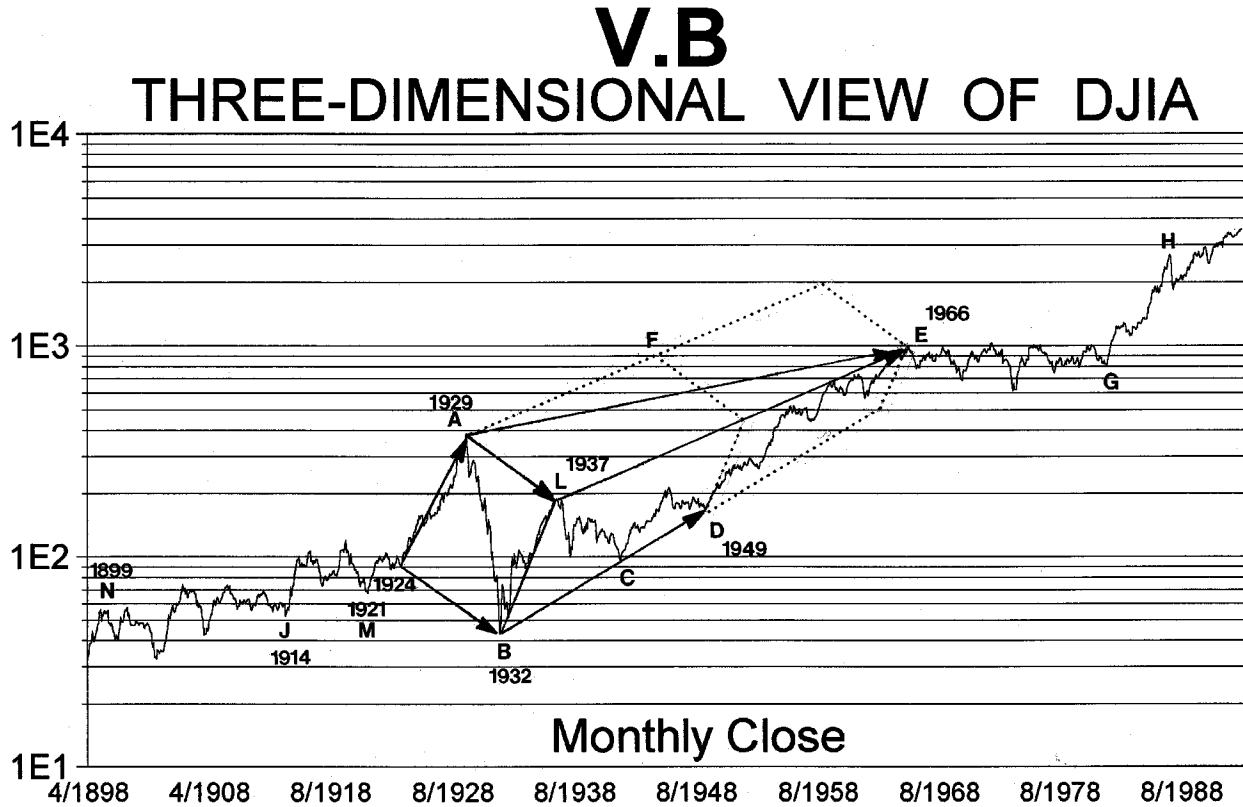
Chart V.B contains several PTVs that were previously shown in Tables 4.1 and 4.2. Those relevant to this discussion are repeated here and grouped with PTVs of similar value.

AE = 1997 BD = 891 BL = 288 (second square of twelve)

BE = 1998 EG = 891 CL = 287

GH = 1994

LE = 1710 JE = 2832 DE = 1209



Three of these PTVs: GH, from the bottom in 1982 to the top in 1987; AE, from the top in 1929 to the top in 1966; and BE, from the bottom in 1932 to the top in 1966, are equal length. Geometrically, these PTVs represent the diagonal of two squares, similar to those shown in Figure 5.14. Also; the length of BD, from the bottom in 1932 to the bottom in 1949, is equal to EG, from the top in 1966 to the bottom in 1982. These PTVs represent sides of squares that define the cube unfolding during this time.

Since BD defines the length of the side of the square, and BE is the diagonal of two such adjacent squares, the length of BE must equal the length of BD multiplied by the square root of five. That is;

$$\text{Theoretical value of BE} = \text{BD} \times \sqrt{5} = 891 \times \sqrt{5} = 1992.3$$

The actual value of BE was 1998, producing an error from the ideal theoretical value calculated above of;

$$\frac{1998-1992.3}{1998} = \frac{5.7}{1998} = 0.28\%$$

Similarly, Chart V.B shows DE, from the bottom in 6/1949 to the top in 2/1966, to be the diagonal of one square⁵⁰; and LE, from the top in 1937 to the top in 2/1966, to be the side of two adjacent squares. Therefore, LE must equal DE times the square root of two. That is;

$$\text{Theoretical value of LE} = \text{DE} \times \sqrt{2} = 1209 \times \sqrt{2} = 1710$$

This theoretical value of LE exactly matched the actual value.

To extend this analysis back in time to the reopening of the stock market in 1914, the relative relationship between JE, from 1914 to 1966, and the rest of the cubic structure is studied.

Figure 5.15 shows a two-dimensional representation of the squares that sequentially presented themselves between 1914 and 1966. The JA square represents a side of the cube that unfolded prior to the start of the cube shown on Chart V.B. This complete cubic structure will be explained in following sections; but for now, it is sufficient to know that the price-time action in three-dimensions rotated along the plane defined by AB, which can be visualized in Figure 5.15 by seeing square JA bent into the page of observation. Since the two-dimensional price-time chart had already recorded the JA square when the cube rotated, the chart represents an unfolded cube.

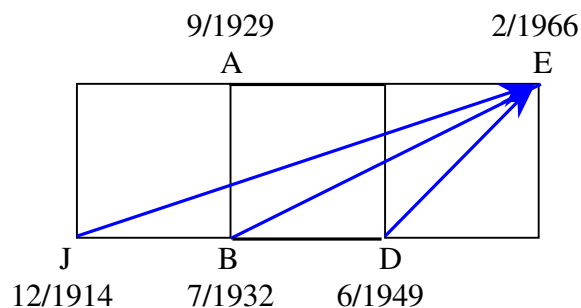


Figure 5.15

Two-dimensional representation of the squares formed in the DJIA from 1914 to 1966

⁵⁰ The PTV, DE, is the diagonal of the square that rotated into view in 1949. As mentioned in Lesson II, **GROWTH PATTERNS**, the diagonal of a square defines W.D. Gann's 45° diagonal angle. The exact angle of DE is given by the trigonometric relationship;

$$\tan^{-1} \frac{840 \text{ points}}{869 \text{ weeks}} = 44^{\circ}$$

This angle provided the support from 1949 until the break in 1962. Between 1962 and 1966 this same 45° angle provided the resistance until the nodal point in 1966 was reached.

BD is the length of the side of the large squares in Figure 5.15 and equals 891. Therefore, the length of JE is given by the square root of TEN times the side of the square, 891. That is;

$$\text{Theoretical value of JE} = \text{BD} \times \sqrt{10} = 891 \times \sqrt{10} = 2818$$

Table 4.2 showed the actual value of JE to be 2832, producing an error from the ideal theoretical value calculated above of;

$$\frac{2832 - 2818}{2832} = \frac{14}{2832} = 0.49\%$$

The relationship of the square root of ten has been previously explained as the square root of two multiplied by the square root of five. It also represents the diagonal of three adjacent squares. This relationship was shown in Figure 5.2.b between EF and the length of the side of the smaller squares during that interval, (i.e., $200 \times \sqrt{10} = 632$).

To further verify the relationship defined above between the squares in Figure 5.15, the ratio between JE and BE must be shown to be the square root of two. That is;

$$\text{Theoretical value of JE} = \text{BE} \times \sqrt{2} = 1998 \times \sqrt{2} = 2825.6$$

Since the actual value for JE was 2832, the error between the actual value and the ideal theoretical value calculated above is;

$$\frac{2832 - 2825.6}{2832} = \frac{6.4}{2832} = 0.22\%$$

SUMMARY OF THREE-DIMENSIONAL STOCK MARKET STRUCTURES

Figure 5.14 showed the three-dimensional characteristics of two cubes placed next to each other with a common face. This figure was overlaid on the price-time chart of the stock market to show the three-dimensional configuration between 1914 and 1966. The vectorial values (PTVs) were calculated between points on Chart V.B to show that the relative relationships between these PTVs were the same as for the sides of Figure 5.14. By calculating these PTVs and the ratios between them, it was shown that the price-time action on Chart V.B takes the three-dimensional form shown in Figure 5.14. Each of the ratios calculated in this section matched the ideal theoretical values within one percentage point! This is well within the reliability of the recorded data, and rules out the possibility of coincidence.

FOUR-DIMENSIONAL CUBIC STRUCTURES IN THE DJIA

While the three-dimensional perspective demonstrated in the previous section can be seen on two-dimensional price-time charts, it does not accurately represent the true

configuration that is unfolding in price-time. The three-dimensional structure is visible only because of the techniques used to record data on two-dimensional price-time charts.

To fully grasp the true nature of price-time, it must be understood that,

THE GEOMETRIC STRUCTURE DEFINING THE SPACIAL RELATIONSHIP BETWEEN POINTS OF FORCE IN PRICE-TIME IS IN MOTION RELATIVE TO THE DIMENSION OF MAN'S PERCEPTION.⁵¹

This initially may sound complicated. However, all it really means is that the geometric solid defining the long-term turning points in the stock market acts like a rotating cube. This appearance of rotation is caused by the twisting nature of the conical helix containing the structure.

For example, the previous section showed two adjacent cubes overlaid on price-time between 1929 and 1966. However, **THE ACTUAL GEOMETRIC STRUCTURE THAT UNFOLDED BETWEEN 1899 AND 1982 WAS A SINGLE CUBE.** The point on Figure 5.14 where it appears the price-time action was transferring from one cube to the next is actually the point in price-time where the cube rotated to expose its next face. This occurred in 1949. In four-dimensional reality, DE did not move to a different cube. Rather, it crossed the face of the cube that is represented by square DF.

Remember, two-dimensional price-time charts only record data happening at that particular instant in time. The face of the geometric structure that lies in the future is hidden from view. In addition, the faces of the structure that have been previously recorded are unfolded onto a two-dimensional plane, as the data is recorded day-by-day. At first, the fact that the cube is rotating into view may create a source of confusion as two-dimensional charts are viewed, but this concept will become clearer when it is further explained in Lesson X, **DIMENSIONAL ASPECTS OF TIME.** As is the case with most new concepts, the more time spent studying the charts the clearer the concept will become.

The conical helix expands as it grows. And since the faces of the cube are exposed as the conical helix twists, it follows that the squares defining these cubes also expand. This explains the increase in energy levels seen as time progresses. The growth process at any particular energy level is complete when the six sides of the cube have completed. After the cube completes, the growth proceeds to the next larger cube, which is stacked on top of the just completed cube. This effectively creates a formation similar to a pyramid with each succeeding cube larger than the previous one, as defined by the expanding conical helix. This was seen in 1949 when the smaller 1899-1949 cube completed and the energy level increased to complete the 1899-1982 cube, **WHICH CONTAINED THE 1899-1949 CUBE.** Therefore, the squares that defined the cube from 1899 to 1982 were larger than the squares that defined the 1899-1949 cube. Similarly, the squares from the 1899 to 1982 cube were smaller than the cube currently under construction (after the increase in energy level in 1982).

⁵¹ Technical Reference: *Modern Physics*, P. 20-23.

The fact that cubes that develop at higher energy levels are composed of squares that are larger than the squares of cubes developed at lower energy levels must be kept in mind, because the following figures will show stacked cubes that appear to be the same size. However, these cubes were drawn in this manner only to show the similarity of structures at different energy levels.

The six faces of the cubic structure from 1899 to 1982 are shown in Figure 5.16. These squares were individually described in Figures 5.4 and 5.5 and are shown on Chart V.H. When viewing this figure, remember that the PTV representing a square is drawn as a line. For example, the PTV from 1899 to 1914 is drawn as a one-dimensional line. However, this PTV defines the square that is the bottom of the cube in Figure 5.16. This explains why 1932 is shown twice on this figure. That is, the drop from 1929 to 1932 completed the entire back square of the cube in Figure 5.16.

The six squares that define the faces of the cubic structure in Figure 5.16 are as follows:

- Face #1 1899 - 1914 Bottom of the cube.
- Face #2 1914 - 1929 Right side of cube. It was crossed diagonally.
- Face #3 1929 - 1932 Back side of cube. Dropped from top of cube to bottom.
- Face #4 1932 - 1949 Left side of cube. It was crossed laterally.
- Face #5 1949 - 1966 Front face of cube. It was crossed diagonally.
- Face #6 1966 - 1982 Top of the cube. It was crossed laterally.

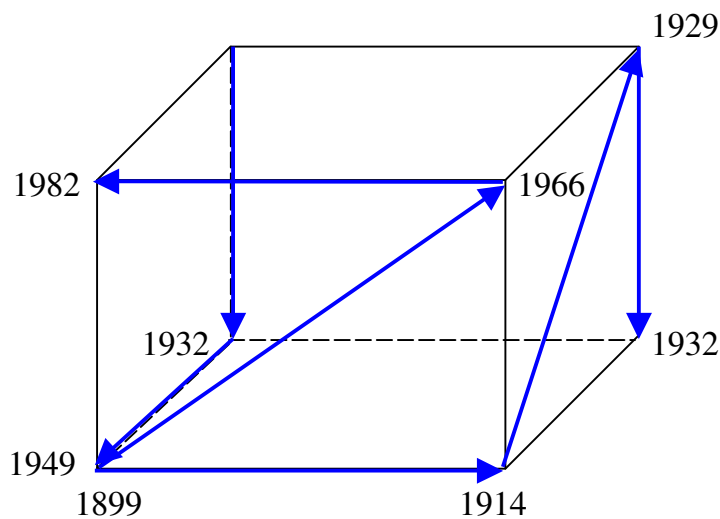


Figure 5.16
Four-dimensional cubic structure of DJIA between 1899 and 1982

CURRENT FOUR-DIMENSIONAL CUBIC STRUCTURE OF THE DJIA

On the date of this writing, (September, 1993), five faces of the cubic structure from 2/1966 to the present have unfolded, as shown in Figure 5.17. The five squares that define the faces of this structure are described below. Reference Figure 5.5 for a detailed description of each square.

Face #1	1966-1982	Formed the bottom of the cube. Its size was defined by its position as the top of the 1899-1982 cube.
Faces #2, #3	8/1982 - 8/1987	Right side and back side of the cube. These two squares were crossed diagonally. As previously shown, the PTV representing these two squares is $\sqrt{5}$ x the 1966-1982 base. That is, $\sqrt{5} \times 891 = 1994$.
Faces #4,#5	3/1988 - Present	Left side and front of cube. These two squares are being crossed diagonally, as were faces 2,3. They compose a single square on the larger cube containing this smaller cube.

Each square in this cube is at a higher energy level than its counterpart in the preceding cube. Therefore, the two squares from 1982 to 1987 in Figure 5.17 compose a single square in a larger cube that contains the cube shown in Figure 5.17. Similarly, the two squares currently being crossed compose another single square on this larger cube. When this larger square is complete (Due in January, 1994 as explained in Part II of this course),

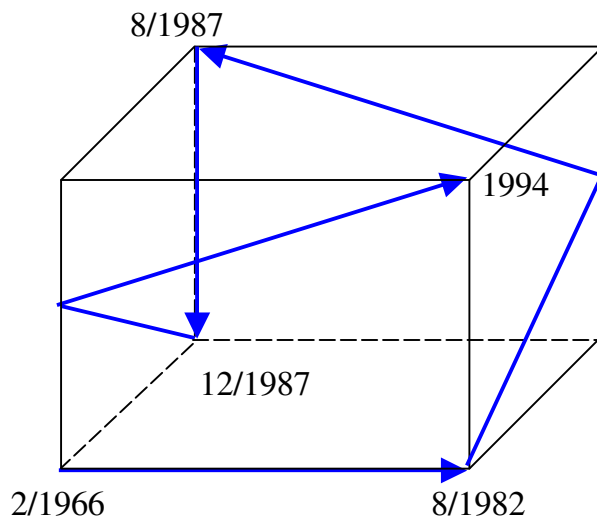


Figure 5.17

Four-dimensional cubic structure of DJIA from 2/1966 to the present

three sides of the larger cube will be complete; i.e., the 1966-1982 square, the 1982-1987 square, and the 1988-1994 square.

This is similar to the 1914-1929 period where two smaller squares were crossed diagonally to define one larger square. Also, the 1899-1914 and 1932-1949 squares each contained two smaller squares, which defined the faces of the 1899-1949 cube.

GEOMETRY OF STACKED CUBES

The square from 1899 to 1914 was crossed laterally, similar to the square from 1966 to 1982. Both these squares represent the base of a cube. The square from 1966 to 1982 was not only the top of the cube from 1899, but also the bottom of a new cube extending from 1966 to the present. In other words, the square from 1966 to 1982 was a common face between two stacked cubes. This is shown in Figure 5.18.⁵²

Do not be confused because the top cube shows the faces reversed from those in Figure 5.17. The two figures show the same cube. One figure views the cube from the front and the other views it from the back. This can be verified by drawing Figure 5.17 on a piece of paper, then turning the paper over and looking at the cube from the other side.

Notice that both the crash of 1987 and the crash of 1929 occurred at the same locations on the two cubes. These dates corresponded with the first time the price-time action touched the top of the cube under construction.

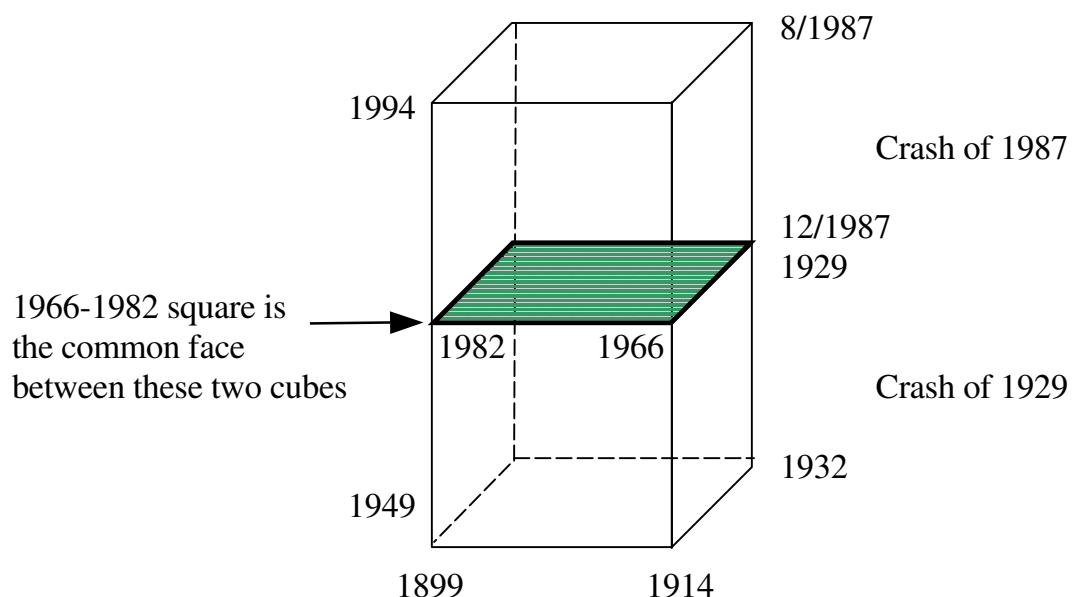


Figure 5.18

Two stacked cubes in the DJIA from 1899-present showing the 1966-1982 square as the common face.

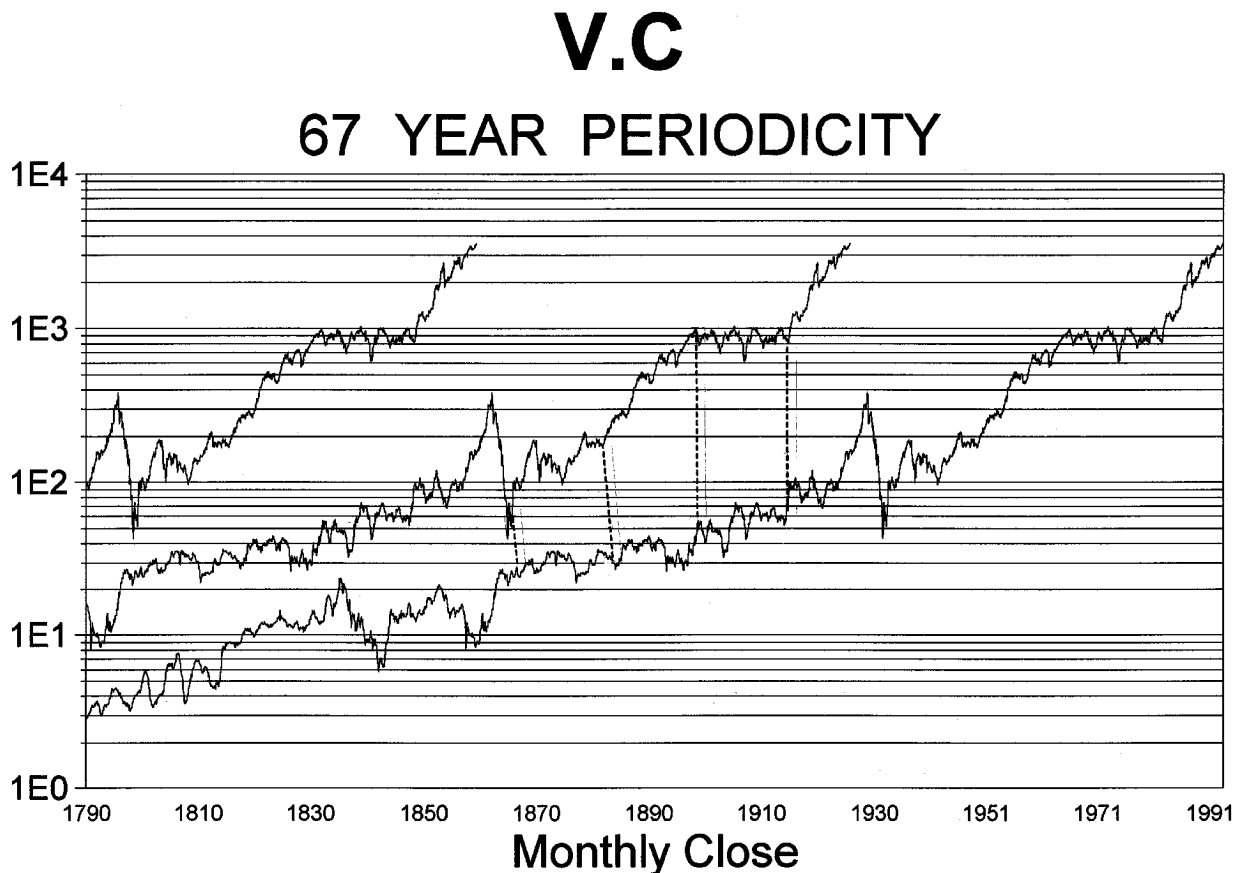
⁵² Technical Reference: *Chemical Principles*, P. 461-462.

SIMILAR PATTERNS FORM ON CORRESPONDING FACES OF CUBES

When two squares form on corresponding faces of two different cubes, the price-time action within these squares is very similar. For example, Chart V.C shows three monthly graphs of the stock market. The lower graph is a complete record from 1790 to 1993. The middle graph is also of the stock market, but it has a 67 year offset from the lower graph. That is, the dates on the middle graph are placed directly over dates 67 years earlier on the lower graph. The upper graph continues this process by shifting this graph 67 years with respect to the middle graph. Notice how the beginning dates of these three graphs; 1790, 1857, and 1924 corresponded with beginning points of some of the largest price advances in history. The reason for choosing the 67 year offset will be explained in Part II of this course, where this period will be shown to correspond with one of the major stock market cycles.

The cubic structures unfolding during each of these time periods are at similar points of development, but at different energy levels. The cubic structure shown in Figure 5.16 began in 1899. Sixty-seven years later, in 1966, the cubic structure shown in Figure 5.17 began to develop.

To verify that similar price-time patterns occur along corresponding squares of different cubes, sections of Chart V.C are expanded for a close-up view. Chart V.D compares a 67-year period between 1869-1935 with the period immediately following it, 1935-present. These two graphs are very similar with the exception of the two five year cycles in 1891 and 1916 turning down with greater energy in the lower graph than their



corresponding cycles on the upper graph, i.e., 1958 and 1983. The location of the larger 84 year cycle explains why there was more energy in the 1958 and 1983 periods. This will be expanded in Lesson VIII.

Charts V.E and V.F provide a more detailed view of these corresponding sections of the market, with twenty year periods graphed on the same chart. Chart V.E compares the two periods between 1896-1915 and 1964-1983. Both these sections contain the squares described in the previous section as bottoms of their respective cubes. Similarly, they both represent tops of different cubes, as described in the section on stacked cubes. In that section it was explained that the 1966-1982 square was the bottom of the cube currently unfolding, and the top of the cube formed between 1899-1982.

The square between 1899-1914 was not only the bottom of the 1899-1982 cube, but also, a common face shared with the cube formed prior to 1899.

Since the 1966-1982 square is the top of the cube originating in 1899, and the 1899-1914 square is the bottom of the same cube, Chart V.E shows the top and bottom of this same cube. Similarly, Chart V.F compares two twenty-year periods between 1870-1890 and 1935-1954.

The reader is encouraged to continue this process and compare the price-time patterns on corresponding squares in different cubes. The long-term view is available on Chart V.C.

CHAOS THEORY AND FRACTALS IN THE STOCK MARKET

This topic is scheduled to be included in future volumes of this course. Hence, only a brief overview will be provided.

Chaos theory is the name given to a relatively new area of study in modern physics. The origin of Chaos theory was in 1961 when a scientist at MIT, Edward Lorenz, tried to create mathematical models to improve weather forecasting. The details of Chaos theory are available from many good books on the subject.⁵³

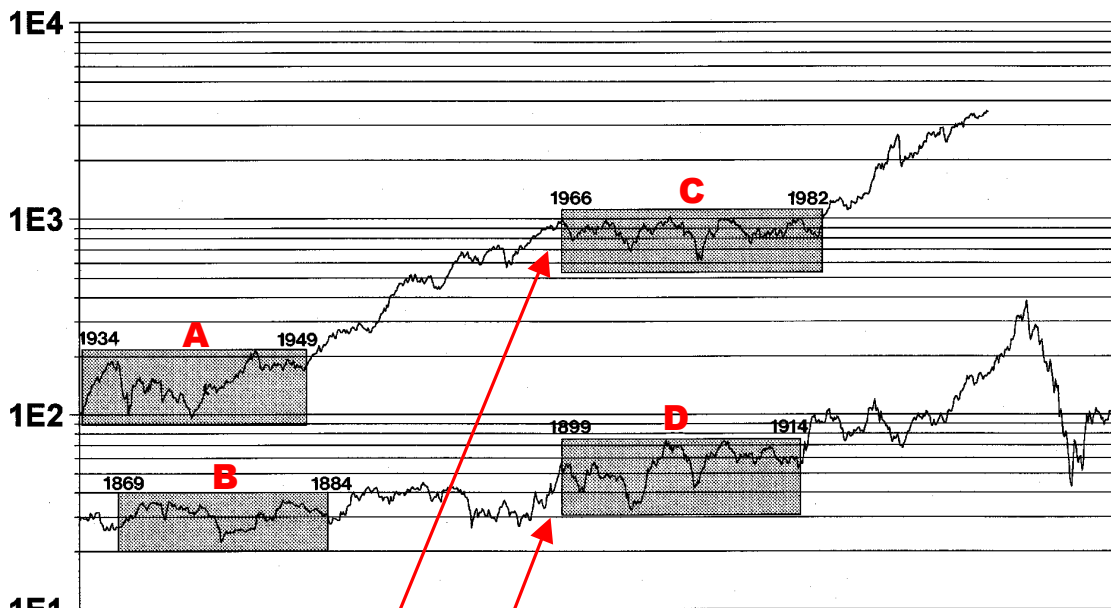
An IBM scientist named Benoit Mandelbrot studied the specific area of Chaos theory called **FRACTALS**. A fractal is a "fractioning" of a larger structure into smaller structures. These smaller structures, fractals, have features similar to the larger structure. This theory states that if a fractal is enlarged to the size of the larger structure the fractal will look like the larger structure.

This theory should be nothing new for students of the Elliott Wave Theory, which applies the 5-3 Elliott Wave pattern to financial market patterns of differing magnitude.

⁵³ Reference: *CHAOS*.

V.D

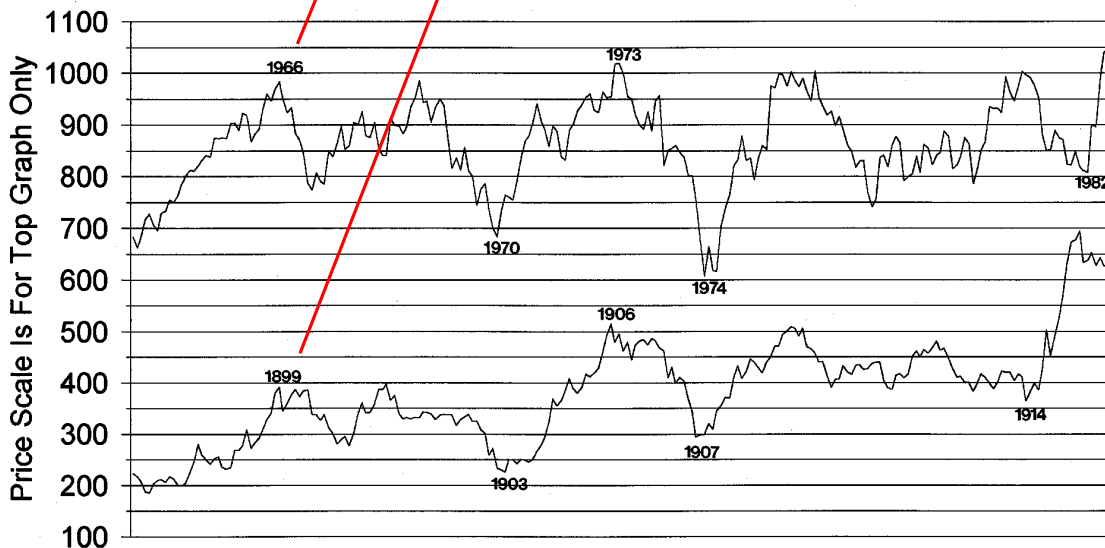
CORRESPONDING SQUARES OF TWO CUBES



Monthly Close

V.E

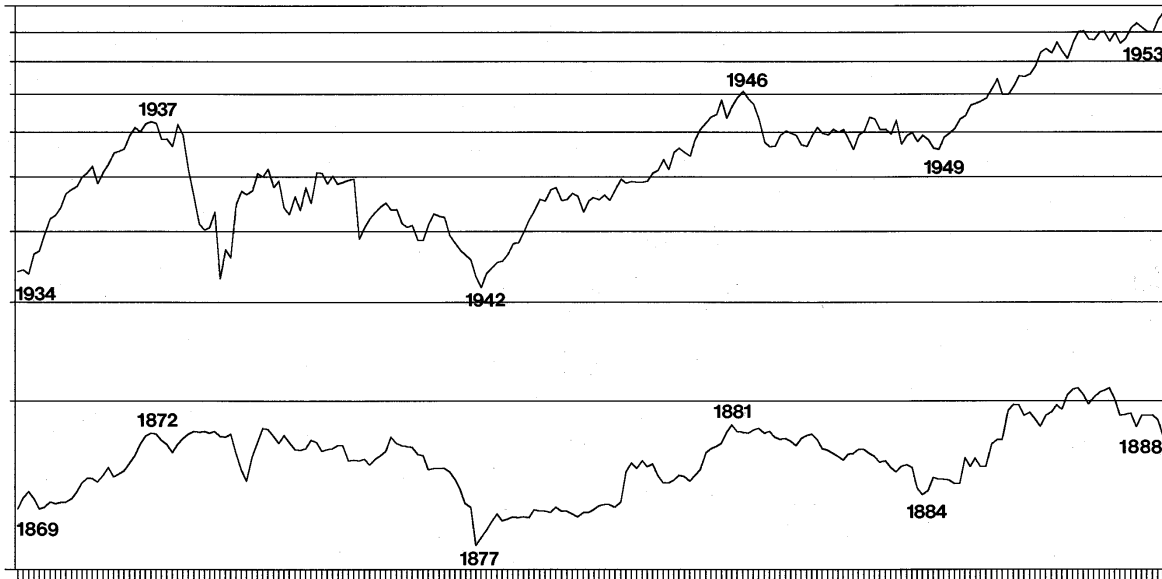
SQUARES C AND D FROM CHART V.D



Monthly Close

V.F

SQUARES A AND B FROM CHART V.D

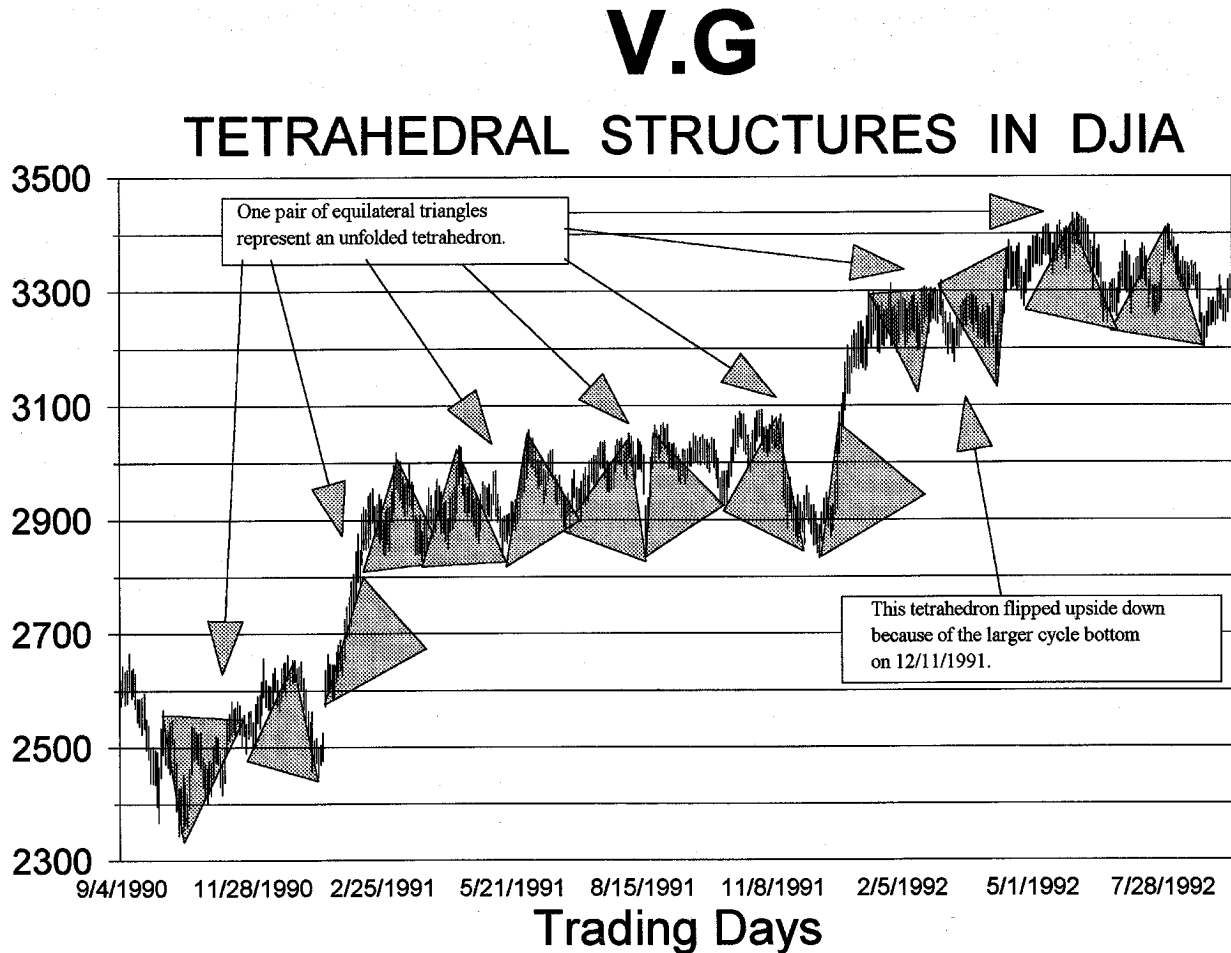


Monthly Close

In application, fractals are used to model growth of natural objects, such as ferns, with nonlinear geometry. The concept of fractals is not new. As was demonstrated earlier in this lesson, the diagonal of the square is used to define the base of the next larger growth phase, which is also contained within a square.

Examples of fractals in the stock market can be seen by comparing the weekly chart between 1966 and 1982 with the daily chart shown on Chart I.A. The length of the PTVs on chart I.A were found to equal 237 when using an hourly time component for the vectors. Similarly, the length of the PTVs connecting the bottoms between 1966-1982 are 237 when using a weekly time component. This also demonstrates the limitations of contemporary cycle analysis. During the 1966-1982 square analysts were unable to find the "cycle" defining the market bottoms. That is because the time between these bottoms varied greatly. However, **THE PTVs CONNECTING THESE BOTTOMS WERE ALL OF EQUAL LENGTH.** Once again, a one-dimensional analysis proved lacking.

Another example of fractals is seen between 1966-1982 by multiplying the 237 value for these PTVs by the square root of five. This value (529) defined the PTV from the 1982 bottom to the 1984 top. Hence, the relationship between the two PTVs, 1978-1982 and 1982-1984 is defined by the square root of five, as is the relationship between the two larger PTVs, 1966-1982 and 1982-1987.



SUMMARY

This concludes Part I of the course. The timing tools presented thus far will now be briefly summarized.

Price-time action is defined within the limits of points of force. The relative spacing between these points can be measured on a two-dimensional plane with radii vectors. The length of these vectors (PTVs) is independent of direction. Whether they point straight down the time axis or straight up in price, their length is constant. If the market is experiencing a vertical movement the analyst can project the terminal point of that movement by measuring the vectorial length from the origin of the movement. If a powerful movement is under way the length of the vector occurs in multiples, most commonly two times, then four times. Similarly, the analyst can use the same technique to project the terminal date of a sideways choppy market where the dominant component of the vector is time.

The triangle is the basic geometric form upon which other structures are based. All **NATURALLY** occurring geometric formations can be constructed with the triangle and

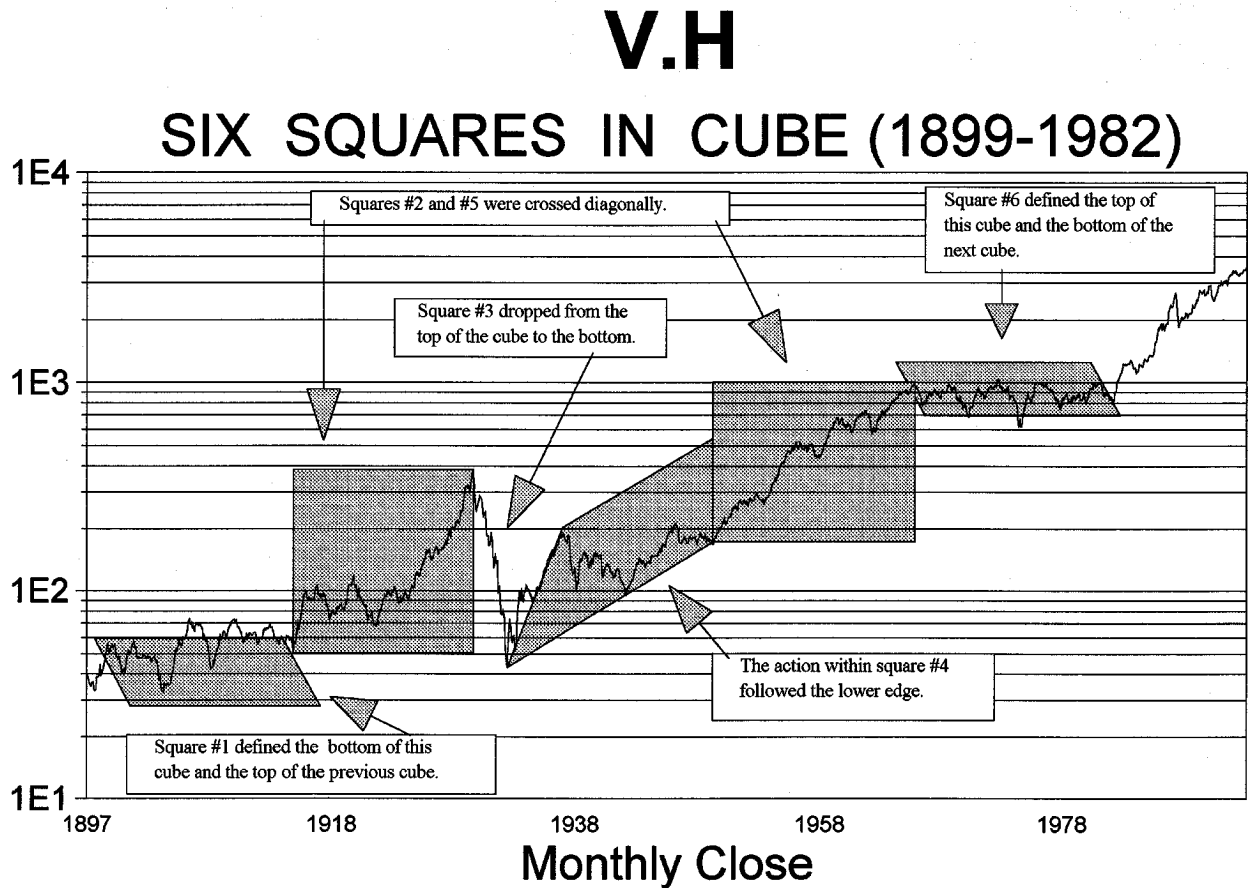
the circle. In the case of the stock market, two vectors interlock to create an equilateral triangle. Therefore, the analyst not only knows in advance the length of the movement under way, but also the direction of that movement, specifically 60° from its mated PTV. Measurement of these equilateral triangles on a daily chart easily allows the analyst to project terminal points of movements within two trading days.

The angle within water was shown to deviate from the ideal tetrahedral angle by five degrees. The two pairs of lone electrons in water cause this deviation. This phenomenon was explained because the DJIA experiences a similar shifting. If the angles are measured within the triangles in the DJIA their exact value will be found to be between 62° and 63° . This two-degree difference within the faces of the DJIA triangles is caused by the shifting within the inner angle of the three-dimensional tetrahedron.

In the case of the stock market, two equilateral triangles seen on a two-dimensional price-time chart compose a three-dimensional tetrahedron. This tetrahedron is unfolded as price-time charts sequentially record the faces as they present themselves. If a market other than the stock market is studied, the composite formed will not necessarily be tetrahedral. However, the triangle will still be the basic construct upon which to build. Rather than the tetrahedral form, the composite may be an octahedron, a dodecahedron, icosahedron, or some other form depending upon the specific lattice of that market.

The tetrahedron is a "cube-centered" solid, meaning it can be placed symmetrically within a cube. The cubic structure in the stock market between 1899 and 1982 was closely analyzed, and detailed measurements were made of each face of this cube verifying its form.

Contained within this larger cube was the smaller cube extending from 1899 to 1949. This can be seen in Figure 5.19 where the smallest cube is the 1899-1949 cube. Two sides of this smaller cube were found to complete one side of the larger cube. When the smaller cube completed in 1949 the fourth side of the larger cube also completed. The length of this fourth side, which extended from 1932 to 1949, was found to equal 891. This value was the length of the top of the larger cube, which extended from 1966 to 1982. The four sides of the larger cube (1899-1982) were found to be progressively increasing in size as the smaller cube unfolded. For example, the 1899-1914 square was slightly smaller than the 1914-1929 square, which in turn was smaller than the 1932-1949 square. The increase in the side length of the larger cube was caused by the expanding conical helix. It is the smaller cube (1899-1949) that is contained within the larger cube that has constant side length. When the smaller cube completed in 1949 there was an increase in energy levels as the fifth side of the larger cube was crossed diagonally to reach its top.



The result of this process is that of one cube stacked on top of another cube, as shown in Figure 5.19. The cube on top is enclosed within a larger cube. This larger cube has another cube stacked on top of it. The cube on top of this larger cube will itself be contained within an even larger cube. This growth process continues, ad infinitum, until growth terminates.⁵⁴

Knowledge of the geometric structure allows the analyst to identify his location within the growth process at any point in time. After the face of the structure has been identified, the limits of that face can be calculated and defined by the PTV. It is within the two-dimensional faces of the structure that accurate cyclic modeling can be performed.

Part II will study the cycles recurring along the faces of the cubic structure identified in Part I. The two-dimensional face of the structure limits the recurrence of these cycles.

⁵⁴ Reference: *Connections – The Geometric Bridge Between Art and Science*, P. 163-166.

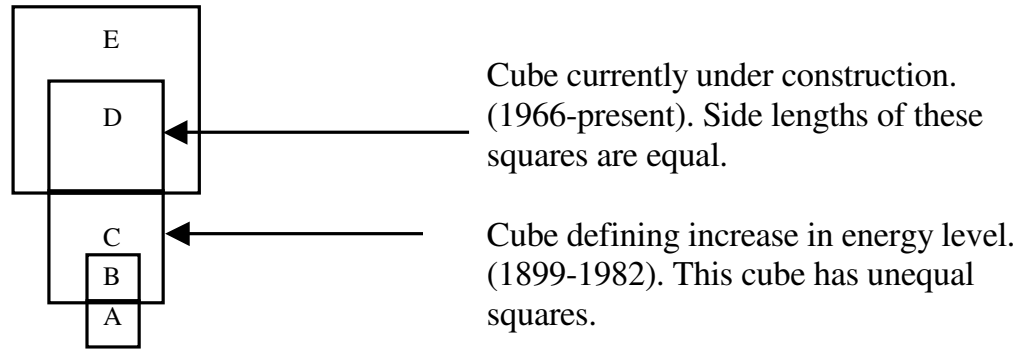


Figure 5.19

Two-dimensional view of stacked cubes contained within other cubes. The cubes with squares that are the same size are those contained within the larger cubes. The cubes containing these smaller cubes are composed of expanding squares to accommodate the expanding conical helix. The two center cubes in this figure are those from Figure 5.18. The smallest cube is that from Figure 5.4.

PART TWO

FOUR-DIMENSIONAL

PRICE-TIME CYCLES

INTRODUCTION

PART TWO

Part one of this course showed how to identify geometric structures in financial markets. It was also shown that with application of the PTV, geometric ratios, and knowledge of the cubic structure, the limits of the square can be determined years in advance.

IT IS WITHIN THE LIMITS OF THE SQUARE THAT CYCLES REPEAT WITH PREDICTABLE PERIODICITY.

When a new square begins the cycles within that square repeat with a periodicity that usually differs from those in the preceding square. Therefore, the knowledge from Part I of this course is critical if accurate cycle analysis is to be performed over any extended period of time.

Traditional cycle analysts err in their approach by attempting to project cycles beyond the limits of the square in which they are defined. As demonstrated in Part I, when a square completes it rotates out of view.

Part II will show how the scientific phenomenon of "sympathetic resonance" synchronizes cycles found in the stock market with the predictable periods of the planets and their harmonics.

Tables will be used extensively in Part II, as they were in Part I, to provide the data supporting all presented postulates. This data provides the indisputable proof of the correlation between stock market cycles and planetary cycles. Numbers do not lie.

Do not be intimidated by tables filled with numbers. They simply record the locations of the planets at different times in history. It is important the reader take the time to review this data, for it is there and in the charts that the ultimate proof lies.

This course makes no claim that a cause-effect relationship exists between planetary motion and stock market cycles. The data is simply gathered and displayed, showing the correlation.

Volumes of material can be written describing the details of these cycles, especially in the areas where double or triple tops or bottoms occur. These types of formations occur when different cycles reach their tops or bottoms close to each other, but not at exactly the same time. As more time is spent studying these multiple tops and bottoms, more awareness of the truth of the theories presented in this course will be gained.

If the reader has difficulty with the concept relating stock market cycles with planetary cycles, the same results can be achieved by looking at the fifteen-degree axes of elliptical cycles, which have the same periodicity as the planets. It is simply easier to use the planets because of the availability of data.

LESSON VI

SYMPATHETIC RESONANCE AND THE LAW OF VIBRATION

I have proven to myself, as well as demonstrated to others, that the Law of Vibration explains every possible phase and condition of the market.
... W.D. Gann

INTRODUCTION

Sympathetic resonance is the scientific term for the natural phenomenon seen when a body is subjected to an external vibrating source with a frequency equal to that of the natural frequency of the body, the body itself begins to vibrate. For example, when two violin strings are in unison and one is bowed, the other will oscillate at the frequency of the bowed string. This will happen even though the second string is not touched by the bow.

In order to explain this phenomenon, a brief explanation of simple vibration is necessary. Initially, it may be difficult to understand how this material relates to financial markets; however, **EVERYTHING** presented in the following explanation is directly applicable to financial markets. If the reader chooses to skip this explanation the material presented later will not make sense. The explanation is brief and broadly covers a variety of characteristics of this phenomenon. For those desiring more information on this subject, books of physics are available giving more detail. As previously stated, it is not the intention of the author to provide information available from other sources. Rather, the reader is referenced to those sources.

A simple way to understand sympathetic resonance is to visualize a child swinging on a swing. If each time the swing returns someone gives the child another push, he will swing higher and higher. This is because the rate at which the swing is pushed equals the period of the swing. The two (the period of the swing and the act of pushing) are synchronous. Similarly, if the swing is pushed every other time it returns it will continue to swing. In this case, the swing and the push are synchronous with a ratio of two to one, i.e., two swings for one push. However, if the swing is pushed before it fully returns, the two will be out of phase and the swing will not swing higher.

In this example the swing is the body being acted upon, the push is the external force, and the period of the swing is the natural frequency of the system.⁵⁵

With respect to financial markets, sympathetic resonance allows an analyst to project, not only exactly where in price a market will advance or decline, but also **WHEN** it will happen. Time has always been the missing element in the projections of market analysts. However, **TIME IS THE MOST IMPORTANT ELEMENT.**

⁵⁵ Technical References: *Fundamentals of Physics – Extended*. P. 387-390, 435-438.
Modern Control Systems, P. 145-146.

SYNCHRONICITY

Nature tends to synchronize elements that initially appear to be disharmonious. At times, achieving this synchronous state requires maximum entropy until a common denominator is obtained, after which, stability occurs. For example, when individual heart cells are removed from two living beating hearts, which are naturally beating at different rates, these two cells will continue to pulse at the rate of the heart from which they were removed. However, when these two cells are placed in contact with each other, both their rates of pulsation will change until a third beat different from either of the two original rates is attained. Both these cells will continue to beat at this third rate as long as oxygen and nutrients are supplied. They have synchronized with each other.

Examples of this law abound in nature. Numerous researchers have found that when women are placed together for several hours each day their menstrual cycles synchronize. Even if the menstrual cycles are, initially, randomly distributed throughout the month, after a short period of time the cycles will synchronize.⁵⁶

Synchrony even occurs with physical appearance. When people live together year after year they tend to start to look alike. Older couples not only attain similar mannerisms, but physically look more similar than they did when they met. These are all examples of nature's force to synchronize.

As with all natural laws, financial markets are not exempt from the phenomenon of synchronizing. In order to accurately time a financial market, it is simply a matter of finding with what other element in nature the particular market has synchronized, then determining if this other element provides predictability.

MUSICAL SCALES

Figure 6.1 shows strings of various lengths in a state of vibration. The string is used because it is the simplest example of a vibrating body. The fundamental tone is shown in 6.1.a, and the remaining tones (6.1.b through 6.1.f) are called "upper harmonics" to the fundamental tone.

The ratios between these tones (and the fundamental tone) define notes on the musical "Diatonic Major Scale". For example, between 6.1.a and 6.1.b the ratio is two, defining the octave. The ratio between 6.1.b and 6.1.c is three to two, defining the musical fifth. The remaining ratios and their respective musical tones are shown on the left side of the figure. On the right side of the figure is the ratio with respect to the fundamental tone, 6.1.a.

Note that these musical intervals consist solely of octaves, fifths, and octaves of fifths. This is the same system used by Pythagoras when he developed the "Diatonic

⁵⁶ Reference: *Nature*, March 1998, Martha McClintock, University of Chicago. The entire menstrual cycle tends to synchronize. This includes the portion known as premenstrual syndrome (PMS). For those working in close proximity to numerous women who are simultaneously experiencing PMS where unpredictable mood swings can occur, this knowledge could be valuable.

Major" musical scale. In this system, called the "succession of fifths", a tone is defined, such as C, as the fundamental tone. One fifth, a ratio of three to two, is taken below this tone. Then a fifth is taken above the fundamental, defining the tone g. Another fifth is taken from g, then another fifth from this tone, and this process is repeated until five octaves are covered. These tones are all reduced into a single octave⁵⁷, creating the "Diatonic Major" musical scale with frequency ratios shown in Table 6.1.

Table 6.1
Frequency Ratios of Diatonic Major Scale
With C As The Fundamental Tone (Key of C)

Musical Tone ⁵⁸	Interval	Frequency Ratio Relative to Fundamental Tone (C)
C	FUNDAMENTAL	1
D	SECOND	9/8
E	MAJOR THIRD	5/4
F	FOURTH	4/3
G	FIFTH	3/2
A	MAJOR SIXTH	5/3
B	SEVENTH	15/8
c	OCTAVE	2/1
g	TWELFTH	3/1

This is the Do, Re, Me, Fa, So, La, Te, Do musical scale. Music played on such a scale, with C as the fundamental tone, is known as "playing in the key of C".

⁵⁷ Reducing tones to a single octave simply means removing the value of unity and keeping the remaining fraction. For example, $3/2 \times 3/2 = 9/4$. From $9/4$ unity is removed, ($4/4$ in this case). The result is $5/4$, which is the frequency ratio of the tone "E", (see Table 6.1), within the single octave of the musical scale.

⁵⁸ Upper case is traditionally used to denote the fundamental tone (C). Lower case letters represent the first octave from the fundamental tone (c). Hyphenated lower case letters represent each successive octave (c', c'', etc.). This is the notation used in Figures 6.1, 6.2, and 6.3.

It is recommended the reader reference additional material concerning construction of the Diatonic Major Scale. This subject will not be further expanded here because this information is available from other sources.

For the purpose of this discussion, remember that a sequence of "fifths" taken above a fundamental tone, and one below the fundamental, and all reduced to a single octave, define the "Diatonic Major" musical scale, as created by Pythagoras.

NODAL POINTS

Having achieved a basic understanding of the musical scale, attention can be focused on Figure 6.1. The lengths and hence, the frequency of the strings shown in this figure are successively divided by two ratios, the octave and the fifth.⁵⁹

The points on this figure where the upper and lower lines come together are called **NODES**, and are places on the string where no motion occurs. For example, in 6.1.b there are two nodes at the end points and one node in the exact middle. Similarly, 6.1.c has two end nodes and two middle nodes, which divide the string into three equal vibrating lengths. The nodes are created as vibrations, which are sent through the string, bounce off the end points and interact with waves progressing in the opposite direction. At the points where nodes occur the waves add together to neutralize each other.

The concept of nodes is very important because, as will be shown, financial markets also possess nodes, i.e., periods of little or no motion where cycles moving in different directions create trendless markets. Lesson IX, **COMPOSITE CYCLES**, expands the concept of nodes.

To be in unison two strings do not have to be of equal length. Strings with lengths in the ratio of simple integers are also in unison. For example, the strings in Figure 6.1.a and 6.1.b are in unison with an integral ratio of two. Strings 6.1.b and 6.1.c are in unison with a ratio of the two integers three and two, and so on for the remaining lengths shown in the figure. Hence, a string is in unison with its harmonics.

If string 6.1.a (the fundamental tone) is set into vibration, string 6.1.b will also begin to vibrate. Also, 6.1.c will vibrate, as will 6.1.d, 6.1.e, and so on. These strings are in unison and will vibrate, sympathetically. Musicians are well aware of this phenomenon, which causes the high-pitched "ringing" sound heard when the string of an instrument is plucked. Without these "upper harmonics" the fundamental alone would have a very dull sound.

It is very important to note **THE STRING LENGTHS DO NOT HAVE TO BE IN EXACT UNISON TO VIBRATE, SYMPATHETICALLY**. If there is a minor difference from the exact integral ratio the bodies will still resonate, sympathetically. However, the further the bodies are from exact unison, the less sympathetic vibration will occur. The importance of this will become apparent as the amount of sympathetic resonance to expect in a financial market is determined given a certain amount of variation from the ideal fundamental. This will be studied in Lesson VIII.

⁵⁹ Technical Reference: *Introduction to Physics for Scientists and Engineers*. P. 581-584.

Rather than striking the fundamental tone shown in Figure 6.1.a, if the string in 6.1.b is struck it will induce sympathetic vibration in its upper harmonics namely, 6.1.c, 6.1.d, 6.1.e, etc. However, the vibration that is sympathetically induced in 6.1.a will have less magnitude than that in the upper harmonics. In other words, when a body is set into vibration the upper harmonics (strings with shorter lengths) will vibrate, sympathetically, with a much greater energy than the "lower harmonics" (strings with greater length than the one set into motion).

This natural phenomenon is the scientific basis for the radio.⁶⁰ A broadcasting station plays a tape or compact disk into a transmitter, which sends out a signal in the form of vibrations. These vibrations cause the circuitry inside the radio to vibrate, sympathetically, recreating the signal that was broadcast.

From radio transmissions to the creation of the musical scale, examples of sympathetic resonance can be found everywhere in nature. This is not limited to phenomena occurring on Earth, but can also be seen in motions in the solar system. For example, **THE RELATIVE PERIODS OF THE PLANETS EXIST IN HARMONIC RATIOS, IMPLYING SYMPATHETIC RESONANCE** was at work on the stellar debris during the formation process of the solar system.

Modern models of planetary formation have residue stellar debris originally distributed evenly in a two-dimensional plane extending from the equator of the sun. According to the theory, this material moved into areas where the least net force acted upon it (nodal points). This migration of the stellar material effectively created areas with large amounts of debris and areas with little or no debris. The areas where debris collected are those where the planets formed. The areas where no debris was present were those with a large net force acting on it, eventually moving the debris out of the area. The areas from where the debris moved represent the spacing between the planets after the formation process completed.

The periods of the planets exist in harmonic ratios. This means the nodal points, which defined the areas in the stellar debris where the material collected and where the planets formed, divided into harmonic ratios.

This process is easily simulated in the laboratory by placing metal filings on a flat sheet and subjecting the sheet to vibration. The metal filings move to areas where the sheet vibrates the least, i.e., nodal points. If the vibration rate is changed the metal filings move to another area on the sheet where the new nodes exist.

The harmonic ratios between the periods of the major planets are shown in Figure 6.2. This figure is the same as Figure 6.1, except the periods of the planets have been inserted in the appropriate positions to show the harmonic relationships.

⁶⁰ In 1909 W.D. Gann stated that his "Law of Vibration" was "the fundamental law upon which the wireless telegraphy, wireless telephones, and phonographs are based. Without the existence of (the Law of Vibration) the above inventions would have been impossible."

As noted earlier in this lesson, the fundamental tone produces upper harmonics. Figure 6.1.f shows an upper harmonic that has 1/12 the length of the fundamental tone, effectively dividing the fundamental tone into 30 degree segments, ($360^{\circ}/12 = 30^{\circ}$). The octave of this division creates an additional upper harmonic along the 15 degree axes. Therefore, a tone produces upper harmonics that are 1/24 the fundamental, i.e., harmonics which coincide with the 15° axes of the fundamental. These 15° axes are critical in correlating planetary motion with the DJIA.

Table 6.2 lists the heliocentric sidereal and synodic⁶¹ periods of the planets.

Table 6.2
Heliocentric Sidereal and Synodic Periods of the Planets

Planet	Sidereal Period	Synodic Period
Uranus	84 years	N/A
Saturn	29.5 years	N/A
Jupiter	12 years	N/A
Mars	22 months (687 days)	N/A
Venus	7 months (225 days)	N/A
Mercury	88 days	N/A
Saturn-Uranus	N/A	45 years
Jupiter-Saturn	N/A	20 years
Jupiter-Uranus	N/A	14 years

With the Saturn-Uranus synodic cycle of 45 years as the fundamental tone, the 20 year Jupiter-Saturn synodic cycle defines the octave, and the 14 year Jupiter-Uranus synodic cycle defines the musical fifth (from the Jupiter-Saturn cycle). The first reaction in seeing this might be that the Jupiter-Saturn cycle is not, EXACTLY, two times the Saturn-Uranus cycle. However, remember what was stated earlier, that two bodies do not have to be in exact unison in order to resonate, sympathetically. If a string of length 45 centimeters is laid next to one of 20 centimeters, and the 45 centimeter string is struck, the 20 centimeter string will vibrate, sympathetically. In addition, we see from Table 6.1

⁶¹ Sidereal periods are measured relative to the fixed stars. One heliocentric sidereal period is the time it takes to make one complete revolution around the sun and return to the same position, as seen from the sun. The heliocentric synodic period is the time interval between two successive conjunctions, as seen from the sun.

that the frequency ratio between "C" and "D" is 8/9. This produces the 40-year period. That is, 45 years x 8/9 years = 40 years, which produces an octave of 20 years.

As even more proof that these two cycles resonate sympathetically, Lesson VIII will show that the 15° and 30° axes of both these cycles provide areas where they synchronize with each other. This is possible due to the elliptical orbits of the planets, causing varying amounts of time to elapse as the planets move through their 15° axes. Even though the cycles of Saturn-Uranus and Jupiter-Uranus are not exact integral multiples, when 15° segments are looked at they tend to synchronize. Saturn-Uranus will move 15° as Jupiter-Saturn moves 30°. This will be proven as the planetary cycles and their harmonics are correlated with the stock market.

THE KEY FACTS TO REMEMBER FROM FIGURE 6.2 IS THAT AS SATURN-URANUS MOVES 15°, JUPITER-SATURN MOVES 30°, JUPITER-URANUS MOVES 45°, AND MARS COMPLETES ONE CYCLE. THESE CYCLES AND THEIR HARMONICS CORRELATE WITH CYCLES IN THE STOCK MARKET.

Figure 6.3 shows the same harmonic relationships shown in Figures 6.1 and 6.2. The difference in Figure 6.3 is that the periods of the minor planets are shown. The Jupiter-Uranus cycle is included in 6.3.a to show the connection between the major and minor cycles. Mars is shown as the fundamental tone in 6.3.b. As Jupiter-Uranus moves 45°, Mars completes one 360° cycle. Therefore, as Jupiter-Uranus moves through its 15° axes Mars moves 120°.

The harmonics of the Mars cycle divide it into 1/3 and 1/4 sections. Venus corresponds with the 1/3 section, defining the musical twelfth. As Mars moves 120°, Venus completes a 360° cycle.

The 1/4 division of the Mars cycle corresponds with the Mercury cycle. As Mars moves 90°, Mercury completes two 360° cycles. Another way to look at this is that Mercury completes one 360° cycle as Mars moves 45°. This means that the Mercury cycle is synchronized with the musical octaves of the Mars cycle. The octaves divide the fundamental tone into 180°, 90°, 45°, ..., sections.

Notice that the relative periods of the planets are numbers in the Fibonacci number sequence. One Mars cycle completes when three Venus cycles and eight Mercury cycles complete. One, three, and eight are numbers in the Fibonacci number series, as explained in Lesson III, **GROWTH PATTERNS**.

Similarly, one Saturn-Uranus completes when two Jupiter-Saturn cycles and three Jupiter-Uranus cycles complete. One, two, and three are successive terms in the Fibonacci number series.

If the relationships between the harmonics of the planets were not made clear by the above description, Lesson VIII, **PLANETARY CYCLES**, should help answer any remaining questions.

Musical Interval / Corresponding Frequency Ratio	Frequency Ratio to Fundamental
-----------------------------------------------------------------	-----------------------------------------------

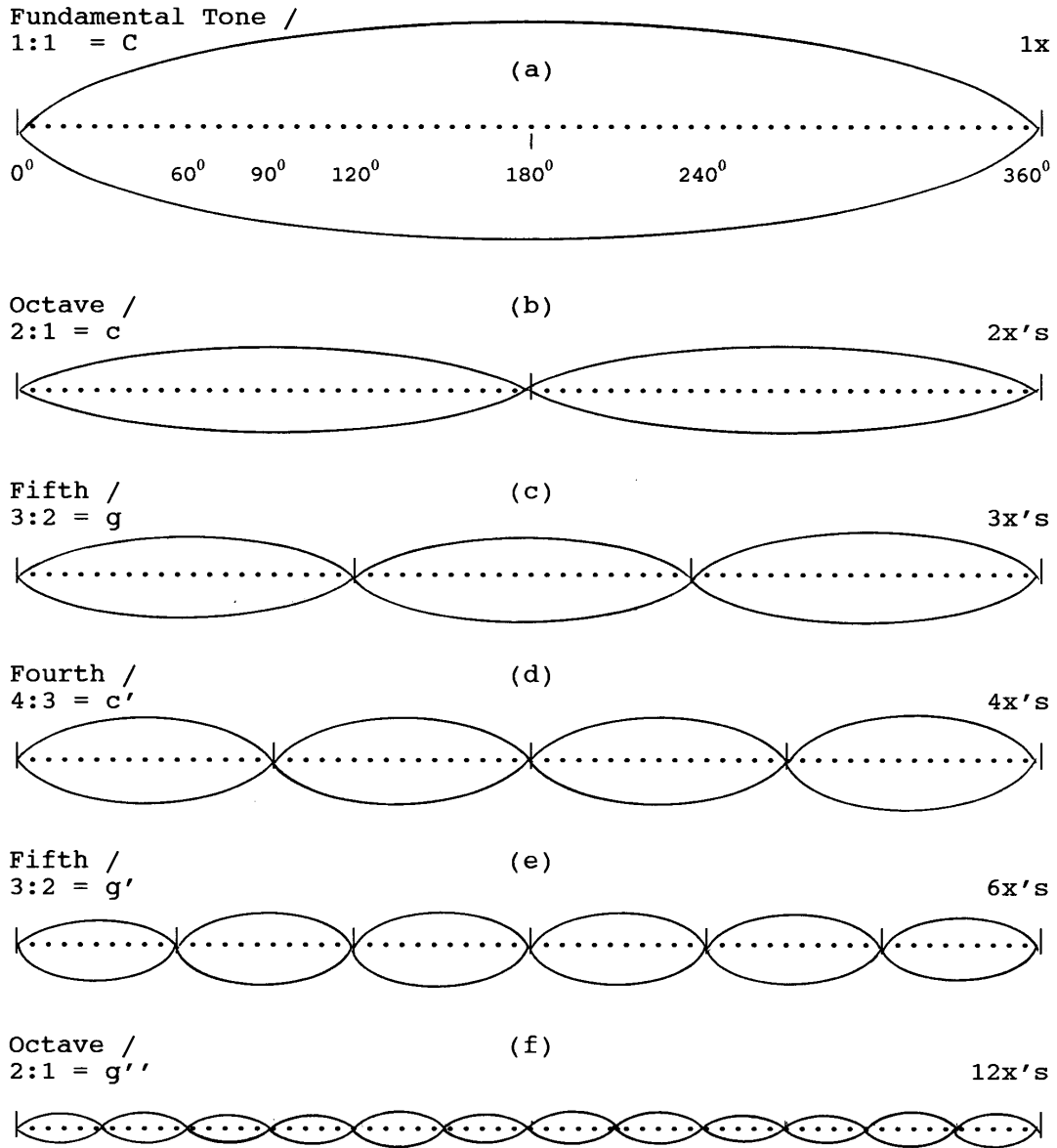


Figure 6.1
Musical intervals and corresponding frequency ratios.

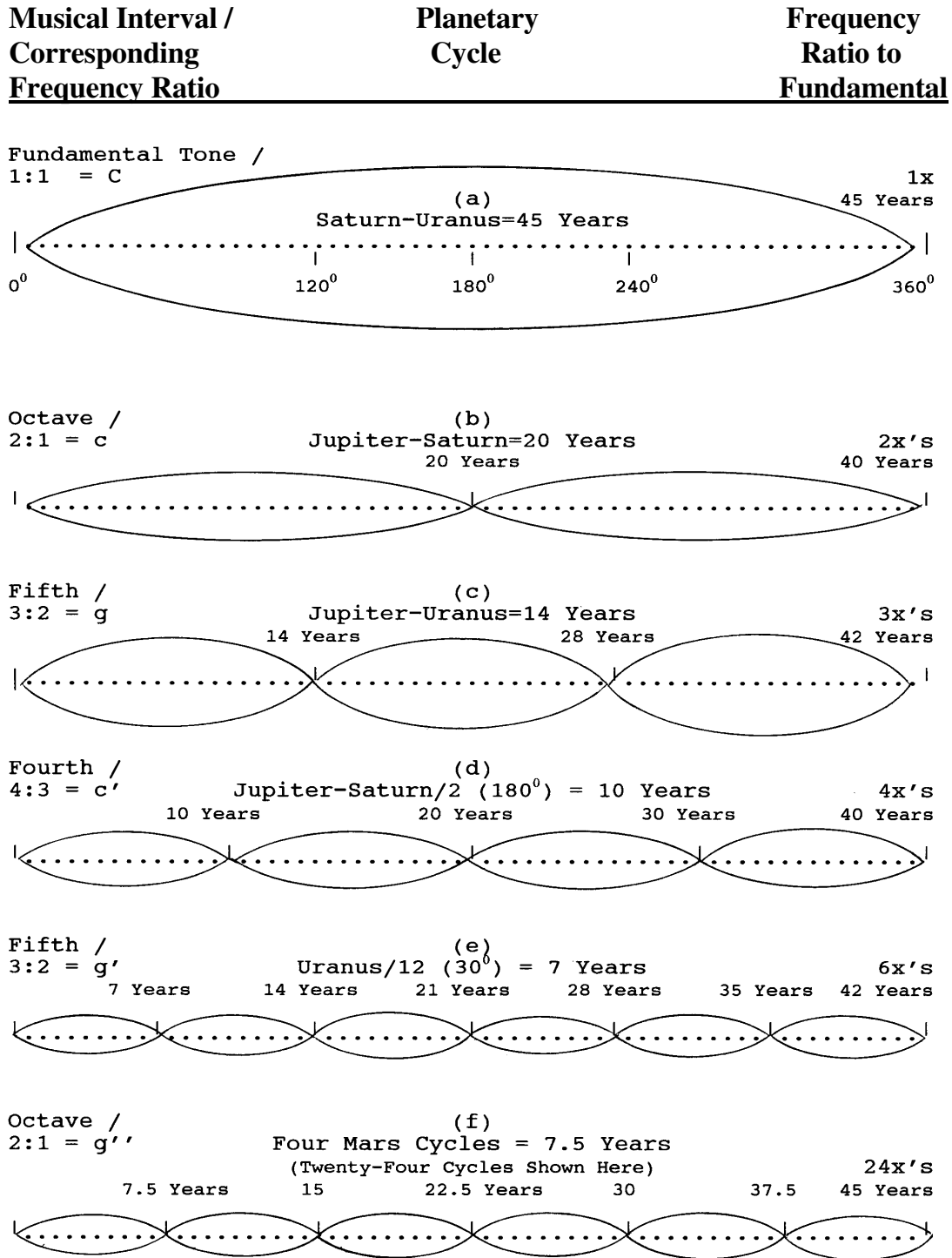
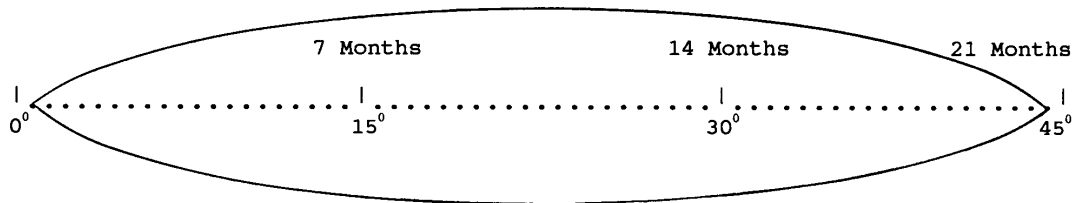


Figure 6.2

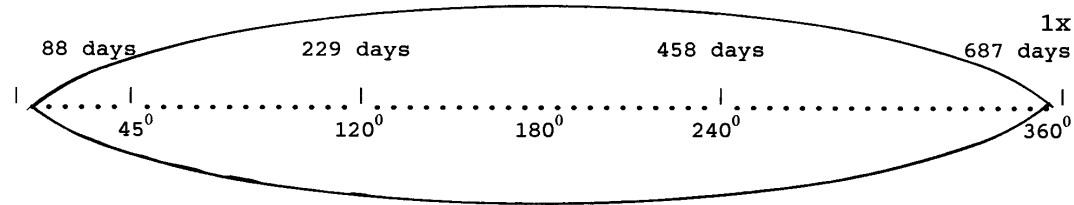
Musical intervals and corresponding major planetary cycles with Saturn-Uranus cycle (a) as the fundamental tone.

<u>Musical Interval / Corresponding Frequency Ratio</u>	<u>Planetary Cycle ⁶²</u>	<u>Frequency Ratio to Fundamental</u>
-----------------------------------------------------------------	------------------------------------------	-----------------------------------------------

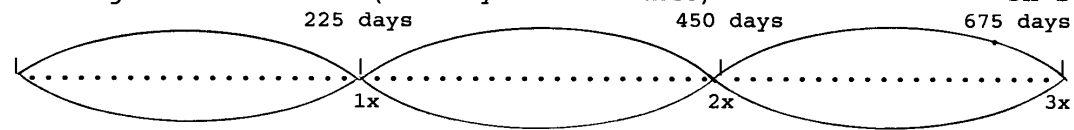
(a)
Cycle From Jupiter-Uranus/8 (45°) = 21 Months 1x
Major Planets⁴⁸



Fundamental Tone (b)
1:1 = C
Mars Cycle = 22.5 Months (687 Days)



(c)
Twelfth / Venus Cycle = 7 Months (225 days) 3x's
3:1 = g
(Three Cycles Shown Here)



(d)
Octave of Fourth / Mercury Cycle = 88 Days 8x's
8:3 = c''
(Eight Cycles Shown Here)

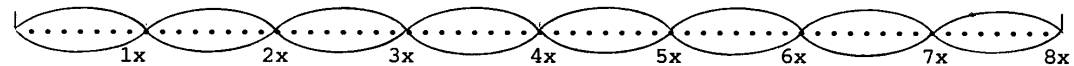


Figure 6.3

Musical intervals and corresponding minor planetary cycles with the Mars cycle (b) as the fundamental tone.

⁶² The major cycle of Jupiter-Uranus, shown in Figure 6.2, is included in this figure to show the connection between the major and minor cycles. The Saturn-Uranus cycle is also synchronized with the Mars cycle.

LESSON VII

CYCLES

Going far means returning.

Lao Tzu (600 B.C.) ... Tao Te Ching

Is there any thing whereof it may be said, See, this is new? it hath been already of old time, which was before us.

... Ecclesiastes 1:10

INTRODUCTION

The subject of financial market cycles is little understood by most market analysts. The traditional methods of Fourier transforms and percent deviations from moving averages originated with scientists and engineers. While these techniques are effective in isolating individual cyclic components of such things as radio signals or compound sound waves, they are little help when the complex topic of repetitive human behavior is studied.

The cyclic component of mass human psychology becomes evident as men repeat the same mistakes committed by their parents and grandparents. When measured in mass, man not only seems incapable of learning from the mistakes of history, but also inclined to repeat the errors committed as recently as the previous generation.

Financial markets are the laboratory where this mass psychology manifests in the form of price-time changes. As masses of people pool their emotions into their hopes and expectations for the future, certain geometric constructs evolve when these emotional changes are recorded as a function of time. The recurrence of behavior at similar locations on these geometric structures defines periodic law.

Financial market cycles begin at a certain point in price-time and progress through their natural growth sequence until they reach completion. After which, the price-time action is contained by a new cycle. The key points to know are; when and where a cycle begins, when and where it ends, and what to expect from the new cycle. This sounds simple, but in practice there are many pitfalls that can trip up the unsuspecting analyst.

This lesson will explain many cycle characteristics, of which contemporary cycle analysts are unaware.

BACKGROUND REVIEW

Traditional methods used by analysts to isolate the cyclic components of a financial market can be summarized in three simplified steps:⁶³

- (1) Establish a moving average from the price-time data.
- (2) Divide the price-time data into the moving average to obtain the percent deviation from the moving average, obtained in step (1).

⁶³ Reference: *Cycles*, Dewey.

- (3) Either visually or by Fourier Transform, obtain the cycles (actually rhythms) from the data in step (2).

DJIA EXAMPLE OF APPLYING CONTEMPORARY CYCLE ANALYSIS

Chart VII.A shows the DJIA from 10/1/1992 to 8/27/1993. This chart has the trend channel drawn in by upper and lower parallel lines, which contain the extremes of the price swings during this time. The median between these two channel lines defines the moving average described above, in step (1), and from which the percent deviation is calculated. This moving average advances at the rate of 400 points in 200 days. That is, it defines a 2x1 diagonal angle. This type of moving average is the simplest to recognize because it is linear over the time frame being studied.

As described above, in step (2), the price-time data is divided into the 2x1 moving average to obtain the percent deviation from the trend. The result of this division is shown on Chart VII.B.

The third step is to determine the rhythms from the detrended data. On Chart VII.B, the first rhythm that immediately stands out is the six-week rhythm, which equals thirty trading days and is shown by vertical lines. Similarly, other rhythms can be found in this chart.

The method followed above is the basic technique applied by contemporary cycle analysts. However, as will be shown in the following section, there are several problems with this approach, which can be overcome with an application of the tools presented in this course.

PROBLEMS WITH CONTEMPORARY CYCLE ANALYSIS

The cycle analysis performed in the previous section contains many examples of the limitations with the approach currently used by cycle analysts. To overcome these limitations, several facts about price-time cycles must be understood. Without an understanding of the cycle characteristics listed below, it is difficult to accurately project future cyclic effects.

- (1) Cycles are elliptical. Hence, as described in Lesson II, **THE ELLIPTICAL NATURE OF PRICE-TIME**, the price-time action either follows the major or minor axis, the upper perimeter, or the lower perimeter. While the price-time action is contained within the ellipse, the definition of the moving average is based upon which path it follows. When the price-time action moves into a new ellipse, a new moving average defines the action within that ellipse.

These ellipses are contained within larger ellipses. The paths taken by the action within larger ellipses defines the larger moving averages.

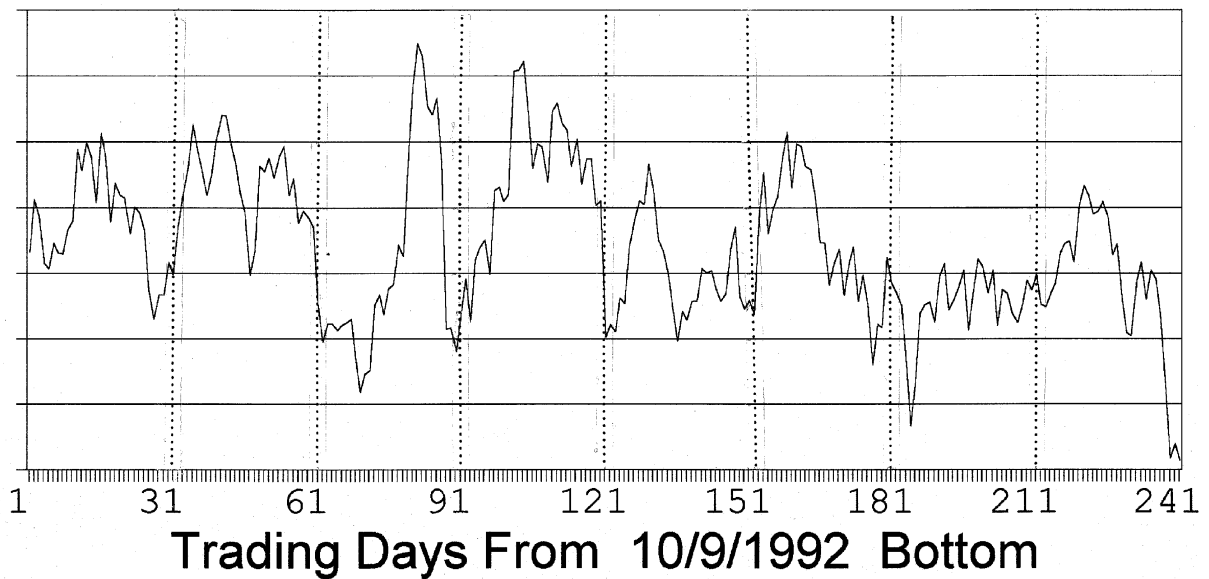
VII.A

DJIA FOLLOWING 1x2 TREND



VII.B

CHART VII.A WITH TREND REMOVED



- (2) The origin of a cycle does not necessarily follow the terminus of the preceding cycle because;

**CYCLES CAN OVERLAP AND THEY CAN
EXPERIENCE VERTICAL OFFSETS.**

Two overlapping cycles were shown on Chart II.A, where equilateral triangle FIK was composed of two overlapping ellipses.

The most obvious examples of vertical offsets happen after gaps. Question #3 at the end of Lesson I calculated the PTV from 1/23/1991 to 3/6/1991, shown on Chart I.D, to be an octave of the cycles occurring during this time interval. The origin of this cycle occurred on 1/23/1991, which is after the vertical offset of the gap preceding it. The origin was not at the absolute price low in 1/14/1991, even though this date was the terminus of the preceding cycle, which began on 12/21/1991.

An example of a vertical offset occurring in the opposite direction of the one described above is shown on Chart II.A. The origin of ellipse FHIJ is at point F, which is below the price high of the preceding ellipse, CFR.

- (3) The terminus of a cycle does not have to occur at its absolute price extreme. That is, the highest price for an advancing cycle or the lowest price for a declining cycle does not necessarily represent its terminus. This was explained in Lesson II, **THE ELLIPTICAL NATURE OF PRICE-TIME**, and can be seen on Chart II.A at point I.
- (4) Financial market cycles do not follow a constant periodicity. Due to the elliptical nature of cycles, it takes less time to move 15° when the cycle is at its faster moving sections. Similarly, when the cycle is at the slower moving part of its cycle it takes longer for a 15° section to complete.

Another important factor causing variance in cycle periodicity is the relative orientation of the equilateral triangles defining the axes of the mated ellipses. This topic is explained in detail later in this lesson.

PATH OF PRICE-TIME WITHIN ELLIPSE DEFINES THE MOVING AVERAGE

The initial step of contemporary cycle analysis, i.e., establishing a reliable moving average, is difficult without knowledge of market geometry. As soon as a reliable moving average is established it changes, ostensibly without warning. The previous example shown on Chart VII.A used the 2x1 linear moving average. The question that cannot be reliably answered by contemporary cycle analysis is; when will this moving average change?

KNOWLEDGE OF THE PTV AND MARKET GEOMETRY ALLOW THE ANALYST TO DEFINE, IN ADVANCE, THE EXACT DURATION OF THE MOVING AVERAGE. WHEN THE PTV HAS REACHED ITS END THE NEW PTV DEFINES THE TERMINAL POINT OF THE NEXT MOVING AVERAGE.

For example, the moving average in the preceding example was found to be a 2x1 diagonal angle, which defined the major axis of the ellipse containing the price-time action. The trend defined by this diagonal angle will continue until the terminal point of the PTV is reached. Contemporary cycle analysts have no idea when this point will be reached. However, with the tools presented in the first five lessons of this course, the analyst can identify in advance when and where this moving average will change.

Do not confuse the PTV with the moving average. Since the moving average can follow the upper or lower perimeter of the ellipse, it does not have to be linear, i.e., follow a straight line. The PTV is a straight line from the origin of a cycle to its terminus. This is shown in Figure 7.1, where the price-time action is shown following the lower perimeter of the ellipse. Hence, this arc defines the moving average. The PTV in this figure connects the origin and the terminus and is not the moving average.

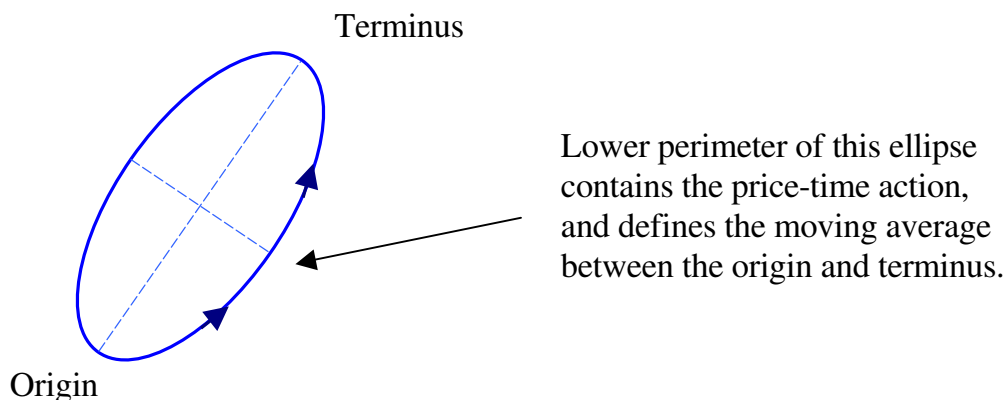


Figure 7.1

Difference between the PTV and the moving average

WHY THE PERIODICITY OF CYCLE TOPS AND BOTTOMS VARY

The varying periodicity of cycle tops and bottoms has always caused a problem for cycle analysts. Bottoms of cycles as small as six weeks can deviate from the ideal rhythm by several days, and tops have been found to deviate even more than bottoms. Exactly when and why this happens has remained a mystery. Tops vary so much that most contemporary cycle analysts do not even use tops to try to predict cycles. Rather, they focus on bottoms and accept the few days of error as an "unexplained" consequence of their technique.

Once again, geometry provides the solution to this old problem. Figure 1.2 showed how the time component of a PTV varies with the angle it assumes with the time axis. When the PTV is parallel to the time axis its time component is at a maximum. As the PTV

rotates upward the time component decreases. When the PTV points in a vertical direction its price component is at a maximum and the time component is zero.

In addition, Lesson II, **THE ELLIPTICAL NATURE OF PRICE-TIME**, identified the formation of the equilateral triangle within mated ellipses, and Figure 2.4 showed how these triangles can assume different orientations. The descriptions of Figures 1.2 and 2.4 should be reviewed at this time.

Figure 7.2 shows three possible configurations of adjacent equilateral triangles, demonstrating the extremes reached in both directions as the triangles rotate. With the orientation shown in 7.2.a the base of both triangles are parallel to the time axis. If cycles always assumed this configuration cycle rhythms would be constant and the distance measured top-to-top and bottom-to-bottom, t_1 , would always be equal.

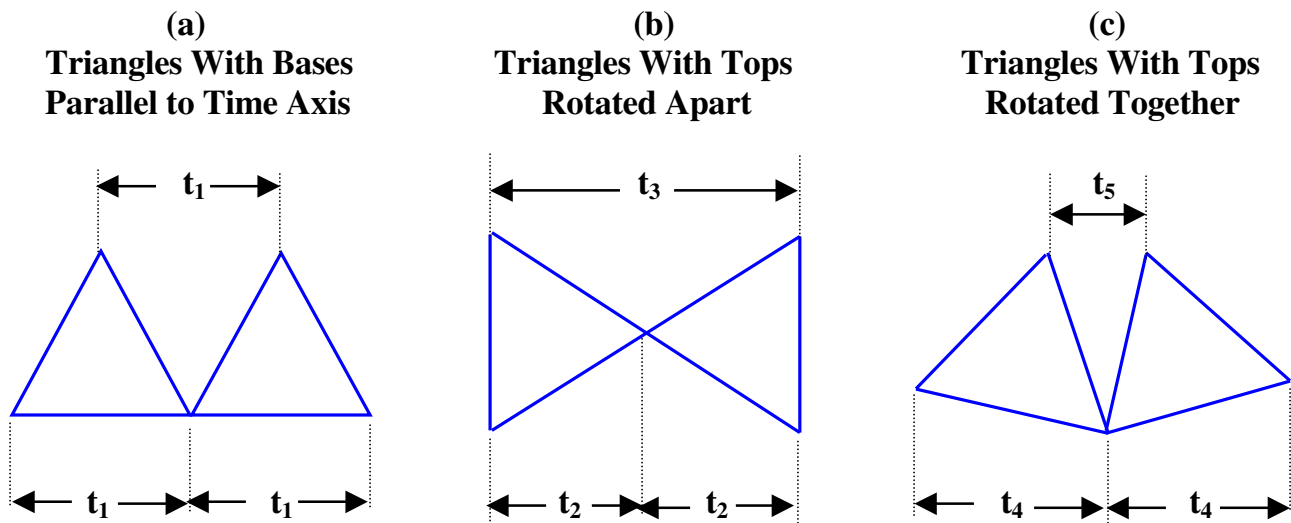


Figure 7.2

Configurations of adjacent equilateral triangles defining variance in periodicity of cycle tops and bottoms

A DJIA example of an equilateral triangle with its base parallel to the time axis was shown on Chart I.A, with triangle ABC. The triangle immediately following it, CDF, was slightly rotated counterclockwise causing the time between the two tops, BD, to be less than the time between the three bottoms, AC and CF.

Lesson II, **THE ELLIPTICAL NATURE OF PRICE-TIME**, showed that the equilateral triangles formed by mated ellipses, can rotate either clockwise or counterclockwise, depending upon the specific geometric configuration at that time. Figure 2.4.a showed the extreme that can be reached as the triangle is rotated counterclockwise. The limitation is reached when the left leg of the triangle is vertical. Similarly, the extreme that can be reached when the triangle is rotated clockwise was shown in Figure 2.4.c, where the right leg is vertical.

If the mirror image of Figure 2.4.a is placed directly after it, the result is the arrangement shown in Figure 7.2.b. Since the left leg of the first triangle is vertical, its top is directly over the first bottom. The triangle on the right is the counterpart to the one on the

left, with its top directly over the bottom at the far right. The result of placing two triangles, rotated in opposite directions, next to each other is the maximum possible separation between the two tops, t_3 . An example of this type of configuration can be seen on Chart I.A, with the tops of the two triangles, IJK and KLM, rotated apart.

The opposite of Figure 7.2.b is shown in Figure 7.2.c, where the tops of the two triangles are rotated toward each other. The result is a very short time interval between these two tops, t_5 . An example of this type of cyclic configuration can be seen on Chart I.A, with triangles EHI and IJK. Notice the spike down between the two tops, H and J.

The above examples, show how the distance between tops of two rotated triangles can vary from nearly zero, as in Figure 7.2.c, to the other extreme of encompassing the entire width of the two triangles, as in Figure 7.2.b. However, even though the distance between the tops can vary greatly, the bottoms vary only slightly. The distance between the bottoms reaches its maximum when the base of the triangles are parallel to the time axis, as in Figure 7.2.a. The distance between the bottoms is at its minimum when the triangles are rotated their maximum amount in opposite directions, as shown in Figures 7.2.b and 7.2.c.⁶⁴

Chart I.A provides a good example of this concept. The base of triangle ABC is parallel to the time axis, and as shown in Table 1.2, the time between these bottoms was 243.5 trading hours. In contrast, triangle IJK was rotated the maximum amount counterclockwise, since its left side is nearly vertical. Table 1.3 shows the time between the bottoms in triangle IJK was 217.0 trading hours, or 26.5 trading hours less than between the bottoms in triangle ABC. This difference of 26.5 trading hours is equal to over four trading days, a significant amount to many traders.

While the bottoms defined by triangles IJK and ABC differed by four days, the shift in the tops was much more dramatic. Since triangle IJK rotated the maximum amount counterclockwise and triangle KLM rotated clockwise, the separation of the tops was close to the maximum. The time between the two tops, JL, was 347 trading hours (54 days), or over one and one-half times longer than the time between the two bottoms, IK, which equaled 217 trading hours. This type of configuration is similar to that shown in Figure 7.2.b. Compare the distance between the tops, JL, with the distance between the tops, HJ, where the triangles take the opposite configuration. The time between the two tops, HJ, equaled 15 trading days, or eight weeks less than JL.

As time progresses, different combinations of paired triangles define the limits of the price-time action along the trend.⁶⁵ Each of these pairs will have different orientations. Their degree of relative rotation defines the separation between cycle tops and bottoms.

⁶⁴ For those who find that equations help make concepts clearer, the following relationships exist in Figure 7.2.

$$t_1 > t_2 ; t_2 = t_4 ; t_3 = t_2 + t_2$$

⁶⁵ Paired triangles are not the same as "mated ellipses". Two mated ellipses form an equilateral triangle. Two equilateral triangles form a pair.

ENERGY LEVELS OF CYCLES

Figure 7.3.a shows a rotating radius vector contained within a circle. This circle represents the energy level that the market is operating within as the PTV rotates.

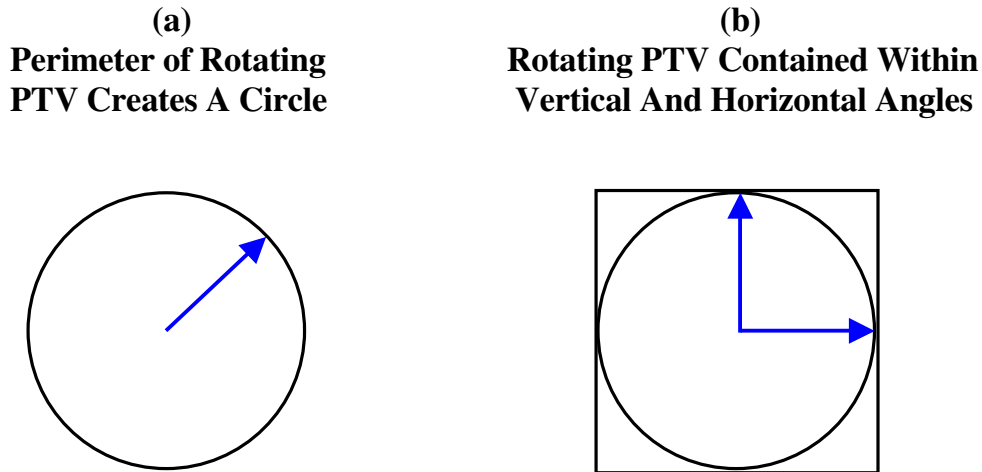


Figure 7.3

Extremes reached by the rotating PTV define the circle and the square.

Figure 7.3.b shows this same PTV with horizontal lines drawn at the top and bottom of the circle where extremes in price are reached, i.e., when the PTV is pointing directly up or down. Also, vertical lines are drawn where the extremes are reached in time, i.e., when the PTV is pointing directly to the right or left. Drawing in the levels at which these price and time extremes are defined effectively encloses the circle in a square.⁶⁶ The vertical lines define when the cycle begins and ends. As shown in Lesson I, when the price-time action enters the new square from the left, as represented on two-dimensional price-time charts, it is contained by the PTV, whose origin had yet to occur in time. The origin of the rotating PTV is located at the center of the circle.

If the growth process is that of composition⁶⁷, the cycle will expand after it reaches completion, and will move to a new energy level. A good example of natural energy levels occurs in chemistry. Electrons revolve around the nucleus of the atom at a stable level in an elliptical orbit until energy is added to the system (such as radiation). As more energy is added the electron moves out and away from the nucleus, effectively expanding its orbit. This transition is not smooth. Rather, it happens in jumps to different energy levels known as "quantum levels". The different energy levels can be seen in Figure 7.4.a, where the electrons are orbiting at a stable level.

⁶⁶ The sides of this square define the vertical and horizontal angles referred to by W.D. Gann. In his *Master Course For Stocks* he stated that the vertical and horizontal angles were more important than the diagonal angles (45^0 , $1x2$, $2x1$, etc.). Unfortunately, current "Gann experts" are selling only the diagonal angles as, so called, "Gann Angles".

⁶⁷ The rules for decomposition reverse the rules for composition.

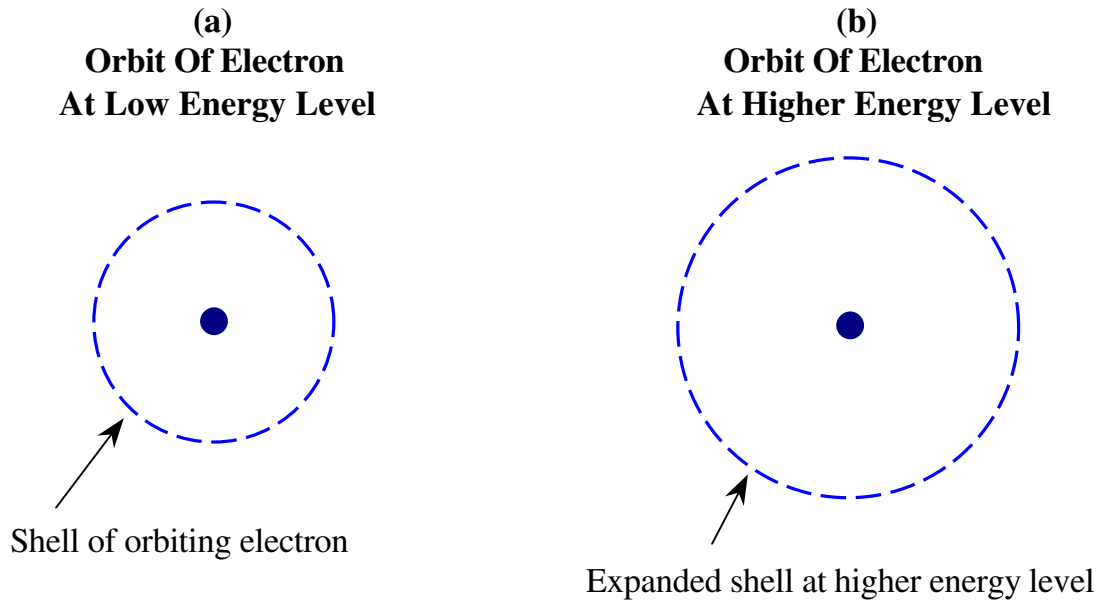


Figure 7.4
Two energy levels of electrons orbiting a nucleus

As more energy is applied, these electrons stay within their orbits until a critical level is reached. When that critical level is passed they make a quantum jump up to the next energy level, as shown in Figure 7.4.b. There they will orbit until more energy is added or removed. To scientists, this is known as the "Bohr model of the hydrogen atom", named after the physicist, Neils Bohr, who postulated it.

Think of the tip of the revolving PTV as an electron spinning around the nucleus of the atom. The length of the PTV is constant for a constant energy level. When the energy level is increased or decreased the length of the PTV changes, accordingly.

Enclosing Figure 7.3.b in a circle creates a figure shown in Figure 7.5, which is the same as Figure 4.2, and the first two energy levels of Figure 4.3. Review the description of these two figures.

Lesson IV showed that the ratio between the diameters of the two circles shown in Figure 4.2 is the square root of two, i.e., 1.414, which represents the diagonal of the square. It also represents the change between two energy levels.

An example in the stock market where there was a transfer from one energy level to the next higher level, occurred during the 1949-1966 square. Lesson V showed that this square was traversed diagonally. Review Figure 5.16, which shows the energy level increasing from the lower level of the cube to the top during the 1949-1966 square. At this higher energy level the price swings covered much greater distance than at corresponding locations at the lower level. Therefore,

STACKED CUBES NOT ONLY REPRESENT COMPLETED GROWTH PATTERNS, BUT ALSO INCREASING ENERGY LEVELS OF CYCLES.

Chart V.E compares squares at corresponding locations on the two different cubes that unfolded between 1899-1982 and 1966-present. Both these squares represent bottoms of cubes, one stacked on top of the other. The square from 1966-1982 was at the higher energy level, while the 1899-1914 square was at the lower energy level.

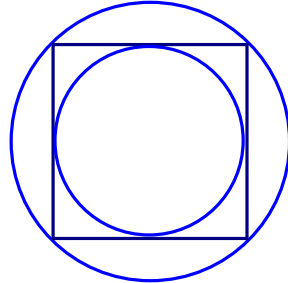


Figure 7.5

Square defining separation between two successive PTV energy levels

LESSON VIII

PLANETARY CYCLES

The ears of man were intended to follow harmonious movements, just as his eyes were intended to detect the motions of the heavenly bodies, those two being sister sciences, as the Pythagoreans declare.

Plato (347 B.C.) ...Republic

INTRODUCTION

Lesson VI showed that the relative motions of the planets exist in harmonic ratios. This lesson will show that these periods and their harmonic ratios are synchronized with cycles in the stock market.⁶⁸

The author spent several years researching potential correlations between geocentric motions of the planets and stock market cycles. The conclusion drawn from this research was that techniques using geocentric positions produce inconsistent results. Analysts using geocentric data claim their results are correct fifty or sixty percent of the time and consider that conclusive evidence of the efficacy of their techniques. It is the author's belief that a fifty or sixty percent correlation is nothing worthy of risking money on.

In contrast, the heliocentric positions of the planets produce a clear and consistent correlation with stock market turning points. Therefore, only heliocentric data is used for all work in this lesson and throughout this course.

This lesson begins with the large planetary cycles to define the larger market trends. After these larger trends are established, the cycles of the smaller planets will be progressively analyzed until the correlation between the Mercury cycle and the stock market is explained. This means that when the larger cycles are studied the smaller cycles will also be exerting their influence. This will cause some deviation at certain points, as a turning point in the stock market is delayed or advanced by one of the smaller cycles. Therefore, when studying precise dates of turning points the larger cycles must have a "window" of tolerance larger than that of the smaller cycles. This should be nothing new for students of cycle analysis. The explanation has been included here for those relatively new to the subject.

As the duration of the cycles become progressively smaller, the "window" of tolerance becomes correspondingly smaller, until even data recorded by the minute can be used for accurate predictions. As mentioned in Lesson V, **GEOMETRIC STRUCTURES**, there is no practical limitation to the size of the time frame to which these techniques can be applied.

⁶⁸ W.D. Gann used the motions of the planets as a market timing tool. The cycles listed in his *Master Course for Stocks* correspond with the periods of the planets.

While Gann claimed the planets were the "cause" of market activity, the author makes no such contention. Rather, it is demonstrated that a synchronicity exists between the relative motions of the planets and financial market activity.

When enough expertise is obtained markets can be timed to within four minutes of resolution. This is well within the reliability of recorded data.⁶⁹

To begin the analysis only monthly charts will be used. This will eliminate, as much as possible, the distortions caused by the smaller cycles.

ON A MONTHLY CHART ALL VISIBLE STOCK MARKET CYCLES ARE EXPLAINED BY THE HELIOCENTRIC SIDEREAL AND SYNODIC MOTIONS OF THE THREE MAJOR PLANETS; URANUS, SATURN, AND JUPITER.

The periods of these cycles and their harmonics are listed in the following section. The correspondence between the harmonics of these cycles is diagramed in Figure 6.2.

BACKGROUND REVIEW

Excluding the Earth and the planets orbiting beyond Uranus, there are three major planets:

(1) Jupiter (2) Saturn (3) Uranus

And three minor planets:

(4) Mercury (5) Venus (6) Mars

These are the planets that will be used to determine the cycles that are synchronous with the stock market. The motions of the major planets are synchronized with the major cycles in the stock market, and the motions of the minor planets are synchronized with the minor cycles.

The periods of the planets are defined by two common systems of measurement. The synodic period measures the time period between two successive conjunctions of two planets. The sidereal period measures the time period of a planet with respect to the fixed stars. Both these systems of measurement have significance in cycle analysis. The synodic and sidereal periods of the major planets that are synchronized with stock market cycles are listed below, along with their harmonic divisions.

⁶⁹ Four minutes is, approximately, how long it takes the Earth to rotate one degree. The details of how to narrow down the projected window to this small a time frame is scheduled to be included in the next volume of this home-study course. For now, accurate timing within one or two days is the objective.

URANUS CYCLE AND ITS HARMONICS

Fundamental Tone	= 84 years		
Octave (180 ⁰)	= 42 years	≅	Saturn-Uranus cycle
Double Octave (90 ⁰)	= 21 years	≅	Jupiter-Saturn cycle
Fundamental / 12	= 7 years	=	1/2 Jupiter-Uranus cycle, 1/3 Jupiter-Saturn cycle, 1/4 Saturn cycle

SATURN-URANUS CYCLE AND ITS HARMONICS

Fundamental Tone	= 45 years	≅	Octave of Uranus
Octave (180 ⁰)	= 22½ years	≅	Double Octave of Uranus
Double Octave (90 ⁰)	= 11.3 years		
Fundamental / 12	= 3.75 years	=	Two Mars Cycles

SATURN CYCLE AND ITS HARMONICS

Fundamental Tone	= 30 years	=	Trine of Saturn-Uranus
Octave (180 ⁰)	= 15 years	=	Trine of Saturn-Uranus
Double Octave (90 ⁰)	= 7½ years		
Fundamental / 6	= 5 years	=	Double Octave of Jupiter-Saturn

JUPITER-SATURN CYCLE AND ITS HARMONICS

Fundamental Tone	= 20 years	=	Trine of Saturn cycle
Octave (180 ⁰)	= 10 years	=	Trine of Saturn cycle
Double Octave (90 ⁰)	= 5 years	=	60 ⁰ of Saturn cycle

JUPITER-URANUS CYCLE AND ITS HARMONICS

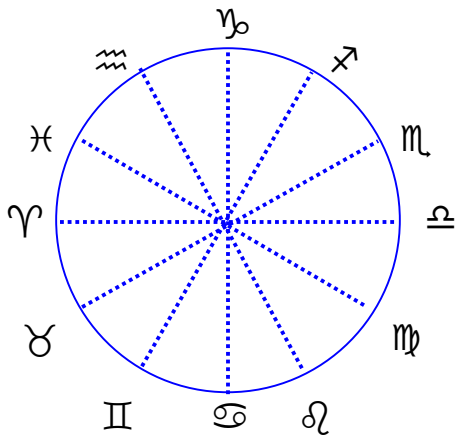
Fundamental Tone	= 14 years	=	60 ⁰ of Uranus cycle
Octave (180 ⁰)	= 7 years	=	30 ⁰ of Uranus cycle
Double Octave (90 ⁰)	= 3.5 years	≅	Saturn-Uranus / 12

SUBDIVISIONS OF THE 360° PLANETARY CYCLE

Lesson VI, **SYMPATHETIC RESONANCE**, showed how the periods of the planets subdivide into harmonic ratios along axes of 15°, and with a major subdivision along the 30° axes. This subdivision provides a convenient means of identifying specific 30° divisions of the orbit, since astronomers (and astrologers) use a system that gives names to each 30° division of the sky. This system of identification will be used here for convenience. The twelve divisions of the heavens and their corresponding names are listed in Table 8.1.

Table 8.1
Names of the Thirty-Degree
Divisions of the Heavens

Degrees From Zero Degree Aires	Name of the Division	Comments
0°	Aries (♈)	This point is chosen as zero degrees, because it defines where the sun crosses the celestial equator moving from south to north.
30°	Taurus (♉)	
60°	Gemini (♊)	
90°	Cancer (♋)	This point is where the sun reaches its furthest point north.
120°	Leo (♌)	
150°	Virgo (♍)	
180°	Libra (♎)	This point is where the sun moves from a northern position to a southern position.
210°	Scorpio (♏)	
240°	Sagittarius (♐)	
270°	Capricorn (♑)	This is the point where the sun reaches its furthest point south.
300°	Aquarius (♒)	
330°	Pisces (♓)	



If you feel more comfortable viewing the 360° circle in graph form, Figure 8.1 shows the circle divided into the twelve 30° sections.

Figure 8.1

Subdivision of the cycles into twelve 30° divisions

ANGLES BETWEEN THE PLANETS AND CORRESPONDING MUSICAL TONES

The angles between the planets that divide the synodic cycle into its harmonics also have traditional names. These names are listed in Table 8.2 and will be used in this lesson.

Table 8.2
Names of Planetary Angles
And Corresponding Musical Tones

Angle Between Planets	Name of Angle	Division of 360° Circle	Corresponding Musical Tone
360 Degrees	Conjunction	1	Fundamental Tone (C)
180 Degrees	Opposition	$\frac{1}{2}$	Octave of Fundamental Tone (c)
120 Degrees	Trine	$\frac{1}{3}$	Twelfth of Fundamental Tone (g)
90 Degrees	Square	$\frac{1}{4}$	Double Octave of Fundamental Tone (c')
60 Degrees	Sextile	$\frac{1}{6}$	Octave of Twelfth (g')
45 Degrees	Semi-Square	$\frac{1}{8}$	Triple Octave of Fundamental Tone (c'')
30 Degrees	Semi-Sextile	$\frac{1}{12}$	Double Octave of Twelfth (g'')

PLANETARY CYCLES AND THE FOUR-DIMENSIONAL STOCK MARKET

Traditional cycle analysts have noted how cycles appear in the stock market, repeat several times, then suddenly disappear. After a period of time these cycles reappear with a phase shift from their original value, repeat for several rhythms, then disappear again. This problem of disappearing cycles has confused cycle researchers, literally, for centuries.⁷⁰ Astrologers used planetary cycles to predict wheat prices at least as far back as the thirteenth century. Even these astrologers wrote about the phenomenon of disappearing cycles.

The four-dimensional understanding of financial markets explains the phenomenon of disappearing cycles.

CYCLES REPEAT ALONG THE FACE OF THE GEOMETRIC STRUCTURE THAT IS PASSING THROUGH MAN'S PERCEPTION AT THAT TIME. WHEN THE FACE OF THIS STRUCTURE IS COMPLETE THE STRUCTURE ROTATES TO EXPOSE THE NEXT FACE OF THE STRUCTURE. THE CYCLES ON THIS NEW FACE HAVE A PHASE SHIFT FROM THE CYCLES ON THE PREVIOUS FACE.

The tools developed in Part I of this course, **PRICE-TIME STRUCTURES**, allow the analyst to identify his relative location within the price-time structure unfolding. More importantly, accurate future projections can be made predicting when the face of the structure will complete and hence, cycle phase shifts can be anticipated.

The fact that the periodicity and phase of a cycle are dependant upon the face of the geometric structure will be proven in this lesson as cycles are identified in the stock market that repeat along the faces of structures, identified in Lesson V, **GEOMETRIC STRUCTURES**. These cycles experienced their phase shifts at the points identified in Lesson V as a completed face of the geometric structure under construction. When the new face rotates into view market analysts are often caught waiting for cycle tops or bottoms that never arrive. That is because they based their projections on a set of conditions that no longer exist. When the face of the structure is complete it rotates out of view, taking with it the conditions that existed on that face.

⁷⁰ Do not confuse disappearing cycles with the phenomenon of "beats". Beats are the result of two or more cycles interfering destructively, to reduce or eliminate their net effect. The concept of beats will be covered further in Lesson IX, **COMPOSITE CYCLES**.

The phenomenon of disappearing cycles has nothing to do with beats. This is proven because when the cycle reappears it has a phase shift. Phase shifts do not occur with beats.

URANUS SIDEREAL CYCLE AND STOCK MARKET CORRELATION

Since the complete cycle of Uranus is 84 years in length, long-term monthly data will be used to examine its correlation with stock market cycles.⁷¹

There are two significant correlations between the heliocentric sidereal motions of Uranus and the stock market. First,

THE QUARTER CYCLE OF URANUS (90⁰), AVERAGING 21 YEARS, CORRESPONDS WITH ALTERNATING ADVANCING AND DECLINING TRENDS IN THE STOCK MARKET.

Charts VIII.A and VIII.B are of detrended US stock market activity from the inception of the NYSE in 1792 to 1914, and from 1914 to 1993, respectively⁷². Two separate charts were used because the markets were closed for a period of 3 1/2 months between 7/31/1914 and 12/12/1914, during World War I. This closure disrupted the existing growth process.⁷³

On the top of these Charts is shown when Uranus completed a quarter-cycle or double octave. The Uranus quarter-cycle averages 21 years and is half of the complete 42-year stock market cycle.

The quarter-cycle of any cycle is extremely important because it defines the square.⁷⁴ In the case of Uranus, the quarter-cycle is reinforced by the synodic period of the Jupiter-Saturn cycle (20 years). That is,

THE URANUS QUARTER-CYCLE, 90⁰, CORRESPONDS WITH ONE JUPITER-SATURN CONJUNCTION.

The quarter-cycle periods are summarized in Table 8.3, where the first column lists the dates of the stock market half-cycle of 21 years. The second column identifies the location of Uranus when the 21-year stock market half-cycle began. Column three lists the location of Uranus when the 21-year stock market half-cycle ended. The fourth column of this table measures the difference between the second and third column, giving the total distance traveled by Uranus during the 21-year stock market half-cycle. The data in this

⁷¹ Appendix F contains a review of the correlation between the periodicity of war in the United States and the quarter-cycle of Uranus.

⁷² The method used for detrending the data in Charts VIII.A and VIII.B is described in Appendix B.

⁷³ In addition, 1914 marked the beginning of a "new era" in the long-term cycles. An explanation of the concept of the new era would require too much space to be included here.

⁷⁴ The 90⁰ division of the cycle is what W.D. Gann referred to when he said, "within the circle forms the square and the triangle." The triangle to which he referred is the trine (120⁰).

table shows how closely the 21-year stock market half-cycle has historically corresponded with 90° motions of Uranus.

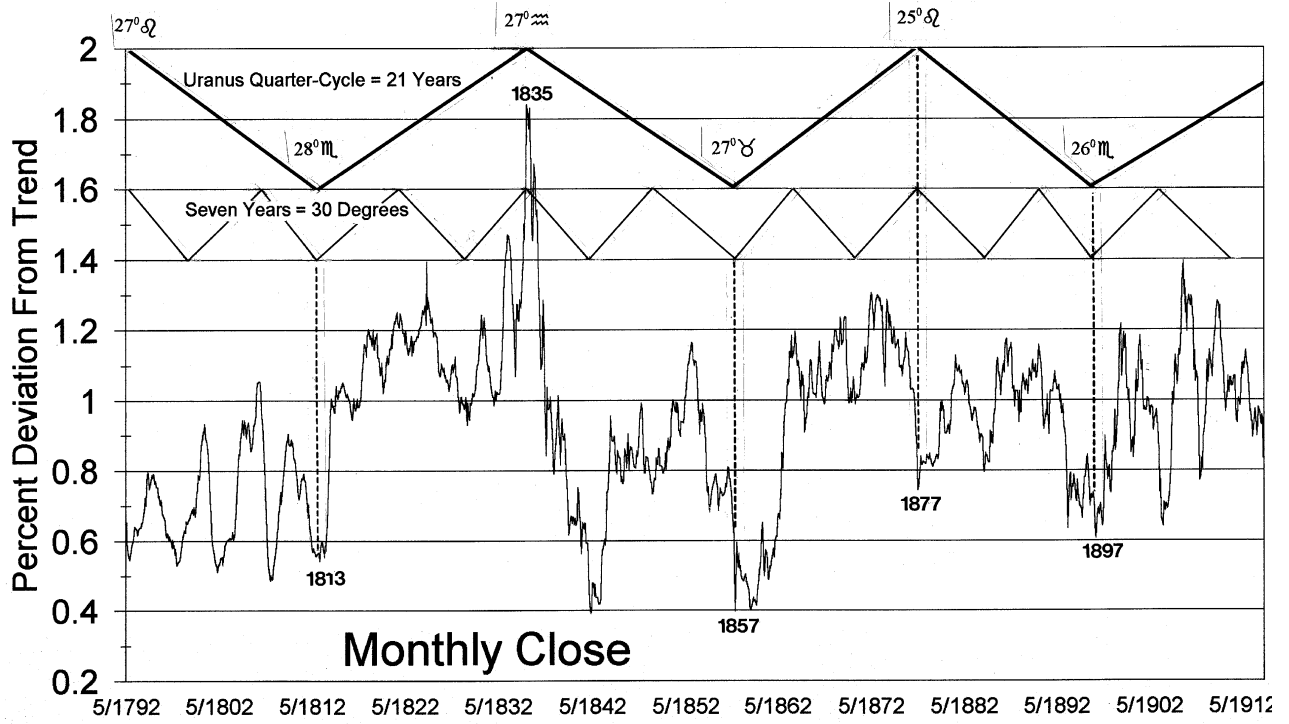
Table 8.3
Twenty-One Year Stock Market Half-Cycle And
Ninety-Degree Motions of Uranus (Quarter-Cycle)
(See Charts VIII.A and VIII.B)

Date of 21-Year Stock Market Half-Cycle	Location of Uranus at Start of Half-Cycle	Location of Uranus at End of Half-Cycle	Degrees Traversed by Uranus During 21-Year Period
9/1794 - 3/1813	29 Leo	26 Scorpio	87 Degrees
3/1813 - 5/1835	26 Scorpio	27 Aquarius	91 Degrees
5/1835 - 10/1857	27 Aquarius	27 Taurus	90 Degrees
10/1857 - 2/1878	27 Taurus	27 Leo	90 Degrees
2/1878 - 4/1897	27 Leo	26 Scorpio	89 Degrees
4/1897 - 11/1919	26 Scorpio	0 Pisces	92 Degrees ⁷⁵
11/1919 - 4/1942	0 Pisces	0 Gemini	90 Degrees
4/1942 - 6/1962	0 Gemini	0 Virgo	90 Degrees
6/1962 - 9/1981	0 Virgo	0 Sagittarius	90 Degrees

⁷⁵ While the market was closed in 1914, Uranus moved 2° . This explains the value of 92° in the table during this time. That is, 26° Scorpio to 0° Pisces is 94° ; and $94^{\circ} - 2^{\circ} = 92^{\circ}$.

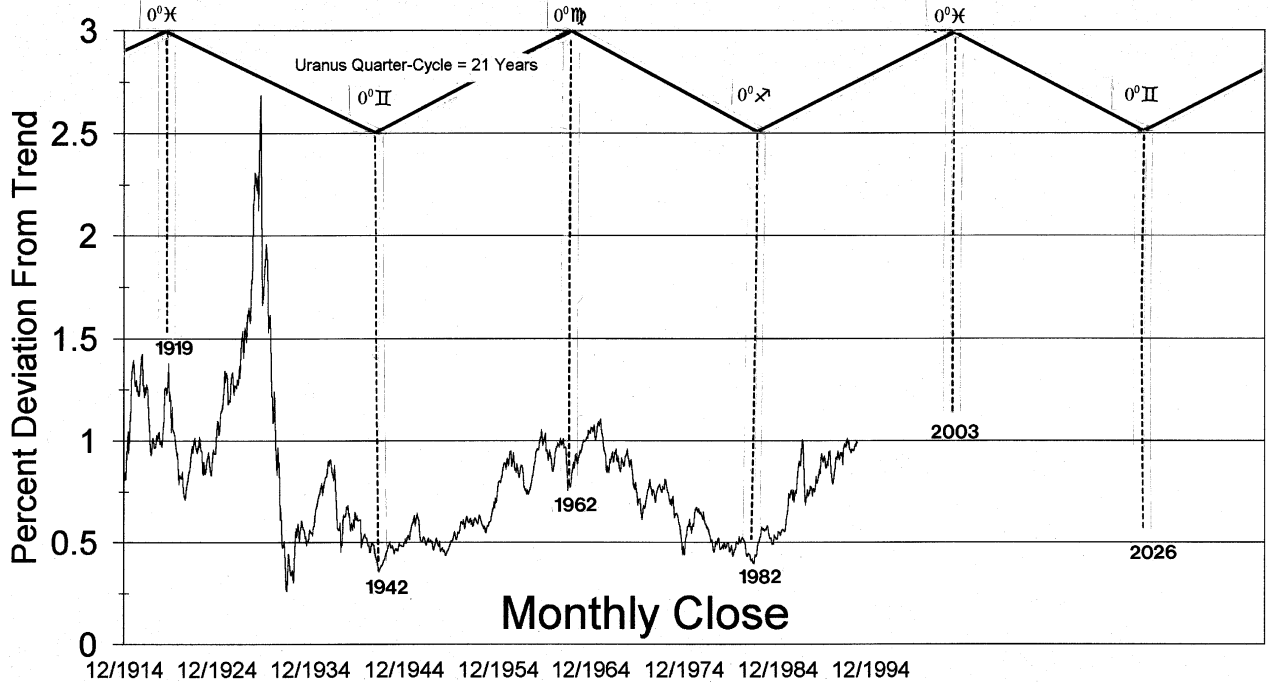
VIII.A

URANUS QUARTER-CYCLES



VIII.B

URANUS QUARTER-CYCLES (1914-2026)



Charts VIII.A and VIII.B show that as Uranus moves through its quarter-cycle of approximately 21 years, the general trend of the stock market alternates between rising and declining prices. This 21 year period of alternating price trends means that a bottom occurs every 42 years when Uranus approaches 0° Gemini and 0° Sagittarius. These bottoms occurred in:

1813 (28° Scorpio)
 1857 (27° Taurus)
 1897 (26° Scorpio)
 1942 (0° Gemini)
 1981 (0° Sagittarius)⁷⁶

Similarly, a top occurs every 42 years when Uranus approaches 0° Pisces and 0° Virgo. These tops occurred in:

1794 (29° Leo)
 1835 (27° Aquarius)
 1878 (27° Leo)
 1919 (0° Pisces)
 1962 (0° Virgo)

Graphically, the location of this square in the circle of 360° is shown in Figure 8.2, where the quarter-cycles are shown as sides of the square. Opposing sides of this square represent similar trends, i.e., either advancing or declining.

THESE FOUR LOCATIONS IN LONGITUDE CORRESPOND WITH THE FOUR EXTREMES REACHED IN LATITUDE: (1) NORTHERN (2) PASSING THROUGH ECLIPTIC NORTH TO SOUTH (3) SOUTHERN (4) PASSING THROUGH THE ECLIPTIC FROM SOUTH TO NORTH.

Projections for this cycle 200 years into the future are included in Figure 8.2. Occurrences of this node are due in 2026, 2065, 2110, 2149, and 2194.

Notice that when the 1878 and 1962 tops arrived, smaller cycles of five and seven years were bottoming. This made the dates of 1877 and 1962 represent periods of sharp decline, as the Uranus axis and the five and seven-year cycles coincided. However, if the general stock market trend is looked at for the Uranus quarter-cycle preceding these dates, a trend of advancing prices is seen.

⁷⁶ These five bottoms varied by as much as four degrees during this 169-year period. The explanation for this deviation is included in the next section covering the seven-year cycle.

TOPS

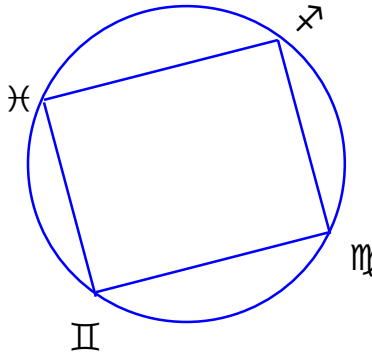
	1835
<u>PAST</u>	<u>1919</u>
FUTURE	2003
	2087
	2149

BOTTOMS

	1813
	1897
<u>1981</u>	<u>PAST</u>
2065	FUTURE

BOTTOMS

	1857
<u>PAST</u>	<u>1942</u>
FUTURE	2026
	2110
	2194

**TOPS**

	1794
	1878
<u>1962</u>	<u>PAST</u>
2046	FUTURE
	2130

Figure 8.2

Quarter-cycles of Uranus showing dates of squares between 1794-2194
(See Charts VIII.A and VIII.B)

Uranus shows how the positions of the planets relate to the cubic structures identified in Lesson V. The position of Uranus in 1899, 3^0 Sagittarius, was exactly the same as at the nodal point of 1982. Both these time periods marked the beginning of a new face of a cubic solid. In addition,

**THE COMPLETE URANUS CYCLE FROM 1899 TO 1982 DEFINED
THE COMPLETE CUBIC STRUCTURE DESCRIBED IN LESSON V.**

SEVEN-YEAR STOCK MARKET CYCLE

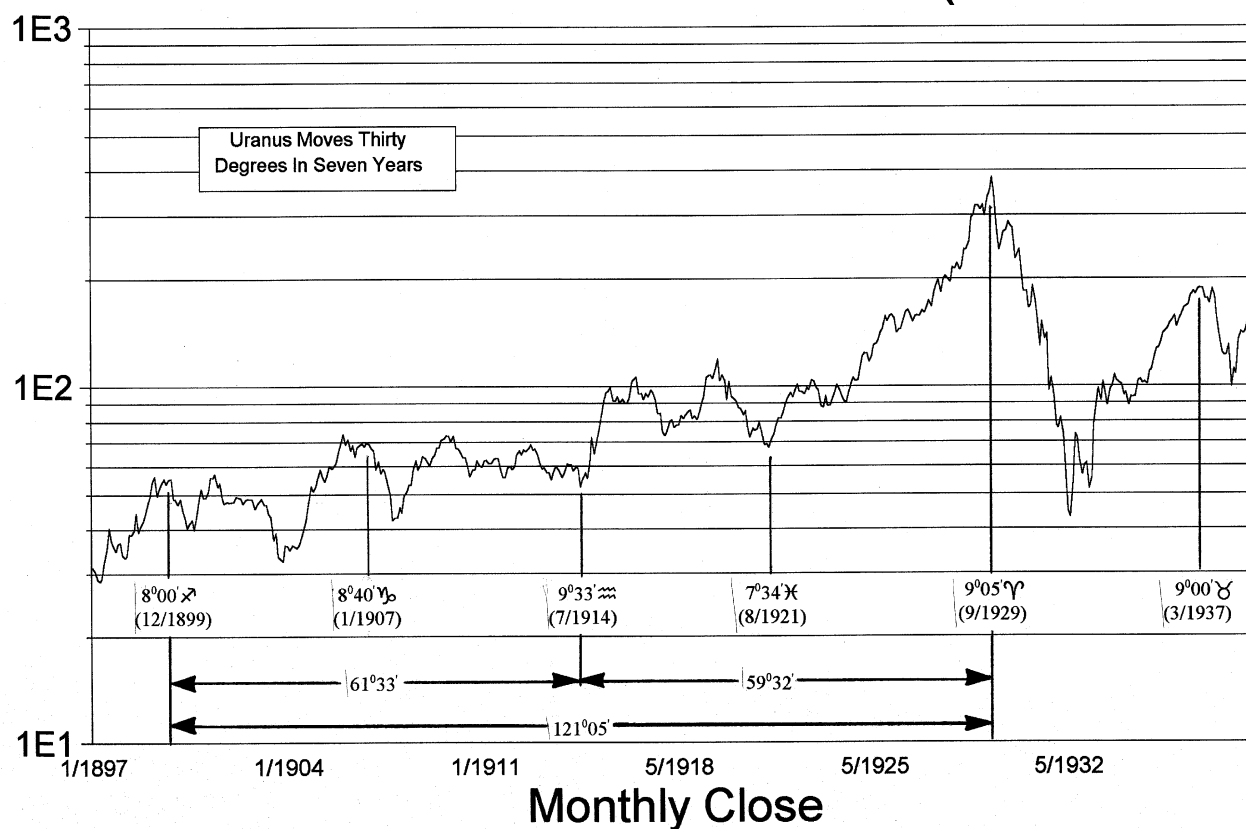
Charts VIII.A, VIII.C, and VIII.D identify the seven-year stock market cycles since the year 1794. The vertical lines on these charts locate the dates of the major turning points. The spacing between each of these vertical lines is 30^0 in the Uranus cycle. This defines the second correlation between the sidereal motion of Uranus and the stock market. That is,

**URANUS CORRESPONDS WITH THE SEVEN-YEAR STOCK
MARKET CYCLE AS IT MOVES ACROSS ITS 30^0 AXES.⁷⁷**

⁷⁷ This cycle is reinforced if the Saturn cycle moves 90^0 at the same time as Uranus moves 30^0 . This will be covered further in the section on the Saturn cycle.

VIII.C

URANUS SEVEN YEAR CYCLE (1897-1939)



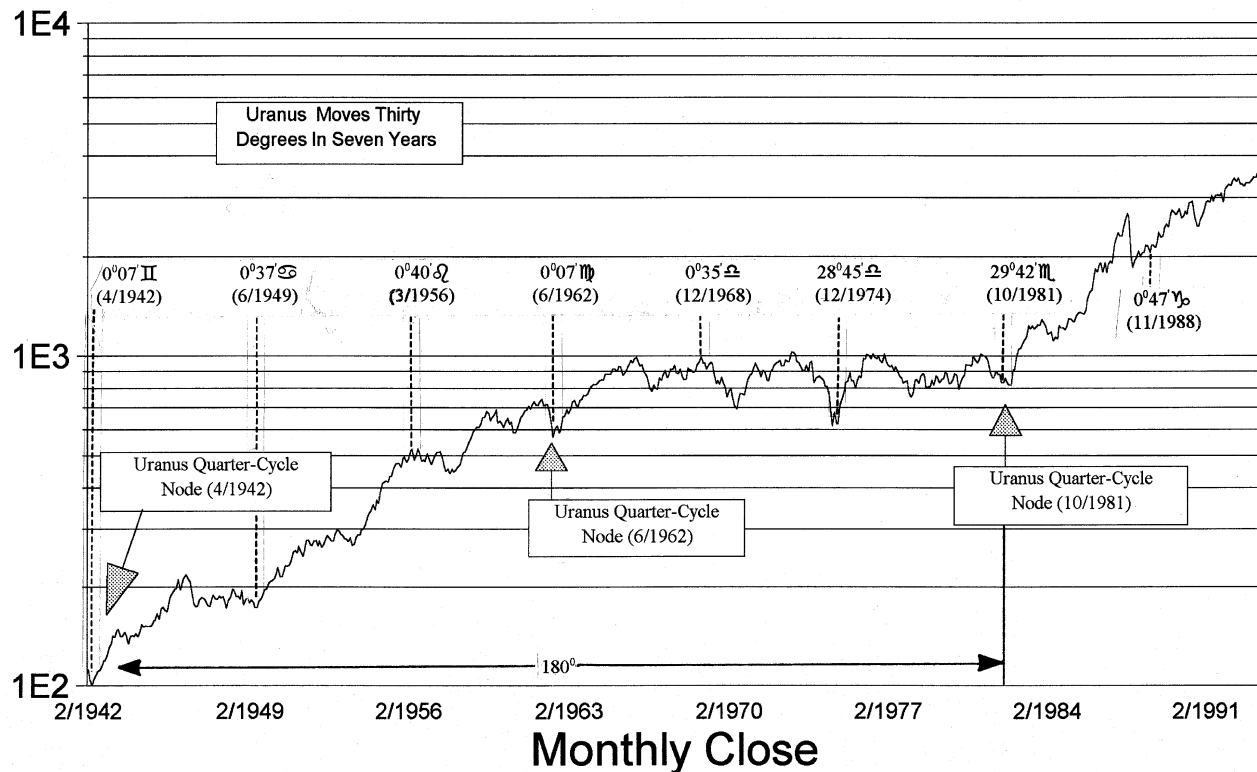
For a closer examination of the correlation between the seven year cycle and 30° motions of Uranus, the data are included in Table 8.4, which is divided into three time periods: (1) 9/1806 - 7/1914; (2) 7/1914 - 4/1942; (3) 4/1942 - 11/1988.

In 1914 World War I broke out and the New York Stock Exchange was closed from 7/31/1914 through 12/12/1914. The cycle did not have a chance to complete its entire 30° motion before the exchange closed. Rather, half this amount, 15° , completed. The seven-year stock market cycle synchronized with the position of Uranus at this point, i.e., 9° Aquarius. This period of stock market activity is shown on Chart VIII.C. Each of the solid vertical lines on this chart represents a 30° division of the Uranus cycle as it crossed 9° of each sign. These locations corresponded with critical turning points in the stock market including the bottom in 1914, the bottom in 1921, the top in 1929, and the top in 1937.

Halfway between these vertical lines are the 15° axes. These axes define important points in the stock market. However, their effect is less than that of the lower harmonics, i.e., the 30° and 60° divisions. This chart shows that Uranus moved 60° between the top in 1899 and the bottom in 1914. It similarly moved 60° from the 1914 low to the top in 1929.

VIII.D

URANUS SEVEN YEAR CYCLE (1942-1993)



The 9^o axis defined the limits of the seven year cycle until April, 1942, when World War II broke out and Uranus conjoined with Saturn. From April, 1942 to the present the seven year cycle has been defined by the position of Uranus at 0^o of every sign, i.e., every 30^o movement. These seven-year cycles are shown on Chart VIII.D, with the 30^o axes of Uranus identified by the dotted vertical lines.

Since 1942, the turning points in the stock market and the corresponding 30^o axes of Uranus have been:

Bottom on	4/28/1942	--	0 ^o 08' Gemini
Bottom on	6/14/1949	--	0 ^o 40' Cancer
Top on	4/5/1956	--	1 ^o 13' Leo
Bottom on	6/27/1962	--	0 ^o 10' Virgo
Top on	12/2/1968	--	0 ^o 32' Libra
Bottom on	12/9/1974	--	28 ^o 45' Libra
Bottom on	9/29/1981	--	29 ^o 43' Scorpio
Bottom on	11/16/1988	--	0 ^o 47' Capricorn

Table 8.4.a
Seven-Year Stock Market Cycles And Thirty-Degree Heliocentric
Motion of Uranus From 1806 to 1914 (See Chart VIII.A)

Date of Seven-Year Cycle	Beginning Location of Uranus	Ending Location of Uranus	Movement of Uranus During Seven-Year Cycle
9/1806 - 3/1813	25 Libra	26 Scorpio	31 Degrees
3/1813 - 7/1821	26 Scorpio	1 Capricorn	35 Degrees
7/1821 - 3/1828	1 Capricorn	29 Capricorn	28 Degrees
3/1828 - 5/1835	29 Capricorn	27 Aquarius	28 Degrees
5/1835 - 3/1843	27 Aquarius	28 Pisces	31 Degrees
3/1843 - 12/1850	28 Pisces	29 Aires	31 Degrees
12/1850 - 10/1857	29 Aires	27 Taurus	28 Degrees
10/1857 - 3/1864	27 Taurus	24 Gemini	27 Degrees
3/1864 - 8/1870	24 Gemini	23 Cancer	29 Degrees
8/1870 - 2/1878	23 Cancer	27 Leo	34 Degrees
2/1878 - 6/1884	27 Leo	27 Virgo	33 Degrees
6/1884 - 6/1890	27 Virgo	25 Libra	28 Degrees
6/1890 - 4/1897	25 Libra	26 Scorpio	31 Degrees
4/1897 - 11/1903	26 Scorpio	25 Sagittarius	29 Degrees
11/1903 - 7/1910	25 Sagittarius	23 Capricorn	28 Degrees
7/1910 - 7/1914	23 Capricorn	9 Aquarius	16 Degrees

Table 8.4.b
Seven-Year Stock Market Cycles And Thirty-Degree Heliocentric
Motion of Uranus From 1914 to 1942 (See Charts VIII.C and VIII.D)

Date of Seven-Year Cycle	Beginning Location of Uranus	Ending Location of Uranus	Degrees Traversed by Uranus During 7-Year Cycle
7/1914 - 8/1921	9 Aquarius	8 Pisces	29 Degrees
8/1921 - 9/1929	8 Pisces	9 Aries	31 Degrees
9/1929 - 3/1937	9 Aries	9 Taurus	30 Degrees
3/1937 - 4/1942	9 Taurus	0 Gemini	Beginning of World War II

Table 8.4.c
Seven-Year Stock Market Cycles And Thirty-Degree Heliocentric
Motion of Uranus From 1942 to 1988 (See Chart VIII.D)

Date of Seven-Year Cycle	Beginning Location of Uranus	Ending Location of Uranus	Degrees Traversed by Uranus During 7-Year Cycle
4/1942 - 6/1949	0 Gemini	1 Cancer	31 Degrees
6/1949 - 4/1956	1 Cancer	1 Leo	30 Degrees
4/1956 - 6/1962	1 Leo	0 Virgo	29 Degrees
6/1962 - 12/1968	0 Virgo	0 Libra	30 Degrees
12/1968 - 12/1974	0 Libra	29 Libra	29 Degrees
12/1974 - 9/1981	29 Libra	0 Sagittarius	31 Degrees
9/1981 - 11/1988	0 Sagittarius	1 Capricorn	31 Degrees

SATURN-URANUS SYNODIC CYCLE AND STOCK MARKET CORRELATION

Saturn and Uranus conjoin every forty-five-years. This means the average time between 30° axes of this cycle is forty-five months, and between 15° axes the average time is 22.5 months.⁷⁸ Figures 6.2 and 6.3 showed that a planet's period divides into harmonics that correspond with periods of other planets.

A historical analysis of the Saturn-Uranus cycle and corresponding stock market cycles since 1896 is summarized in the following sections. The information contained in Tables 8.5.a, 8.5.b, 8.5.c, 8.5.d, and 8.5.e is shown on Charts VIII.E, VIII.F, and VIII.G, VIII.H, VIII.I, respectively. Solid vertical lines show the 30° axes on these charts. The angles between Saturn and Uranus at key turning points are listed, as well as the distance these two planets traveled between the dates of these turning points. While studying the charts described in the following sections, note how precisely the 30° axes of the Saturn-Uranus cycle coincided with turning points in the stock market.

The data contained in these charts are divided into separate tables to cover the individual growth sections in the stock market. The reason for dividing the analysis into different sections was explained earlier in this lesson. Specifically, when the face of the geometric structure that is unfolding in price-time is complete the next face that rotates into view may have cycles with a phase shift from the earlier face. The exception to this rule occurs when completion of the face of the structure coincides with arrival of the cycle at its 15° axis. For example, at the transition between the two squares 1899-1914 and 1914-1929, the Saturn-Uranus cycle was at its 15° axis, as defined by the 1899-1914 period. Therefore, when the 1899-1914 square completed and the Saturn-Uranus cycle was aligned with its location at that time, there was no phase shift for the new set of cycles within the new square between 1914-1929.

An example when completion of a square did not coincide with a 15° axis of the Saturn-Uranus cycle occurred in 1949. When the Saturn-Uranus cycle arrived at its 15° axis in 1946 the 1932-1949 square had not yet completed. When the square was complete in 1949 the angle between Saturn-Uranus was 66° . This was the point in time when the Saturn-Uranus cycle synchronized with the stock market cycles for the duration of the 1949-1966 square. The 66° axis was not on the 15° axes of the 1932-1949 square. Rather, it was the origin of the cycles in the 1949-1966 square.

Since the 1949-1966 square is one face of a cubic geometric solid, the data covering this period is included in a separate table. Similarly, 1899-1914, 1914-1929, 1966-1982, and 1982-1987 are faces of cubes and hence, their data is included in separate tables. The exception to this is the 1899-1929 period when there was no phase shift between the squares, as explained above. Therefore, the data for these two squares are included in a single table.

⁷⁸ This 22.5-month period corresponds with the sidereal period of Mars.

HISTORICAL ANALYSIS OF SATURN-URANUS CYCLE (1896-1929)

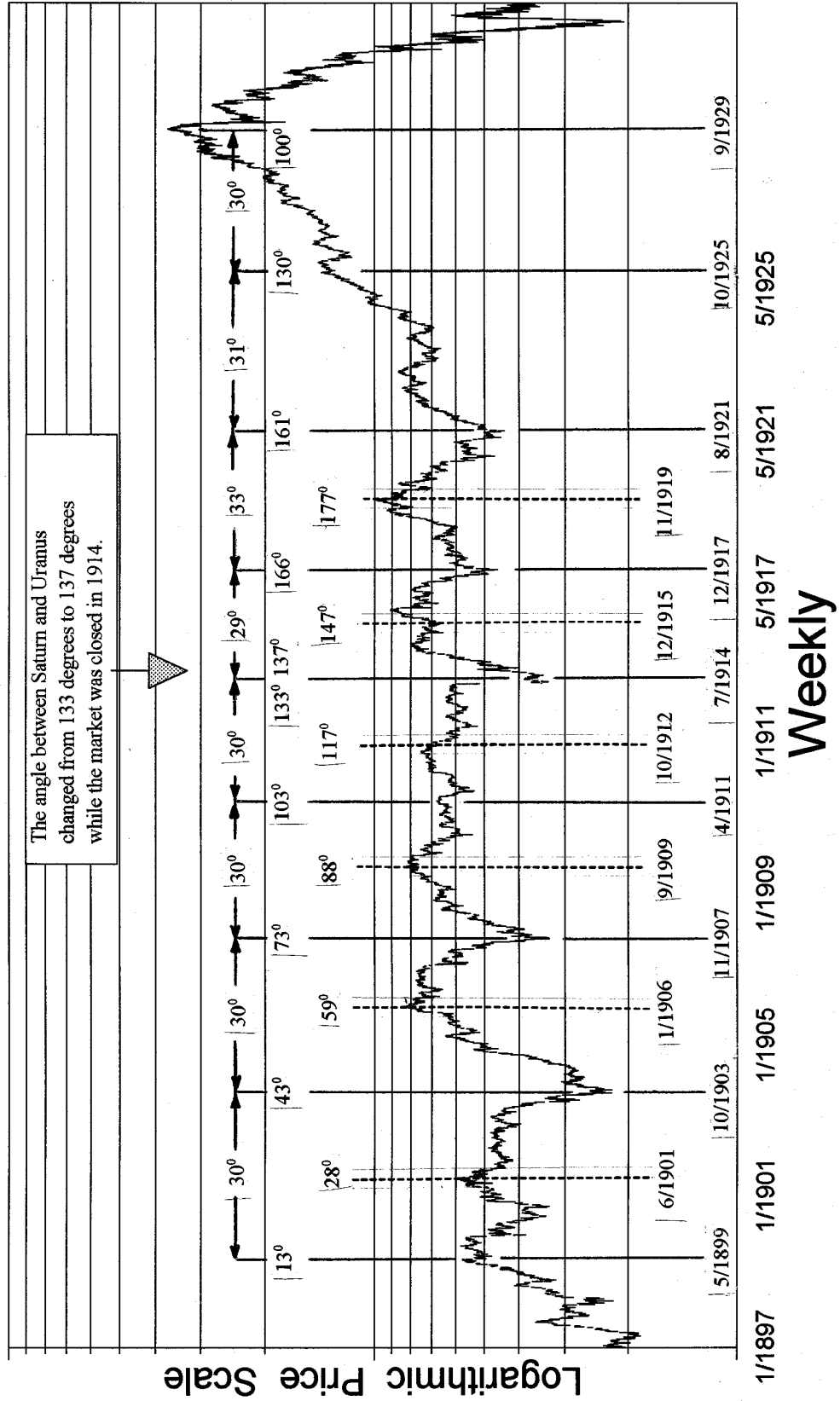
The data contained in Table 8.5.a, and graphed on Chart VIII.E, covers one of the easiest periods in stock market history to study. Across these two faces of the cube the major cycles and their harmonics were very closely synchronized hence, they tended to reinforce each other, rather than interfere destructively. As explained in the previous section, the Uranus cycle was at its nodal point in 1899. This was the same nodal point as in 1981. Within the larger Uranus cycle the Saturn-Uranus cycle subdivides stock market turning points along its 15⁰ axes, as shown on Chart VIII.E.

Table 8.5.a
Saturn-Uranus Synodic Divisions of Fifteen Degrees And
Corresponding Turning Points in the DJIA (1896-1929)
 (See Chart VIII.E)

Date of Turning Point in DJIA	Angle Between Saturn and Uranus	Change From Last Point
12/1896	Two Degrees Before Conjunction	N/A
4/1899	13 Degrees After Conjunction	15 Degrees
6/1901	27 Degrees	14 Degrees
10/1903	43 Degrees	16 Degrees
1/1906	59 Degrees	16 Degrees
11/1907	74 Degrees	15 Degrees
9/1909	89 Degrees	15 Degrees
4/1911	103 Degrees	14 Degrees
10/1912	117 Degrees	14 Degrees
7/1914	133 Degrees	16 Degrees
7/1914 - 12/1914	STOCK MARKET CLOSED	Moved 4 ⁰ While Closed
12/1914	137 Degrees	N/A
12/1917	166 Degrees	29 Degrees
8/1921	161 Degrees	33 Degrees
9/1929	100 Degrees	61 Degrees

VIII.E

SATURN-URANUS AXES (1897-1929)



The square from 1899 to 1914 was crossed laterally, similar to the square from 1966 to 1982. Both these squares represent the base of a cube. The square from 1966 to 1982 was not only the base of the cube extending from 1966 to the present, but also the top of the cube from 1899 to 1982. Lesson V and Chart V.E showed the similarities of the market action within these two squares.

The cycles on Chart VIII.E are clearly evident. Rather than provide a cycle-by-cycle description of that chart, it is recommended the reader spend the time to thoroughly familiarize himself with the cycles identified there.

While studying this chart, notice that the 1899-1914 square coincided with the trine (120° movement) of the Saturn-Uranus cycle, as did the 1914-1929 square. The half-trine (60°) defined the bottom of the 1907 "rich man's panic" in the first square, and the 1921 bottom in the second square. Every turning point in the stock market during this time coincided with a harmonic of the Saturn-Uranus cycle, all the way down to the 15° harmonic.

HISTORICAL ANALYSIS OF SATURN-URANUS CYCLE (1929-1937)

The stock market topped out in 9/1929 when the Saturn-Uranus cycle arrived at its trine from the 1914 low, the double trine from the 1899 top, and 180° from the 1907 low of the "rich man's panic".

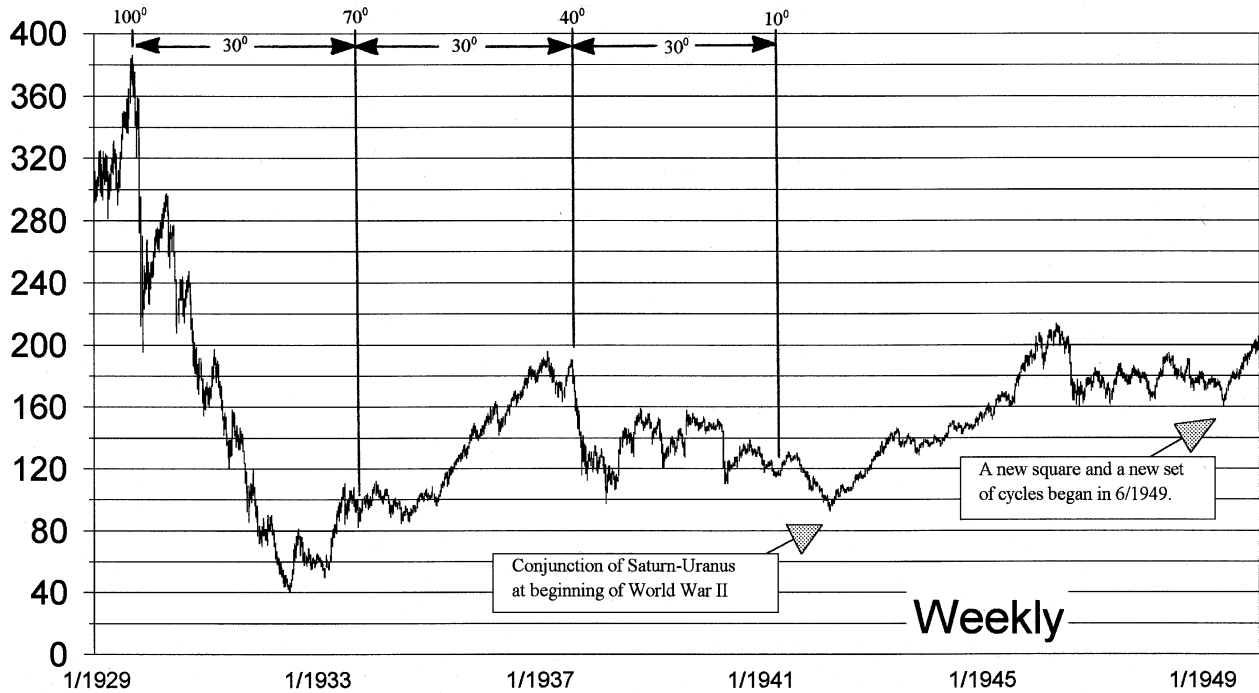
From the 1929 top, the 30° sections of the Saturn-Uranus cycle defined the bottom in 10/1933 and the major top in 8/1937. These cycles are shown on Chart VIII.F, and the data are included in Table 8.5.b. The 1937 top was not only 60° from the 1929 top, but also 120° from the 1921 bottom, 180° from the 1914 bottom, and 240° from the bottom of the 1907 "rich man's panic".

Table 8.5.b
Saturn-Uranus Synodic Movements of Thirty Degrees And
Corresponding Turning Points in the DJIA (9/1929 - 8/1937)
(See Chart VIII.F)

Date of Turning Point In DJIA	Angle Between Saturn and Uranus	Change From Last Point
9/1929	100 Degrees	N/A
10/1933	70 Degrees	30 Degrees
8/1937	40 Degrees	30 Degrees

VIII.F

SATURN-URANUS AXES (1929-1942)



VIII.G

SATURN-URANUS AXES (1949-1971)

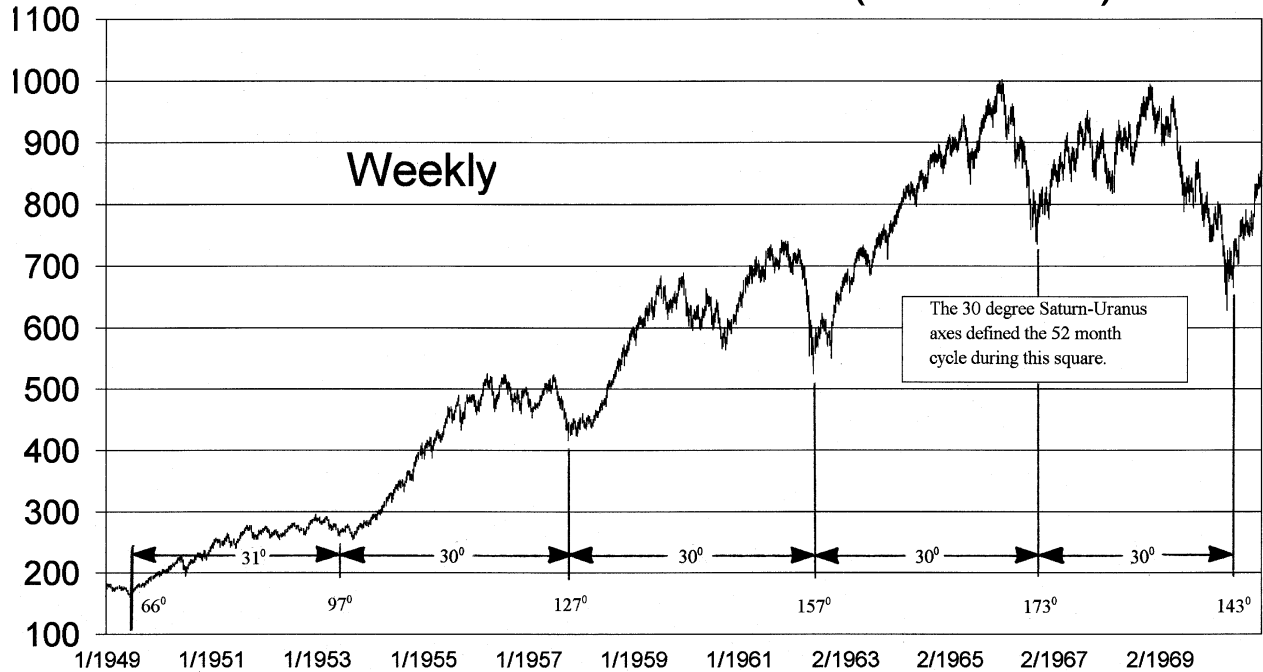


Table 8.5.c
Saturn-Uranus Synodic Movements of Fifteen Degrees
And Corresponding Turning Points in the DJIA;
Showing The 52-Month Cycle Between 1949-1966
(See Chart VIII.G)

Date of Turning Point in DJIA	Angle Between Saturn and Uranus	Change From Last Point	Number of Months
6/1949	66 Degrees	N/A	N/A
7/1951	81 Degrees	15 Degrees	25
6/1953	97 Degrees	16 Degrees	23
9/1955	112 Degrees	15 Degrees	27
10/1957	127 Degrees	15 Degrees	25
1/1960	141 Degrees	14 Degrees	27
6/1962	157 Degrees	16 Degrees	29
8/1964	172 ⁰ (Before the Opposition)	15 Degrees	26
10/1966	173 ⁰ (After the Opposition)	15 Degrees	26

Study the double top in 1937. The March top coincided with the Uranus cycle arriving at its 9⁰ axis, as described in the previous section. The August top coincided with the Saturn-Uranus cycle arriving at its axis, as described above. When cycles are not simultaneously arriving at their axes multiple tops or bottoms are formed. When cycles are synchronized, such as during the 1899-1929 square, sharp turning points are defined.

The larger Uranus cycle arrived at its node in 1942, coinciding with entrance of the United States into World War II⁷⁹. This combination of events occurred during the conjunction of Uranus and Saturn and affected the stock market cycles synchronized with the Saturn-Uranus cycle. During this period, the Uranus cycle and the Saturn-Uranus cycle were not simultaneously arriving at their 30⁰ axes, as they were during the 1899-1929 square. This made the bottoms associated with each cycle less clearly defined.

The square completed in 1949, causing the stock market cycle related with the Saturn-Uranus cycle to align with its location (66⁰) at that time. Future cycles were defined along 30⁰ axes from that point.

⁷⁹ Notice that the Uranus cycle has shifted phase twice in history, during the two World Wars. The phase shift of the synodic cycles (Saturn-Uranus) occurs at the completion of squares.

HISTORICAL ANALYSIS OF SATURN-URANUS CYCLE (1949-1966)

A new square began in 6/1949, and the Saturn-Uranus cycle aligned at that time at 66° . From that point the 30° divisions of the Saturn-Uranus cycle defined successive stock market bottoms in the square from 1949 to 1966.

Anyone seriously involved in stock market cycle analysis has heard of the fifty-two month cycle. This cycle is covered in detail at the end of this section. The disappearance of the fifty-two month cycle when it was due to bottom in 1971 has remained an unsolved mystery for years. However, with an understanding of the four-dimensional geometry involved this puzzle is resolved. During the period 1949-1966, the fifty-two month cycle synchronized with 30° motions of Saturn-Uranus, as shown on Chart VIII.G.

Table 8.5.c contains the data for this side of the cube, which defines the fifty-two month cycle. The data in the last column of this table is from bottom-to-top or top-to-bottom. Therefore, to get a complete cycle bottom-to-bottom add together the two values.

The major drop in 1962 occurred when the Uranus cycle was 90° from its location in 1942, (i.e., Uranus quarter-cycle), while at the same time the Saturn-Uranus cycle was 90° from the beginning of the square in 1949. This was a deadly combination, and a sure giveaway for a significant shake-up in the market.

HISTORICAL ANALYSIS OF SATURN-URANUS CYCLE (1966-1982)

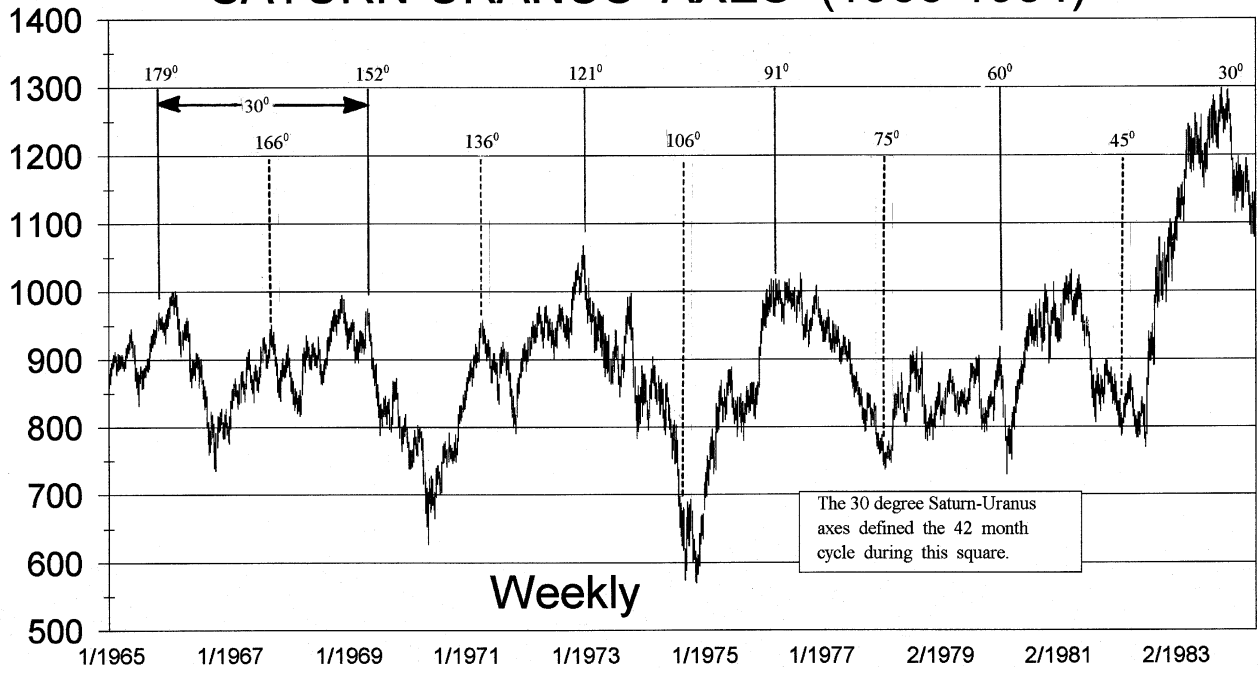
When the square completed in 1966, the new stock market cycle began with a period averaging forty-two months, as shown on Chart VIII.H. This stock market cycle was still synchronized with the Saturn-Uranus cycle. However, during this time the Saturn-Uranus cycle was moving faster than it was during the 1949-1966 square and it only took forty-two months to move 30° . This cycle ran from 1966 to 1982 until the side of the cube was complete, as described in Lesson V. The data for the forty-two month cycle (which was the fifty-two month cycle on the previous face of the cube) are contained in Table 8.5.d. Measured from the beginning of the 1966 square;

The 5/1969 top was 27° ,
 The 1/1973 top was 59° ,
 The 5/1976 top was 90° ,
 The sharp drop in 2/1980 was 120° ,
 The 3/1982 bottom was 136° .

The 3/1982 bottom was 60° from the 12/1974 bottom and 31° from the 3/1978 bottom.

VIII.H

SATURN-URANUS AXES (1966-1984)



VIII.I

SATURN-URANUS AXES (1980-1993)



Study Chart VIII.H and notice how neatly the turning points in the stock market aligned with 15° axes of the Saturn-Uranus cycle. The 15° section defining the decline between 1/1973 and 10/1974 will be studied in greater detail later in this lesson after the smaller cycles have been explained.

In 1982 the Uranus cycle returned to its nodal point, as described in the section on the Uranus cycle, and the long-term cube from 1899 was complete.

Table 8.5.d
Saturn-Uranus Synodic Movements of Fifteen Degrees
And Corresponding Turning Points in the DJIA;
Showing The 42-Month Cycle Between 1966-1982
(See Chart VIII.H)

Date of Turning Point in DJIA	Angle Between Saturn and Uranus	Change From Last Point	Number of Months
2/1966	180 Degrees	N/A	N/A
9/1967	165 Degrees	15 Degrees	19
5/1969	153 Degrees	12 Degrees	20
4/1971	136 Degrees	17 Degrees	23
1/1973	121 Degrees	15 Degrees	21
10/1974	106 Degrees	15 Degrees	21
5/1976	90 Degrees	16 Degrees	19
3/1978	75 Degrees	15 Degrees	22
2/1980	60 Degrees	15 Degrees	23
3/1982	44 Degrees	16 Degrees	25

HISTORICAL ANALYSIS OF SATURN-URANUS CYCLE (1981-1991)

The resolution of the data used to study this section of the stock market is given to the minute, rather than to the degree, as was done in previous sections. This was done because this time period occurred more recently and is therefore more familiar to most market analysts. Consequently, this time period will be more closely scrutinized in later lessons.

When the 1982 square began the speed of the Saturn-Uranus cycle had returned to that of the 1949-1966 period. This means **THE 52-MONTH CYCLE RETURNED DURING THIS PERIOD.**

Chart VIII.I shows the Saturn-Uranus cycle from 1981 to 1993. When the top arrived in 4/26/1981 the Saturn-Uranus cycle was at $50^{\circ}24'$. Thirty degrees of the Saturn-Uranus cycle measured from this axis defined the 52-month cycle. One and one-half times this amount (45°) defined the 78-month cycle.

For example, the top in 8/25/1987 occurred at $5^{\circ}23'$, which was $45^{\circ}01'$ from the top on 4/26/1981.

Exactly 52-months after the top on 8/25/1987 the stock market bottomed on 12/11/1991. During this time, the Saturn-Uranus cycle moved from $5^{\circ}23'$ through the conjunction to $24^{\circ}03'$, or a distance of $29^{\circ}26'$. The halfway point in this cycle was 10/10/1989, when the "mini-crash of 1989" occurred. This date was exactly 15° from the 12/11/1991 low. That is,

$$24^{\circ}03' - 9^{\circ}03' = 15^{\circ}.$$

When is the next 15° axis due? Add 45° to the 8/25/1987 top and the sum is $39^{\circ}37'$. This angle arrives in January, 1994. Similarly, add 15° to the 12/11/1991 bottom and you get $39^{\circ}03'$. Again, due in January, 1994. Or, add 90° to the 4/26/1981 high to get $39^{\circ}36'$. Again, due in January, 1994. The net result of this will be a turning point in January that will be identifiable on a monthly chart.

Table 8.5.e
Saturn-Uranus Synodic Movements of Fifteen Degrees
And Corresponding Turning Points in the DJIA
Between 1981-1991 Showing The 52-Month Cycle
(See Chart VIII.I)

Date of Turning Point in DJIA	Angle Between Saturn and Uranus	Change From Last Point	Number of Months
4/26/1981	$50^{\circ}24'$	N/A	N/A
4/26/1983	$35^{\circ}27'$	$14^{\circ}57'$	24
5/02/1985	$21^{\circ}08'$	$14^{\circ}19'$	25
8/25/1987	$5^{\circ}23'$	$15^{\circ}45'$	27
10/10/1989	$9^{\circ}03'$	$14^{\circ}26'$	26
12/11/1991	$24^{\circ}03'$	$15^{\circ}00'$	26

SIXTY-SEVEN YEAR PERIODICITY AND SATURN-URANUS SYNODIC CYCLE

The Saturn-Uranus cycle not only coincides with turning points in the stock market along its 15° axes, but also defines significant turning points with its larger harmonics. For example, one and one-half cycles lasts 67-years. This 67-year period defined the interval between the beginning dates of the faces of the cubes described in Lesson V. The large cube developed its base beginning in 1899. Sixty-seven years later, in 1966, the base of the next cube started. Compare how closely stock market patterns repeated within this 67-year interval, as shown on Chart V.E.

The data from Chart V.E is included in Table 8.6. Study this table and see how corresponding turning points are located one and one-half Saturn-Uranus cycles apart.

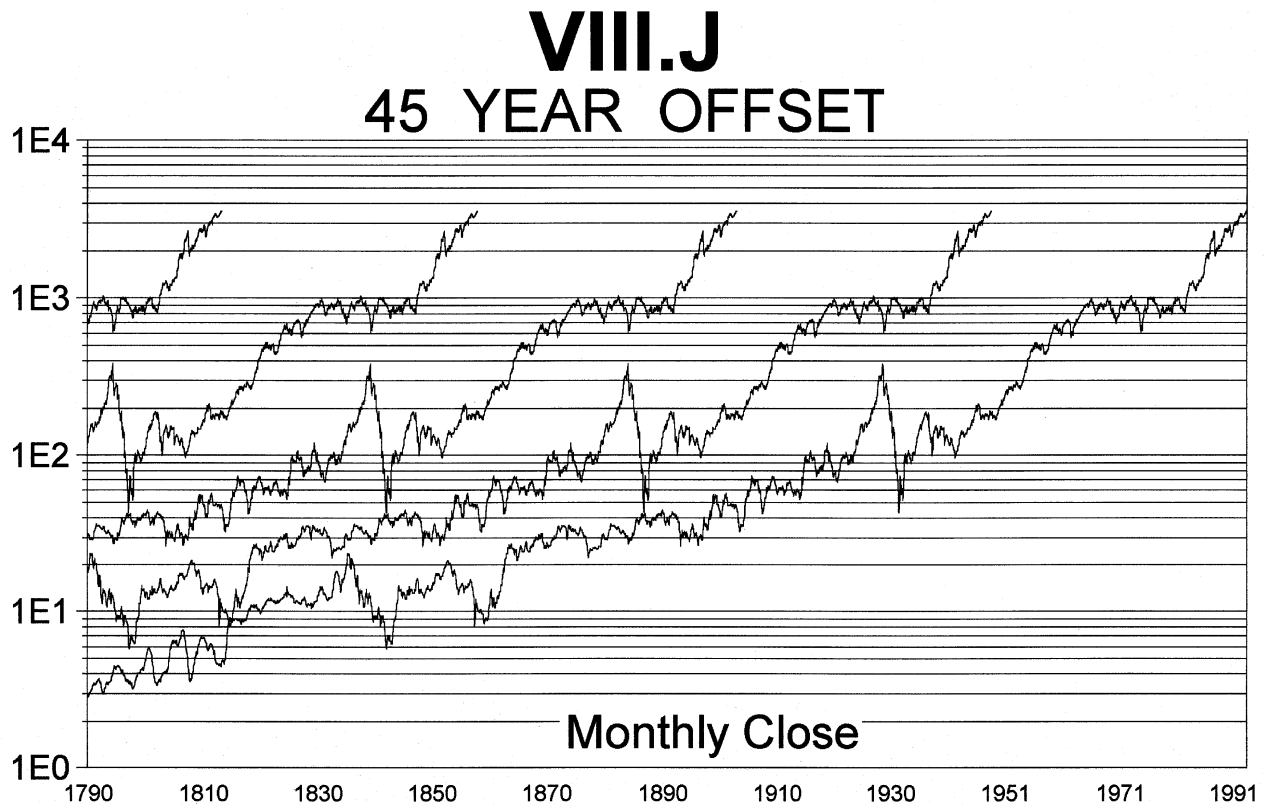
Table 8.6
Sixty-Seven Year Stock Market Patterns
And 540° Saturn-Uranus Synodic Movements
(See Chart V.E)

Corresponding Points on 67-Year Stock Market Pattern	Degrees Traversed by Saturn-Uranus Cycle Between the Two Dates in Column One
4/1899 - 2/1966	529°00
1/1906 - 1/1973	540°00
11/1907 - 10/1974	541°00
12/1914 - 6/1982	541°00

FORTY-FIVE-YEAR PERIODICITY AND SATURN-URANUS SYNODIC CYCLE

One complete Saturn-Uranus cycle lasts 45 years. This interval coincides with similar conditions in the stock market.⁸⁰ Chart VIII.J overlays the stock market with 45-year intervals. Compare the graphs on this chart, and note how turning points tend to coincide with the 45-year interval; for example, 1929 and 1974, 1937 and 1982, 1921 and 1966, 1942 and 1987, etc.

⁸⁰ This time period was so important to W.D. Gann that he wrote a book titled, "*45 Years On Wall Street*".



LONG-TERM HARMONICS AND STOCK MARKET TURNING POINTS

Table 8.7 lists some of the turning points in the stock market that have coincided with multiples of the Saturn-Uranus half-cycle of twenty-two years.

Because Table 8.7 does not include all the relevant harmonics of the Saturn-Uranus cycle, the reader is encouraged to independently study this cycle's harmonics and related stock market turning points. For example, compare stock market patterns separated by time periods of 45 and 67-years, such as the completed five-year cycle from 1937-1942 and its inverse from 1982-1987.

RESOLVING THE MYSTERY OF THE DISAPPEARING 52-MONTH CYCLE

Many financial market cycle analysts have noted the existence of the fifty-two month cycle. This cycle repeated with remarkable accuracy for several years. However, they are unable to explain why the cycle suddenly changed when the 1971 bottom was expected. In addition, they are at a loss to explain why the cycle appeared in 1949, when previous to that date it did not exist. To quote one such reputable analyst, "the fifty-two month cycle seemed to appear out of nowhere in 1949". This analyst was more correct than even he realized. The "nowhere", to which he referred was actually the face of a cube that did not rotate into view until 1949. Prior to that date, this face was in the "nowhere" of a different dimension. As previously shown,

Table 8.7
Saturn-Uranus Half-Cycle of Twenty-Two Years And
Corresponding Turning Points in the Stock Market (1792-2019)

Stock Market Turning Points	Number of Saturn-Uranus Cycles From the Birth of NYSE (5/1792)
5/1792 - Birth of NYSE	N/A
1813 - Bottom before steady advance into 1835	One Half Cycle
1835 - Highest top between 1792 - 1863	One Cycle
1859 - Beginning of five-year cycle, starting huge advance during civil war	One and a Half Cycles
1884 - Bottom that starts side of square from 1884-1899	Two Cycles
1907 - "Rich Man's Panic"	Two & Half Cycles - From 1792 One Cycle - From 1861
1929 - Peak before the "Great Depression"	Three Cycles - From 1792 One & Half Cycles - From 1861 One Half Cycle - From 1907
1949 - Bottom that starts side of square from 1949-1966	Three & Half Cycles - From 1792 Two Cycles - From 1861
1974 - Bottom of market	Four Cycles - From 1792 Three Cycles - From 1835 One & Half Cycles - From 1907 One Cycle - From 1929
1997	Four & Half Cycles - From 1792 One & Half - From 1929
2019	Five Cycles - From 1792 Two Cycles - From 1929 One Cycle - From 1974

THE FIFTY-TWO MONTH CYCLE IN THE DJIA FROM 1949 TO 1966 WAS SYNCHRONIZED WITH 30⁰ MOVEMENTS OF THE SATURN-URANUS CYCLE.

The DJIA cycle did not begin on the exact 30⁰ axis of the Saturn-Uranus cycle. Rather, the cycle began in 1949 when the Saturn-Uranus cycle was at an angle of 66⁰. From this point, the fifty-two month DJIA cycle bottomed every time Saturn-Uranus moved 30⁰. Refer to the section covering this time period in the Saturn-Uranus cycle. The

period from 1949 to 1966 represents a face of the cubic structure described in Lesson V, **GEOMETRIC STRUCTURES**. During this time the DJIA moved across the diagonal of square DE as shown on Chart V.B, at an angle of 44° . This face of the cube completed in 1966. On that date, the new face of the cube rotated into view and the 30° axes of the Saturn-Uranus cycle synchronized with the new DJIA cycle. This new cycle had a periodicity of 42-months, rather than 52-months of the previous cycle. This shifting in the length of the cycle is caused by the elliptical nature of the planets orbits. After 1966, Saturn was moving much faster, relative to Uranus, than it was before 1966. The DJIA cycle of 42-months still corresponded with 30° movements of Saturn-Uranus, it just took less time for that distance to be covered.

This new set of cycles began in 1966 and continued across the new face of the cube until 1982 when that square completed. This cycle topped in 1966, 1969, 1973, 1976, and 1980. Chart VIII.H showed that each of these tops corresponded with a 30° motion of Saturn-Uranus. Notice that tops were used for this face of the cube, while bottoms were used for the 1949-1966 structure. This is because the 1966-1982 square represents the top of the cubic structure, while 1949-1966 was the diagonal of a square composing a side of the cube.

When the 1966-1982 square completed the speed of the Saturn-Uranus cycle had increased to that of the 1949-1966 square, corresponding to the return of the 52-month cycle at that time. The precise dates of this cycle and corresponding locations of Saturn-Uranus are listed in Table 8.5.e.

SATURN SIDEREAL CYCLE AND STOCK MARKET CORRELATION

Saturn completes one revolution relative to the fixed stars in 29.5 years. This cycle and its harmonics are key to stock market timing because,

FIVE-YEAR STOCK MARKET GROWTH PATTERNS ARE SYNCHRONIZED WITH 60° MOTIONS OF SATURN.

It is critical the stock market analyst is aware of this relationship. For example, the five-year bull market from June, 1982 to October, 1987 began when Saturn entered 21° Virgo in June, 1982 and abruptly terminated in October, 1987 when Saturn crossed 21° Scorpio, which was 60° from its position at the beginning of the bull market.

Similarly, the five-year component of the "great bull market" of the 1920's began in May, 1924 when Saturn crossed 0° Scorpio, and continued until September, 1929 when the 60° interval had been spanned by Saturn as it crossed 0° Capricorn.

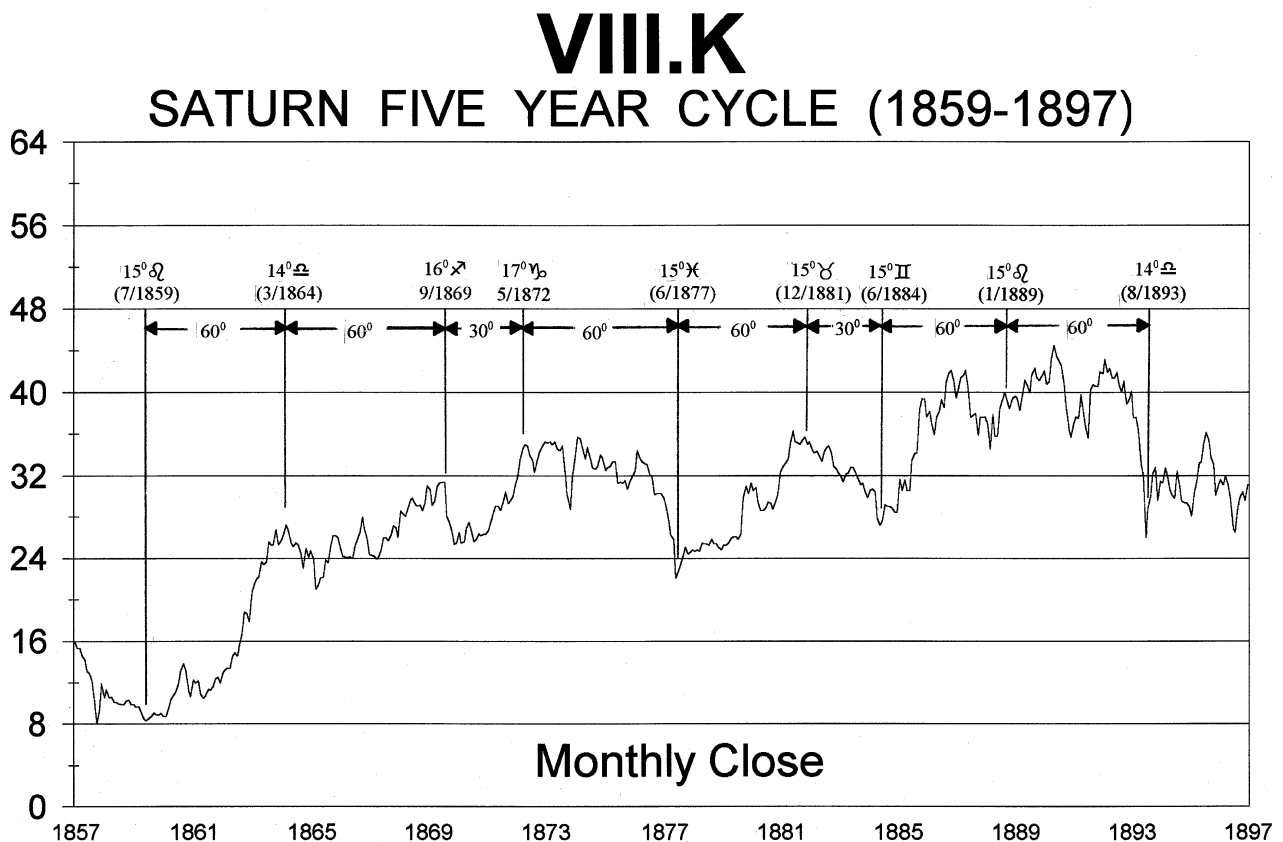
Numerous examples exist proving the correlation between the five-year stock market cycle and the 60° interval of Saturn. Table 8.8 chronicles these five-year cycles, since 1859. As with the Uranus cycle, the data in Table 8.8 is divided into two parts. The

time period before the close of the market in July, 1914 is included in Table 8.8.a, while that after the reopening of the market in December, 1914 is included in Table 8.8.b.

It is recommended the reader compare the data in Tables 8.8.a and 8.8.b with the charts showing the five-year cycles: Charts VIII.K, VIII.L, VIII.M, and VIII.N.

Charts VIII.K through VIII.N include periods when the beginning of a five-year cycle did not immediately follow the terminus of the previous five-year cycle. During these "gaps" Saturn typically moved 30°, rather than the 60° interval of a complete five-year cycle. The explanation for these "gaps" requires an understanding that the larger Uranus cycle contains the cycles of the smaller Saturn cycle. And since 60° sections of the Saturn cycle do not fit into the Uranus quarter-cycle an integral number of times, there is a certain amount of "extra space" in the Uranus cycle to accommodate. A more extensive explanation of these "gaps" between the five-year cycles is included later in this section.

The close of the stock market in 7/31/1914 coincided with completion of the 1909-1914 five-year cycle. At the close Saturn was located at 23° Gemini. When it reopened in December, 1914 Saturn had moved 6° to 29° Gemini. The five-year cycles realigned themselves with the location of Saturn at that time. This axis served to define the succeeding five-year cycles, including the bottom in 5/1924 and the cycle that terminated in September, 1929, beginning the "Great Depression". The location of Saturn in September, 1929 was 180° from its position at the reopening of the stock market in



VIII.L

SATURN FIVE YEAR CYCLE (1897-1932)

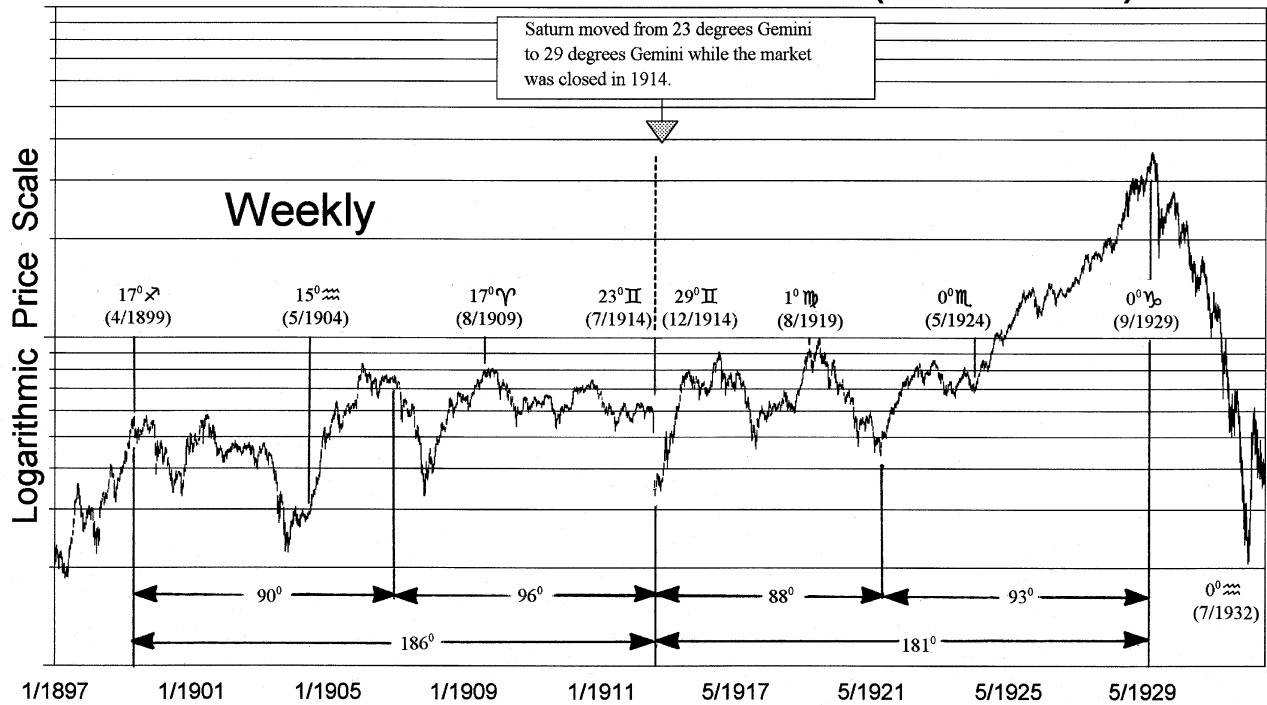


Table 8.8.a
Five-Year Stock Market Cycles And
Sixty-Degree Sidereal Motions of Saturn (1859-1914)
 (See Charts VIII.K, VIII.L)

Date of Five-Year Cycle	Beginning Location of Saturn	Ending Location of Saturn	Degrees Traversed by Saturn
7/1859 - 3/1864	15 Leo	14 Libra	59 Degrees
3/1864 - 7/1869	14 Libra	15 Sagittarius	61 Degrees
5/1872 - 6/1877	16 Capricorn	15 Pisces	59 Degrees
6/1877 - 7/1882	15 Pisces	17 Taurus	62 Degrees
6/1884 - 1/1889	14 Gemini	16 Leo	62 Degrees
1/1889 - 7/1893	16 Leo	14 Libra	58 Degrees
7/1893 - 4/1899	14 Libra	18 Sagittarius	64 Degrees
4/1899 - 5/1904	18 Sagittarius	15 Aquarius	57 Degrees
5/1904 - 8/1909	15 Aquarius	17 Aries	62 Degrees
8/1909 - 7/1914	17 Aries	23 Gemini	66 Degrees (Close)

December, 1914 and 360° from its position at the beginning of the square in 1899 (plus the 6° it moved while the market was closed). The 1899 top was flat during which Saturn moved from 18° Sagittarius in 4/1899 to 26° Sagittarius 12/1899.

Cycles are easiest to study when they align with other cycles or their harmonics. In the case of the Saturn cycle, it is easiest to identify the five-year stock market cycle when the Uranus cycle is reaching its axes at the same time as is Saturn. One such period existed between 1899 and 1929. This time frame is excellent to study in great detail. The Saturn cycle for this period is shown on Chart VIII.L. And the Saturn-Uranus cycle is shown on Chart VIII.E. Notice from these two charts, how the two cycles were aligned with each other at major turning points in the stock market. The period from 1899 to 1914 was 120° in the Saturn-Uranus cycle, 180° in the Saturn cycle, and hence, 60° in the Uranus cycle.

Similarly, the period from 1914 to 1929 had identical cyclical relationships between these two planets. During this time, Saturn moved 180° , Saturn-Uranus moved 120° , and Uranus moved 60° . Therefore, between 1899 and 1929; Saturn moved a complete cycle of 360° , Saturn-Uranus moved 240° , and Uranus moved 120° . This thirty-year period had to be one of the easiest stock markets ever to time! Spend some time reviewing the charts covering the cycles in this time period. This knowledge will make it easier to analyze time frames when the cycles are not exactly aligned.

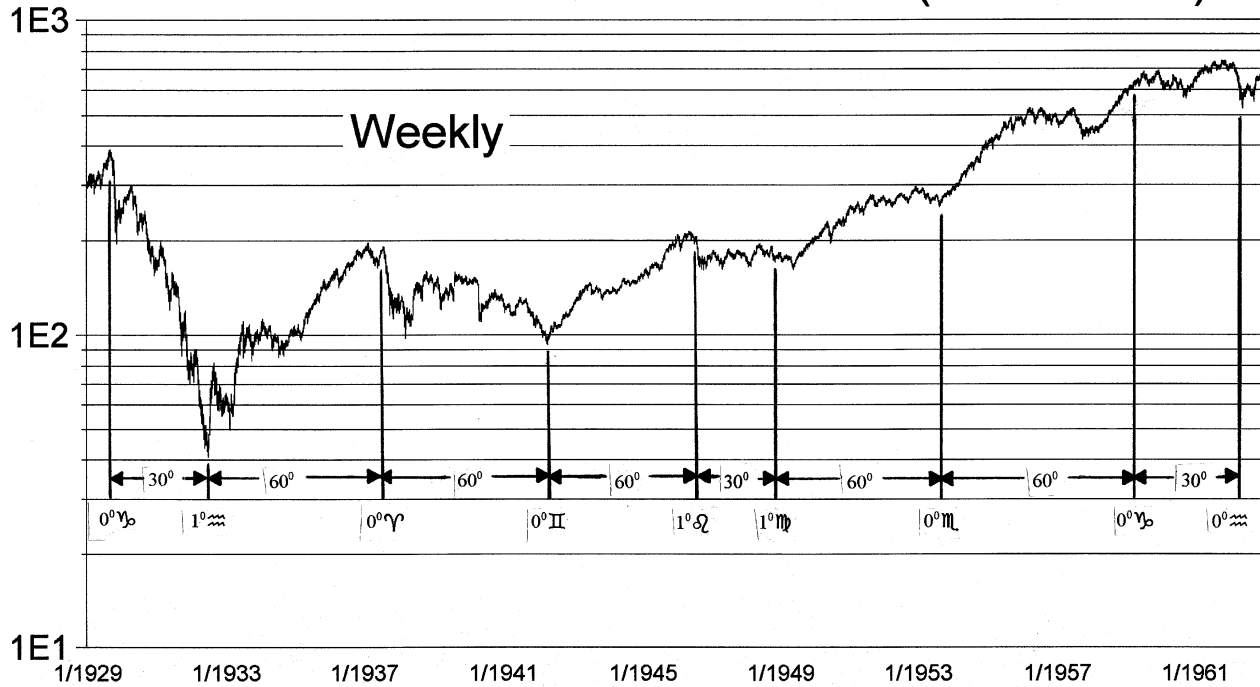
The section on the Uranus cycle showed that major bottoms in the stock market coincide with Uranus entering Gemini and Sagittarius. These locations are 180° apart and also coincide with major turning points in the Saturn cycle. Since the period of Saturn is 29.5 years, its 180° nodal areas are 15 years apart. These nodal areas have been:

Top in	9/1824	Saturn at	1°	Gemini
Bottom in	11/1839	Saturn at	12°	Sagittarius
Bottom in	12/1854	Saturn at	12°	Gemini
Top in	9/1869	Saturn at	17°	Sagittarius
Bottom in	6/1884	Saturn at	14°	Gemini
Top in	4/1899	Saturn at	18°	Sagittarius
Bottom in	7/1914	Saturn at	23°	Gemini
Top in	9/1929	Saturn at	$29^{\circ}35'$	Sagittarius
Bottom in	4/1942	Saturn at	1°	Gemini
Top in	8/1956	Saturn at	2°	Sagittarius
Top in	1/1973	Saturn at	19°	Gemini
Top in	10/1987	Saturn at	21°	Sagittarius

Saturn will return to this nodal area in the year 2002, which coincides with Uranus returning to the nodal area shown in Figure 8.2.

VIII.M

SATURN FIVE YEAR CYCLE (1929-1962)



VIII.N

SATURN FIVE YEAR CYCLE (1966-1987)

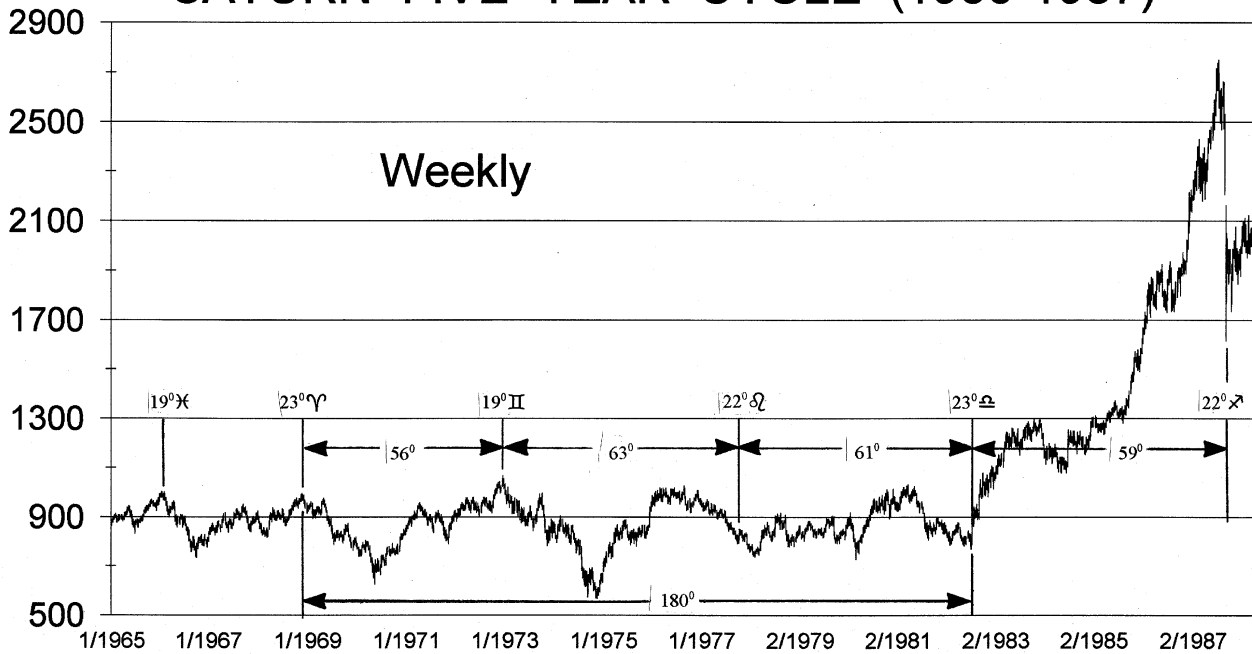


Table 8.8.b
Five-Year Stock Market Cycles And
Sixty-Degree Sidereal Motions of Saturn (1914-1987)
(See Charts VIII.L, VIII.M, VIII.N)

Date of Five-Year Cycle	Beginning Location of Saturn	Ending Location of Saturn	Degrees Traversed by Saturn
12/1914 - 8/1919	29 Gemini	1 Virgo	62 Degrees
8/1919 - 5/1924	1 Virgo	0 Scorpio	59 Degrees
5/1924 - 9/1929	0 Scorpio	0 Capricorn	60 Degrees
7/1932 - 8/1937	1 Aquarius	0 Aries	59 Degrees
8/1937 - 4/1942	0 Aries	1 Gemini	61 Degrees
4/1942 - 8/1946	1 Gemini	0 Leo	59 Degrees
12/1948 - 9/1953	0 Virgo	29 Scorpio	59 Degrees
9/1953 - 5/1959	29 Scorpio	2 Capricorn	63 Degrees
11/1968 - 1/1973	23 Aires	19 Gemini	56 Degrees
1/1973 - 10/1977	19 Gemini	22 Leo	63 Degrees
10/1977 - 6/1982	22 Leo	21 Libra	59 Degrees
6/1982 - 10/1987	21 Libra	21 Sagittarius	60 Degrees

Analysis of Charts VIII.K through VIII.N demonstrates an important characteristic concerning the origin of the five-year Saturn cycles.

IT IS ALONG THE 15⁰ AXES OF THE LARGER URANUS CYCLE AND SATURN-URANUS CYCLE THAT THE FIVE-YEAR SATURN CYCLE ORIGINATES.

The five-year stock market cycle should be viewed as a "package unit". It is a completed growth spiral in price-time. This spiral has its origin or terminus aligned with the larger cycle ("wheels within wheels").

Because the five-year cycle is a "package unit", and aligns its origin or terminus with the nodes of the larger cycles, the beginning point of the five-year cycle is not always aligned with the 0⁰ axis of Saturn. For example, the June, 1982 to October, 1987 cycle ran from 21⁰ Virgo to 21⁰ Scorpio. Also, the 1859-1864 cycle ran from 15⁰ Leo to 15⁰ Libra. The reason for this is that smaller cycles form within larger cycles ("wheels within wheels"). The sidereal cycle larger than the Saturn cycle is the Uranus cycle. The synodic cycle larger than the Saturn cycle is the Saturn-Uranus cycle. The position of Uranus in 1859 was exactly one and one-half Uranus cycles from its position in 1982 (3⁰ Gemini to 3⁰

Sagittarius, as shown in Figure 8.2). The five-year Saturn cycles began from these nodal points on the Uranus cycle.

Figure 8.2 also identified 1942 as a nodal point in the Uranus cycle (0° Gemini). This point is 180° from the two nodal points in 1982 and 1899. Compare the five-year Saturn cycles that aligned themselves with these nodal points; i.e., 1899-1904, 1937-1942, and 1982-1987. All these cycles were aligned with Uranus nodal points.

A comparison of the charts of the Uranus quarter-cycles (VIII.A and VIII.B) with the charts of the five-year Saturn cycles shows that the five-year cycles will not fit into a Uranus quarter-cycle an integral number of times. This means that a "gap" is left over after the maximum number of five-year cycles are fitted into the Uranus quarter-cycle. This extra space also aligns along the 30° axes of the Saturn cycle.

Table 8.9 contains the six Uranus quarter-cycles since 1857, and the five-year Saturn cycles that fit into each of these quarter-cycles. The 30° sections of the Saturn cycle that were not part of a five-year cycle are shown in the third column.

Table 8.9
Saturn Five-Year Cycles Within Uranus Quarter-Cycles
(Uranus Quarter-Cycles Are Shown in Table 8.3)

Uranus (90°) Quarter-Cycles	Saturn (60°) Five-Year Cycles	Saturn (30°) "Gap"
1857-1878	1859-1864 1864-1869 1872-1877	1869-1872 (30°)
1878-1897	1877-1882 1884-1889 1889-1893 1893-1899	1882-1884 (30°)
1897-1919	1899-1904 1904-1909 1909-1914 1914-1919	1897-1899 (30°)
1919-1942	1919-1924 1924-1929 1932-1937 1937-1942	1929-1932 (30°)
1942-1962	1942-1946 1948-1953 1953-1959	1946-1948 (30°) 1959-1962 (30°)
1962-1981	1968-1973 1973-1977 1977-1982	1966-1968 (34°)

For example, the Uranus quarter-cycle from 1857 to 1878 contained three completed five-year cycles; 1859-1864, 1864-1869, 1872-1877, as shown on Chart VIII.K. The "gap" was between 1869 and 1872. During this time, Saturn moved 30° , from 17° Sagittarius to 17° Capricorn. Similarly, the Uranus quarter-cycle from 1897 to 1919, contained four completed five-year cycles; 1899-1904, 1904-1909, 1909-1914, 1914-1919, as shown on Chart VIII.L. The "gap" was from 1897 to 1899. During this time Saturn moved 30° , from 26° Scorpio to 26° Sagittarius.

The Uranus quarter-cycle from 1919 to 1942 contained four completed five-year cycles; 1919-1924, 1924-1929, 1932-1937, 1937-1942, as shown on Charts VIII.L and VIII.M. The "gap" was the crash between 1929 and 1932. During this time Saturn again moved 30° , from 0° Capricorn to 0° Aquarius.

Because the price-time action within the 1949-1966 square traversed it diagonally, effectively defining the increasing energy level, prices experienced a strong upward force during this period. This made it difficult to clearly identify the smaller cycles, including the five-year cycle.

JUPITER-SATURN CYCLE AND STOCK MARKET CORRELATION

Jupiter and Saturn conjoin every twenty years. Therefore, each 30° movement of Jupiter relative to Saturn averages twenty months. Each conjunction moves about 240° relative to the fixed stars from the previous conjunction. This means that every sixty years the third conjunction between these two planets occurs in approximately the same position in the heavens. During this sixty-year period Uranus completes three quarter-cycles, or 270° .

When a conjunction occurs at the same longitude and latitude as a previous conjunction, it is known as a "first order conjunction". This period is 60 years for the Jupiter-Saturn cycle. The 60-year cycle was one listed by W.D. Gann in his *Master Course For Stocks* as a major cycle.

Financial astrologers have used the Jupiter-Saturn cycle for years to try to predict financial market prices and is the basis of the decennial period (10 Year) identified by Edgar Lawrence Smith, W.D. Gann, et. al.⁸¹

A complete record of the New York Stock Exchange from 1790 to 1993 can be charted. When these charts are divided into twenty-year periods, an easy comparison of the stock market during separate Jupiter-Saturn cycles is possible. Compare similar points on these charts to see for yourself if there is anything to the twenty-year stock market period.⁸²

⁸¹ W.D. Gann produced and made available to the public "Annual Forecasts", which he sold for large sums of money. These forecasts were based upon the decennial period. Appendix C contains an example of how W.D. Gann made his annual forecasts.

⁸² Appendix D contains a discussion of the twenty-year presidential cycle. Briefly stated, the president elected every 20 years, during the Jupiter-Saturn conjunction, dies in office.

Long-term wheat data allows the reader to extend this analysis back to the year 1290. Along with the 200-year rhythm, 60-year spikes in price corresponding with the Jupiter-Saturn cycle are clearly present in the wheat market. On a smaller magnitude, a ten-year rhythm can also be clearly seen on that chart.

20-MONTH JUPITER-SATURN HARMONIC AND STOCK MARKET CYCLES

THERE IS A CYCLE OF ALTERNATING ADVANCING AND DECLINING PRICES IN THE STOCK MARKET CORRELATED WITH 15° MOTIONS OF THE JUPITER-SATURN CYCLE. THESE CYCLES AVERAGE 20 MONTHS FROM BOTTOM-TO-BOTTOM OR TOP-TO-TOP.

Since this cycle only defines a ten-month trend, a smaller time frame will be used to study its effects in the stock market. Chart VIII.O shows the DJIA from 1/1980 to 6/1993 with the 15° axes of the Jupiter-Saturn cycle drawn in. There are two sets of vertical lines on this chart. The dotted lines define the 15° axes. The solid lines also define 15° axes, however they are spaced to identify the sympathetic resonance between the Jupiter-Saturn cycle and the harmonics of the larger Saturn-Uranus cycle. In other words, the solid vertical lines on Chart VIII.O are spaced either 30° or 45° apart, depending upon which of these two divisions corresponds more closely with the 15° axes of the larger Saturn-Uranus cycle shown on Chart VIII.I. Compare these two charts and see how closely the harmonics of these two planetary cycles correspond.

Chart VIII.O shows that there are sometimes two and sometimes three divisions of the larger Saturn-Uranus cycle by the smaller Jupiter-Saturn cycle. That is, the Saturn-Uranus 15° harmonic sometimes corresponds with 30° on the Jupiter-Saturn cycle and sometimes with 45°. Whichever division is taking place, the two cycles are synchronous. It is critical that this relationship is understood, because this is the mechanism used to determine the subdivisions of the cycles. **A CYCLE IS MORE PRONOUNCED IF IT IS REINFORCED BY THE HARMONICS OF ANOTHER CYCLE.**⁸³ The solid vertical lines on Chart VIII.O show where these two major cycles reinforce each other, effectively identifying key turning points in the stock market. This concept of subdivision of larger cycles by the smaller cycles is expanded later in this lesson.

The exact data for the Jupiter-Saturn cycle are contained in Tables 8.10.a and 8.10.b. Having the data in table format allows the reader to identify the precise location of the Jupiter-Saturn cycle when turning points in the DJIA occurred. As in previous tables, the location of the Jupiter-Saturn cycle is given at the beginning and end of the related advance or decline in the stock market. The change in relative position of the Jupiter-Saturn cycle, during the advance or decline, is included in the last column. Even when the

⁸³ Technical Reference: *Fundamentals of Physics – Extended*, P. 409-412.

turning point in the stock market did not precisely align itself with a 15° axis of the Jupiter-Saturn cycle, a 30° distance was covered when the entire cycle is looked at, i.e., bottom-to-bottom or top-to-top.

Two tables are used because the geometric growth pattern, which began in 1982, completed in 1987, after which the new Jupiter-Saturn cycle synchronized with the DJIA on 3/2/1988.

Study these tables, especially the data concerning the reinforced harmonics of the Saturn-Uranus cycle. Notice how precisely these major harmonics identified turning points in the stock market, such as the "crash of 1987".

The top in 10/1987 represented the end of the growth pattern that began in 1982, that is, a completed five-year cycle, which represented the diagonal of two stacked squares, as explained in Lesson V. When this growth pattern completed, the ensuing correction was severe enough to be known as the "crash of 1987". The cycles in the growth pattern that followed the crash had a phase shift from the pattern preceding it. The concept of phase shift after completion of a geometric growth pattern was explained earlier in this lesson.

Between the dates shown in Table 8.10.b (3/2/1988-12/18/1991) there were 961 trading days. During this time the Jupiter-Saturn cycle moved a total of 75°04'. Hence, it follows that during this time the Jupiter-Saturn cycle averaged 12.8 trading days per degree. This is calculated as follows:

$$\frac{961 \text{ trading days}}{75^{\circ}04'} = \frac{12.8 \text{ trading days}}{1 \text{ degree}}$$

VIII.O JUPITER-SATURN AXES (1980-1993)

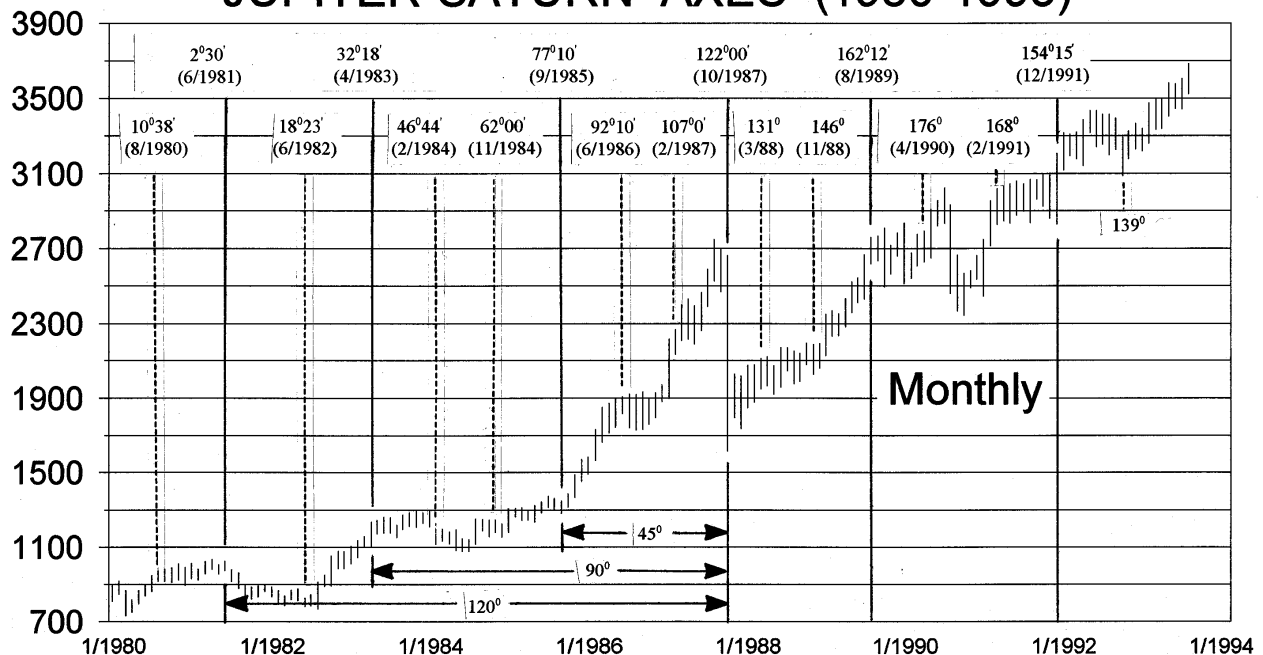


Table 8.10.a
Jupiter-Saturn Synodic Movements of Fifteen Degrees
And Corresponding Turning Points in the DJIA
From 1981 to the Crash of 1987
(See Chart VIII.O)

Date of Half-Cycle in DJIA	Angle Between Jupiter-Saturn at Beginning	Angle Between Jupiter-Saturn at End	Degrees Traversed by Jupiter-Saturn
6/15/1981 - 6/21/1982	2 ⁰ 30	18 ⁰ 23	15 ⁰ 53
6/21/1982 - 5/06/1983	18 ⁰ 23	32 ⁰ 46	14 ⁰ 23
5/06/1983 - 2/23/1984	32 ⁰ 46	46 ⁰ 48	14 ⁰ 02
2/23/1984 - 12/19/1984	46 ⁰ 48	62 ⁰ 10	15 ⁰ 22 ⁸⁴
12/19/1984 - 9/18/1985	62 ⁰ 10	77 ⁰ 12	15 ⁰ 02
9/18/1985 - 6/03/1986	77 ⁰ 12	92 ⁰ 23	15 ⁰ 11
6/03/1986 - 2/11/1987	92 ⁰ 23	107 ⁰ 30	15 ⁰ 07
2/11/1987 - 10/5/1987	107 ⁰ 30	122 ⁰ 00	14 ⁰ 30

Table 8.10.b
Jupiter-Saturn Synodic Movements of Fifteen Degrees And
Corresponding Turning Points in the DJIA After the Crash of 1987
(See Chart VIII.O)

Date of Half-Cycle in DJIA	Angle Between Jupiter-Saturn at Beginning	Angle Between Jupiter-Saturn at End	Degrees Traversed by Jupiter-Saturn
3/02/1988 - 11/16/1988	131 ⁰ 08	146 ⁰ 40	15 ⁰ 32
11/16/1988 - 8/11/1989	146 ⁰ 40	162 ⁰ 12	15 ⁰ 32
8/11/1989 - 4/30/1990	162 ⁰ 12	176 ⁰ 24	14 ⁰ 12
4/30/1990 - 2/19/1991	176 ⁰ 24 (Before 180 ⁰)	168 ⁰ 27 (After 180 ⁰)	15 ⁰ 09
2/19/1991 - 12/18/1991	168 ⁰ 27 (After 180 ⁰)	153 ⁰ 48	14 ⁰ 39

⁸⁴ The effect of this cycle was attenuated by the July, 1984 cycle bottom. The reason why the 7/1984 cycle bottom was so strong is explained later in this lesson. In addition to the cyclic effects, the price-time action had reached the lower perimeter of the ellipse originating in 1982. From this point the price-time action snapped up to meet the terminus of the ellipse.

Since the actual DJIA turning points in Tables 8.10.a and 8.10.b rarely deviated from the Jupiter-Saturn 15^0 axes by more than one-half degree, this represented an average error of 6-7 trading days. This error must be viewed in the context that it is measured within a large cycle with an average trend of ten months. A deviation of six trading days in a cycle lasting ten months represents an error of less than 3%. For comparison, a 3% error in an eight-week cycle is about one trading day.

The error is even less than 3% when measurements are made top-to-top or bottom-to-bottom. The 3% value represents the worst-case scenario of top-to-bottom or bottom-to-top, defined by the 15^0 axes.

JUPITER-URANUS CYCLE AND STOCK MARKET CORRELATION

The Jupiter-Uranus cycle completes one synodic period every fourteen years. This means that Jupiter-Uranus moves 180^0 as Uranus moves 30^0 , relative to the fixed stars, completing a seven-year cycle. As with other cycles, the Jupiter-Uranus cycle has axes every fifteen degrees, which last on average seven months.

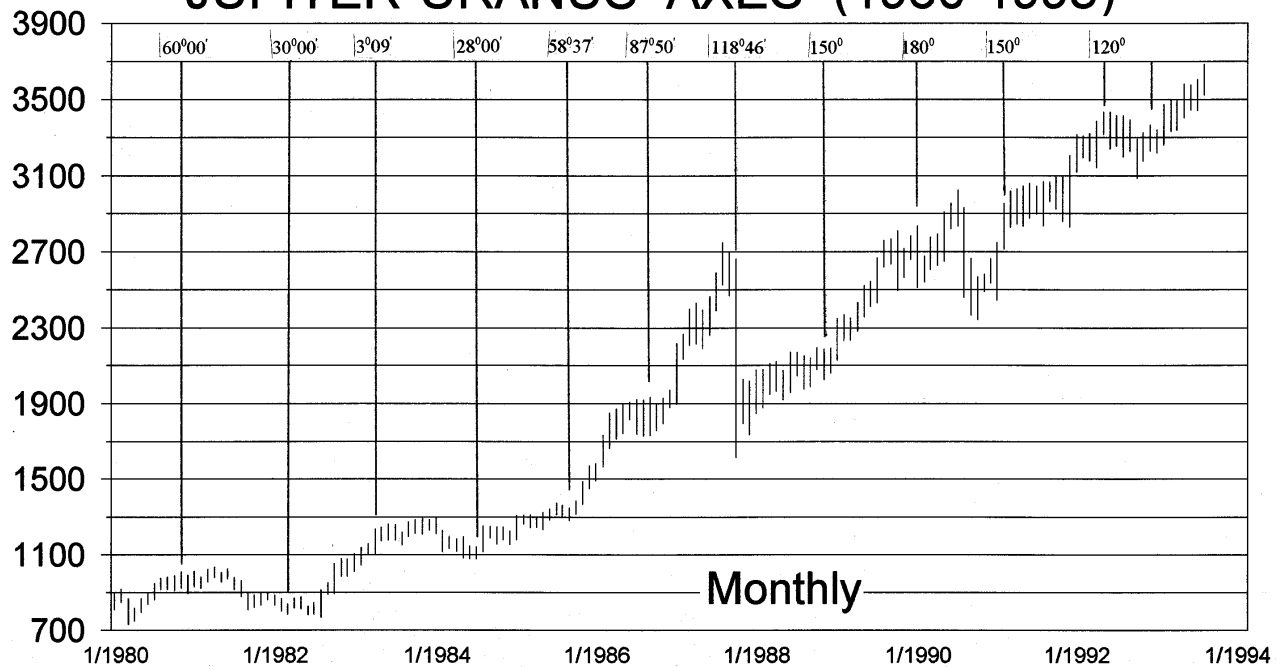
FIFTEEN-DEGREE SECTIONS OF THE JUPITER-URANUS CYCLE DEFINE THE SEVEN-MONTH STOCK MARKET CYCLE.

As with the Jupiter-Saturn cycle, a smaller time frame will be used to study the effects of this cycle in the DJIA because it has a smaller period. For example, Chart VIII.P shows the DJIA between 1/1980 and 6/1993. The vertical lines show the 30^0 harmonics of the Jupiter-Uranus cycle.

Just as the harmonics of the Jupiter-Saturn cycle correspond with the harmonics of the Saturn-Uranus cycle, the Jupiter-Uranus harmonics correspond with both the Saturn-Uranus and the Jupiter-Saturn harmonics. Hence, all three of these major cycles reinforce each other. Compare the 15^0 harmonics of the Saturn-Uranus cycle on Chart VIII.I with the Jupiter-Uranus cycles shown on Chart VIII.P. Also, compare the Jupiter-Saturn harmonics on Chart VIII.O with those of Jupiter-Uranus shown on Chart VIII.P. These three charts show how the major cycles synchronize along their 15^0 axes.

The fifteen-degree axes of the Jupiter-Uranus cycle and corresponding turning points in the DJIA between March, 1980 and the crash of October, 1987 are listed in Table 8.11.a. The data after October, 1987 are included in Table 8.11.b.

VIII.P JUPITER-URANUS AXES (1980-1993)



It is critical to understand that two possible conditions define how the larger Saturn-Uranus cycle is divided into its harmonics by the smaller Jupiter-Uranus and Jupiter-Saturn cycles. Depending upon the relative speeds of their elliptical orbits, the Saturn-Uranus 15° harmonic is either:

- (1) Divided into three parts by the 15° Jupiter-Saturn harmonics and four parts by the 15° Jupiter-Uranus harmonics.
- (2) Divided into two parts by the 15° Jupiter-Saturn harmonics and three parts by the 15° Jupiter-Uranus harmonics.

Depending upon which of these two possible conditions exists, the Jupiter-Uranus cycle will be strongest at either its 45° harmonic or at its 60° harmonic, because one of these harmonics will coincide with the Saturn-Uranus 15° harmonic.

After the crash in October, 1987, the orb-of-influence of the Jupiter-Uranus cycle changed to that shown in Table 8.11.b. This coincided with completion of the 1982-1987 square. After the crash, the orb-of-influence was less than one degree, while during the 1982-1987 square it was approximately two degrees.

To show how closely these Jupiter-Uranus 30° axes coincided with DJIA tops and bottoms, the distance the Jupiter-Uranus cycle traveled per trading day will be compared with the deviation this cycle had from the ideal 15° axes.

Table 8.11.a
Jupiter-Uranus Synodic Movements of Fifteen Degrees
And Corresponding Turning Points in the DJIA (3/1980 - 10/1987)
(See Chart VIII.P)

Date of 7-Month DJIA Half-Cycle	Angle Between Jupiter-Uranus at Beginning	Angle Between Jupiter-Uranus at End	Change in Location
3/27/1980 - 11/19/1980	75 ⁰ 15	60 ⁰ 00	15 ⁰ 15
11/19/1980 - 6/25/1981	60 ⁰ 00	46 ⁰ 12	13 ⁰ 48
6/25/1981 - 3/09/1982	46 ⁰ 12	30 ⁰ 07	16 ⁰ 05
3/09/1982 - 10/22/1982	30 ⁰ 07	14 ⁰ 50	15 ⁰ 17
10/22/1982 - 5/06/1983	14 ⁰ 50	2 ⁰ 29	12 ⁰ 21
5/06/1983 - 1/10/1984	2 ⁰ 29	14 ⁰ 16	17 ⁰ 45
1/10/1984 - 7/25/1984	14 ⁰ 16	28 ⁰ 00	13 ⁰ 44
7/25/1984 - 3/04/1985	28 ⁰ 00	44 ⁰ 06	16 ⁰ 06
3/04/1985 - 9/18/1985	44 ⁰ 06	58 ⁰ 41	14 ⁰ 35
9/18/1985 - 3/27/1986	58 ⁰ 41	73 ⁰ 15	14 ⁰ 34
3/27/1986 - 9/29/1986	73 ⁰ 15	87 ⁰ 50	14 ⁰ 35
9/29/1986 - 4/07/1987	87 ⁰ 50	102 ⁰ 57	15 ⁰ 07
4/07/1987 - 10/22/1987	102 ⁰ 57	118 ⁰ 46	15 ⁰ 49

Table 8.11.b
Jupiter-Uranus Synodic Movements of Fifteen Degrees
And Corresponding Turning Points in the DJIA After Crash of 1987
(See Chart VIII.P)

Date of 7-Month DJIA Half-Cycle	Angle Between Jupiter-Uranus at Beginning	Angle Between Jupiter-Uranus at End	Change in Location
11/16/1988 - 5/22/1989	149 ⁰ 37	164 ⁰ 00	14 ⁰ 23
5/22/1989 - 1/03/1990	164 ⁰ 00	179 ⁰ 12 (After 180 ⁰)	16 ⁰ 48
1/03/1990 - 7/20/1990	179 ⁰ 12	165 ⁰ 00	14 ⁰ 12
7/20/1990 - 2/19/1991	165 ⁰ 00	150 ⁰ 00	15 ⁰ 00
2/19/1991 - 10/09/91	150 ⁰ 00	134 ⁰ 18	15 ⁰ 42
10/09/91 - 6/2/1992	134 ⁰ 18	118 ⁰ 44	15 ⁰ 34

Between the dates shown in Table 8.11.b (11/16/1988-6/2/1992) there were 894 trading days. During this time the Jupiter-Uranus cycle moved a total of $91^{\circ}39'$. Hence, its average movement during this time was 9.8 trading days per degree. This is calculated as follows:

$$\frac{894 \text{ trading days}}{91^{\circ}39'} = \frac{9.8 \text{ trading days}}{1 \text{ degree}}$$

Therefore, when the actual DJIA turning point, measured top-to-top or bottom-to-bottom, deviated from the Jupiter-Uranus cycle by one degree, this represented an error averaging 9.8 trading days. This two-week window is measured within a fourteen-month cycle. A deviation of 9.8 trading days in a cycle lasting fourteen months represents an error of 3%.

When a harmonic larger than 30° is used the error becomes much less than 3%. For example, between 11/16/1988 and 6/2/1992 the actual movement of Jupiter-Uranus was $91^{\circ}39'$. This deviated from the ideal angle by only one degree, spanning a period of 3 1/2 years.

MARS SIDEREAL CYCLE AND STOCK MARKET CORRELATION

The cycles studied thus far have been long-term. The smallest of which is the Jupiter-Uranus cycle with a bottom-to-bottom or top-to-top period averaging fourteen months. The worst-case scenarios for these major cycles allow the analyst to project tops or bottoms within 1-2 weeks. This section on the Mars cycle begins an analysis of the minor cycles. These cycles allow the analyst to narrow the "window" of tolerance down to 1-2 trading days.

Mars has special significance in the planetary cycles. It cannot be grouped with the major planets. Nor, is it entirely one of the minor planets. Rather, it provides a link between these two groups of planets.⁸⁵

Mars is the planet Johannes Kepler studied while developing his laws of elliptical motion.⁸⁶ It is fortunate that Tycho Brahe focused his efforts on Mars while recording the data used by Kepler because Mars has a clearly defined elliptical orbit. If Venus had been used instead of Mars Kepler may have never discovered the elliptical orbits because Venus orbits in a nearly circular path.

Mars returns to its position relative to the fixed stars every 22.5 months. This time period corresponds with the fifteen-degree axes of the Saturn-Uranus cycle and the forty-five degree axes of the Jupiter-Uranus cycle. These correlations provide the "link" between

⁸⁶ W.D. Gann used what he called the "MOF". Which is an abbreviation for the "Mean of Five". He took the "mean" of the locations of the five planets with mars left out, and tried to associate that value with price values. The mean is the halfway point between two extremes.

⁸⁷ Reference: *Kepler's Geometrical Cosmology*.

the harmonics of the major planets and the periods of the minor planets, as shown in Figures 6.2 and 6.3.

The previous section on the Jupiter-Uranus cycle measured the difference between the date of the actual DJIA top or bottom and the date the Jupiter-Uranus axes were reached. Several of these deviations were caused by the synchrony that exists between the Mars trine and the Jupiter-Uranus 15^0 harmonic. The DJIA bottoms and tops deviated from the ideal Jupiter-Uranus 15^0 axes when the Mars trine and the Jupiter-Uranus axes were not perfectly aligned.

Two critical areas of the Mars cycle deserve special attention. They are located sixty degrees apart at 19^0 Virgo and 19^0 Scorpio. These two points often identify bottom-to-top or top-to-bottom swings in the stock market. The reason why these two areas are so important is explained in the next section on the musical twelfth of the Mars cycle. In short, this is where the Mars cycle shifts between two trines (120^0) when it becomes asynchronous with the 15^0 Jupiter-Uranus harmonic.

Chart VIII.Q shows a period of twenty-seven years with these two critical areas of the Mars cycle identified. The data for the Scorpio turning points from 5/1969 to 11/1991 are listed in Table 8.12.a, and those for 19^0 of Virgo are listed in Table 8.12.b. Chart VIII.Q shows how almost every major turning point between 1965 and 1992 coincided with these two locations in the Mars cycle.

Recently, the dates 3/27/1980, 1/10/1984, and 10/2/1987 are all well-known turning points in the DJIA that corresponded with the location of 19^0 Virgo in the Mars cycle.

Since Mars moves 360^0 in approximately 465 trading days, it averages 1.3 trading days per degree. Therefore, it averages 3^0 motion in four trading days. Three degrees on either side of 19^0 is 16^0 - 22^0 , which encompasses most of the items in Tables 8.12.a and 8.12.b. This $\pm 3^0$ range provides a window of tolerance of ± 4 trading days.

When calculating the error it must be realized that many of the turning points listed in Tables 8.12.a and 8.12.b were not sharply defined. Many times the actual DJIA high or low did not occur very far from the day the ideal Mars angle was crossed.

OCTAVES (1/2; 1/4; 1/8) OF THE MARS CYCLE AND THE STOCK MARKET

Mars is synchronized with the period of Mercury in the ratio of eight to one, defining the triple octave. When Mars completes one cycle, Mercury completes eight. Or,

**THE COMPLETE MERCURY CYCLE IS SYNCHRONIZED WITH
THE 45^0 HARMONIC OF THE MARS CYCLE.**

VIII.Q

MARS VIRGO AND SCORPIO POINTS

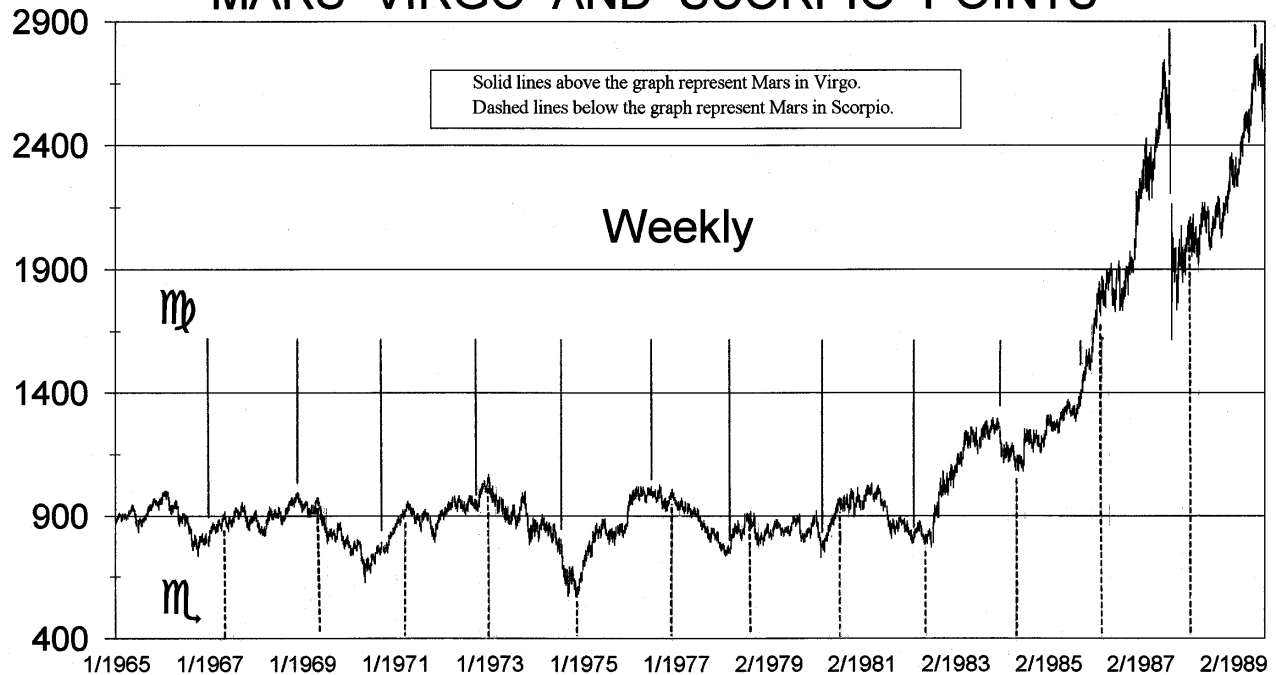


Table 8.12.a
Mars Scorpio Cycle And Corresponding
Turning Points in the DJIA (5/1969-11/1991)
 (See Chart VIII.Q)

Date of Cycle	Location of Mars At Start of Cycle	Location of Mars At End of Cycle
5/09/1969 - 3/18/1971	28 ⁰² Scorpio	23 ²⁷ Scorpio
3/18/1971 - 1/11/1973	23 ²⁷ Scorpio	12 ²⁷ Scorpio
1/11/1973 - 12/09/1974	12 ²⁷ Scorpio	17 ²⁸ Scorpio
12/09/1974 - 9/22/1976	17 ²⁸ Scorpio	5 ⁵⁵ Scorpio
9/22/1976 - 9/11/1978	5 ⁵⁵ Scorpio	16 ³¹ Scorpio
9/11/1978 - 8/08/1980	16 ³¹ Scorpio	21 ³⁵ Scorpio
8/08/1980 - 6/21/1982	21 ³⁵ Scorpio	19 ⁰⁷ Scorpio
6/21/1982 - 5/29/1984	19 ⁰⁷ Scorpio	29 ⁵³ Scorpio
5/29/1984 - 3/27/1986	29 ⁵³ Scorpio	19 ⁴¹ Scorpio
3/27/1986 - 3/02/1988	19 ⁴¹ Scorpio	29 ²⁷ Scorpio
3/02/1988 - 1/03/1990	29 ²⁷ Scorpio	21 ⁴⁶ Scorpio
1/03/1990 - 11/14/1991	21 ⁴⁶ Scorpio	18 ¹⁷ Scorpio

Table 8.12.b
Mars Virgo Cycle And Corresponding
Turning Points in the DJIA (12/1968-7/1991)
(See Chart VIII.Q)

Date of Cycle	Location of Mars at Start of Cycle	Location of Mars at End of Cycle
12/2/1968 - 10/28/1970	14 ⁰ 12 Virgo	17 ⁰ 45 Virgo
10/28/1970 - 9/26/1972	17 ⁰ 45 Virgo	23 ⁰ 04 Virgo
9/26/1972 - 8/08/1974	23 ⁰ 04 Virgo	20 ⁰ 27 Virgo
8/08/1974- 6/18/1976	20 ⁰ 27 Virgo	17 ⁰ 25 Virgo
6/18/1976 - 4/03/1978	17 ⁰ 25 Virgo	3 ⁰ 01 Virgo
4/03/1978 - 3/27/1980	3 ⁰ 01 Virgo	19 ⁰ 14 Virgo
3/27/1980 - 3/08/1982	19 ⁰ 14 Virgo	29 ⁰ 53 Virgo
3/08/1982 - 1/10/1984	29 ⁰ 53 Virgo	23 ⁰ 43 Virgo
1/10/1984 - 10/7/1985	23 ⁰ 43 Virgo	1 ⁰ 25 Virgo
10/7/1985 - 10/2/1987	1 ⁰ 25 Virgo	18 ⁰ 04 Virgo
10/2/1987 - 8/11/1989	18 ⁰ 04 Virgo	14 ⁰ 36 Virgo
8/11/1989 - 7/08/1991	14 ⁰ 36 Virgo	18 ⁰ 35 Virgo

Chart VIII.R shows turning points in the DJIA correlated with 180⁰ sections (first octave) of the Mars cycle. The data for this period are contained in Table 8.12.c. These 180⁰ sections are synchronized with four Mercury cycles, shown on Chart VIII.W. The synchronous nature of these cycles can also be seen in Figure 6.3, and they are summarized below:

- 180⁰ of the Mars cycle**
- = Four Mercury cycles**
- = One and one-half Venus cycles**

One example of this combination in the DJIA occurred between 8/11/1989 and 7/20/1990. Review this section of the stock market on the respective charts of the Mars, Mercury, and Venus cycles.

VIII.R

MARS 180 DEGREE HARMONICS

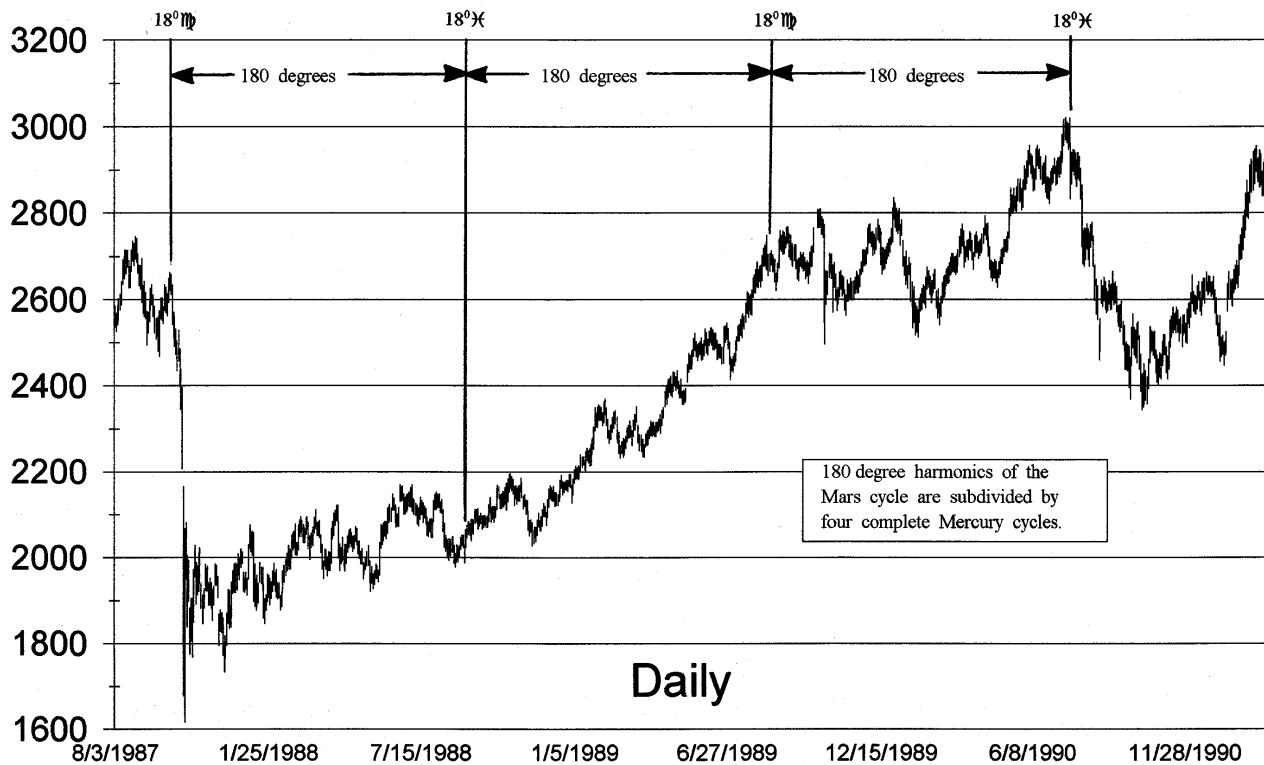


Table 8.12.c
Mars 180° Harmonics And Corresponding Turning
Points in the DJIA (10/2/1987 - 6/8/1992)
 (See Chart VIII.R)

Date of Cycle	Location of Mars at Start of Cycle	Location of Mars at End of Cycle	Degrees Traveled by Mars During Cycle
10/2/1987 - 9/01/1988	18°04 Virgo	18°12 Pisces	180 Degrees
9/01/1988 - 8/11/1989	18°12 Pisces	14°36 Virgo	177 Degrees
8/11/1989 - 7/20/1990	14°36 Virgo	18°16 Pisces	183 Degrees
7/20/1990 - 7/08/1991	18°16 Pisces	18°35 Virgo	180 Degrees
7/08/1991 - 6/08/1992	18°35 Virgo	19°33 Pisces	181 Degrees

MUSICAL TWELFTH (1/3) OF THE MARS CYCLE AND THE STOCK MARKET

The link between the harmonics of Mars and the periods of the minor planets is shown in Figure 6.3, where it can be seen that the period of Venus is in the ratio of three to one with Mars. That is,

WHEN MARS MOVES 120° VENUS COMPLETES ONE CYCLE.

Because Venus moves in a nearly circular orbit there are periods where it separates from the Mars trine. This will be explained in the section covering the Venus cycle.

Previous sections showed that the Mars trine is also synchronized with the 15° axes of the Jupiter-Uranus cycle. Therefore, these three synchronized harmonics can be summarized as follows:

$$\begin{aligned}
 & \mathbf{15^\circ \text{ Jupiter-Uranus cycle}} \\
 = & \mathbf{120^\circ \text{ In the Mars cycle}} \\
 = & \mathbf{\text{One complete Venus cycle}}
 \end{aligned}$$

Charts VIII.S and VIII.T show combinations of the Mars trine and the Jupiter-Uranus 15° harmonic correlated with DJIA turning points. The Mars trines are identified with vertical lines drawn above the graph. These sections represent the musical twelfth (1/3) and are synchronized with one complete Venus cycle, as demonstrated in Figure 6.3. Compare these 120° sections of the Mars cycle with the Venus cycle from Charts VIII.U and VIII.V. Closely synchronized cycles allow the analyst to identify where future nodal points are certain to occur. The date of the first such point shown on these charts was October 2, 1987, just before the great crash. One trine later, on May 27, 1988, the stock market reached a critical bottom. The market bottomed again on November 16, 1988 when Mars reached its next trine. The ensuing rally lasted until August 11, 1989 when Mars reached its third trine, returning to the same position as October 2, 1987.

The vertical lines drawn below the graphs in Charts VIII.S and VIII.T show the 15° axes of the Jupiter-Uranus cycle. Note how precisely these 15° axes align with the Mars trines shown above the graph.

There is one point on Chart VIII.S where the Mars trine and the Jupiter-Uranus 15° harmonic did not align. That occurred at the August 11, 1989 top. During this period the Mars cycle shifted to its next trine. The elliptical orbits of the planets caused this shift in the Mars trine. The Mars cycle does not divide into the Jupiter-Uranus cycle a perfectly integral number of times. This difference is reflected in the Mars cycle by it shifting to the second trine when the Jupiter-Uranus cycle becomes asynchronous with it. This shifting in trines occurs when Mars is at the slowest point in its orbit, at aphelion in Virgo.

VIII.S MARS 120 DEGREE HARMONICS

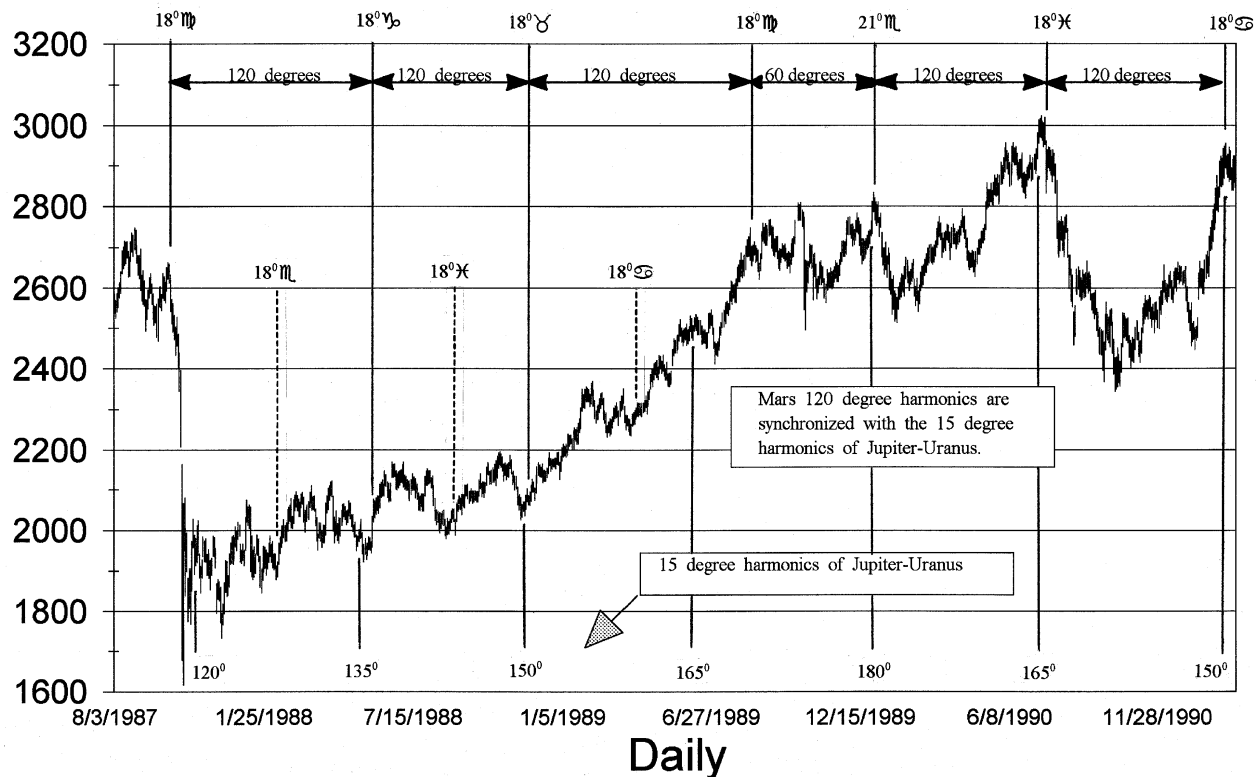


Chart VIII.T shows the turning points in the DJIA between the dates 1/3/1990 and 6/5/1992 which coincided with the three synchronized cycles: 15° Jupiter-Uranus, Mars trine, and one complete Venus cycle. By comparing the lines above the graph on Chart VIII.T, which represent the Mars trine, with the lines drawn below the graph, which represent the Jupiter-Uranus 15° harmonic, it can be seen that these two cycles were synchronized during this time.

Figure 8.3 shows the two Mars trines between 1/23/1987 and 6/5/1992. The shifting between these two trines occurred when the Mars trine became asynchronous with the Jupiter-Uranus cycle between 8/11/1989 and 1/3/1990. The second Mars trine, shown in Figure 8.3.b, aligned with the Jupiter-Uranus 15° harmonic for the time frame shown on Chart VIII.T.

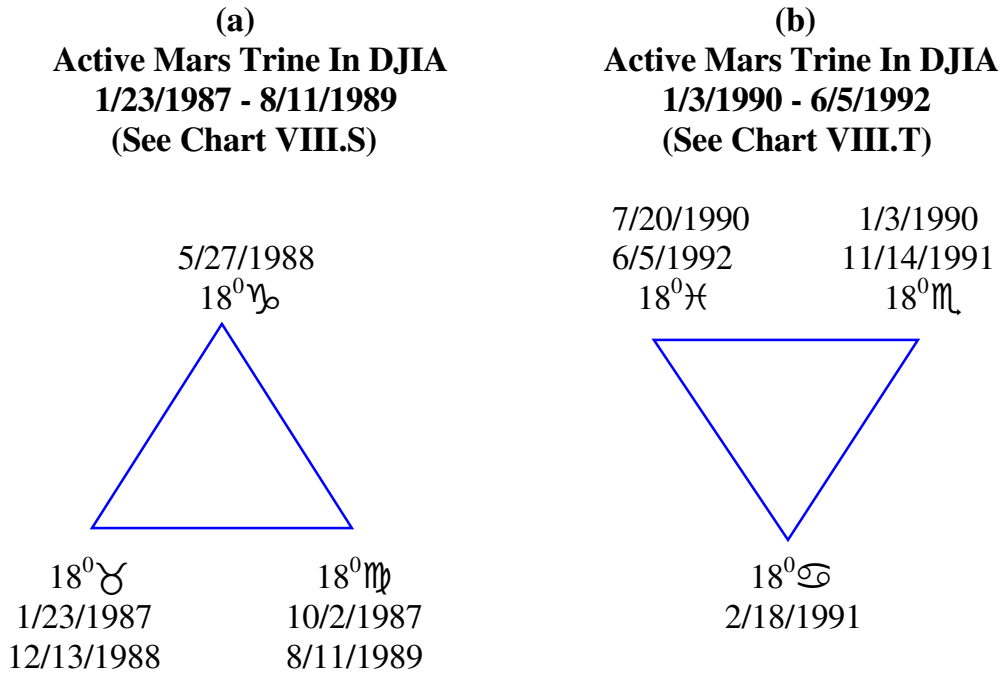


Figure 8.3

Two Mars trines that were synchronized with the 15° axes of the Jupiter-Uranus cycle in DJIA between 1/1987-6/1992. The shift between the two trines occurred between 8/11/1989 and 1/3/1990.

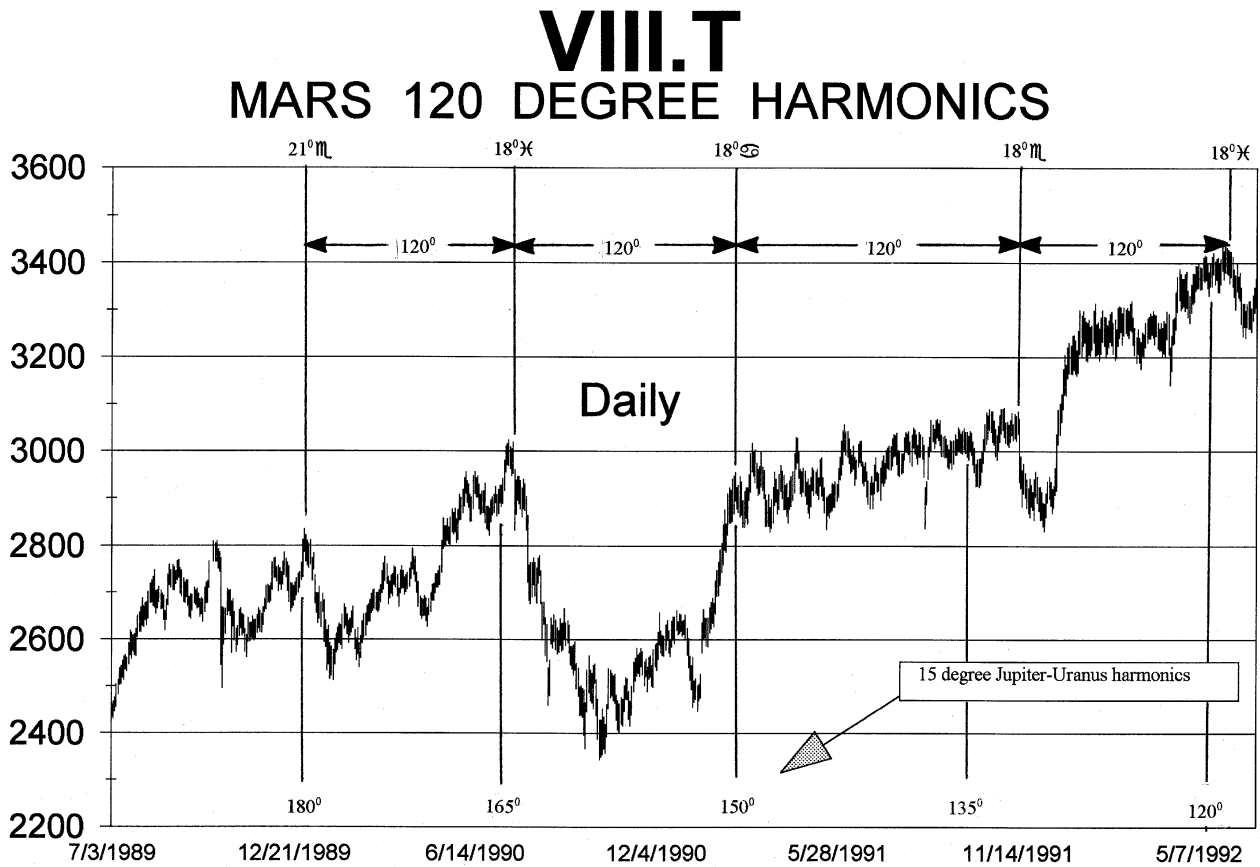


Table 8.12.d contains the location of Mars for the trine shown in Figure 8.3.a. The first date in this table, 1/23/1987, occurred during a powerful uptrend. On this date the DJIA made a 120 drop in the final hour of trading, from up 60 points to down 60 points.

Table 8.12.d
Mars 120° Harmonics And Corresponding Turning
Points in the DJIA (1/23/1987 - 8/11/1989)
 (See Figure 8.3.a and Chart VIII.S)

Date of Cycle	Location of Mars at Start Of Cycle	Location of Mars at End Of Cycle	Degrees Traveled by Mars During Cycle
1/23/1987 - 10/2/1987	18°25 Taurus	18°04 Virgo	120 Degrees
10/2/1987 - 5/27/1988	18°04 Virgo	17°35 Capricorn	120 Degrees
5/27/1988 - 12/13/88	17°35 Capricorn	20°00 Taurus	122 Degrees
12/13/88 - 8/11/1989	20°00 Taurus	14°36 Virgo	115 Degrees

Table 8.12.e contains the location of Mars during the second trine shown in Figure 8.3.b. These 120° sections are also synchronized with the 15° axes of the Jupiter-Uranus cycle and one complete Venus cycle.

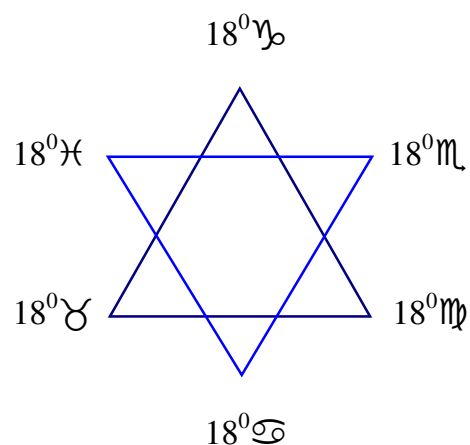
Table 8.12.e
Mars 120° Harmonics And Corresponding Turning
Points in the DJIA (1/3/1990 - 6/5/1992)
 (See Figure 8.3.b and Chart VIII.T)

Date of Cycle	Location of Mars at Start Of Cycle	Location of Mars at End Of Cycle	Degrees Traveled by Mars During Cycle
1/03/1990 - 7/20/1990	21°46 Scorpio	18°16 Pisces	117 Degrees
7/20/1990 - 2/19/1991	18°16 Pisces	16°42 Cancer	118 Degrees
2/19/1991 - 11/14/1991	16°42 Cancer	18°17 Scorpio	121 Degrees
11/14/1991 - 6/05/1992	18°17 Scorpio	17°39 Pisces	120 Degrees

MARS TRINES IN DJIA (1/87-6/92) FORM THE HEBREW "STAR OF DAVID"

When the two triangles from Figures 8.3.a and 8.3.b are superimposed they create the Hebrew "Star of David" shown in Figure 8.4. This is no coincidence because the ancient Hebrews relied heavily on cyclic law and the motions of the planets. Twelve was used to reflect the twelve months in the year, which is the approximate time between successive full moons. The Hebrews committed considerable effort to studying the motions of the planets, and incorporated their findings into their form of astrology, and even into their religion. Much forgotten knowledge of planetary cycles can be gained by studying the works of these ancient astrologers. The hard part is finding reliable historic information and correctly interpreting its meaning.

The last few centuries have allowed mass human emotional swings to be recorded in the form of financial market price data. The analysis of this data verifies that these ancient Hebrews did not erroneously correlate the motions of the planets with cyclic characteristics of life on Earth.



18°♎ to 18°♌ defines the 60° transition from one trine to the next, which occurred between 8/11/1989 - 1/3/1990.

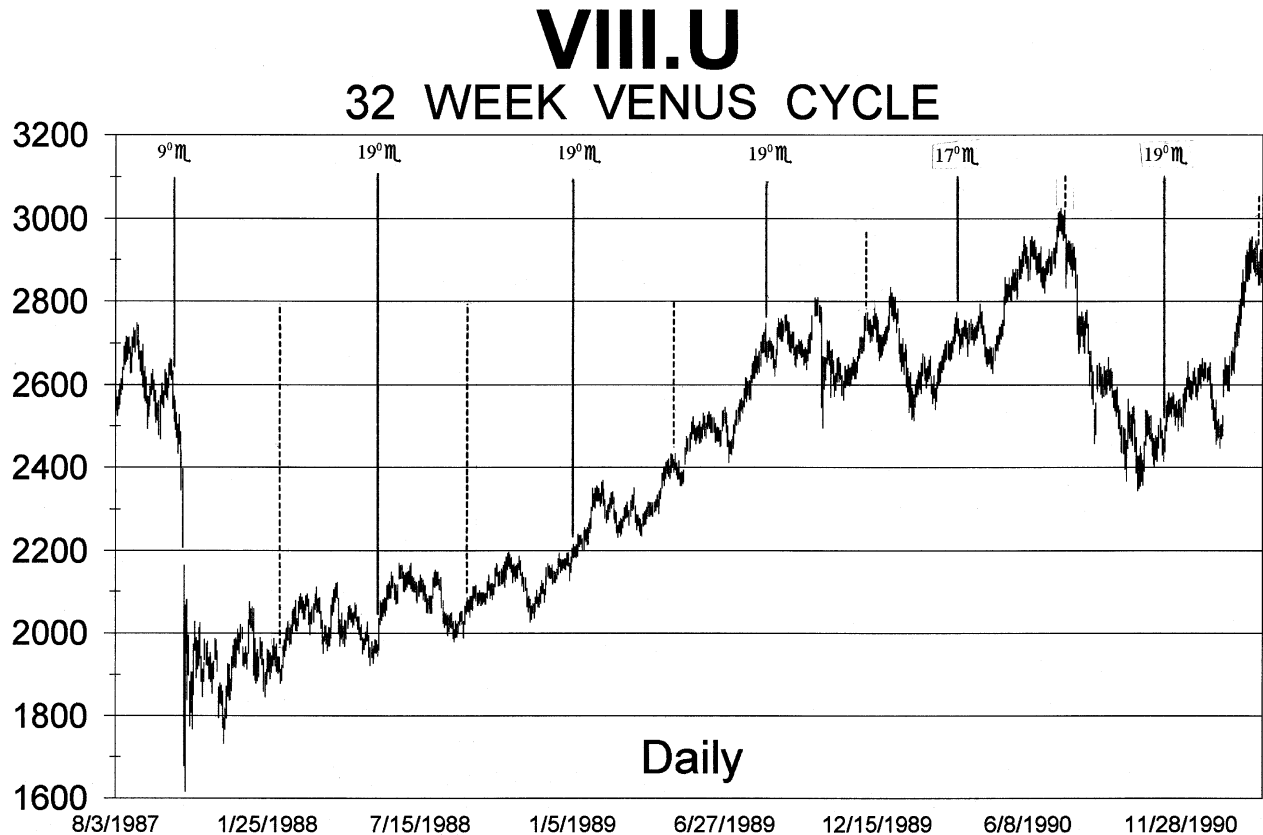
Figure 8.4

The two Mars trines in the DJIA between 1/23/1987 and 6/5/1992 that are synchronized with the Jupiter-Uranus 15° axes form the Hebrew "Star of David". (See Figure 8.3 and Charts VIII.S and VIII.T)

VENUS SIDEREAL CYCLE AND STOCK MARKET CORRELATION

Venus completes one sidereal period every 225 days. Figure 6.3.c showed that this period is synchronized with the harmonics of the Mars cycle. When Venus completes one cycle Mars moves 120°. In other words, Venus responds to the musical "twelfth" of Mars. Compare the 180° Venus harmonics shown on Chart VIII.U with the Mars half-trines shown on Chart VIII.S.

The periods of these two planets are so close to a perfect three to one ratio, ($687/225 = 3.05$), that it can be difficult to tell with which cycle the stock market has synchronized. However, because the orbit of Venus is less elliptical than that of Mars there are periods when these two cycles separate from each other, effectively isolating the individual cycles.

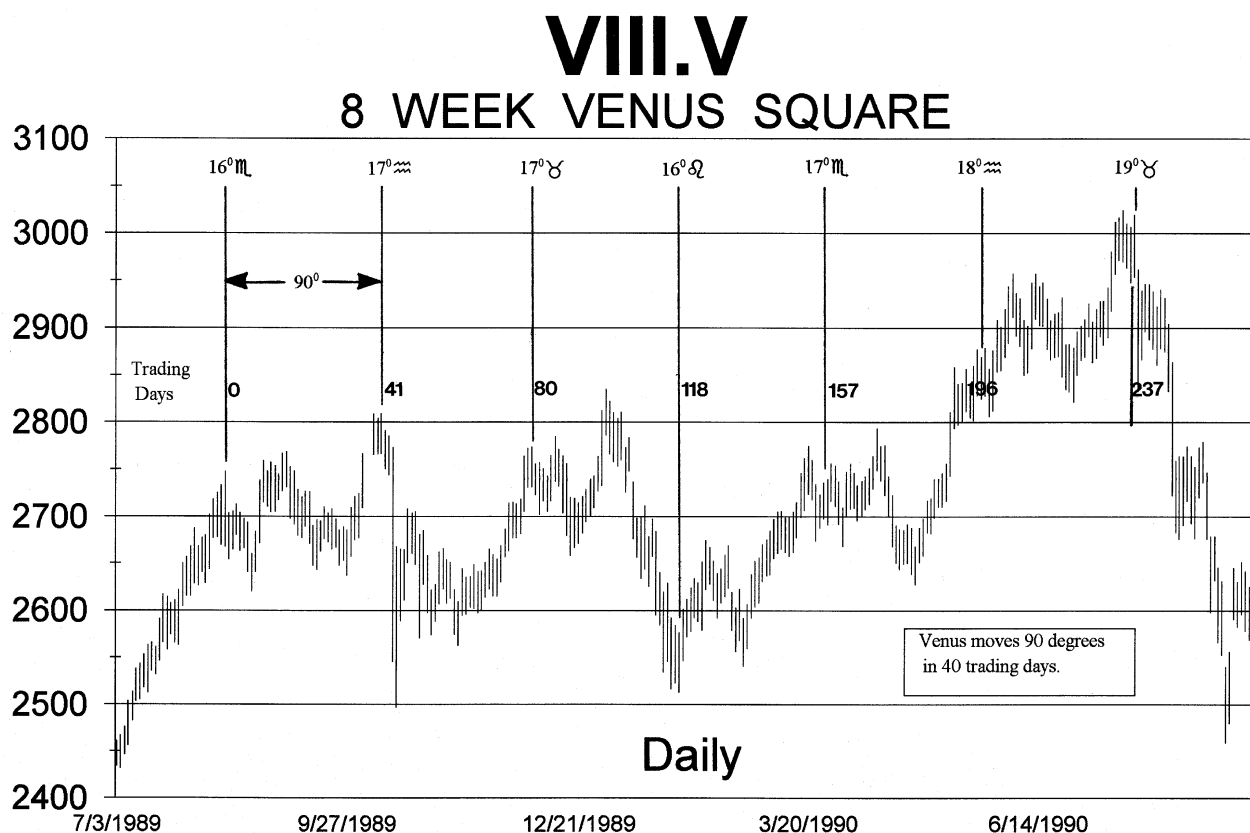


At these times the cycles can be clearly identified. For example, Chart VIII.T showed that the 1/3/1990 top coincided with the Mars trine in Scorpio. However, Chart VIII.V shows that the Venus cycle does not align with this top, rather its axis arrived 19 trading days earlier on 12/5/1989. These two charts show how two cycles create a "double top" or a "double bottom" when they become asynchronous.

The general rule in finding the cyclic component with the greatest effect is to find with which harmonic of another cycle the cycle under study is most closely synchronized. For example, to find the reinforced harmonics of the Venus cycle, it is a matter of finding which harmonic of the larger cycles coincide with the Venus cycle. As mentioned above, Venus is very closely aligned with the trine (120°) of Mars. Therefore,

**WHEN THE MARS CYCLE SUBDIVIDES INTO ITS HARMONICS
OF 30° VENUS WILL HAVE MOVED THREE TIMES THIS
AMOUNT, OR 90° .**

Since the complete cycle of Venus lasts 225 days (32 weeks), division of the Venus cycle into 90° sections creates four eight-week cycles. And since Venus's orbit is very nearly circular, the duration of these four cycles are very similar. In other words,



THE VENUS 90° HARMONIC DEFINES THE EIGHT-WEEK STOCK MARKET CYCLE.

Chart VIII.V shows the DJIA from 7/1989 to 9/1990. The vertical lines on this chart identify the 90° sections of the Venus cycle. Table 8.13.a shows how closely these 90° harmonics corresponded with the eight-week cycle in the DJIA.

The squares (90°) in the Venus cycle explain why the 1/30/1990 cycle bottom happened when it did. The Mars cycle was not due to bottom until it reached its 30° axis on 2/23/1990, and the Mercury cycle was not due to bottom until February when it reached 6° Scorpio. However, on 1/30/1990 the Venus cycle was exactly 180° from the 10/10/1989 top; 270° from the 8/11/1989 top; and 90° from the 12/5/1989 top. Also, the bottom in 1/30/1990 defined the halfway point between the top in 8/11/1989 and the top in 7/17/1990. Between these two tops Venus moved 540°, or 1 1/2 cycles.

In addition to the correlation with the Mars cycle, the harmonic relationship between the Venus and Mercury cycles is apparent when Chart VIII.U is compared with Chart VIII.W.⁸⁷ Specifically, one complete Mercury cycle is aligned with 135° of the Venus cycle, or two complete Mercury cycles are aligned with 270° of the Venus cycle.

⁸⁸ The Mercury cycle is explained in the following section.

Since the 90° section of Venus is correlated with the eight-week stock market cycle, three of these sections, 270° , correspond with three eight-week cycles. This relationship is important because it defines the musical fifth, (ratio of 3:2), with the Mercury cycle. That is, three 90° sections of the Venus cycle correspond with two complete Mercury cycles. Or,

RELATIVE MOVEMENTS OF VENUS AND MERCURY DEFINE THE MUSICAL FIFTH

Table 8.13.a
Venus Ninety-Degree Motions And Corresponding
Eight-Week Cycle in the DJIA (8/1989 - 7/1990)
(See Chart VIII.V)

Date of Eight-Week DJIA Cycle	Location of Venus At Start Of Cycle	Location of Venus At End Of Cycle	Distance Traveled By Venus During Cycle
8/14/1989 - 10/10/1989	16 Scorpio	17 Aquarius	91 Degrees
10/10/1989 - 12/5/1989	17 Aquarius	16 Taurus	89 Degrees
12/5/1989 - 1/30/1990	16 Taurus	16 Leo	90 Degrees
1/30/1990 - 3/28/1990	16 Leo	18 Scorpio	92 Degrees
3/28/1990 - 5/22/1990	18 Scorpio	16 Aquarius	88 Degrees
5/22/1990 - 7/17/1990	16 Aquarius	15 Taurus	89 Degrees Also, 270° from 1/30 540° from 8/89

Lesson VI, **SYMPATHETIC RESONANCE**, showed how important the relationship of the fifth is for creation of the musical scale. The "Diatonic Major Musical Scale" is created by taking fifths from a fundamental tone and reducing them into a single octave. This same ratio that is the basis of music is present in the relative periods of Venus and Mercury, and their reflection in the stock market with the eight and twelve-week cycles.

The preceding section on the Mars cycle showed that the Mars and Mercury cycles exist in the harmonic relationship of the octave. Therefore, the harmonics between Mars and Mercury, and between Mercury and Venus, contain the two necessary elements to define the complete "Diatonic Major Musical Scale"; that is, the octave and the fifth.

On a larger time scale, several complete Venus cycles are shown on Chart VIII.U. This chart shows how one and one-half Venus cycles ($1\frac{1}{2} = 540^{\circ}$) are reinforced by the 180° harmonics of Mars, which are shown on Chart VIII.R.

For example, one and one-half Venus cycles completed between the 10/5/1987 top and the 9/1/1988 bottom. Between these two dates Mars moved 180° , from 18° Virgo to 18° Pisces. Another one and one-half Venus cycles (or three complete cycles from the 10/5/1987 top) completed between the 9/1/1988 bottom and the 8/11/1989 top. This top coincided with Mars moving 180° from its location at the 9/1/1988 bottom (or one complete cycle from the 10/5/1987 top). Continuing this process, one and one-half Venus cycles completed between the 8/11/1989 top and the 7/17/1990 top. The 7/17/1990 top led to a 600+ point drop in the DJIA in three months. This top was 180° on the Mars cycle from the 8/11/1989 top and one and one-half cycles from the 10/5/1987 top.

The data for the larger harmonics of the Venus cycle shown on Chart VIII.U are contained in Table 8.13.b.

Venus completed one cycle between 10/5/1987 and 5/17/1988. There were 155 trading days during this 360° cycle. Therefore, Venus averages;

$$\frac{360 \text{ degrees}}{155 \text{ trading days}} = 2.3 \text{ degrees per trading day}$$

Since Venus's orbit is nearly circular, this average speed will be relatively constant throughout the 360° cycle.

Table 8.13.b
Venus Cycle And Corresponding
Turning Points in the DJIA (10/1987 - 3/1991)
 (See Chart VIII.U)

Date of Cycle	Location Of Venus At Start Of Cycle	Location Of Venus At End Of Cycle	Distance Traveled By Venus During Cycle
10/5/1987 - 5/19/1988	9 Scorpio	12 Scorpio	363°
5/19/1988 - 8/11/1989	12 Scorpio	12 Scorpio	720° (2 Cycles)
8/11/1989 - 1/30/1990	12 Scorpio	16 Leo	274° (3/4 Cycle)
1/30/1990 - 7/17/1990	16 Leo	15 Taurus	269° (3/4 Cycle)
7/17/1990 - 11/8/1990	15 Taurus	19 Scorpio	184°
11/8/1990 - 3/5/1991	19 Scorpio	25 Taurus	186°

The average of 2.3 degrees that Venus travels per trading day means that when Venus's location did not align with the ideal cycle by four degrees, as it did at places shown in Table 8.13.b, this corresponded with less than two trading days.

Notice that as the cycles become smaller, the "window of tolerance" is becoming correspondingly narrower. The Venus cycle was shown above to produce results within a two trading day window. This is much narrower than the 7-10 days for the Jupiter-Saturn and Jupiter-Uranus cycles.

12-WEEK MERCURY CYCLE AND STOCK MARKET CORRELATION

Mercury has a sidereal period of 88 days, which is approximately 60 trading days (twelve weeks). The Mercury cycle is one of the easiest to identify in the stock market because its period precisely subdivides the periods of the other planets, establishing a close relationship with their harmonics. This cycle is synchronized with the third octave (45⁰ axes) of the Mars cycle, as shown in Figure 6.3.d.

THE MERCURY CYCLE IS SYNCHRONIZED WITH THE TWELVE-WEEK STOCK MARKET CYCLE.

Since this cycle only lasts twelve weeks, a daily chart of the DJIA is used to study its effect. Chart VIII.W identifies the twelve-week cycle with vertical lines and the corresponding locations of Mercury listed at the tops of these lines.

The data from Chart VIII.W are outlined in Table 8.14 where thirteen twelve-week cycles are listed with corresponding locations of Mercury. The return of Mercury to 6⁰ Scorpio rarely deviated from these DJIA cycles by more than one or two trading days.

There are several items of special significance in Chart VIII.W. This time period is a "close-up" view of a section of the Jupiter-Saturn cycles shown on Chart VIII.O. The section describing the Jupiter-Saturn cycle identified the dates 3/2/1988, 11/16/1988, 8/11/1989, and 4/30/1990 as alternating tops and bottoms in the DJIA (see Table 8.10.b), correlated with the Jupiter-Saturn cycle. Review these dates on Chart VIII.W and notice how neatly the Mercury cycle fits into these time intervals. The Jupiter-Saturn cycle topped out in 3/2/1988 when Mercury was at 6⁰ Scorpio. During this 15⁰ interval of the Jupiter-Saturn down cycle the market moved sideways. Within this interval Mercury completed exactly three cycles. Chart VIII.X shows how the interval between 3/2/1988 and 11/16/1988 subdivided into three sections (the musical twelfth).

The Jupiter-Saturn cycle advanced between its 15⁰ axes from 11/16/1988 to 8/11/1989. Within this time interval Mercury again completed exactly three cycles. Therefore, the complete 30⁰ cycle of Jupiter-Saturn from 3/2/1988 to 8/11/1989 contained exactly six Mercury cycles.



On 8/11/1989 the Jupiter-Saturn cycle turned down until it bottomed on 4/30/1990. During this period Mercury again completed exactly three cycles. Chart VIII.X compares the time period from 8/11/1989 to 4/30/1990, with the period from 3/2/1988 to 11/16/1988. As explained above, these two sections are 30° apart in the Jupiter-Saturn cycle and six complete Mercury cycles. Within these two sections the movement is characterized by three twelve-week cycles, the first running from the top to the first bottom. The remaining two twelve-week cycles run bottom-to-bottom. The first twelve-week cycle had to run top-to-bottom because it was contained within the larger Jupiter-Saturn cycle, which ran top-to-bottom. If the Jupiter-Saturn cycle ran bottom-to-top the first Mercury cycle within that trend would run bottom-to-bottom and the last cycle would run bottom-to-top. The remaining turning points on Chart VIII.W correspond with completed Mercury cycles; i.e., 7/20/1990, 10/17/1990, 1/14/1991.

DETERMINING STRONGEST PLANETARY HARMONICS IN A TIME PERIOD

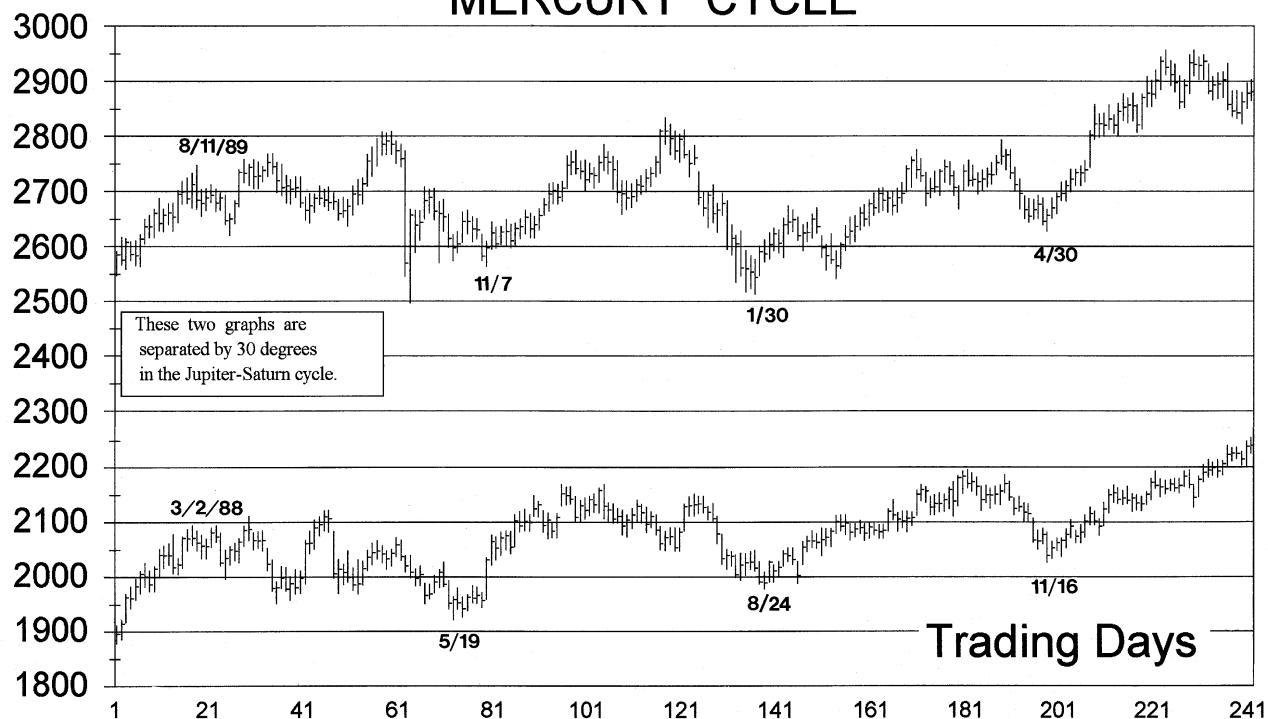
The techniques outlined below are universal. Study very closely the procedure followed, it will be used in the next lesson when the technique for modeling future price-time action is presented. The material presented in this section is vitally important to understanding financial market cycles, because it lets the analyst know to which harmonics to devote the most attention.

Table 8.14
Twelve-Week Mercury Cycle And Corresponding
Turning Points in the DJIA (12/1987 - 1/1991)
 (See Chart VIII.W)

Date of 12-Week Cycle	Location of Mercury at Beginning	Location of Mercury at End of Cycle
12/04/1987 - 3/02/1988	6 Scorpio	7 Scorpio
3/02/1988 - 5/27/1988	7 Scorpio	3 Scorpio
5/27/1988 - 8/24/1988	3 Scorpio	7 Scorpio
8/24/1988 - 11/21/1988	7 Scorpio	9 Scorpio
11/21/1988 - 2/17/1989	9 Scorpio	9 Scorpio
2/17/1989 - 5/15/1989	9 Scorpio	7 Scorpio
5/15/1989 - 8/11/1989 -	7 Scorpio	7 Scorpio
8/11/1989 - 11/7/1989	7 Scorpio	7 Scorpio
11/7/1989 - 1/30/1990	7 Scorpio	24 Libra
1/30/1990 - 4/30/1990	24 Libra	1 Scorpio
4/30/1990 - 7/20/1990	1 Scorpio	7 Libra
7/20/1990 - 10/17/1990	7 Libra	10 Libra
10/17/1990 - 1/14/1991	10 Libra	14 Libra

To accurately time turning points in any financial market the cycles and their dominant harmonics must be isolated. As explained earlier in this lesson, cycles are most pronounced when they are reinforced by other cycles or their harmonics.

VIII.X MERCURY CYCLE



When the objective is to project market turning points on monthly charts spanning a time frame less than five-years, it is adequate to focus on the Saturn-Uranus cycle and the cycles contained within it, as long as the locations of the larger cycles are known. The smaller synodic cycles within the Saturn-Uranus cycle are the Jupiter-Saturn cycle, the Jupiter-Uranus cycle, and the minor cycles defined in previous sections of this lesson.

Based on the relative speed of the Saturn-Uranus cycle, there are two possibilities for the relative relationships between the three major cycles listed above:

- (1) Either, the Jupiter-Saturn cycle will move 45° and the Jupiter-Uranus cycle will move 60° , while the Saturn-Uranus cycle moves 15° .
- (2) Or, the Jupiter-Saturn cycle will move 30° and the Jupiter-Uranus cycle will move 45° , while the Saturn-Uranus cycle moves 15° .

These two possibilities are graphically shown in Figure 8.5, where Figure 8.5.a shows the Jupiter-Saturn cycle moving 45° and the Jupiter-Uranus cycle moving 60° , while the slower moving Saturn-Uranus cycle moves across its 15° axis. Figure 8.5.b shows the Jupiter-Saturn and Jupiter-Uranus cycles moving much slower, relative to the Saturn-Uranus cycle, than in Figure 8.5.a. In Figure 8.5.b the Jupiter-Saturn cycle moves 30° and the Jupiter-Uranus cycle moves 45° , while the Saturn-Uranus cycle moves across its 15°

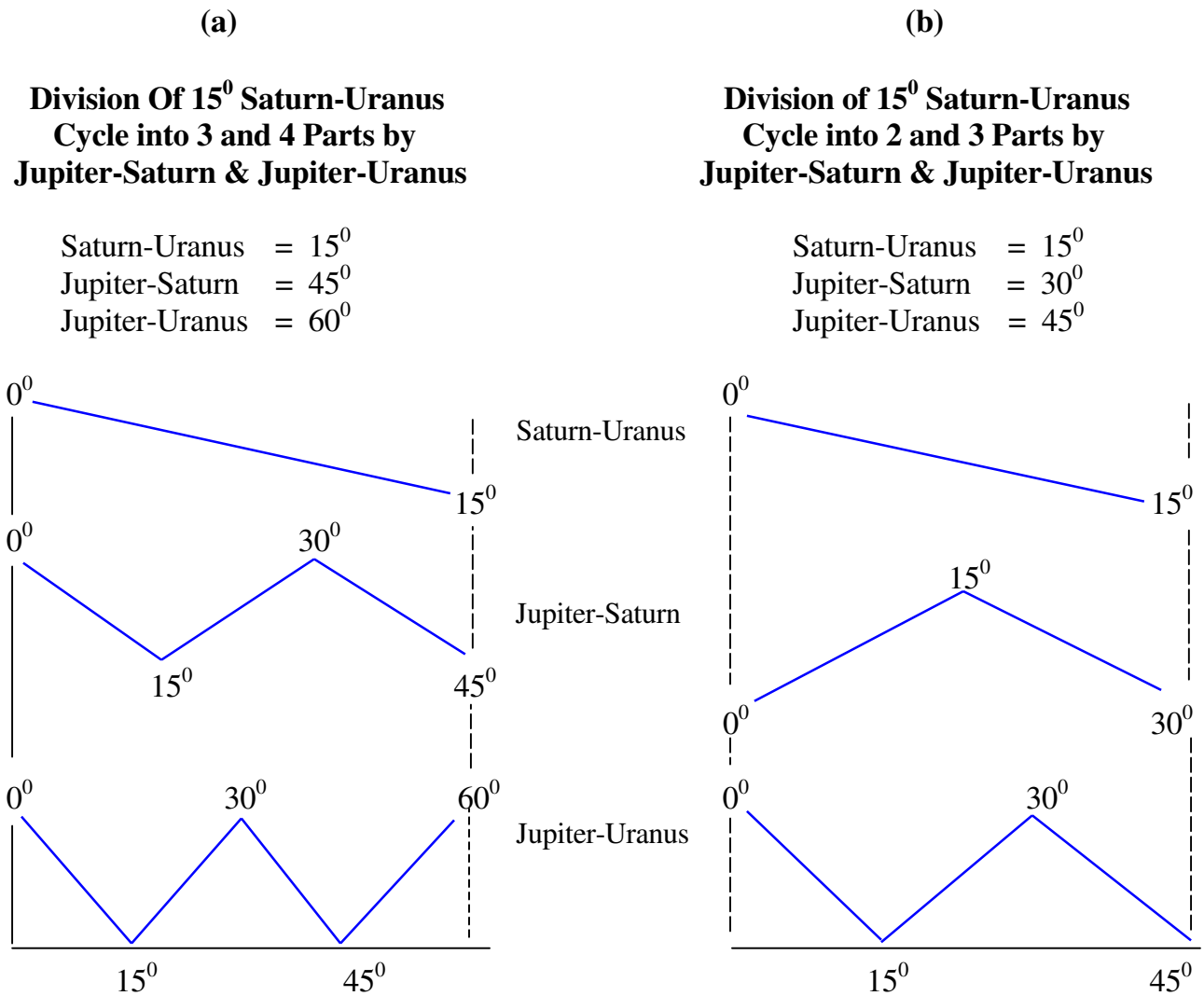


Figure 8.5

Two possible subdivisions of the Saturn-Uranus cycle by the Jupiter-Saturn and Jupiter-Uranus cycles

axis. This is the same relationship shown in Figure 6.2, which assigned musical tones to the ratios between the average periods of the major planets.

The division of a cycle into its reinforced harmonics is another application of the law of "Sympathetic Resonance" described in Lesson VI.

Examples of both these cyclic combinations abound in financial market charts. Between June 15, 1981 and April 26, 1983 the conditions existed as defined in Figure 8.5.b. During this time, the Saturn-Uranus cycle moved 15^0 , the Jupiter-Saturn cycle moved 30^0 , and the Jupiter-Uranus cycle moved 45^0 . Charts VIII.I, VIII.O, and VIII.P show these three cycles during this time period, and provide verification of their integral multiples.

Immediately following the time period described above, cyclic conditions existed as shown in Figure 8.5.a. Between April 26, 1983 and September 17, 1985 the Jupiter-Saturn

cycle moved 45° and the Jupiter-Uranus cycle moved 60° , while the Saturn-Uranus cycle moved across its 15° axis.

The Saturn-Uranus and Jupiter-Saturn harmonics shown in Figure 8.5.a begin and end in phase. While the harmonics with the configuration shown in Figure 8.5.b begin out of phase and end in phase. The phasing shown in these two figures are not the only ones possible. For example, the 1982-1987 period had the Jupiter-Saturn cycle 180° out of phase from that shown in Figure 8.5.b. This period will be studied in great detail in the next lesson.

At this point, the reader should understand that the Saturn-Uranus cycle is subdivided into integral amounts by the smaller cycles depending upon the relative speed of the three major planets. This is important because;

THE RELATIVE SPEEDS OF THE SATURN-URANUS, JUPITER-SATURN, AND JUPITER-URANUS CYCLES DEFINE THE HARMONICS THAT HAVE THE GREATEST CORRELATION WITH FINANCIAL MARKET CYCLES.

In Figure 8.5.a the Jupiter-Saturn cycle crosses three 15° axes during the time the Saturn-Uranus cycle crosses one 15° axis. As with all cycles, the octave of the Jupiter-Saturn cycle occurs when it has moved halfway between the starting point and the end point. Figure 8.5.a shows the starting point to be 0° and the end point to be 45° . Halfway between these two points is $22^{\circ}30'$.

THE EFFECT OF THE $22^{\circ}30'$ ANGLE IN THE JUPITER-SATURN CYCLE IS MOST PRONOUNCED WHEN ITS SPEED IS SUCH THAT IT MOVES 45° WHEN THE SATURN-URANUS CYCLE MOVES 15° , CAUSING THE $22^{\circ}30'$ JUPITER-SATURN HARMONIC TO BE REINFORCED BY THE FIRST OCTAVE OF THE 15° SATURN-URANUS CYCLE.

A stock market example when the $22^{\circ}30'$ harmonic of the Jupiter-Saturn cycle was reinforced by the first octave of the 15° Saturn-Uranus cycle occurred between April 26, 1983 and September 17, 1985. This period was previously identified as 15° on the Saturn-Uranus cycle and 45° on the Jupiter-Saturn cycle. The octave of the Jupiter-Saturn cycle occurred halfway between these two dates when the Jupiter-Saturn cycle had moved $22^{\circ}30'$. This harmonic defined the July 25, 1984 bottom. The exact angle between Jupiter-Saturn at the high of April 26, 1983 was $32^{\circ}18'$. The exact angle between Jupiter-Saturn at the bottom of July 25, 1984 was $54^{\circ}28'$, or a difference of $22^{\circ}10'$.

Another example with conditions nearly identical to those described above existed between August 11, 1989 and December 18, 1991. During this time the Saturn-Uranus cycle moved 15° and the Jupiter-Saturn cycle moved 45° . Therefore, the $22^{\circ}30'$ octave of the Jupiter-Saturn cycle occurred at the well-known bottom on October 11, 1990. Between August 11, 1989 and October 11, 1990, the Jupiter-Saturn cycle moved from $162^{\circ}12'$ to $175^{\circ}00'$, for a total of $22^{\circ}48'$.

Similarly, the top just before the crash on October 5, 1987 occurred when the Jupiter-Saturn cycle reached $122^{\circ}00'$. This was $22^{\circ}48'$ from the bottom on September 29, 1986 and $44^{\circ}50'$ from the bottom on September 17, 1985. Therefore, the bottom on September 29, 1986 coincided with the octave of the 45° Jupiter-Saturn cycle, measured between September 17, 1985 and October 5, 1987.

The deviations from the ideal $22^{\circ}30'$ octave and the date of the actual turning points rarely lasted more than one or two trading days. Remember, the Jupiter-Saturn cycle is one of the larger cycles. To narrow the exact date of the turning point smaller cycles are used.

The examples given above of the $22^{\circ}30'$ harmonic occurred within time frames when the cyclic combinations were as shown in Figure 8.5.a. The effect of this harmonic is greatly attenuated when the Jupiter-Saturn cycle moves 30° within the Saturn-Uranus 15° cycle, as shown in Figure 8.5.b. The reason for this becomes clear if Figure 8.5.b is studied. When the Jupiter-Saturn cycle moves $22^{\circ}30'$, with the type of arrangement shown in Figure 8.5.b, it will not coincide with the first octave of the Saturn-Uranus 15° cycle. Rather, the Saturn-Uranus cycle will have moved through three-quarters of its cycle, corresponding with the second octave. The magnitude of the second octave is less than the first octave. Similarly, this $22^{\circ}30'$ harmonic of the Jupiter-Saturn cycle is not reinforced by a major harmonic of the Jupiter-Uranus cycle, this cycle moving approximately 34° during this time.

An example of the cyclic combination shown in Figure 8.5.b occurred between June 15, 1981 and April 26, 1983. During this time the Jupiter-Saturn cycle moved 30° within the larger Saturn-Uranus 15° cycle. The $22^{\circ}30'$ harmonic is measured from the node defining the beginning of this cycle on June 15, 1981. This $22^{\circ}30'$ harmonic arrived in November, 1982 and had minimal effect on the stock market, as can be seen on Chart VIII.O. The Jupiter-Saturn octave during this period was not the $22^{\circ}30'$ division, rather it occurred at 15° . This harmonic corresponded with the major bottom in March, 1982.

To make this concept clearer, Figure 8.6 shows how the dominant harmonic changes from 15° to $22^{\circ}30'$ during a theoretical period of time. Figure 8.6.a shows the larger Saturn-Uranus cycle moving across three 15° axes. In Figure 8.6.b the Jupiter-Saturn cycle moves 30° during the first Saturn-Uranus 15° cycle, and 45° during the second and third Saturn-Uranus 15° cycles. Figure 8.6.c shows the octave of the Jupiter-Saturn cycle shown in Figure 8.6.b. The duration of the first two half-cycles in Figure 8.6.c is 15° of the Jupiter-Saturn cycle. However, the remaining half-cycles in Figure 8.6.c have $22^{\circ}30'$ durations. All the cycles in Figure 8.6.c are the result of subdividing the Jupiter-Saturn cycle shown in Figure 8.6.b into two parts, but the values change from 15° to $22^{\circ}30'$ because the larger Jupiter-Saturn cycle changes from 30° to 45° .

This theoretical example actually happened between the dates of June 15, 1981 and October 5, 1987, as shown on Charts VIII.I and VIII.O.

The conclusion to be drawn from the above discussion is that measuring $22^{\circ}30'$ from a node on the Jupiter-Saturn cycle identifies a significant turning point in the stock market only if the relative speed of the cycles are as shown in Figure 8.5.b. That is, the Jupiter-Saturn cycle must move through 45° during a 15° motion of the larger Saturn-Uranus cycle.

The octave divides this 45^0 section in half. This is critical to the cycle analyst, because as he tries to identify the effects of each harmonic, sometimes the 15^0 division and sometimes the $22^030'$ division is used, depending upon the relative speed of the larger cycle.

The method used to project the relative strength of the Jupiter-Uranus harmonics is the same as that used above for the Jupiter-Saturn cycle. That is, when its harmonics correspond with a major harmonic of another cycle its strength is greatly enhanced. Figure 8.5.b shows Jupiter-Uranus moving 45^0 as Saturn-Uranus moves 15^0 . Therefore, just as was explained for the Jupiter-Saturn cycle, the octave is defined by a $22^030'$ movement within this time period.

An example of the configuration shown in Figure 8.5.b occurred between the dates of June 15, 1981 and April 26, 1983. During this time the Jupiter-Uranus cycle moved 45^0 . The $22^030'$ octave of this cycle corresponded with the June, 1982 bottom.

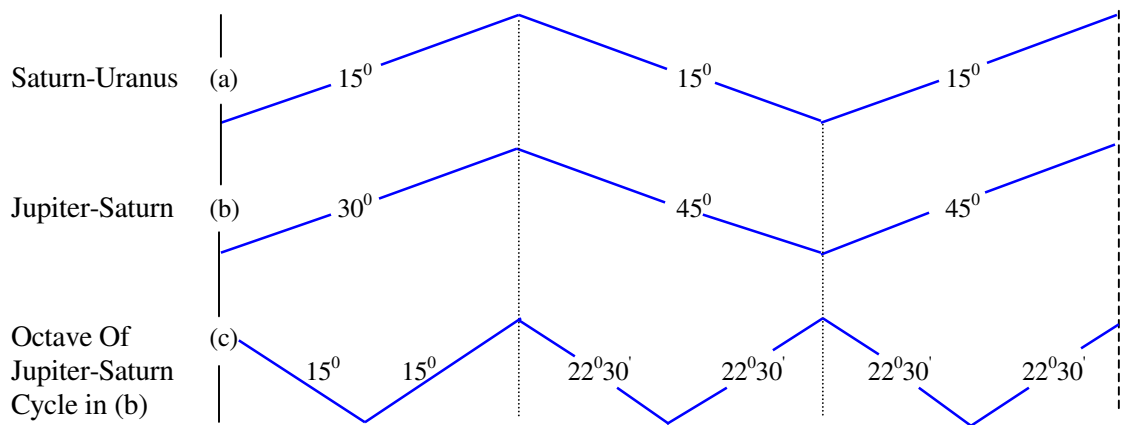


Figure 8.6

Two possible harmonic divisions of the Jupiter-Saturn cycle: 15^0 and $22^030'$

Figure 8.5 shows that, depending upon which of the two configurations the three cycles assume, the $22^030'$ harmonic will be strong in either the Jupiter-Saturn cycle or the Jupiter-Uranus cycle, **BUT NOT BOTH WITHIN THE SAME SATURN-URANUS 15^0 CYCLE.**

EXAMPLE PROJECTING TURNING POINTS USING PLANETARY CYCLES

Knowledge of planetary cycles would be little more than an academic exercise unless a technique can be applied using these cycles to accurately project price-time turning points. This section provides a practical application of locating stock market cycles, using the harmonics of the planets described in this lesson. Because the 1973-1974 stock market decline is well known to most analysts, it will be used as the example.

January, 1973 would have easily been identified in advance as a turning point in the stock market for a variety of reasons. Just a few of these reasons are:

- (1) Uranus seven-year cycle was 30^0 from the beginning of the square in 2/1966, and due to bottom when it reached its 0^0 axis in two years.
- (2) Uranus cycle was 180^0 from the low in 7/1932.
- (3) Saturn-Uranus cycle was 60^0 from the beginning of the square in 2/1966.
- (4) Saturn-Uranus cycle was 30^0 from the top in 5/1969.
- (5) Saturn-Uranus cycle was completing a 360^0 cycle from the top in 9/1929.
- (6) Saturn cycle was 90^0 from the beginning of the square in 2/1966.
- (7) Saturn was in Gemini; as it was in 1942, 1914, 1884, etc.
- (8) Jupiter-Uranus cycle was 90^0 from the top in 5/1969, and 60^0 from the bottom in 7/1970.
- (9) Jupiter-Saturn cycle was 60^0 from the top in 12/1968.
- (10) Mars returned to 19^0 Scorpio, which was its location at the tops in 4/1971 and 4/1969.

For the reasons outlined above, the analyst would have concluded that January, 1973 represented a cyclic turning point in the stock market. If it is not clear how this conclusion was reached, reread the sections in this lesson describing these cycles.

Even if the date of this top had not been identified in advance, within two weeks it would have been clear that a major decline was under way, since prices declined nearly ten percent during the first two weeks.

Since prices had been increasing into the January, 1973 turning point, the task became one of determining how long the ensuing decline would last and when intervening countertrend rallies would occur within this decline.

As explained in the section on the Uranus cycle, the twenty-one year Uranus quarter-cycle and seven year Uranus cycle were pointing down during this time. Therefore, the objective focuses on projecting what will happen for the two or three years between the nodal point in January, 1973 and the expected seven year Uranus cycle bottom in early 1975. The largest cycle corresponding with this time frame occurs along the 15^0 axes of the Saturn-Uranus cycle, which averages 22.5 months per 15^0 axis.

The first step in the analysis is to find where in the future the Saturn-Uranus cycle will have moved 15^0 from the January, 1973 node. The exact angle between Saturn-Uranus on 1/11/1973 was 121^033 . Fifteen degrees from this location is 116^033 , which occurred on 9/12/1974. Therefore, the Saturn-Uranus cycle would be expected to define a declining trend as it moved 15^0 between 1/11/1973 and 9/12/1974.

After identifying the terminal point of the 15^0 Saturn-Uranus cycle, the next step is to determine how far the smaller cycles move within this 15^0 section of the Saturn-Uranus cycle. This will reveal which of the harmonics reinforce each other in this particular section.

The ephemeris shows that between the 15^0 Saturn-Uranus axes from 1/11/1973 to 9/12/1974 the Jupiter-Saturn cycle moved $30^036'$ and the Jupiter-Uranus cycle moved $45^034'$. Notice how neatly these three cycles fit together along their 15^0 axes. The two smaller cycles only deviated by about one-half of one degree from a perfect fit. This difference represents less than one week.

This cyclic configuration was shown in Figure 8.5.b, where it was shown that the strongest harmonics from such a configuration are:

- (1) 15^0 Saturn-Uranus cycle
- (2) 15^0 Jupiter-Saturn cycle
- (3) $22^030'$ Jupiter-Uranus cycle
- (4) 15^0 Jupiter-Uranus cycle

The $22^030'$ Jupiter-Uranus harmonic is reinforced by the 15^0 Jupiter-Saturn cycle and the octave of the 15^0 Saturn-Uranus cycle.

The $22^030'$ Jupiter-Saturn harmonic is not included in this list, because it was not reinforced by the major harmonic of another cycle stronger than the second octave. This harmonic will have an effect, it will just be less than the four listed above.

Figure 8.7 shows the locations of these four major harmonics. The 15^0 Saturn-Uranus cycle is shown in Figure 8.7.a.

Figure 8.7.b shows the three Jupiter-Saturn 15^0 axes during this time period. They occurred at the beginning, middle, and end; i.e., at $148^015'$ on 1/11/1973, $133^015'$ on 11/14/1973, and at $118^015'$ on 9/2/1974.

Figure 8.7.c shows that the Jupiter-Uranus $22^030'$ harmonic was so closely synchronized with the Jupiter-Saturn 15^0 harmonic that they both topped on the same trading day, 11/14/1973.

Previous sections showed that the strength of the Jupiter-Saturn and Jupiter-Uranus $22^030'$ cycles is determined by their relative location within the larger Saturn-Uranus cycle. Similarly, the locations of the 15^0 axes of the Jupiter-Uranus cycle are determined by the Mars trine reinforcing them. The 15^0 Jupiter-Uranus harmonics for this time period are shown in Figure 8.7.d.

There is a very critical characteristic of this harmonic of which the analyst must be aware. The starting date of the Jupiter-Uranus 15^0 axis is 1/25/1973. This date was determined by the synchrony that exists between this harmonic and the Mars trine. However, the starting date for the Jupiter-Uranus $22^030'$ harmonic is determined by its synchrony with the larger Saturn-Uranus and Jupiter-Saturn harmonics.

EVEN THOUGH THE RELATIVE MOTION OF THE SAME TWO PLANETS (JUPITER AND URANUS) DEFINES THE 15^0 AND $22^030'$ HARMONICS, THE PRECISE LOCATIONS OF THESE TWO HARMONICS ARE DETERMINED BY THEIR SYNCHRONY WITH THE HARMONICS OF DIFFERENT PLANETS. THE 15^0 HARMONIC IS SYNCHRONIZED WITH THE MARS TRINE AND THE $22^030'$ HARMONIC IS SYNCHRONIZED WITH THE SATURN-URANUS AND JUPITER-SATURN CYCLES.

The active Mars trine for this period is shown in Figure 8.7.e. This is the same trine shown in Figure 8.3.b. The first three axes of this trine were closely synchronized with the Jupiter-Uranus 15^0 axes shown in Figure 8.7.d. These two harmonics became asynchronous when Mars slowed down as it approached aphelion in Virgo. At this point the Jupiter-Uranus 15^0 harmonic became synchronized with the new Mars trine shown in Figure 8.3.a. This "decoupling" from the first Mars trine can be seen in Figures 8.7.d and 8.7.e where the Jupiter-Uranus cycle bottomed on 9/20/1974 and the Mars trine bottomed three months later on 12/12/1974.

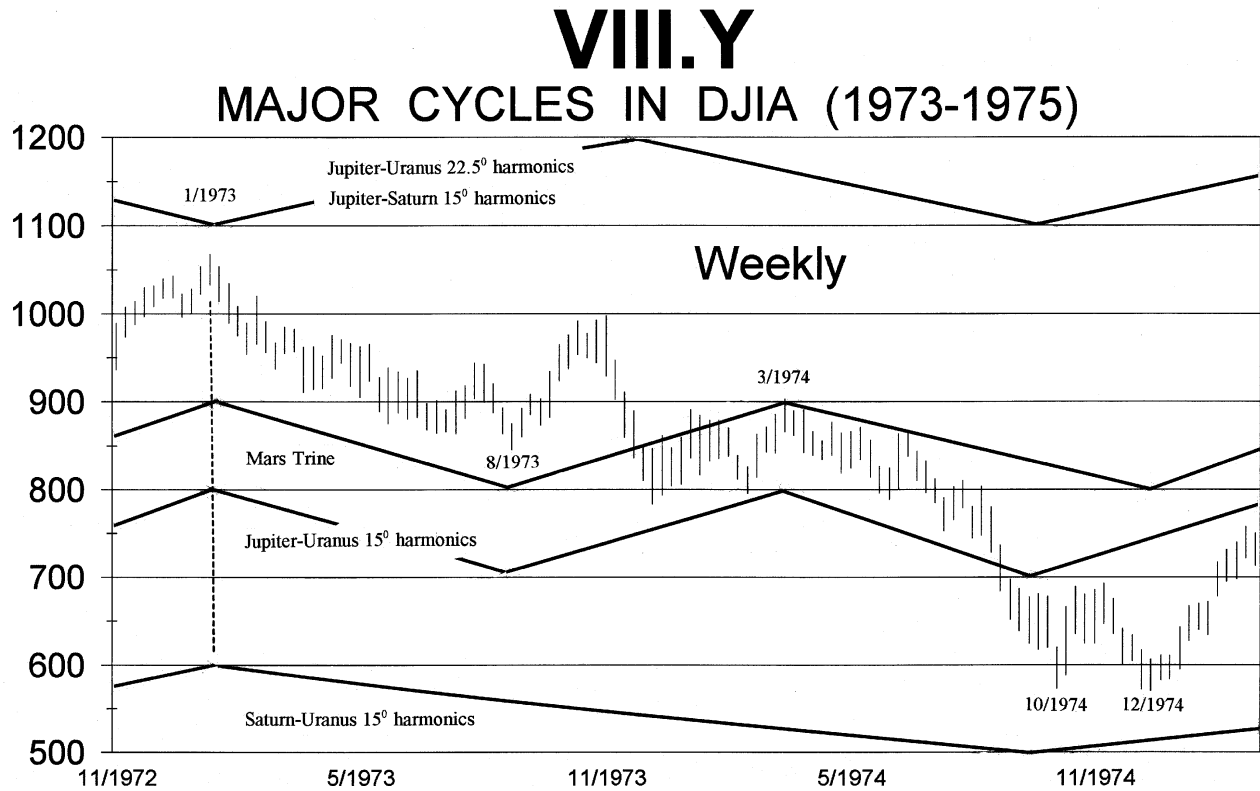
Chart VIII.Y shows the cycles from Figure 8.7 overlaid on the DJIA. The Jupiter-Saturn 15^0 harmonic and the Jupiter-Uranus $22^030'$ harmonic were so closely synchronized that they are shown as the same cycle on this Chart. The axes of these two combined harmonics coincided with the dramatic decline in November, 1973.

The 15^0 Jupiter-Uranus harmonic and its associated Mars trine turned up between August, 1973 and March, 1974. These cycles coincided with the countertrend rally during this time. The two bottoms in October, 1974 and December, 1974 coincided with the Jupiter-Uranus 15^0 harmonic and the Mars trine becoming asynchronous at that time, as shown in Figures 8.7.d and 8.7.e. This was an example of the double bottom formation caused by cycles not arriving at their axes simultaneously.

SUMMARY

This lesson analyzed the correlation between each of the planetary cycles and stock market cycles. Briefly summarized, the topics included:

- A. Stock market cycles resonate sympathetically with the heliocentric motions of the planets.



- B. The sidereal and synodic periods of Uranus, Saturn, Jupiter, Mars, Venus, and Mercury correspond with cycles in the stock market.
- C. The periods of the planets subdivide into harmonics with lengths equal to the periods of faster moving planets. This was summarized in Figures 6.2 and 6.3.
- D. There are axes every fifteen degrees of planetary motion. The magnitude of the correlation of stock market cycles with these axes increases as the harmonic number decreases. That is, there is an increasing order of magnitude as follows:

$$15^{\circ}, 30^{\circ}, 45^{\circ}, 90^{\circ}, \dots \text{ etc.}$$

For example, the 90° axis has a more pronounced correlation with stock market turning points than the 45° axis or the 30° axis.

- E. Uranus 30° axes correspond with the seven-year stock market cycle. This cycle is reinforced if it corresponds with ninety-degree motions of Saturn.

- F. The Uranus quarter-cycle averages twenty-one years and corresponds with an alternating trend of stock market prices.
- G. Saturn 60^0 axes correspond with the five-year stock market cycle.
- H. Saturn has two significant nodal areas located 180^0 apart in Gemini and Sagittarius. These nodes are in the same signs as the Uranus nodes.
- I. The Saturn-Uranus synodic cycle of forty-five-years has axes every 15^0 , averaging 22.5 months, that correspond with changing trends in the stock market.
- J. The Saturn-Uranus synodic cycle defined the 52-month stock market cycle during the 1949-1966 and 1982-1987 squares.
- K. The Saturn-Uranus synodic cycle defined the 42-month stock market cycle during the 1966-1982 square.
- L. One and one-half Saturn-Uranus synodic cycles corresponded with the 67-year interval between similar faces of the two major cubes defined in Lesson V.
- M. The Jupiter-Uranus synodic cycle of fourteen years has axes every 15^0 , averaging 7 months, that correspond with changing trends in the stock market.
- N. The Jupiter-Saturn synodic cycle of twenty years has axes every 15^0 , averaging 10 months, that correspond with changing trends in the stock market.
- O. The $22^030'$ harmonic is most pronounced in either the Jupiter-Saturn cycle or the Jupiter-Uranus cycle, depending upon which of these two cycles moves 45^0 within the larger Saturn-Uranus 15^0 harmonic.
- P. The Mars trine corresponds with the 15^0 Jupiter-Uranus harmonic, and shifts to a new trine when these two cycles become asynchronous. This typically happens when Mars is at the slowest point in its orbit, in Virgo.
- Q. The Mars square (90^0) corresponds with two Mercury cycles and two twelve-week stock market cycles.
- R. The Venus square (90^0) corresponds with the eight-week stock market cycle.
- S. The Mercury cycle corresponds with the twelve-week stock market cycle.

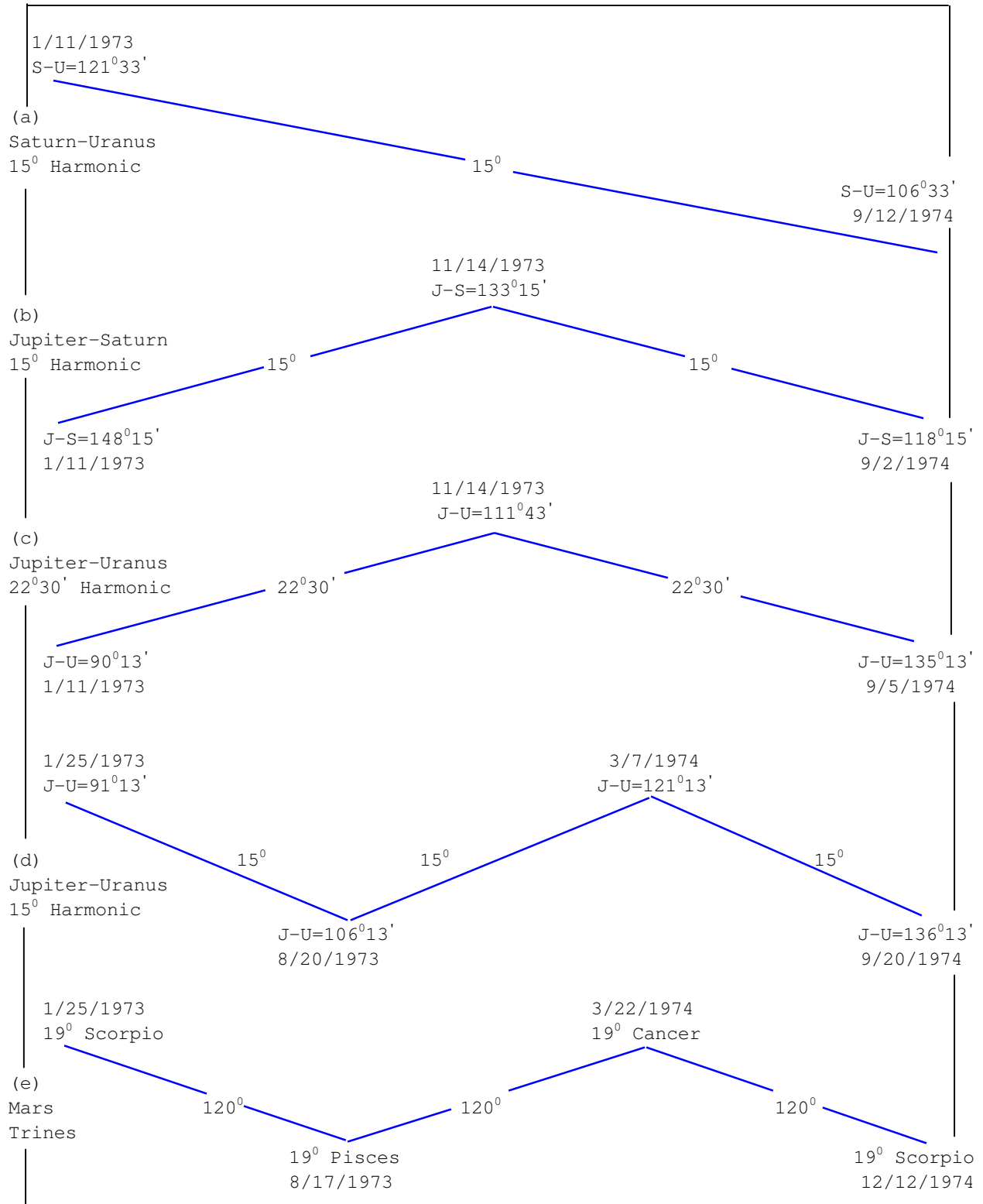


Figure 8.7 TIME
 Locations of the four major planetary harmonics and the active Mars trine
 January 11, 1973 and December 12, 1974

LESSON IX

COMPOSITE CYCLES: PUTTING IT ALL TOGETHER

It is sufficiently agreed that all things change, and that nothing really disappears, but that the sum of matter remains exactly the same.

Francis Bacon (1626 A.D.) ...Cogitationes de Natura Rerum

INTRODUCTION

Previous lessons studied the correlation between cycles in the stock market and motions of the planets across their 15⁰ axes. Each of these cycles and their harmonics exert their own influence on mass human psychology, which can be identified and measured by studying relative price-time changes. The net effect of these individual cycles, known as simple components, is called the "composite wave", and is what is seen on price-time charts.

This lesson will use the planetary cycles and their harmonics, identified in Lesson VIII, **PLANETARY CYCLES**, as simple components to create a composite wave that accurately models stock market price-time behavior. The techniques employed are unique in the fact that they are based upon a determination of dominant planetary harmonics and the boundaries containing these effects based upon the geometry from Part I. Regardless of the time period studied, past or future, the techniques used below to create the composite wave can be used to model price-time. The principles are equally applicable to any time period because the motions of the planets and their corresponding harmonics are not only easily calculated years in the past, but also into the future.

To develop a composite wave from individual simple cycles the technique described in Lesson VII, **CYCLES**, which removed the individual components from existing stock market data, is reversed. This approach differs from those used by contemporary cycle analysts who try to create an accurate composite model by adding together a variety of simple components and expect this **SUM** to model financial market behavior. However, as was demonstrated in Lesson VII, **CYCLES**, this sum only creates the **PERCENT DEVIATION FROM THE TREND**. To arrive at the final model, **THE SUM MUST BE MULTIPLIED BY THE LARGER TREND**.

CONTEMPORARY METHODS FOR CREATING COMPOSITE WAVES

Market analysts have tried for years to create a composite wave that reliably predicts financial market behavior. The most commonly used approach is the simple "sum of sin waves", which uses sin waves as simple components. These "cycles", which are actually rhythms, are shown in Figure 9.1.

The effort to create an accurate model from sin waves is frustrated when the results follow the real-life data for a short period of time then "suddenly" deviate from it. Regardless of the periods of the rhythms used to create the composite wave, only marginal success has ever been attained. The fatal flaw in the approach used by these analysts is a lack of understanding of the nature of the "simple components". That is, they do not know what cycles to add together, and for what period of time these simple components will predictably repeat. The reasons for their problems are:

- (1) **THE DURATION OF THE EFFECT OF A SIMPLE CYCLE IS DEFINED WITHIN THE LIMITS OF THE FACE OF THE UNFOLDING GEOMETRIC STRUCTURE.** This was demonstrated in Lesson VII, **PLANETARY CYCLES**, where the phase and periodicity of the cycles were shown to change when the price-time action moved into a new square, such as when the 1949-1966 square completed.
- (2) Simple components do not follow a constant periodicity. Lesson V, **CYCLES**, showed how the time component of a cycle depends upon the angle the base of the equilateral triangle assumes with the time axis.
- (3) Since cycles are elliptical, their speed is not constant, resulting in varying amounts of time elapsing as the cycles sweep across their 15^0 axes.
- (4) Simple components can overlap, as explained in Lesson II, **THE ELLIPTICAL NATURE OF PRICE-TIME.**
- (5) Simple components do not necessarily begin or end at price lows or highs. This was also explained in Lesson II, **THE ELLIPTICAL NATURE OF PRICE-TIME.**

USING TRIANGLE WAVES AS SIMPLE COMPONENTS

Waveforms other than sin waves are also used to create composites. The most common of these is the simple triangle wave, which will be used in the following discussion for an easy understanding of basic theory.

Figure 9.2 shows two triangle waves with simple cycle A completing six rhythms in the same time interval that B completes just over four. To simplify this analysis the "amplitude", or height, of both waves are the same. Although many analysts actually use this type of model to try to project price-time, the reader should now be aware of the oversimplification of this approach. Previous lessons have proven that price-time rhythms do not follow linear paths, as shown in Figure 9.2. Rather, cycles are elliptical.

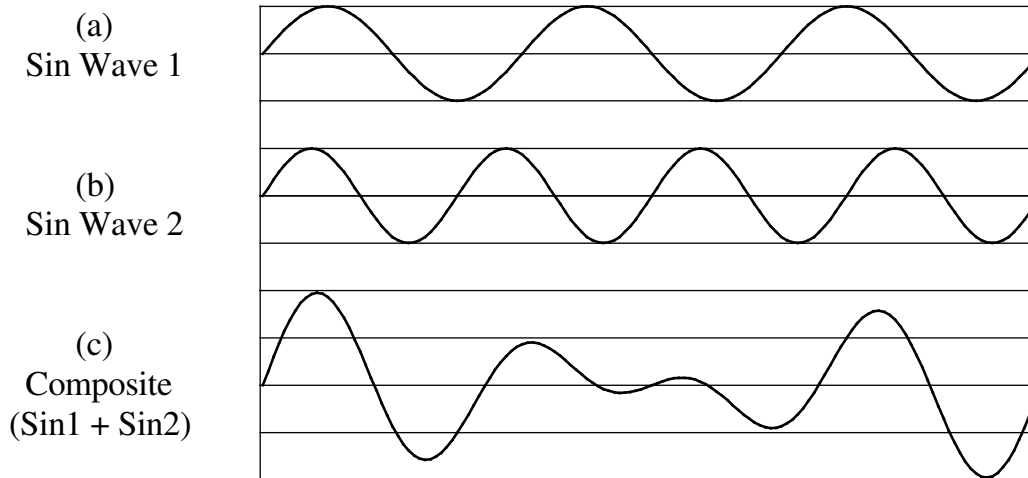


Figure 9.1
"Sum of Sin Waves": The traditional method of creating composites

Figure 9.2.c shows the "composite" wave, i.e., the sum of the two simple cycles. This figure shows areas where the composite has very little net movement and areas where there are large swings. Areas where there are large net swings occur when the simple components "interfere constructively". This happens when the two waves are moving in the same direction at the same time, effectively reinforcing each other.

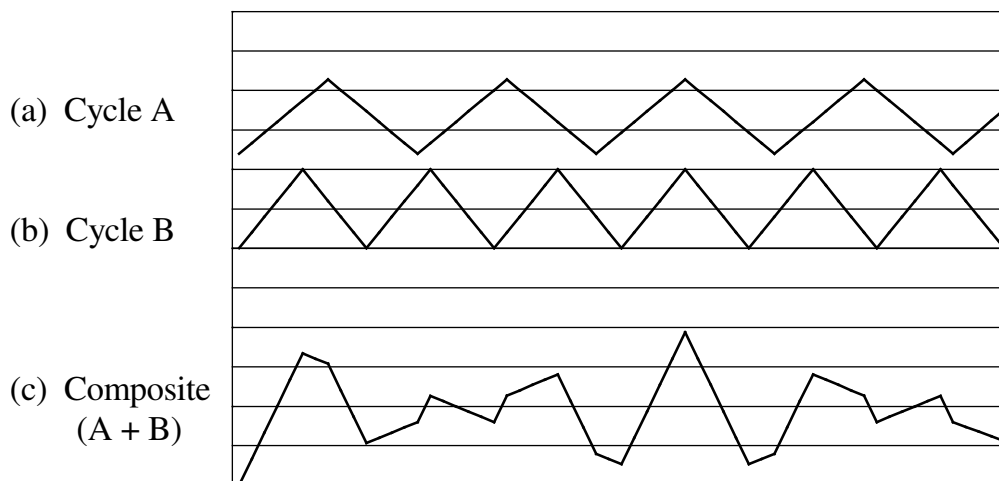


Figure 9.2
Composite of simple triangle waves

STOCK MARKET "BEATS"

Cycles "interfere destructively" when they move in opposite directions, reducing their combined net effect. There are two areas in Figure 9.2.c where the two simple components produce a near zero composite. Areas of little net movement are called "nodes" and have been referred to several times in this course. Musicians recognize nodes as "beats", which occur when sound waves with different frequencies add together to produce a reduced net effect. This is heard as a pulsating rhythm. How often these beats occur is called the "beat frequency", and is determined by subtracting the frequencies of the two simple components. For example, the difference between the two simple waves in Figure 9.2 is two, i.e., six minus four equals two.⁸⁸

Financial market nodes are present on all time scales and occur where the price-time action is described as trendless and "choppy". For example, between February, 1966 and August, 1982 one very large node existed. This coincided with the down phase of the Uranus quarter-cycle, effectively interfering with the net positive growth process. On a smaller time scale, a node existed for six months between March 27, 1986 and September 29, 1986. This node coincided with the Jupiter-Uranus and Jupiter-Saturn cycles turning down within the larger upward trend. These cycles were explained in Lesson VIII, **PLANETARY CYCLES**.

Similarly, data that is recorded by the minute show nodal areas where short-term simple cycles have turned in the opposite direction of the larger trend.

COMPOSITES OF MULTIPLE CYCLES

Figure 9.3 shows four simple triangle waves with periods of 52, 20, 14, and 2 months. All these cycles begin "in phase". That is, they all begin at the same bottom and are increasing. If any of these cycles are shifted out of phase with the others the composite will change.

The sum of the simple waves (the composite) is shown below the four simple waves. The reader should take the time to study how this composite changes form as each simple component reverses direction.

Figure 9.4 shows the same four triangle waves from Figure 9.3 with a 1x1 linear trend added into the composite. Compare this type of model with the 1949-1970 period.

An easy way to study the effects of various simple waves on a composite is with a computer spreadsheet program. These programs add together as many simple cycles as your computer's internal memory will allow. Having this process automated allows experimentation with a variety of combinations in a short period of time.

⁸⁹ Technical Reference: *Fundamentals of Physics – Extended*, P. 437-438.

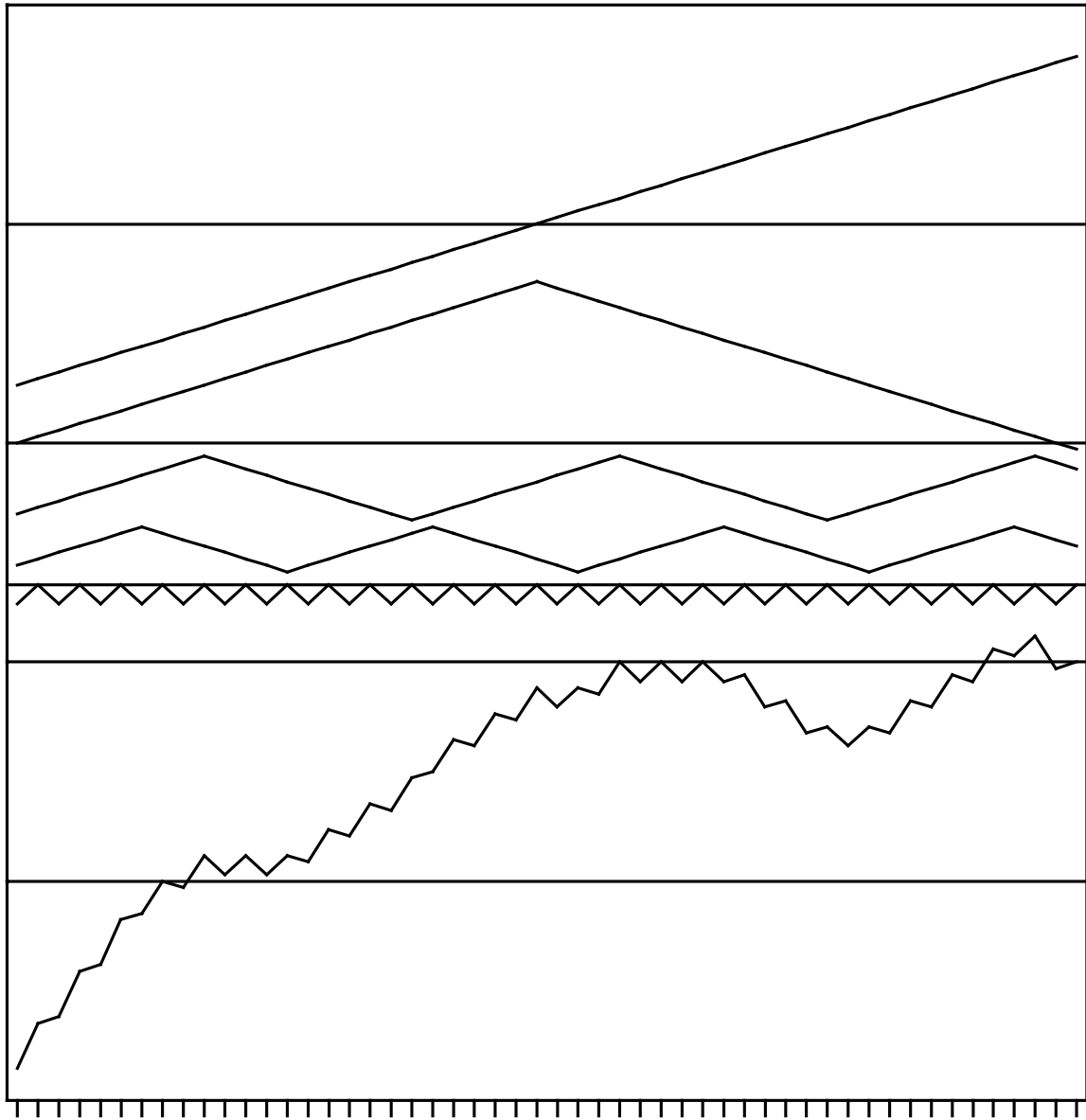


Figure 9.4
Composite waves from Figure 9.3 with 1x1 linear trend added in.

CREATING THE REAL-LIFE COMPOSITE OF THE STOCK MARKET

Lesson V, **CYCLES**, showed how cycles are traditionally isolated in financial markets by analysis of the percent deviation from a moving average. This approach starts with a composite wave, removes the trend by dividing the price-time data into the moving average, then subtracts out each individual cyclic component, i.e., the simple cycles.

To produce a composite wave the methods used in Lesson V are reversed. That is,

- (1) The individual cyclic components are added together producing the percent deviation from the underlying trend.
- (2) The future trend is determined by analysis of the locations of the longest cycles. This trend is a function of the length of the time frame being studied. If a seven-year trend is large enough the motion of Uranus between its 30^0 axes is used. If a trend longer than seven years is needed the 21-year Uranus quarter-cycle is used, and the seven-year cycle becomes another simple component to be added into the composite.

The Saturn five-year cycle is used for the trend if the analysis covers five-years or less the.

- (3) The result of the addition of the simple components in step (1) is multiplied by the trend from step (2).

To demonstrate how closely this method predicts stock market activity, the well-known period from the low on August 11, 1982 until the crash in October, 1987 will be modeled. Lesson III, **GROWTH PATTERNS** identified this period in the DJIA as a completed five-year growth pattern.

The first step in developing an accurate stock market composite is to determine each individual simple component. This step is the most important because after the simple components are determined it is simply a matter of applying mechanical techniques to derive the composite.

Because the speed of the Jupiter-Saturn cycle during this time was such that it moved 45^0 during each of the 15^0 Saturn-Uranus sections, the $22^030'$ Jupiter-Saturn octave was reinforced by the 15^0 Saturn-Uranus octave, and is therefore used as one of the simple components. The method for determining that this harmonic is a significant cycle was explained at the end of Lesson VIII, **PLANETARY CYCLES**.

During this five-year growth pattern the Saturn five-year cycle defined the larger trend of one point per trading day. That is, the linear approximation of the trend followed the 45° angle on the daily chart.

The cycles added together to produce the percent deviation from the trend are:

- (1) 15° heliocentric motions of the Saturn-Uranus cycle.
- (2) 15° heliocentric motions of the Jupiter-Saturn cycle.
- (3) 15° heliocentric motions of the Jupiter-Uranus cycle.
- (4) $22^{\circ}30'$ heliocentric motions of the Jupiter-Saturn cycle.

Figure 9.5 shows the four simple components listed above, including the angle between the planets and the respective date.

The $22^{\circ}30'$ Jupiter-Uranus harmonic is not included in this composite because it was not reinforced by a harmonic of another cycle stronger than the second octave. This contrasts with the 1973-1974 period described in the previous lesson where the $22^{\circ}30'$ Jupiter-Uranus cycle was included and the $22^{\circ}30'$ Jupiter-Saturn harmonic was not. If this explanation does not sound familiar review the last section of Lesson VIII, **PLANETARY CYCLES**, where this technique was explained.

Although the spacing between the axes of the cycles in Figure 9.5 are as defined above in steps (1) - (4), these angles are not on a 15° axis. Each planetary combination experiences the effect of its axes a characteristic number of degrees from the perfect angle.⁸⁹ The deviation from the perfect angle is only fixed within the face of the geometric structure in view. For example, within the 1982-1987 square the Saturn-Uranus axes are located $5^{\circ}30'$ before the perfect angle. On April 26, 1983 the 15° Saturn-Uranus cycle turned down when the angle between them was $35^{\circ}30'$, which was $5^{\circ}30'$ before the perfect angle of $30^{\circ}00'$. Similarly, each of the angles shown in Figure 9.5.a are $5^{\circ}30'$ before the ideal 15° axes. The fact that the effects of a cycle are experienced before the ideal angle is not a problem because;

THE RELATIVE SPACING BETWEEN AXES IDENTIFIES THE TURNING POINTS.

The spacing between the axes of the Saturn-Uranus cycle between April 26, 1983 and August 25, 1987 was $30^{\circ}00'$.

⁹⁰ Astrologers have identified this characteristic and labeled it the "orb of influence", which is the distance before the ideal angle where the effects begin to be experienced. Because many readers already understood this term it will be used in this lesson.

To create the composite wave the angles between the Jupiter-Saturn and Jupiter-Uranus cycles will be measured to the degree, rather than to the minute, making it easier for the reader to verify data. Since these two cycles are relatively fast moving, the error introduced by only measuring to the degree will be less than one week. Because the Saturn-Uranus cycle moves much slower than the others, its data will be measured to the half-degree. The angles used for each simple component are as follows:

- (1) Saturn-Uranus $5^{\circ}30'$ before the 15° axes
- (2) Jupiter-Saturn $2^{\circ}00'$ before the 15° axes
- (3) Jupiter-Uranus $2^{\circ}00'$ before the 15° axes

Notice, the faster moving cycles experience their effects much closer to the perfect 15° axes than do the slower moving cycles.

If greater resolution is desired, the angles measured to the minute where the cycles actually turned are listed below:

- (1) Saturn-Uranus $5^{\circ}27'$ before the axes
- (2) Jupiter-Saturn $2^{\circ}10'$ before the axes
- (3) Jupiter-Uranus $1^{\circ}30'$ before the axes

When the four simple cycles shown in Figure 9.5 are added together the composite shown in Figure 9.6.a is created. This composite establishes the percent deviation from the underlying trend, as explained in Lesson V, **CYCLES**.

Figure 9.6.b shows the trend during this five-year growth period. This trend advanced at the rate of one point per trading day (45° angle on the daily chart) within the confines of the 60° movement of Saturn, i.e., 21° Libra to 21° Sagittarius. When this 60° distance had been spanned the five-year growth pattern was complete.

When the sum from Figure 9.6.a is multiplied by the trend shown in Figure 9.6.b, the resultant product is the model for the stock market during this time period. This product is shown on Chart IX.A. Graphed below the model is the actual DJIA during this same time period. The differences between the model and the actual data were caused by reasons previously described. If the simple cycles are modified to take into account the items listed below, the result will be a more accurate stock market model.

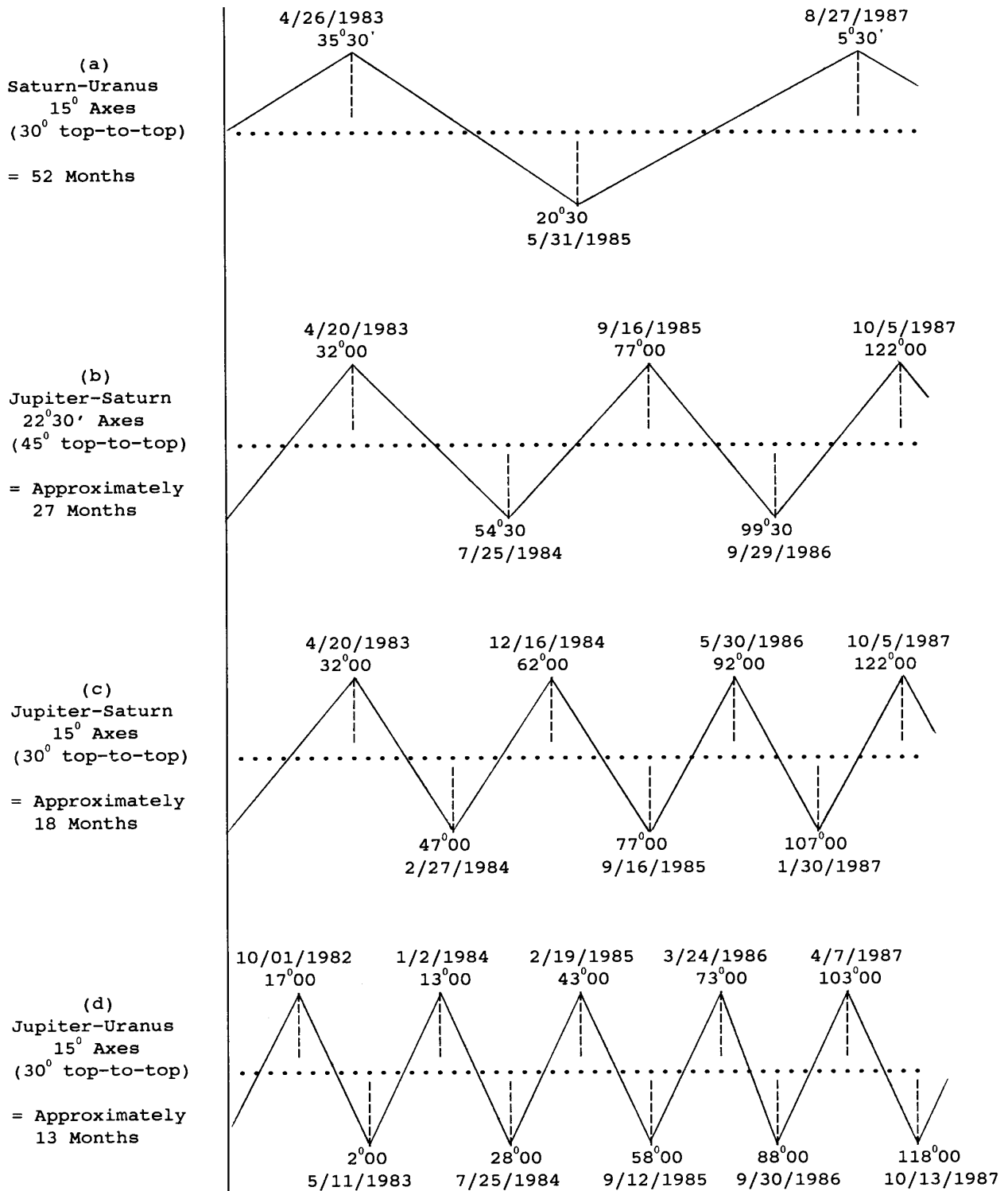
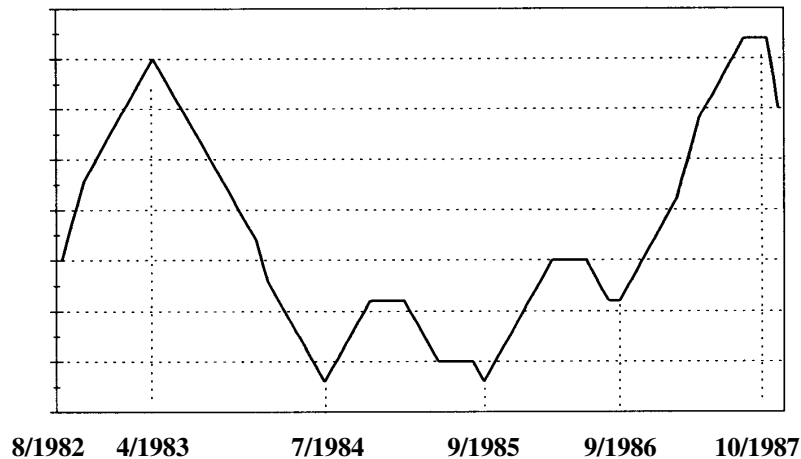


Figure 9.5

Planetary cycles defining the simple components of the DJIA composite wave from 8/1982 to 12/1987 (See Chart IX.A)

(a)
Composite of planetary cycles between 1982-1987
defining the percent deviation from the underlying trend



(b)
Underlying trend of one point per trading day
defined by 60° movement of Saturn (6/1982-10/1987)

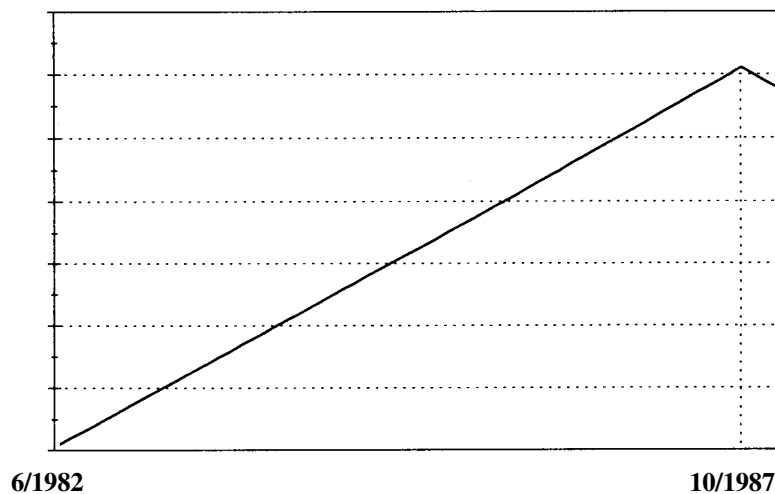
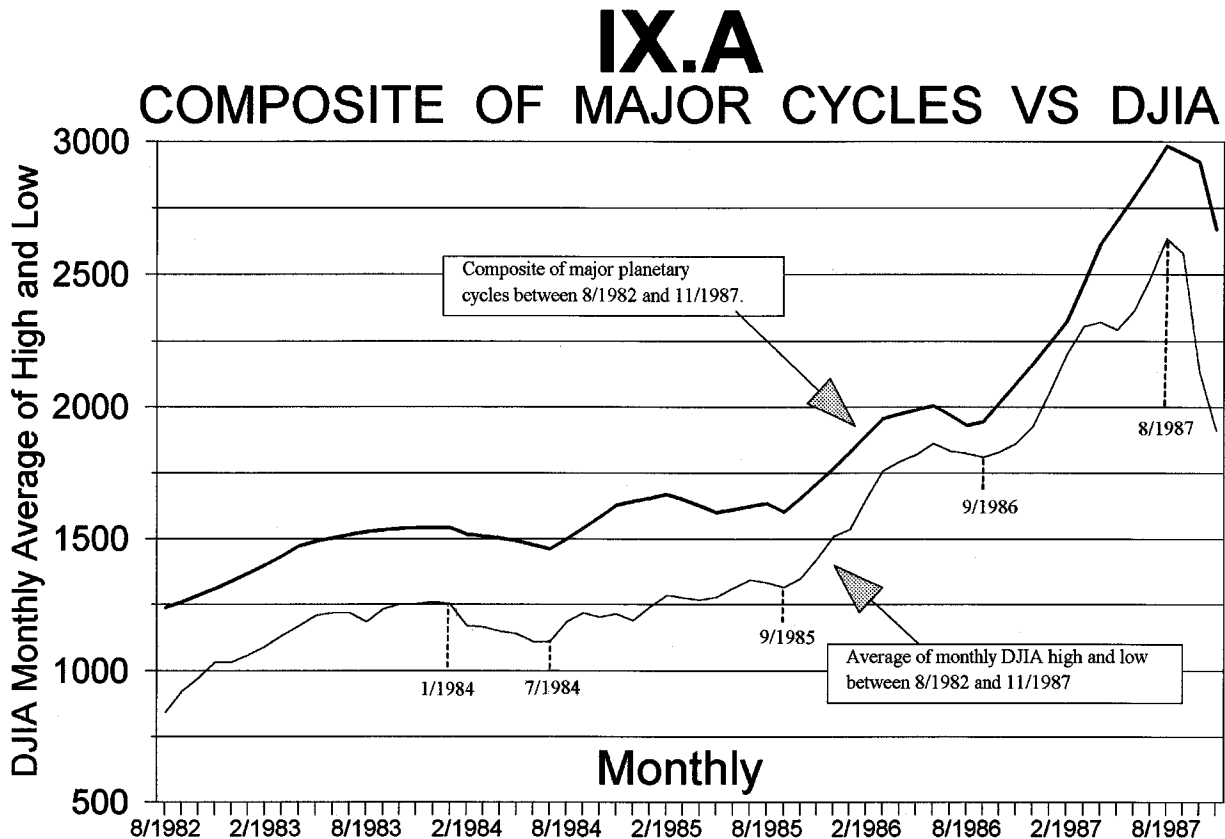


Figure 9.6

(a) Composite (sum) of the individual planetary cycles shown in Figure 9.5

(b) Linear trend of one point per trading day (1982-1987)

- (1) The minor deviation that occurred in November, 1985 was at the terminal point of the ellipse shown on Chart II.D.
- (2) The smaller cycles, such as the Mars cycle, were not included in the composite.
- (3) Triangle waves were used, rather than the actual elliptical construct, so the general technique could be easily understood.
- (4) The orb of influence is measured to the degree, rather than to the minute.



CHANGING ORBS OF INFLUENCE

As with many other problems in financial market analysis, the changing "orb of influence" is explained by market geometry. The orbs of influence listed in the preceding section are only in effect while the face of the cube under construction is in view. When the cube rotates to expose a new face the orb of influence changes to the value characteristic to that face. That is,

**THE DISTANCE BETWEEN THE IDEAL ANGLE AND WHERE
THE CYCLIC EFFECTS ACTUALLY OCCUR CHANGES WHEN
THE FACE OF THE GEOMETRIC STRUCTURE CHANGES.**

Financial market analysts who have tried in the past to show a correlation between planetary cycles and financial market behavior have erred in setting a fixed orb of influence, which they have assumed does not change. This distance must be adjusted when the geometric structure rotates and exposes a new face.

After the new face has rotated into view, determining the new orb of influence is a simple matter of observation. What is known as an orb of influence is simply the alignment of cycles within the newly exposed geometric face. This concept was demonstrated in Lesson VIII, **PLANETARY CYCLES**, where stock market cycles were shown to synchronize with the angles between the planets when the new face of the cube began. For example, it has already been shown that during the 1949-1966 square the fifty-two month cycle was synchronized with 30^0 motions of the Saturn-Uranus cycle. This square began in

1949 when the Saturn-Uranus cycle was at 66° . The 66° angle was 6° **AFTER** the perfect angle of 60° . This 6° orb of influence was in effect during the entire 1949-1966 square. During this time each of the axes occurred 6° **AFTER** the ideal angle, i.e.,

66° in 6/1949	(6° after the axis)
96° in 6/1953	(6° after the axis)
126° in 10/1957	(6° after the axis)
156° in 6/1962	(6° after the axis)
173° in 10/1966	(7° after the axis)

Chart VIII.G shows the fifty-two month cycle in the DJIA during this time and the corresponding locations of the Saturn-Uranus cycle.

LESSON X

DIMENSIONAL ASPECTS OF TIME

And swear by him that liveth for ever and ever, who created heaven, and the things that therein are, and the earth, and the things that therein are, and the sea, and the things that are therein, that there should be time no longer.

... Revelation 10:6

INTRODUCTION

The objective of this course has been to increase awareness of the multi-dimensional reality in which man exists, while at the same time providing practical applications in the form of financial market timing.

Time has been the common theme underlying each of the preceding lessons. This lesson will provide a clearer perspective of this elusive concept, allowing the analyst to better understand what is truly happening in the world around him.

To study the periodic recurrence of mass human behavior, this course used price-time charts of the stock market, not only because of the availability of recorded historical data, but also because of the generally inquisitive nature of financial market analysts. The reader should now realize that applications of the concepts presented in this course extend well beyond financial markets.

Lesson V, **GEOMETRIC STRUCTURES**, demonstrated the progressive evolution of geometric structures as price-time unfolds. To understand the four-dimensional structures that are unfolded onto two-dimensional price-time charts, it must be seen how man, as a three-dimensional being, perceives two-dimensional and one-dimensional objects. The perspective gained by these exercises can then be used to understand that what man is experiencing at any given time is simply a piece of a continuum contained in a higher dimension.

Volumes of material can be written on the subject presented in this lesson. However, the focus will only be on that which clarifies the nature of four-dimensional stock market structures.

BACKGROUND REVIEW

The three dimensions can be represented as shown in Figure 10.1. Each of these figures represents the previous figure set into motion. For example, if the line in Figure 10.1.a is placed into motion it sweeps out the two-dimensional plane shown in Figure 10.1.b. Similarly, if the plane in Figure 10.1.b is placed into motion the three-dimensional cube in Figure 10.1.c is defined. These three figures effectively establish the relationship between motion and changing dimension. That is, as a geometric form in one dimension

is placed into motion it defines another geometric form in a higher dimension. The importance of this relationship will be seen in this lesson as the four-dimensional geometric structures that are unfolding in financial markets are modeled as three-dimensional structures in motion relative to man's perception.

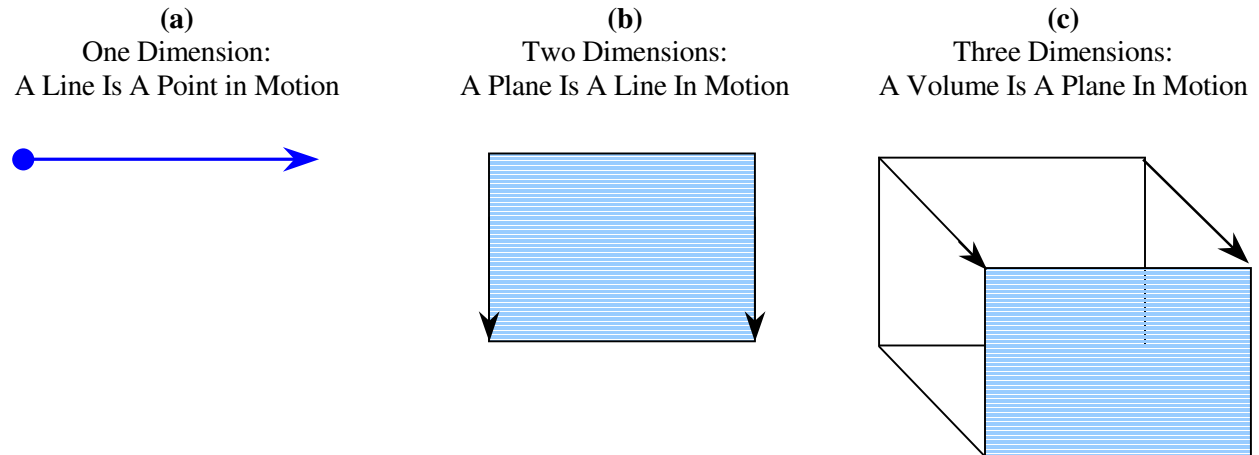


Figure 10.1

Relationship between motion and dimension

TIME IS MOTION IN A HIGHER DIMENSION

The traditional technique used by philosophers and conceptual scientists, such as Albert Einstein, to understand the relationship between a higher dimension and man's three-dimensional perception is to create analogies with one and two dimensions. When various spatial relationships are established from one dimension to two, and from two dimensions to three, the extrapolation is made from three dimensions to the higher fourth dimension.⁹⁰

By studying the perception of motion and time in lower dimensions we are able to recognize the "cause-effect" relationship between events happening in our world and motion of a higher dimension. To demonstrate this concept an analogy using the perceptual awareness of a two-dimensional being will be studied.

Figure 10.2 shows a two-dimensional plane where some hypothetical being lives. Passing through this two-dimensional world is a rotating wheel divided into six equal parts, each with a different color.

⁹¹ Reference: *Tertium Organum*.

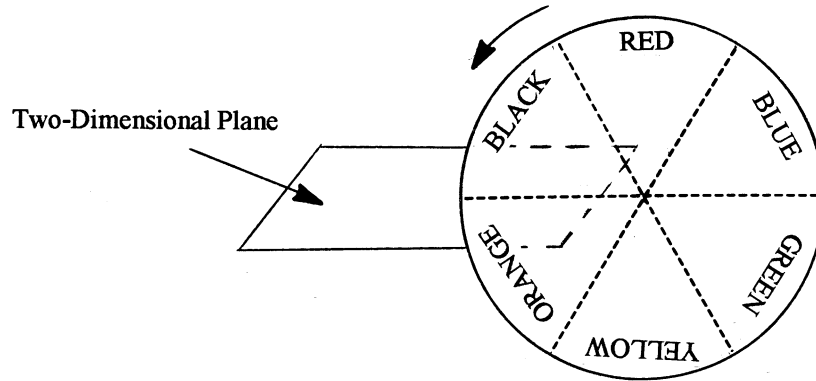


Figure 10.2

Motion of a three-dimensional color wheel through a two-dimensional plane

This two-dimensional being is only aware of an existence on his plane. He is unaware of the rotating wheel because everything above or below the plane is unknown to him. However, the rotating wheel creates a change in the two-dimensional world as it passes through. This change will be perceived as a sequence of repeating colors. The two-dimensional plane will turn black, then red, blue, green, yellow, orange, and back to black, as the sequence repeats itself. Our two-dimensional being will notice this repeating sequence and will be able to predict into the future exactly when any color is due to appear. He will most likely make a simple mathematical model predicting the change, and since this model is verified by observation in nature, it will have passed the scientific method and can be called a "Law of Nature".

If this sequence of repeating colors were recorded on a two-dimensional chart, it would appear as in Figure 10.3.

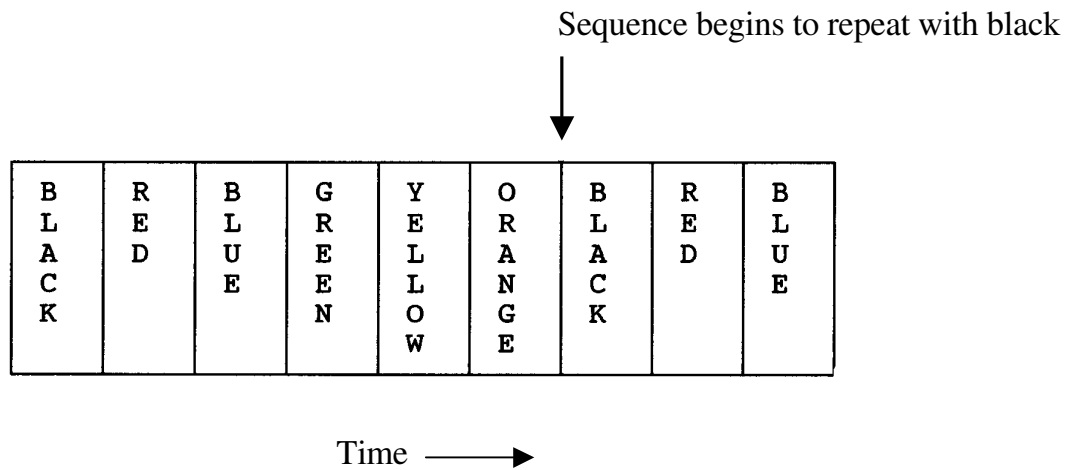


Figure 10.3

Two-dimensional time chart of three-dimensional rotating color wheel

In other words, what we as three-dimensional beings know as **MOTION** of a rotating wheel is perceived by the two-dimensional being as a repeating sequence of colors changing with **TIME**. The two blacks in Figure 10.3 are actually the same section of the color wheel. If this two-dimensional being were clever enough to wrap this chart around, so the same colors overlapped, he would see the actual construct of the wheel.

SIMILARLY, WHAT MAN AS A THREE-DIMENSIONAL BEING SEES IN TWO-DIMENSIONAL FINANCIAL MARKET CHARTS AS PRICES CHANGING AS A FUNCTION OF TIME IS ACTUALLY THE MOTION OF A FOUR-DIMENSIONAL LATTICE ROTATING THROUGH HIS THREE-DIMENSIONAL PERCEPTION.

FOUR-DIMENSIONAL PRICE-TIME

Figure 5.10 showed that when equilateral triangle CDF was rotated the true structure of a tetrahedron was revealed. Similarly, rotating triangle IJK revealed another tetrahedron. This exercise was the same as performed above, where the end point of the color sequence was wrapped back around to the beginning point, effectively revealing the true structure of the wheel. Rather than a three-dimensional wheel rotating through a two-dimensional plane, a four-dimensional tetrahedral lattice rotated through man's three-dimensional perception. In addition, as these tetrahedra unfolded they were sequentially recorded on a two-dimensional price-time chart. The limitation of two-dimensional price-time charts explains why the paper had to be mentally folded to reveal the true three-dimensional structure of the tetrahedra.

Lesson V identified the tetrahedron as one of the "cube centered" structures, i.e., it can be placed symmetrically within a cube. This cubic structure was located on a chart of the DJIA for a period extending 100 years into the past.

Therefore, if a cube is used as the four-dimensional structure rotating through man's three-dimensional perception, the model in Figure 10.4 can be used to understand its effect.

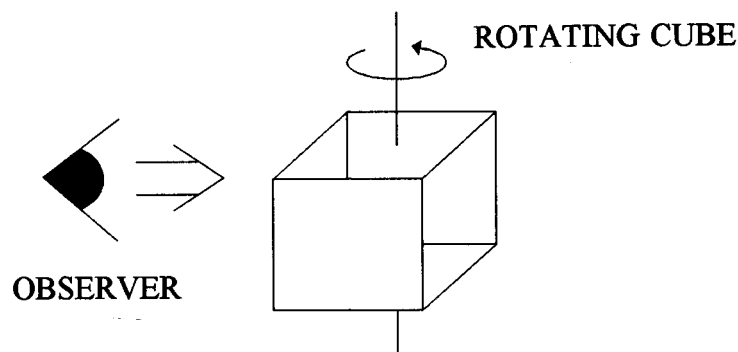


Figure 10.4

Three-dimensional cube rotating through the perception of a two-dimensional observer

TIME CONTINUUM

At any single moment in time man is experiencing a condition that is the net sum of all individual forces acting upon him. Any point in time is a small part of a larger continuum, whose structure and existence extends in a smooth and unbroken manner beyond the three-dimensional perception of man.

Most things in the universe are well beyond man's understanding. His existence and perception is truly minuscule when viewed from the extraordinary complexity and order in the universe. The experiences of *deja vu* everyone has experienced may actually be locations in three-dimensional perception where a common point in four-dimensional space-time has occurred. For example, Chart I.A revealed points B and D to be a single common point at the apex of a four-dimensional tetrahedron. However, in our three-dimensional world they were perceived as occurring thirty-two days apart. In other words, **WHEN POINT D OCCURRED IT HAD ALREADY OCCURRED THIRTY-TWO DAYS EARLIER AT POINT B.**

At any given time, a point on a price-time chart represents the net result of all optimism and pessimism pushing and pulling prices up or down. When two of these points occur simultaneously in four-dimensions, as with points B and D, they represent an identical net condition of optimism and pessimism in the human condition, and nowhere is the human condition better represented and recorded than in financial markets.

In this course, stock market charts have been provided as **PROOF OF THE CONTINUUM CALLED TIME.** Manifestation of this continuum in man's perception is a function of the specific method of observation. If historical stock market charts are used, the structures outlined in this course will be revealed. However, if charts of a different financial market are studied different forms may be seen. This is because each element in nature has its own characteristic resonant frequency and lattice structure. Similarly, each financial market responds in its own characteristic way to the common stimulus of the time continuum.

APPENDIX A

CRASH OF 1987 ANALYSIS OF RETRACEMENT RATIO

Many market analysts have incorrectly identified the crash of 1987 as a PHI (1.62) retracement of the advance from 1982 to 1987. This is an example of the limitation of one-dimensional analysis. In this case, the analysts are using the single dimension of price to calculate the retracement. Even if closing values are chosen for the data an unacceptable error is produced.

Using closing values, the advance from 8/12/1982 to 8/25/1987 was:

$$2722 - 777 = 1945 \text{ points}$$

To calculate the projected PHI retracement, analysts multiply this advance by 0.618:

$$\text{Projected retracement} = 1945 \times 0.618 = 1202 \text{ points}$$

They then subtract this projected retracement from the high on 8/25/1987 to arrive at their projected low:

$$\begin{aligned} \text{Projected low} &= \text{high in 1987} - \text{projected retracement} \\ &= 2722 - 1202 = 1520 \end{aligned}$$

Even if the intraday low on 10/20/1987 (1616) is used as the actual low, the projected retracement missed this value by 100 points.

The PTV is used as a means of comparing the results obtained by Fibonacci analysts, with those obtained by applying the methods in this course.

As calculated in Table 4.1, the PTV from 8/9/1982 to 8/25/1987 was 1994. Therefore, a perfect 50% retracement would be:

$$\text{Projected retracement} = 1994 / 2 = 997$$

Table 4.1 calculated the actual retracement to be 1013. Therefore, the error between the projected value and the actual retracement is calculated as follows:

$$\frac{1013 - 997}{997} = \frac{16}{997} = 1.6\%$$

APPENDIX B

EQUATIONS USED FOR DETRENDING THE MONTHLY STOCK MARKET DATA SINCE 1790 (See Charts VIII.A and VIII.B)

The equation used for detrending the data is that for exponential growth⁹¹, i.e.,

$$q = q_0 e^{kt} \quad \text{where,} \quad k = \frac{1}{t_2 - t_1} \ln\left(\frac{q_2}{q_1}\right)$$

$$\text{and,} \quad q_0 = q_1 \left(\frac{q_1}{q_2}\right)^{\frac{t_1}{t_2 - t_1}}$$

For the exponential trend between 1914 and 1992 the following data was used in the above equations:

$$\begin{aligned} t_0 &= 12/1914 \\ t_1 &= 10/1987 = 874 \text{ months} \quad ; \quad q_1 = 2662 \\ t_2 &= 2/1992 = 926 \text{ months} \quad ; \quad q_2 = 3313 \end{aligned}$$

Therefore, the equation defining the trend between 1914 and 1992 is:

$$q = 67.332 \times e^{.004207 t}$$

This equation was divided into the monthly data to arrive at the detrended Chart VIII.B.

The same technique was applied to the 1790-1914 period to arrive at the trend equation:

$$q = 5.378 \times e^{.001672 t}$$

This equation was divided into the monthly data to arrive at the detrended Chart VIII.A.

⁹² Technical Reference: *Calculus for Scientists and Engineers*, P. 453-456. Many biology texts also address the natural growth equation when calculating the amount of bacterial present in a culture at any given time.

APPENDIX C

W.D. GANN'S ANNUAL FORECASTS

W.D. Gann made available to the public annual forecasts for a variety of financial markets including stocks and grains. His forecasts for the stock market were well known for their accuracy, and sold for \$100 during the great depression in the 1930's.

Gann shrouded the basis of his forecasts in great secrecy, primarily because of their simplicity. If the public knew how these forecasts were made they would not have to pay the high prices for them. This brief writing will identify the basic principle behind W.D. Gann's annual forecasts. Although there are other considerations that must be taken into account to fine-tune the forecast, there is a single basic foundation to the approach.

In the introduction to his 1919 stock market forecast Gann stated, "History repeats itself in the stock market as well as in the lives of men." He also said that he based his annual forecasts on, "... a time factor which I discovered", and that this time factor was the basis for his "Master Time Factor".

Simply stated, Gann went back ten and twenty years in the financial market he was forecasting and used the dates of turning points in those years for his forecast.

The astrological correlations with this time period are successive conjunctions and oppositions of the Jupiter-Saturn cycle, which occur every ten years.

A copy of Gann's "*Forecast of the Stock Market for 1922*" is included in Figure C.1. Below his forecast are one-year graphs of the stock market in 1912 and 1902, which were ten and twenty years before the year Gann was forecasting.

For all the mystery and price associated with these forecasts and the "Master Time Factor", it certainly was a simple concept.

Forecast of the Stock Market for 1922

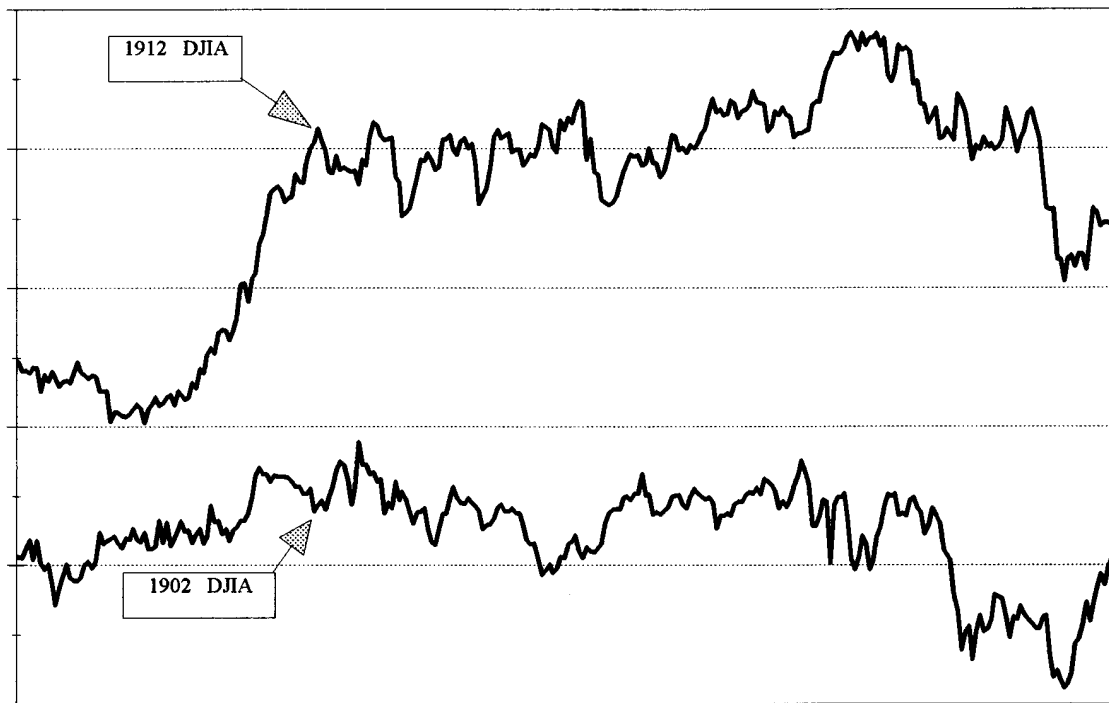
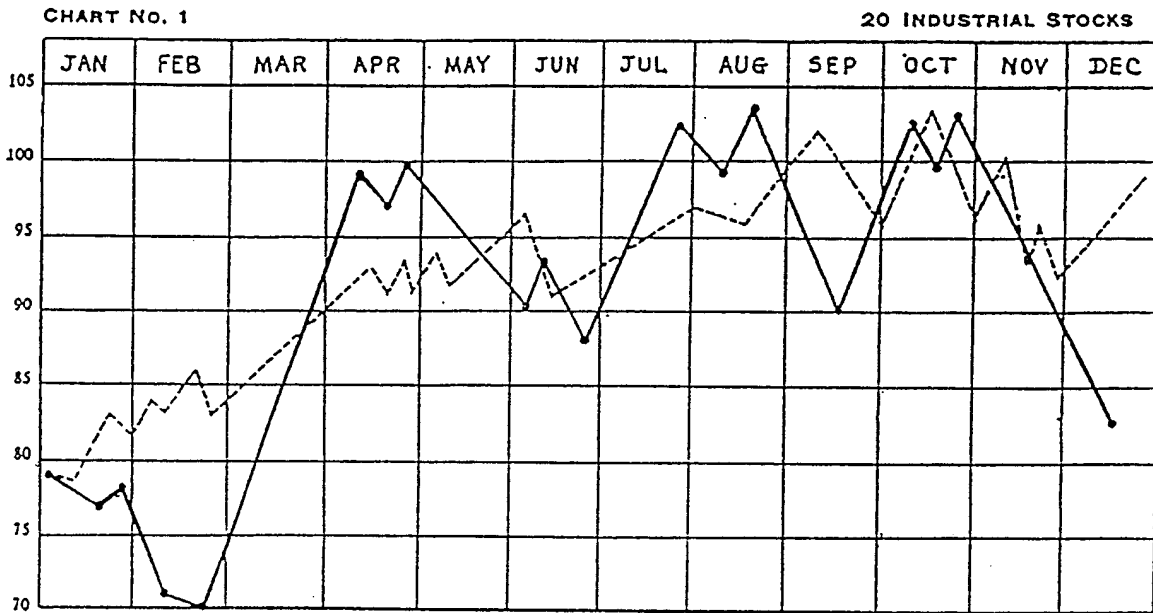


Figure C.1

W.D. Gann's annual stock market forecast for 1922 (top graph); and the stock market ten years earlier in 1912, and twenty years earlier in 1902 (bottom graphs).

APPENDIX D

TWENTY-YEAR PRESIDENTIAL CYCLE

The twenty-year presidential cycle is well known among astrologers. Basically, the president taking office in the year of the Jupiter-Saturn conjunction has died in office. Since these conjunctions occur at regular twenty-year intervals, this cycle recurs accordingly. Recurrences of this cycle have been:

William Harrison	took office in 1841
Abraham Lincoln	took office in 1861
James A. Garfield	took office in 1881
William McKinley	took office in 1901
Warren Harding	took office in 1921
Franklin Roosevelt	took office in 1941
John Kennedy	took office in 1961

The president does not necessarily die in the term of the twenty-year cycle in which he was elected. For example, Abraham Lincoln was killed in 1865, shortly after being reelected to his second term. The Jupiter-Saturn conjunction occurred in his first term.

Nor, does this conjunction necessarily coincide with his first term in office. McKinley was reelected to his second term in 1900, placing him in office during the 1901 conjunction.

William Harrison died April 4, 1841 after one month in office. To show how tough he was, he delivered his inauguration address in a cold rain without a coat. He died one month later from pneumonia.

Abraham Lincoln was assassinated April 15, 1865, officially by John Wilkes Booth. Lincoln was the president in office during the 1861-1865 term when the conjunction occurred.

James A. Garfield died September 19, 1881 eighty days after being shot on July 2, 1881 by Charles J. Guiteau.

William McKinley died September 14, 1901 one week after being shot by Leon Czolgojz.

Warren Harding died August 2, 1923 of thrombosis in the third year of his term.

Franklin D. Roosevelt died April 12, 1945 of heart failure.

John F. Kennedy was assassinated November 22, 1963, officially by Lee Harvey Oswald.

Astronomically, these twenty-year time periods coincide with Jupiter-Saturn conjunctions. Figure D.1 shows the locations and dates of the Jupiter-Saturn conjunctions between 1841 and 1961.

Figure D.1 shows the trine formed by successive conjunctions of Jupiter and Saturn. This configuration is known as a "triplicity", and results because every sixty years the third conjunction of Jupiter and Saturn takes place at approximately the same location relative to the fixed stars.

Every third conjunction of Jupiter and Saturn does not take place at EXACTLY the same location in the sky. Rather, this point migrates, on average, nine degrees. This fact can be seen in Figure D.1 where the sixty year intervals define the complete circle of 360° plus nine degrees.

For example, the conjunctions that occurred in Capricorn took place at 7° in 1841, then 16° in 1901, and finally 24° in 1961. Each of these points are located nine degrees apart.

This nine degree migration of the location of the conjunctions resulted in the Jupiter-Saturn conjunction moving into a new triplicity with the 1981 conjunction, at 7° Libra. Similarly, 1841 was the first year this conjunction occurred within this triplicity, and the first year of this presidential jinx.

The change in triplicity in 1981 coincided with the presidential cycle being broken with the election of Ronald Reagan. Although he was shot in office, he did not die.

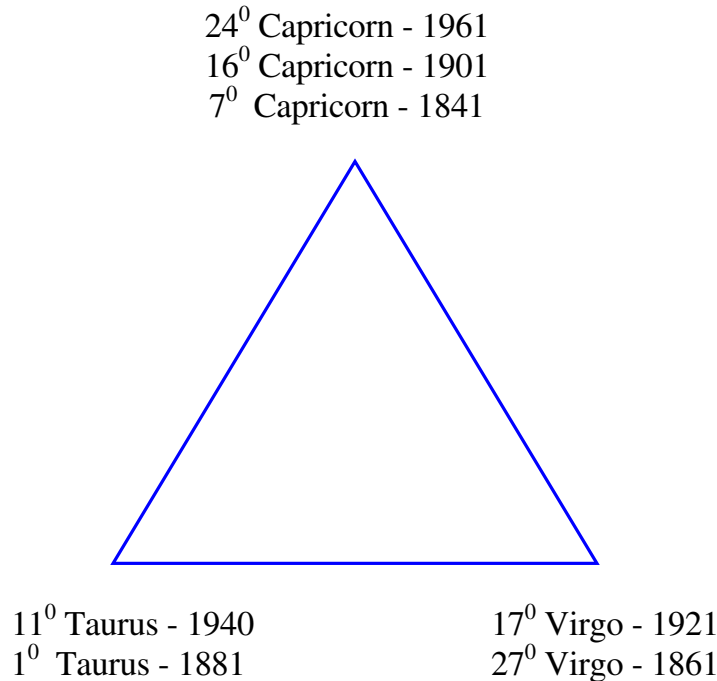


Figure D.1

Locations of the Jupiter-Saturn conjunctions between 1841 and 1961 defining the triplicity

APPENDIX E

FORMAT OF DATA AND TABLES USED IN THIS COURSE

FORMAT OF STOCK MARKET DATA

The price values used in calculations in this course are intraday high and low Dow Jones Industrial Averages. The time values are when the hourly highs and lows occurred, as recorded in the Wall Street Journal. Using intraday values instead of hourly readings allows greater accuracy, since large price swings can occur between two hourly readings. This method will introduce a certain amount of error. However, the availability of long-term historical data in the intraday format makes this approach the most accurate for the given data.

Also, since the Dow Jones Industrial Averages is a non-homogeneous index composed of a variety of stocks, each vibrating at its own characteristic frequency, this index does not produce as accurate results as would be achieved using a single stock or commodity. However, once again, the availability of long-term historical data (or lack of) is a consideration here. This approach makes more sense as vibration rates lasting for several decades and extending back in time into the eighteenth century are studied.

FORMAT OF TABLES USED IN THIS COURSE

Tables are used extensively throughout this course to display all data used in calculations. This allows the skeptical reader to independently verify conclusions.

Almost all the tables in Part I contain data used to calculate PTVs. The format of all these tables is the same. Each row contains the data for one PTV. The eight columns contain the data used for the calculation of each of the PTVs, and are structured as follows:

- First column - "Price-Time radius vector" lists the letters identifying the PTV from the chart identified in the table header.
- Second column - "Date & Time of High" gives the date and time of day the highest price was reached. This may be the beginning or the end point of the PTV, depending upon whether the PTV was descending or ascending, respectively.
- Third column - "Price High" gives the value of the highest price reached by the PTV. This value is reached on the date listed in the second column of the table. If the PTV is measured between two bottoms the value in the third column will be the **INTRADAY LOW** on the date listed in the second column.

For all other situations the value in this column will be the **INTRADAY HIGH** on the date listed in the second column.

An example where the high value for the PTV is an intraday low is seen on Chart I.A with PTV CF. Point F is the high point for the PTV. However, since point F is a bottom, the price high used to calculate CF is the intraday low on the date at point F.

- Fourth column - "Date & Time of Low" gives the date and time of day the lowest price was reached. This may be the beginning or the end point of the PTV, depending upon whether the PTV was ascending or descending, respectively.
- Fifth column - "Intraday Low" gives the value of the PTV price low reached on the date listed in the fourth column. If the PTV is measured between two tops the value in this column will be the **INTRADAY HIGH** on the date listed in the fourth column. For all other situations the value in this column will be the **INTRADAY LOW** on the date listed in the fourth column.
- Sixth column - "Time Change (in hours)" gives the total trading hours that elapsed between the date of the high and low, as listed in the second and fourth columns.
- Seventh column - "Price Change (points)" gives the total change in price that occurred between the high and low, i.e., the value listed in the third column minus the value listed in the fifth column.
- Eighth Column - "Vector Value (PTV)" uses the values from column six and column seven to calculate the PTV, as described in Figure 1.1.

The tables in Part II have a variety of formats. When planetary cycles are being studied the first column lists the beginning and ending dates of the related stock market cycle. The second and third columns list the heliocentric locations of the associated planet on the dates listed in the first column. The final column subtracts the second and third column, giving the total distance traveled by the planet between the dates listed in the first column.

APPENDIX F

URANUS CYCLE AND THE PERIODICITY OF AMERICAN WAR

Volumes of material can be written on the subject of the periodicity of war. However, because of limited space this writing will only serve as a general introduction to the subject. The focus will be on the correlation between the Uranus quarter-cycle and American war.

Gemini is the "ruling sign" of the United States, as defined by the locations of the planets at its birth. Also, Uranus is known as the "revolutionary planet", causing disruption and war. This discussion will show that the Uranus quarter-cycle of 21 years corresponds with war in this country.

The three most significant wars in American history in terms of affecting the form of government and the relative number of lives lost have been:

- (1) The Revolutionary War officially began with the signing of the Declaration of Independence on July 4, 1776. This date defined the birth of the United States.
- (2) The Civil War officially began on April 12, 1861 with the firing on Fort Sumter. This date was one Uranus cycle (84 years 9 months) after the signing of the Declaration of Independence in 1776.
- (3) World War II ended in Europe on April 30, 1945 when Adolf Hitler committed suicide. This date was one Uranus cycle (84 years) after the start of the Civil War in 1861 and two Uranus cycles after the signing of the Declaration of Independence in 1776.

The three major wars listed above coincided with Uranus returning to the same location in the heavens.

Figure F.1 shows the location of Uranus during each of the major wars in the United States. Since the birth of the United States in 1776, Uranus has entered Gemini three times. These dates are shown on the bottom of Figure F.1. When the Declaration of Independence was signed in 1776 Uranus was at 10^0 Gemini. At the beginning of the Civil War in 1861 Uranus was at 11^0 Gemini. Similarly, the end of World War II in 1945 coincided with Uranus arriving at 12^0 Gemini. Notice that this area in the Uranus cycle was also identified in Lesson VIII as stock market nodal points, shown on Charts VIII.A and VIII.B.

Uranus will again return to this location in the year 2029, which also coincides with the 45-year Saturn-Uranus cycle returning to its same location as at the stock market nodal point in 1982.

On the opposite side of the circle from Gemini is Sagittarius, which is shown at the top of Figure F.1. This area coincided with the "minor" wars of:

- (1) The War of 1812 ended on December 24, 1814 when Uranus was at 3^0 Sagittarius.
- (2) The Spanish-American War ended on December 10, 1898 with the signing of the Treaty of Paris. On this date Uranus was at 4^0 Sagittarius.

These two opposing locations in Gemini and Sagittarius are the points where Uranus reaches zero degrees latitude. They have coincided with every major American war except two:

- (1) World War I ended on November 9, 1918.⁹²
- (2) US involvement in the Vietnam War began in December, 1962 when Kennedy authorized the military "advisors", which he sent there, to "return fire if fired upon", and increased their numbers to 11,000.

The locations of Uranus during both these wars were 90^0 from the previously listed major wars.

Compare the dates of the seven wars shown in Figure F.1 with the nodal points in the stock market shown in Figure 8.2 and on Charts VIII.A and VIII.B. The dates when Uranus arrived at its nodes not only coincided with changing trends in the stock market, but also with all major wars in the United States.

⁹³ World War I began in the geographic area near the country now called Bosnia. The current tensions in Bosnia have coincided with Uranus returning to its location at the outbreak of World War I.

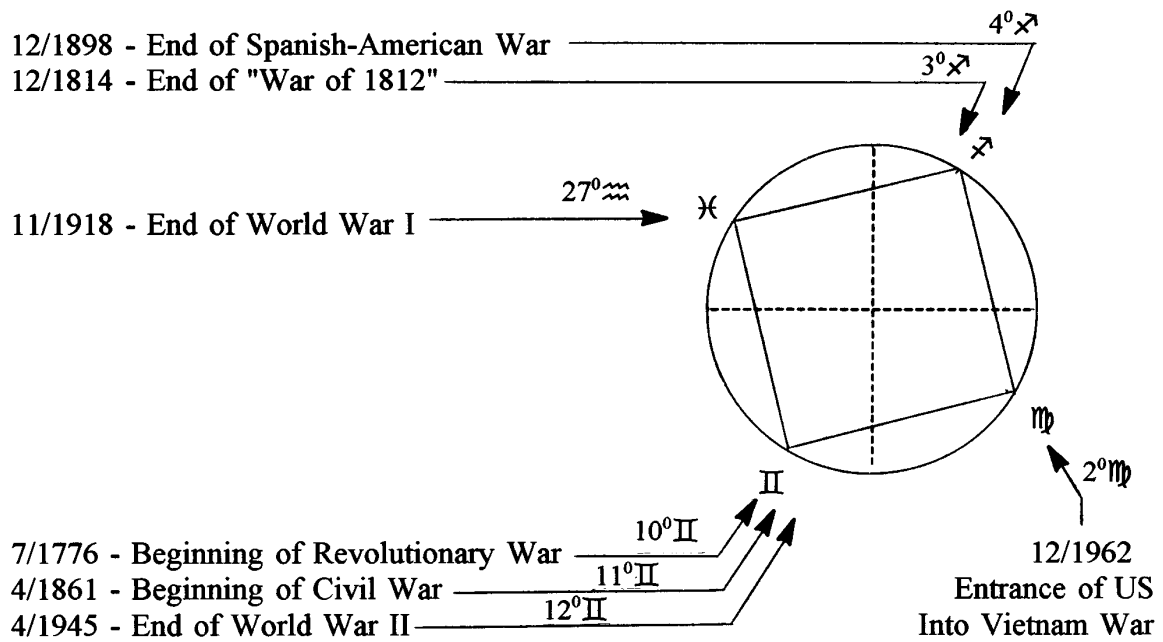


Figure F.1
Coincidence of Uranus Squares With American War

APPENDIX G

SQUARE ROOT OF FIVE STOCK MARKET GROWTH SPIRALS

This analysis was included in an appendix because some readers may find it a little too technical. Although there is nothing more complicated than a simple trigonometric relationship, some readers are uncomfortable with mathematics in general.

The "tangent" is the trigonometric function that defines the relationship between opposite and adjacent sides of a triangle that are not the hypotenuse. It is used in this analysis to find the angle the PTV assumes with the price and time axes. The reader does not have to understand the mathematics used to derive these angles to grasp the main point of this section. However, if he wishes to verify the numbers used in this analysis all data and results are contained in Table G.1.

The growth spiral based on the Fibonacci ratio is the most commonly used by financial market analysts. This spiral was shown in Figure 3.2 and defined the subdivisions of the five-year growth pattern between 1982 and 1987. This spiral is known as the Golden Spiral because each successive wrap is defined by radii vectors with proportion to the preceding vector in the ratio of PHI (1.618). Natural growth spirals are not limited to the Fibonacci ratio. For example,

STOCK MARKET GROWTH SPIRALS ARE DEFINED BY THE SQUARE ROOT OF FIVE RATIO.⁹³

This is why in Lesson IV, **PRICE-TIME RATIOS MORE IMPORTANT THAN FIBONACCI**, the square root of five was described as "the most important ratio in stock market analysis". Each successive wrap in stock market growth spirals are in the proportion of the square root of five to the preceding vector. This has produced a source of confusion among contemporary analysts as they have tried to force stock market data into the Fibonacci spiral. Because the Golden Spiral is closely related to the square root of five, as shown in Figure 4.4.b, it provides just enough "bait" for analysts to continue their pursuit down the wrong path. A good example of this was given in Lesson III, **GROWTH PATTERNS**, where the Golden Section was used to determine successive wraps on the spiral. However, a closer look at Chart III.B shows that this vector was actually the diagonal of two squares, which defines the root five relationship.

The root five growth spiral is shown in Figure G.1. Each of the triangles shown in this figure are similar and have sides in the root five proportion. The inner angles are given by the relationships:

$$\begin{aligned}\text{TAN}^{-1}(2.236) &= 65.9^{\circ} \\ \text{TAN}^{-1}(0.447) &= 24.1^{\circ}\end{aligned}$$

⁹⁴ Reference: *The Geometry of Art and Life*.

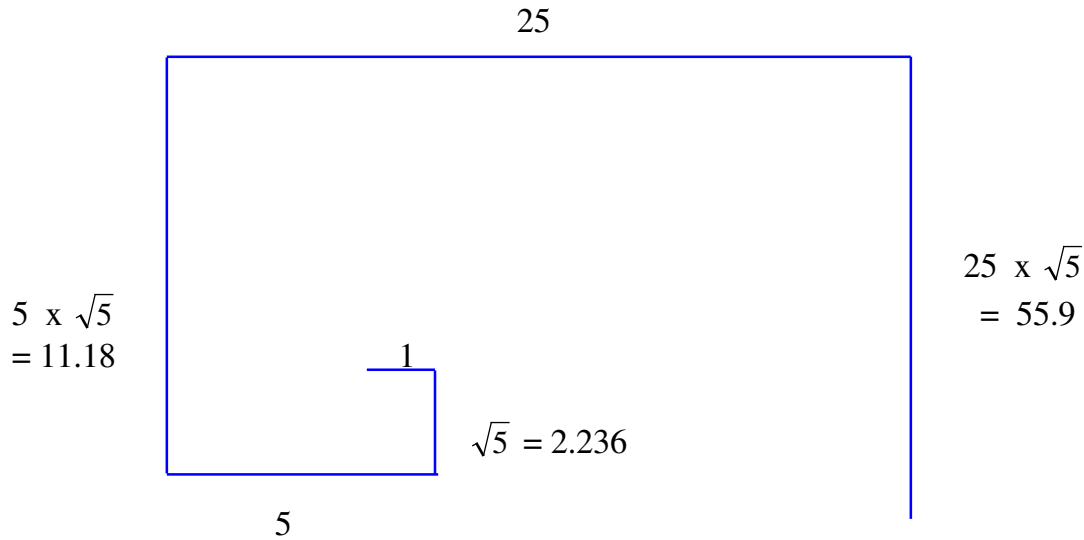


Figure G.1
Square root of five growth spiral

STOCK MARKET EXAMPLES OF THE ROOT FIVE GROWTH SPIRAL

Figure G.2 shows the PTVs connecting the major turning points in the DJIA between 12/1914 and 6/1942. The horizontal and vertical legs of these triangles are the time and price components of each PTV, whose data is contained in Table 4.2. These triangles represent successive wraps on the square root of five growth spiral. If the triangle from 9/1929 to 7/1932 were rotated 90° and each leg multiplied by the square root of five, the triangle from 12/1914 to 9/1929 would be formed as follows:

Triangle ABO 9/1929 - 7/1932		Triangle JAO 12/1914 - 9/1929
AO = 345 POINTS	$\times \sqrt{5} =$	JO = 769 WEEKS
BO = 148 WEEKS	$\times \sqrt{5} =$	AO = 333 POINTS
AB = 375	$\times \sqrt{5} =$	JA = 838

These two triangles present a good example demonstrating the intimate connection between price and time. Since they are successive wraps on the growth spiral, these triangles are rotated 90° from each other. Hence,

THE ROOT FIVE PROPORTION BETWEEN THE TWO TRIANGLES IS FROM PRICE IN THE FIRST TRIANGLE TO TIME IN THE SECOND TRIANGLE, AND FROM TIME IN THE FIRST TRIANGLE TO PRICE IN THE SECOND TRIANGLE.

That is, the decline from 9/1929 to the bottom in 7/1932 lasted 148 weeks. And the advance from the bottom after the reopening of the market in 12/1914 to the top in 9/1929 was 333 points, which is the square root of five times the 148 week decline from 9/1929 to 7/1932.

Similarly, the decline from 9/1929 to 7/1932 was 345 points. And the advance from 12/1914 to 9/1929 lasted 769 weeks, which is the square root of five times the 345 point drop from 9/1929 to 7/1932.

The angles within the triangles in Figure G.2 are calculated in Table G.1. If the angles formed between the vertical price axis and the two PTVs in Figures G.2.a and G.2.b are added together the result is a nearly perfect 90° angle. That is,

$$\begin{array}{r} \text{JAO} = 66.59^{\circ} \\ + \text{BAO} = 23.27^{\circ} \\ \hline = \text{JAB} = 89.86^{\circ} \end{array}$$

In other words, the two PTVs defining the stock market action from 12/1914 to the top in 9/1929 and from 9/1929 to the depression low in 7/1932 are at a right angle to each other and in proportion of the square root of five, effectively forming a root five rectangle with sides of 838 and 375.

Note that the root five triangle from 9/1929 to 6/1942, shown in Figure G.2.c, overlaps the root five triangle in Figure G.2.b. This is because the 9/1929-7/1932 PTV is not in the same two-dimensional plane as the triangle in Figure G.2.c.

In conclusion, analysts would have better results if they redirected their efforts away from Fibonacci ratios and toward those produced by the square root of five.

Table G.1
Angles of PTVs in Figure G.2 Relative to the Price and Time Axes
(Price and Time Values in Middle Column are From Table 4.2)

Angle In Figure G.2	Opposite Side / Adjacent Side	TAN ⁻¹ of Opposite / Adjacent From Preceding Column
AJO in Figure G.2.a	$\frac{333 \text{ Points}}{769 \text{ Weeks}} = 0.43$	TAN ⁻¹ (0.43) = 23.27 ⁰
JAO in Figure G.2.a	$\frac{769 \text{ Weeks}}{333 \text{ Points}} = 2.31$	TAN ⁻¹ (2.31) = 66.59 ⁰
BAO in Figure G.2.b	$\frac{148 \text{ Weeks}}{345 \text{ Points}} = 0.43$	TAN ⁻¹ (0.43) = 23.27 ⁰
ABO in Figure G.2.b	$\frac{345 \text{ Points}}{148 \text{ Weeks}} = 2.33$	TAN ⁻¹ (2.33) = 66.78 ⁰
CAO in Figure G.2.c	$\frac{659 \text{ Weeks}}{293 \text{ Points}} = 2.25$	TAN ⁻¹ (2.25) = 66.03 ⁰
ACO in Figure G.2.c	$\frac{293 \text{ Points}}{659 \text{ Weeks}} = 0.44$	TAN ⁻¹ (0.44) = 23.75 ⁰

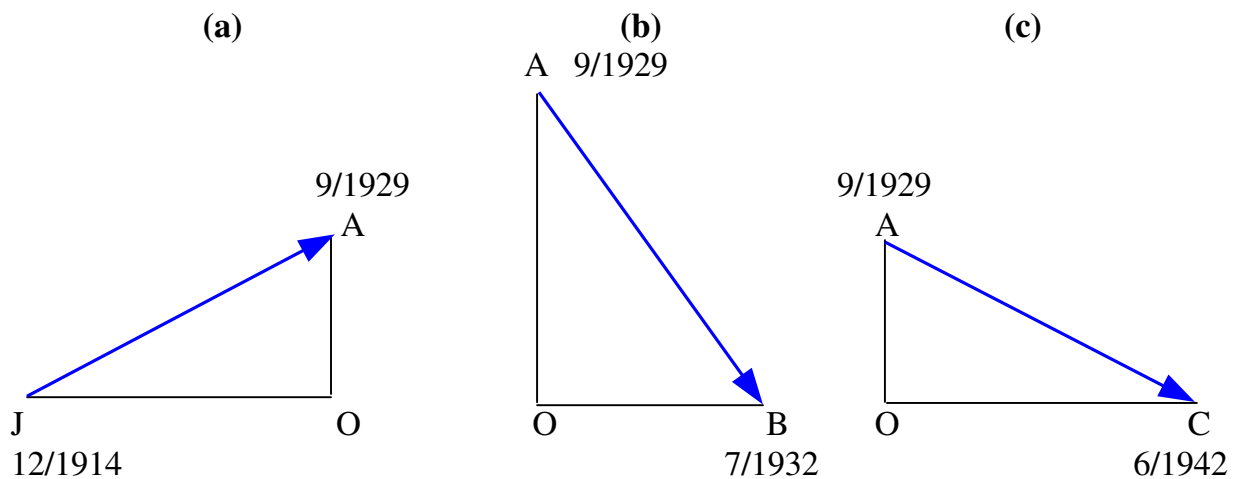


Figure G.2
 Similar triangles formed by PTVs between 1914 – 1942

REFERENCES

The books used as references in both the “Technical Reference” and “Reference” footnotes are listed below. Some of these are college level science and engineering texts which require some technical background to fully understand. Others require no previous training.

American Heliocentric Ephemeris 1901-2000, Neil Michelsen, (1982), Astro Computing Services, ISBN 0-917086-36-8

Calculus With Analytic Geometry, Munem & Foulis, (1978), Worth Publishers, ISBN 0-87901-087-8

Chaos, James Gleik

Chemical Principles, Dickerson, Gray, Darensbourg, (1970), Benjamin/Cummings Publishing, ISBN 0-8053-2422-4

Chemistry, Reactions, Structure, and Properties, Dillard & Goldberg, (1978) MacMillan Publishing, ISBN 0-02-329580-5

Connections – The Geometric Bridge Between Art and Science, Jay Kappraff, (1990), McGraw-Hill, ISBN 0-07-034251-2

Curves of Life, Theodore Andrea Cook, (1979), Dover Publications, ISBN 0-486-23701-X

Cycles, Dewey, (1971), Hawthorn Books, Library of Congress 70-130730

Electronic Devices and Circuit Theory, Boylestad & Nashelsky, (1978), Prentice-Hall, ISBN 0-13-250340-9

Elements of Dynamic Symmetry, Jay Hambridge

Engineering Circuit Analysis, Hayt & Kemmerly, (1978), McGraw-Hill, ISBN 0-07-027393-6

Feedback and Control Systems, (1967), Stefano, Stubberud, Williams, McGraw-Hill

Fundamentals of Physics – Extended, Halliday, Resnick, Wakler, (1997), John Wiley, ISBN 0-471-10559-7

Geometry of Art and Life, Matila Ghyka, (1977), Dover Publications, ISBN 0-486-23542-4

Introduction to Physics for Scientists and Engineers, Bueche, (1969), McGraw-Hill, ISBN 0-07-008871-3

Kepler’s Geometrical Cosmology, (1988), J.V. Field, University of Chicago Press, ISBN 0-226-24823-2

Modern Control Systems, Doft, (1980), Addison-Wesley, ISBN 0-201-01258-8

Modern Physics, Gautreau & Savin, (1978), McGraw-Hill, ISBN 0-07-023062-5

Sacred Geometry, Robert Lawlor, (1989), Thames & Hudson, ISBN 0-500810303

Tertium Organum, Petyr Demianovich Ouspensky

BOOKS AND SOFTWARE BY THIS AUTHOR

Please visit www.cycle-trader.com for details on any of these books.

Pentagonal Time Cycle Theory

Cowan's latest book published in 2009.

Four-Dimensional Stock Market Structures And Cycles

The first ten lessons of this series are contained within these two books. Lessons one through five deal with the four-dimensional geometric structures in financial markets. The last five lessons identify the cycles correlated with turning points within these structures. These cycles are applicable to any market.

Market Science Volume I - Square Of Twelve

This book contains lessons eleven and twelve and proves that the square of twelve is the elemental unit of measurement within the soybean market.

- XI - Square Of Twelve
- XII - Vectorial Partitioning

Market Science Volume II - Market Dynamics

This book contains lessons thirteen through sixteen and an update on stock market cycles and the growth spiral unfolding in that market, as of July 1995.

- XIII - Non-Euclidean Price-Time Geometry
- XIV - Quantum Energy Levels Of Freely Traded Markets
- XV - Soybean Cycles
- XVI - Square Of Fifty-Two
- Also - Stock Market Cycle Update And Current Growth Spiral
- Also - Applications Of The Musical Fifth To Timing
- Also - Dimensions Of Ancient Monuments And Soybean Spirals

W.D. Gann Commodity Trading Courses – Edited by Bradley F. Cowan

W.D. Gann Stock Market Trading Courses – Edited by Bradley F. Cowan

The Rare Writings Of W.D. Gann – Edited by Bradley F. Cowan

CycleTimer Software – Automates Many of the Techniques Used in This Book

Stock Market Geometry; P.O. Box 9756; San Diego, CA 92169-0756 USA